Some oxidative reactions of silanes and related compounds catalysed by copper(II) and palladium(II) complexes

A thesis submitted for the award of the degree of

Doctor of Philosophy

By

Arup Purkayastha

Roll No: 004701

to the

Department of Chemistry

INDIAN INSTITUTE OF TECHNOLOGY, GUWAHATI

GUWAHATI 781039, INDIA

MAY, 2003

Dedicated

to my

Mother

INDIAN INSTITUTE OF TECHNOLOGY, GUWAHATI

Department of Chemistry

CERTIFICATE

It is certified that the work contained in the thesis entitled "**Some oxidative reactions of silanes and related compounds catalysed by copper(II) and palladium(II) complexes**" by Mr. Arup Purkayastha, a student of the Department of Chemistry, Indian Institute of Technology, Guwahati for the award of the degree of Doctor of Philiosophy has been carried out under my supervision and this work has not been submitted elsewhere for a degree.

May, 2003

Dr. JUBARAJ B. BARUAH
Associate Professor
Department of Chemistry
IIT-Guwahati

INDIAN INSTITUTE OF TECHNOLOGY, GUWAHATI

Department of Chemistry

Statement

I hereby declare that the matter embodied in the thesis is result of research carried out by me in the Department of Chemistry, INDIAN INSTITUTE OF TECHNOLOGY, GUWAHATI, INDIA under the supervision of Dr. Jubaraj Bikash Baruah.

.

I. I. T. Guwahati

Arup Purkayastha

Arup Purkayastha

ACKNOWLEDGEMENTS

I express my sincere gratitude to my research supervisor Dr. Jubaraj Bikash Baruah, Associate Professor, Department of Chemistry, Indian Institute of Technology, Guwahati, who motivated me to do research in this area. His scientific thinking, valuable suggestions, discussion and constant support helped me a lot during the total course of my investigation.

I would like to acknowledge all the faculty member of the chemistry department, for their help and valuable suggestions in my Ph.D. tenure. My thanks are also due to all Research scholars, Project staff, and technical staff of our Department for all the help and assistance, which I received during my stay at IIT Guwahati.

I thank the Council of Scientific and Industrial Research, New Delhi for the financial support received by me. I thank the Indian Institute of Technology, Guwahati for all the facilities that were made available to me.

My sincere thanks are due to Professor P. Balaram, Molecular Biophysics Division, Indian Institute of Science, Bangalore for MALDI mass spectra and Central Drug Research Institute, Lucknow, Indian Institute of Science Bangalore, Indian Institute of Chemical Technology, Hyderabad for recording various types of spectra and other analyses. Dr. R. Kataky for SEM and Dr. A. E. Goeta of university of Durham for crystal structure

I would like to thank my mother for her constant encouragement and my other family members for supporting me in various stages of my Ph. D programme.

Arup Purkayastha

Arup Purkayastha

ABSTRACT

The results included in the thesis are mainly on silicon-oxygen bond forming reactions. Some physicochemical studies of tetrachlorocuprate complexes to establish a structure-reactivity correlation are also included. There are five chapters in the thesis.

A general introduction on synthetic methodology for siloxanes, their classification and utility is given in the chapter 1. A rationalisation in this chapter is made to show the scope for development of newer reagents for silicon-oxygen bond forming reactions. Different reactions of silanes as well as various mechanisms involved in the preparation of Si-Si and Si-hetero atom bonds are also included in this chapter.

The chapter 2 contains the synthesis and characterisation of few tetrachlorocuprates. In this chapter it has been demonstrated that the tetrachlorocuprates have flexible co-ordination geometry and suitable redox couple of Cu(II)/Cu(I) that are essential features for various types of catalytic reactions.

In the chapter 3 the utility of tetrachlorocuprate complexes as catalyst for the synthesis of silylether from Si-H bond activation is discussed. These copper complexes are also used as catalyst for oxidation of some related aromatic compounds. The role of metallic copper in the silicon-oxygen bond formation is also discussed in this chapter.

In the chapter 4 a few palladium(II) complexes having nitrogen donor ligands are described. These palladium complexes have been used as catalyst for synthesis of silylether as well as siloxane oligomers from silanes. Based on various observations and literature reports various possible mechanistic aspects for silicon-oxygen bond forming reactions have

been demonstrated. The limitation of the tetrachlorocuprate catalysts in the silicon-oxygen bond forming reaction is also discussed in this chapter.

The chapter 5 gives details of the experiments with relevant spectroscopic and other analytical data of the various compounds synthesised in chapter 2, chapter 3 and chapter 4. The references are compiled at the end of the thesis.

Contents

Chapter 5

Experimental section

Experimental section of Chapter 2

Experimental section of Chapter 3

Experimental section of Chapter 4

Chapter 1

Introduction

1.1 General features of silicon compounds

Silicon containing compounds are abundant in nature. They have versatile applications as hybrid materials[1], plastic and in opto-electronic materials[2]. Most abundant form of silicon in nature is in the form of its oxide; it makes up three quarters of the earth crust. The silicon and carbon are in the same group in the periodic table thus have similar outer electronic configuration, so their reactivity are comparable. Comparison of thermodynamic property as well as the reactivity of carbon and silicon compounds provides information on equivalence of carbon and silicon in terms of reactivity. Some bond energies of carbon and silicon with another atom that forms stable bonds are listed in the table 1.1. This table clearly shows that silicon-oxygen single bond is more stable bond than carbon-oxygen. The silicon-carbon bond, silicon-silicon and carbon-carbon bond energies are comparable. But silicon has a less tendency to form silicon-silicon bond in comparison with carbon to form carbon-carbon bond. This may be attributed to lower electronegativity of silicon than carbon; the lesser electronegativity makes the silicon to form more polar bond as compared to carbon. This also explains the susceptibility of a silicon-silicon bond towards nucleophilic attack over a carbon-carbon bond; the possible involvement of a hypercoordinated reaction intermediate is also another factor that favors such a process. In spite of the comparable bond strength of SiH bond as compared to a CH bond, the polarity of the former generally makes SiH bond more reactive. The silicon analog of

methane is silane, which is very reactive towards oxygen; methane requ conditions for similar reaction.

Table 1.1

	Si (kJ/mol)	**C** (kJ/mol)
-Si	322	372
-O	535	346
-C	372	335
-H	376	404

The properties of silicon in organosilanes are quite different from those of carbon in organic hydrocarbons; the figure 1.1 lists the various types of silicon bond and its analogy with carbon skeleton.[3] The availability of d-orbitals in silicon allows silicon to have higher co-ordination numbers. Thus, *penta-* and *hexa-* coordinate silicon are common.

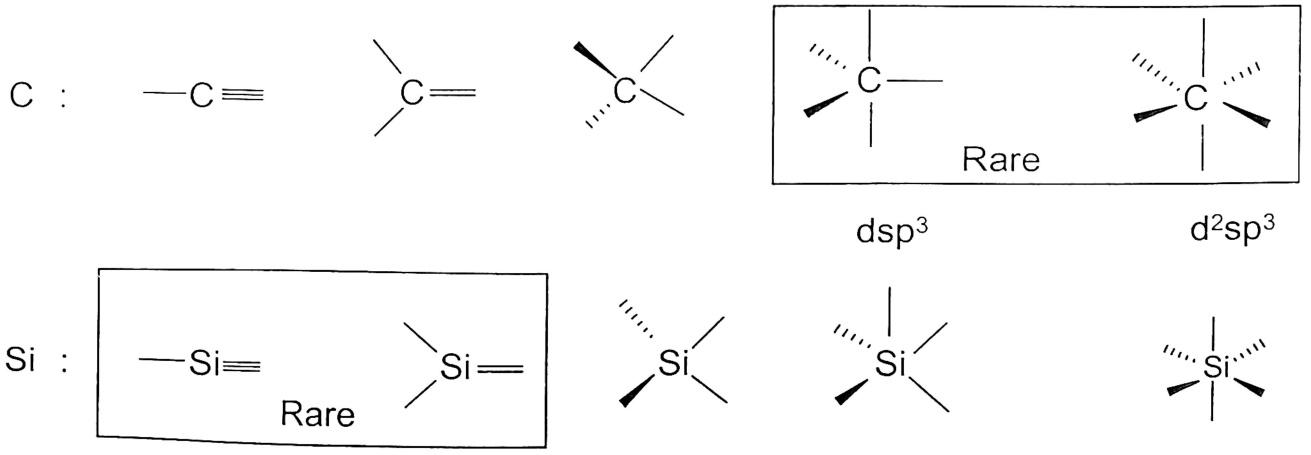

Figure 1.1

The SiF bond is the most stable bond followed by silicon-oxygen bond. The SiF bond is thermodynamically stable but is kinetically labile. This allows the nucleophilic substitution at the silicon center as well as cleavage of silicon-oxygen bond with the help of reagent containing fluoride ions, like tertiarybutylammoniumfluoride.[4a] One important feature of silicon compounds is that the silicon-oxygen bond are thermally stable. But

silicon-oxygen bonds are generally unstable in the presence of acid, base or fluo [4c]

1.2 Multiple bonds to silicon

The multiple bonded silicon compounds are not common, but there are many examples of silicon compounds having multiple bonds at the silicon center. The synthetic methodology describing synthesis of SiC, SiSi bonds are also available in literature.[5a, 5b] Among the multiple bonded compounds, the very bulky group around silicon, like mesityl group can stabilize SiSi as well as SiC bonded compounds. Two illustrative examples of stable SiSi and Si=C containing compounds are shown in structure 1. I and 1. II

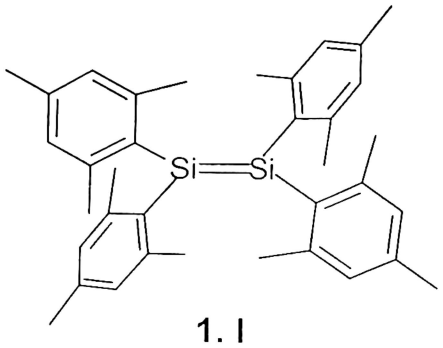

1. I

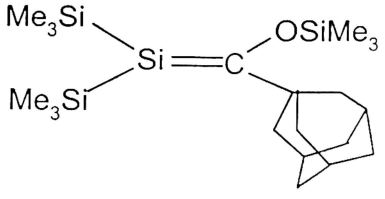

1. II

There are also examples of stable compounds containing SiSi double bond in cyclic units and also in spiro compounds.[5c, 5d] Two such examples are shown in structures **1.III** and **1.IV**.

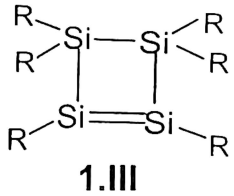

R = *t*-BuMe$_2$Si

1.III

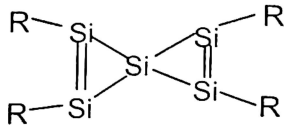

R = *t*-Bu$_2$MeSi

1. IV

The aromatic silicon containing compounds such as (**1.V, 1.VI**) namely silabenzene having the silicon atom attached to a bulky group like 2,4,6-tris{bis (trimethyl silyl) methyl}phenyl (Tbt) group are isolated and characterised in order to make a comparisons of aromaticity with corresponding aromatic counterpart such as naphthalene and benzene

respectively. Silabenzenes are generally not stable at room temperature; some tra like acetylene, methanol and benzophenone are used as matrix for stabilization and isolation of the silabenzenes.[6-8]

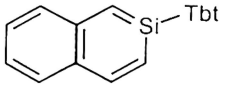

1. V

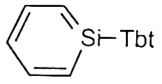

1. VI

Tbt = 2,4,6-tris{bis(trimethyl silyl)methyl]phenyl

The carbonyl analogue of silicon, the silanone intermediate [9,10] are proposed to be involved in the preparation of cyclic siloxane; but existence of silanone as independent species is yet to be realized. In this context we can bring an example of such a reaction between diphenyldichlorosilane with DMSO and 2,2,5,5 tetramethyl-1-oxa-2,5 disilacyclopentane that gives different type of cyclic siloxane. Proof for participation of silanone as an intermediate in these reactions comes from the product analysis during the course of the reactions. Verification of this hypothesis comes from the reaction between diphenyldichlorosilane[11] and DMSO in the presence of 2,2,5,5 tetramethyl-1oxa-2,5 disilacyclopentane (**1.VII**). In this reaction silanone intermediate is trapped by insertion into a strained ring containing silicon-oxygen single bonds. In fact, from this reaction it has been possible to isolate 4,4,7,7 tetramethyl 1,-3 dioxa-2,2 diphenyl-2,4,7 trisilacycloheptane (**1.IX**) and 6,6,9,9 tetramethyl-1,3,5-trioxa 2,2,4,4 tetraphenyl 2,4,6,9 tetrasilacyclononane (**1.X**). The (**1.IX**) could have been formed by insertion of diphenylsilanone into a SiO single bond of (**1.VII**). Alternatively, (**1.X**) may be formed from the reaction of oxobridged dimeric intermediate (**1.VIII**) with (**1.VII**). The proposed reaction scheme[10] explaining the product formation is shown in the scheme-1. I

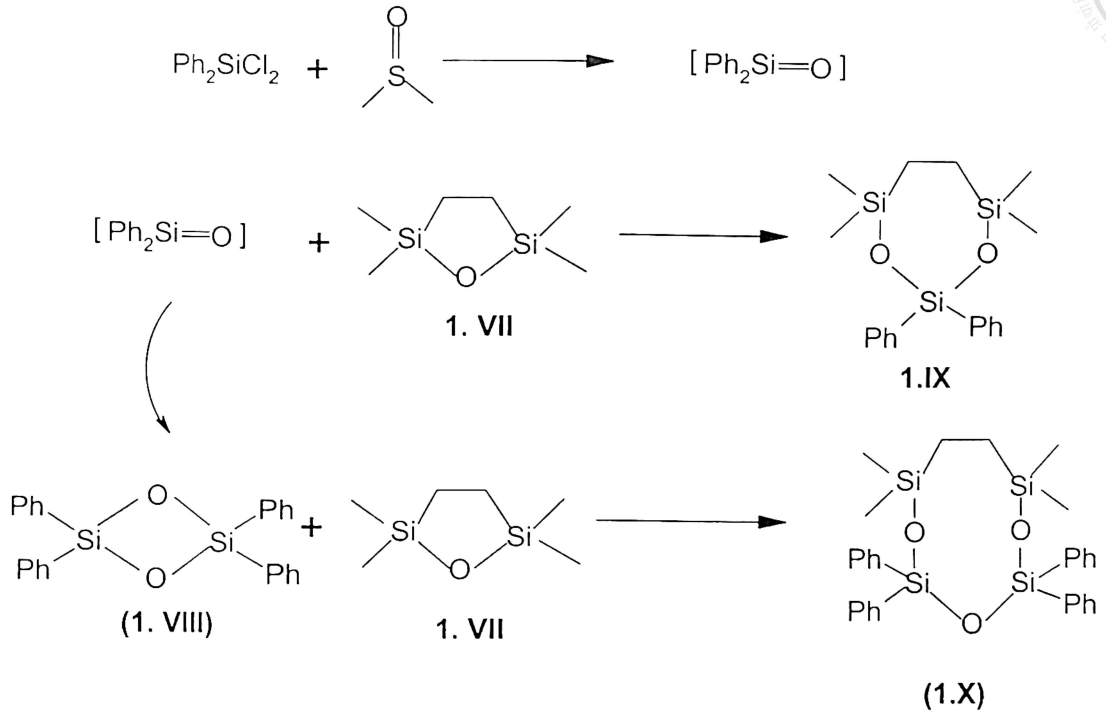

Scheme 1.1

The foregoing discussion shows that there is a distinct difference in the reactivity pattern of silicon compounds with corresponding carbon analogue. The instability of multiple bonds on silicon limits the synthetic strategies in silicon chemistry as compared to the available methodologies in organic chemistry. This results several synthetic challenges to overcome in silicon chemistry. There are scopes for new methodology on the synthesis of following types of compounds.

(i) Isolation of silanone intermediate is yet to be achieved.

(ii) Stable silicon containing triple bonded compounds are limited.

(ii) Synthesis of silicon-silicon π-delocalized conjugated polymers, which may have highly unusual electronic properties.

1.3 Siloxanes

Siloxanes are silicon containing compounds having silicon oxygen bond. However, a pure inorganic silicon-oxygen network is called silicate. The silicates are abundant in nature. In organic chemistry the silicon-oxygen bond is frequently used as a protective group for

alcohols and phenols. This stems from both easy formation as well as cleavag oxygen bond. Among the silicon-oxygen bonded compounds the trialkyl silyl ethers are prone towards hydrolysis during chromatography. The hydrolytic cleavage can be reduced by increasing the steric bulk around a silicon-oxygen bond, which leads to more stable silylethers.[12] Based on rate of hydrolysis of a silicon-oxygen bond the effective steric effect of trialkylsilyl groups on stabilizing a silylether can be realized. The stability of the trialky/aryl silylether in the increasing order are as follows: $Me_2SiH < Me_3Si < PhMe_2Si < EtMe_2Si < Ph_3Si <$ (n-Bu)$Me_2Si <$ (*iso*-Bu)$Me_2Si <$ (n-Bu)$_2$MeSi $< Et_3Si <$(cyclohexyl)$Me_2Si <$ (*i*-pr)$_2$MeSi $<$ (*t*-Bu)$Me_2Si <$ (*iso*-Pr)$_3$Si$<$ (*t*-Bu)$Ph_2Si <$ (*t*-Bu)$_3$Si $<$ (cyclohexyl)$_3$Si.[13] Thus, the relative stability of the silyl ether and selectivity in deprotection are two important factors that decide the success of protection and deprotection of alcohols or phenols.

There are several methods that can lead to silicon-oxygen bond formation are:

i) The reaction of silicon halides with alcohol (equation 1.1) gives corresponding silylether. These reactions are generally carried out in presence of base like pyridine, imidazole and tertiary amine etc.[14]

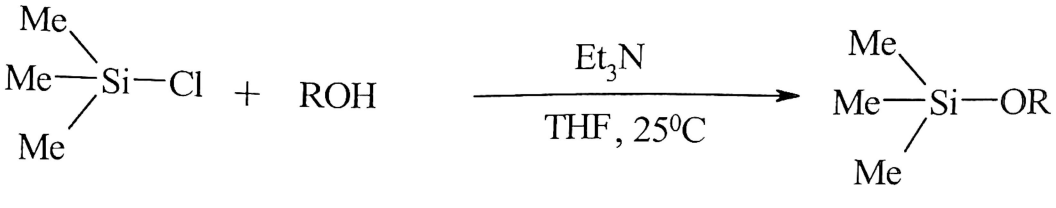

Equation 1.1

The disadvantage of this method is that an acid scavenger is required for removal of the liberated acid which otherwise can cleave a silicon-oxygen bond. Such reactions also require aqueous workup to remove the ammonium salts formed in the reaction. The reaction

of tri-isopropylsilylchloride with alcohols in dimethylformamide in the presence or pyridine is a commonly used reaction for alcohol protection.[15]

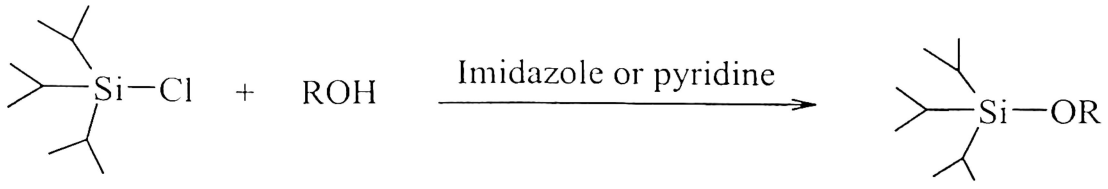

Equation 1.2

The presence of bulky isopropyl substituents on the silicon lowers the rate of reactions as compared to other conventionally used silylating agent such as trimethylsilylchloride (TMS) or *t*-butyldimethylsilylchloride (TBDMS). Another advantage of using tri-isopropyl silyl chloride is that; it selectively silylate primary alcohols even in the presence of a secondary alcohol. The reaction of silyltriflates with alcohols also leads to silylether.[16] An example of such a reaction involving the retention of optical active center is shown in equation 1. 3

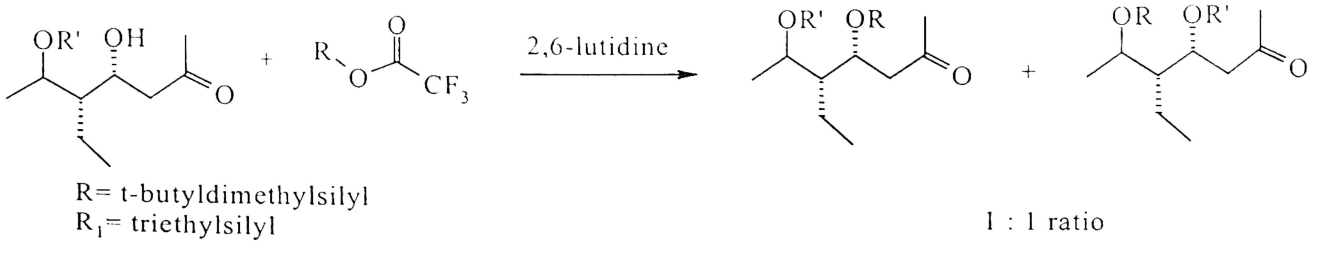

R= t-butyldimethylsilyl
R_1= triethylsilyl

1 : 1 ratio

Equation 1.3

ii) Another widely studied method of silicon-oxygen bond formation is the dehydrogenative coupling reactions of silanes with alcohols in presence/absence of a catalyst[17] (equation 1.4)

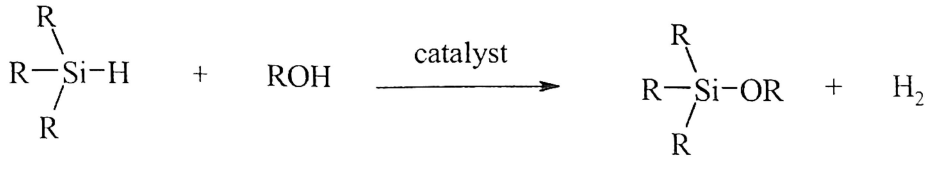

Equation 1.4

The dehydrogenative coupling reaction is advantageous over other reactic ease in the product isolation and possibility of continuous processing. A large number of metal complexes can act as catalyst for this reaction. The activation of Si-H also can be achieved by metal powders.

These reactions are also catalyzed by alkoxide and amines. The use of catalytic amount of potassium hydroxide (mol 9%) 18-crown-6 ether (mol 3%) in dichloromethane[18] under mild condition demonstrates an example of supramolecular catalysis in synthesis of silylether. A wide varities of silyl ethers are prepared by this method.

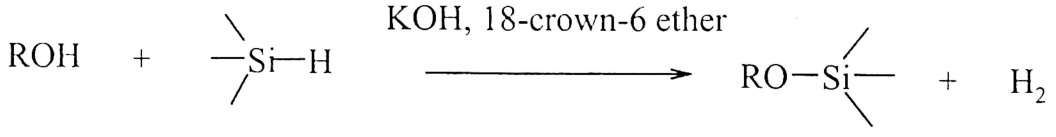

Equation 1.5

iii) Siloxy ether of dihydroxy aromatic compounds can be prepared by the reductive disilylation of quinones by disilanes. Such reactions are catalyzed by palladium and rhodium catalysts.[19]

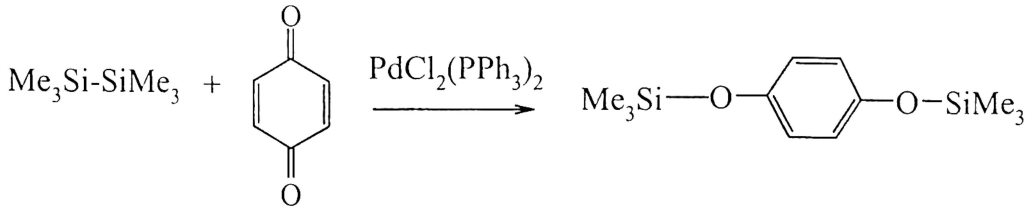

Equation 1.6

The equation1.6 depicts the palladium-catalyzed disilylation of 1,4-benzoquinones with hexamethyldisilane. In a relatively recent work, such methodology is extended to co-polymerization reaction of hydrosilanes with 1,4-benzoquinone to give silicon-oxygen bonded oligomers.[20]

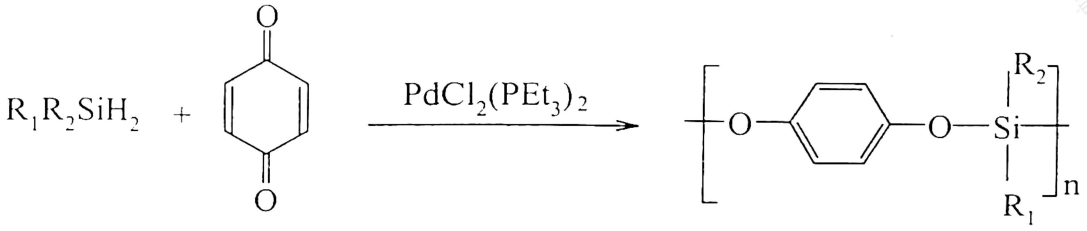

Equation 1.7

iv) Another method for silicon-oxygen bond formation reaction is by the acid catalyzed condensation of silanols.[21]

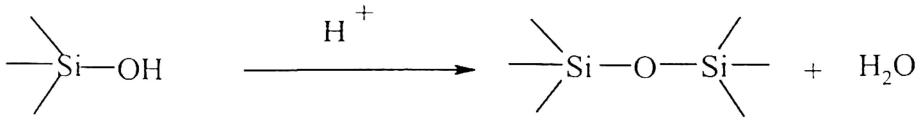

Equation 1.8

This reaction is widely used for the synthesis of various macromolecular siloxane architectures, such as linear siloxane, silsesquioxane and silica network and glasses.[22a] However, the use of strong acid in these reactions causes equilibration of the reaction. [22b]

v) Unsaturated silicon containing compounds such as silenes, disilenes react efficiently with alcohols to give addition products.[5a] Nucleophilic addition of alcohols and water to disilene[23,24] (equation 1.9) require slightly elevated temperature in absence of catalyst but the reactions are much slower than nucleophilic addition reactions of silenes. [25,26](equation 1. 10).

R' = Mesityl group

Equation 1.9

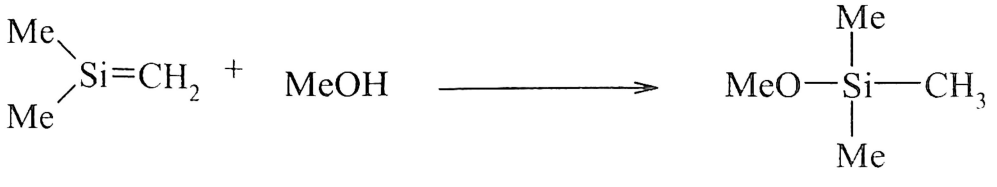

Equation 1.10

vi) The silicon-nitrogen bonds are relatively unstable, they can be easily conve ethers and such reactions are used for preparations of silylether attached to a phenolic group through intervening carbon atom (equation 1. 11)[27]

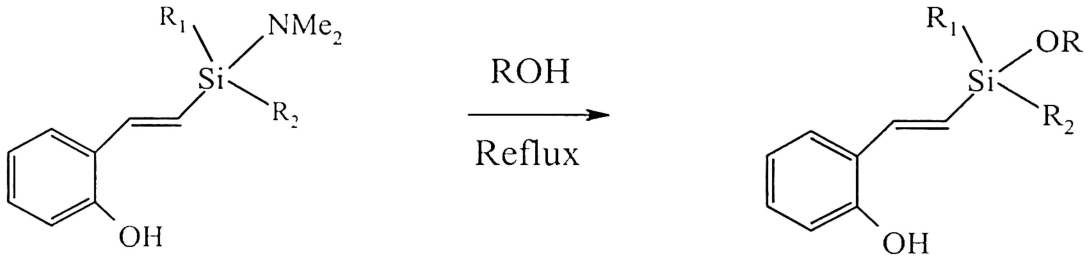

Equation 1.11

I. 4 Silicon-oxygen bonded compounds as precursor in organic synthesis

In the earlier section different synthetic methods used for silicon-oxygen bond formation is emphasized. However, utility aspects of such reactions are realized when these reactions are applied to some useful organic transformations. Some of the synthetically useful organic reactions that involve silicon-oxygen bonded compounds are listed below to show the utility of silicon-oxygen bonded compounds.

1. Acid catalyzed aldol reaction of silylenol ethers with an aldehyde is catalyzed by Lewis base to give stereoselective carbon-carbon bond formation.[28,29,30] (equation 1.12)

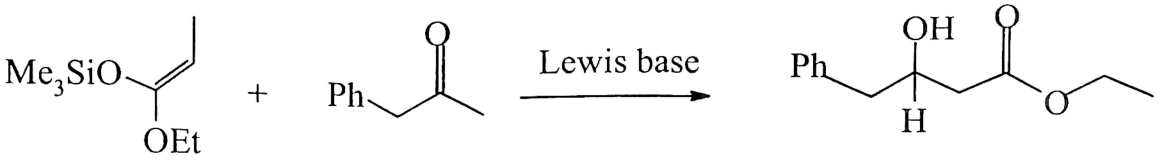

Equation 1.12

The reaction of (**1.XI**) with benzaldehyde (**1.XII**) is catalyzed by $TiCl_4$ to give 63:37 ratio of **1.XIII**) and (**1.XIV**).

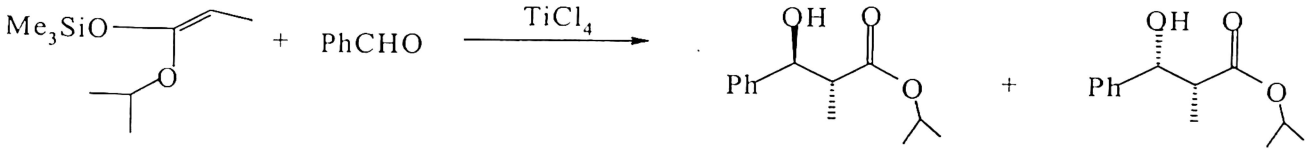

1.XI **1.XII** **1.XIII** **1.XIV**

63 : 37

Equation 1.13

2) Oxygen protected carboxylic acid gives cyclic compound through intermolecular aldol reaction. [31](equation 1.14)

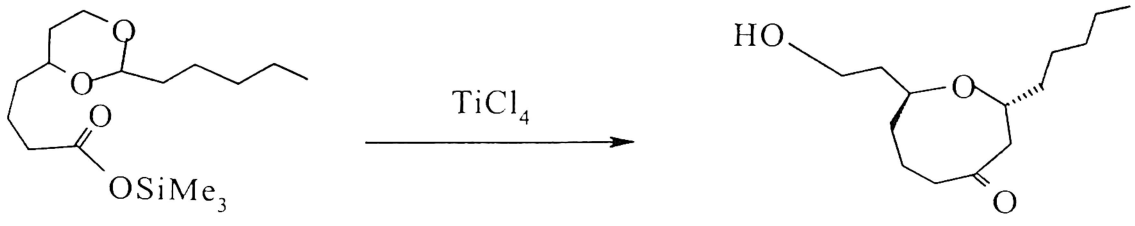

Equation 1.14

The reaction shown in equation 1.14 gives ring expansion with stereospecific transformation.

3) Preformed silylenol ethers are used for Michael addition reaction of a α, β unsaturated carbonyl compounds (equation 1.15). [32]

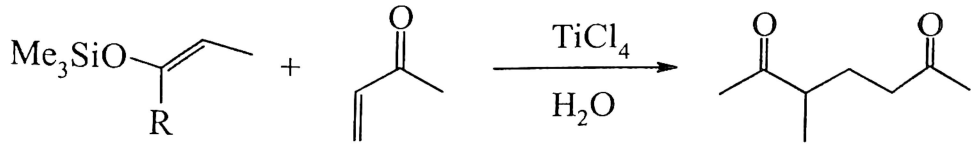

Equation 1.15

4) Spirocyclic skeleton (**1.XVI**) can be prepared from suitable silylenol ethers ig 1,4-Dicyanonaphthalene (DCN) as an electron acceptor in acetonitrile. [33,34] This reaction proceeds in presence of light.

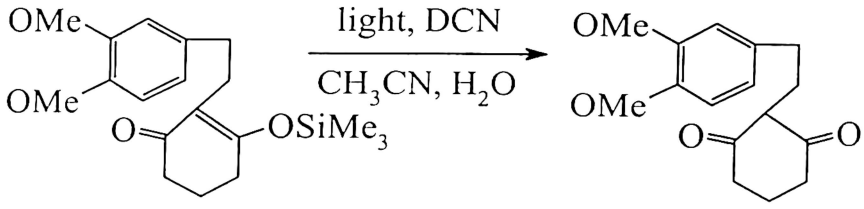

1. XV **1.XVI**

Equation 1.16

5) Trimethylsiloxy α-diazo-β-ketophosphate (**1. XVII**) in the presence of catalytic amount of $Rh_2(OAc)_4$ gives a mixture of α-phosphono-δ lactone (**1.XVIII**) and 2-phosohano cyclopentenone (**1.XIX**).[35]

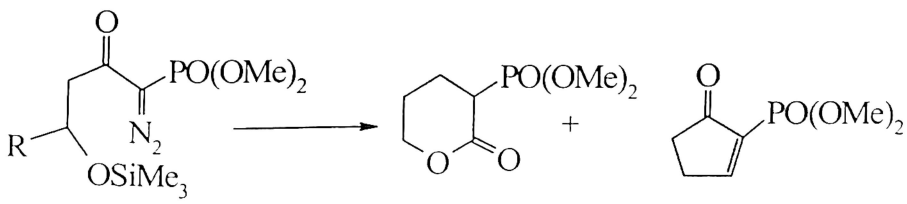

1.XVII **1. XVIII** **1. XIX**

Equation 1.17

6) The reaction of ethyl (4-methoxy phenyl) silanediol with 4-octyne in presence of $[Rh(OH)_2(COD)]_2$ as catalyst (where COD = cyclooctadiene) results in carbon-carbon bond formation. [36,37] to give (**1.XX**).

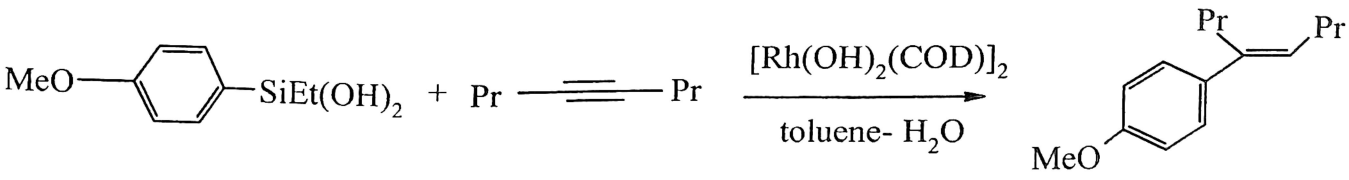

1 .XX

Equation 1.18

I. 5 Types of siloxane

Based on structure, functional group/s on the silicon and organic spacer between two silicon centers; siloxane are broadly classified into the following classes, according to scheme1.2

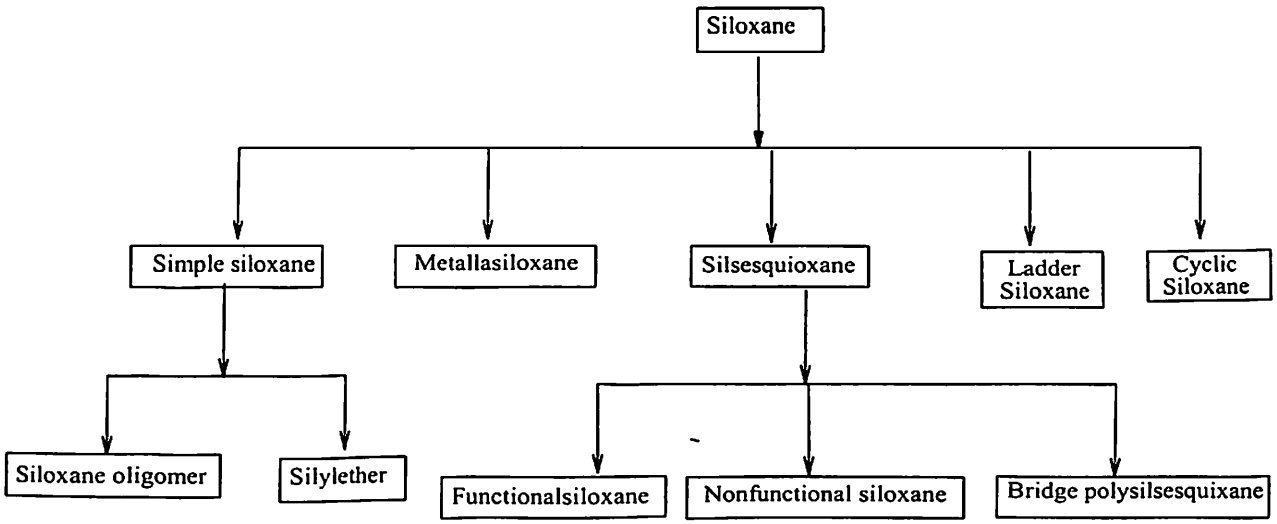

Scheme 1.2

I.5 (i) Silylether

Silylethers are the simplest form of all silicon-oxygen bonded compounds. They may be mono, di, tri and tetra silyl ether as shown below:

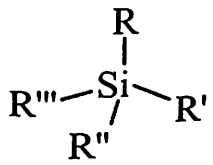

R = R	R' = R'	R''= R''	R''' = OR	**1.XXI**	monosilylether
R = R	R' = R'	R''= OR	R''' = OR	**1.XIXII**	disilylether
R = R	R' = OR	R''= OR	R''' = OR	**1.XXIII**	trisilylether
R = OR	R' = OR	R''= OR	R''' = OR	**1.XXIV**	tetrasilylether

I.5 (ii) Linear oligomeric siloxanes

This class of silicon oxygen containing oligomers has direct silicon oxygen bond to build an one-dimensional network (**1.XXV**). They can also have intervening bifuntional groups as linker to link silicon-oxygen bonds (**1.XXVI**). The starting materials for linear siloxane oligomers are generally dichlorosilane, dihydro silane or dialkoxy silane.[38,39] The dehydrogenative coupling reaction of alkoxy silanes with bifunctional alcohols can give linear siloxanes with high molecular weight.[39] These oligomers are also called silicones. They find application as silicon oil, foam stabilizing agent and surfactant.

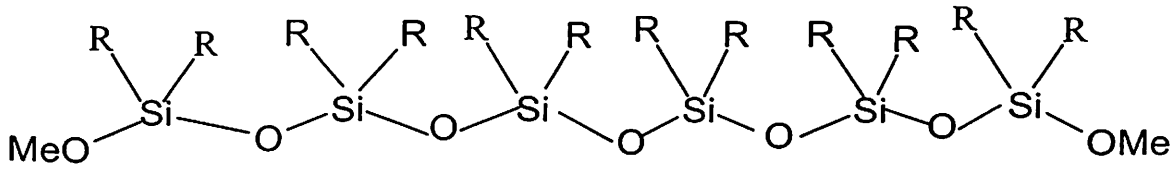

1.XXV

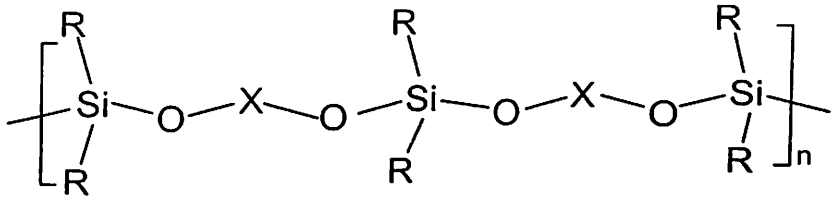

Where X is a binding unit such as methylene group.

1.XXVI

I. 5 (iii) Metallasiloxanes

Metallasiloxanes are siloxanes having some of the silicon atoms replaced by an appropriate metal. In-corporation of metal into a siloxane framework leads to two or three dimensional or linear network. Metallasiloxanes can be derived from silanediols, disilanol,

silanetriols and trisilanols. For example, transesterification reaction of Ti(C h sterically hindered silanediol {(*t*-Bu O-)$_3$SiO}$_2$Si(OH)$_2$ gives cyclic siloxane (**1.XXVII**). Similarly, cyclic dihalotitanasiloxanes [*t*-Bu$_2$Si(O)OTiX$_2$]$_2$ (X = Cl, Br, I) can be prepared by the direct reaction of the corresponding titaniumtetra chlorides with *t*-Bu$_2$Si(OH)$_2$.[40] Such compounds are made of eight membered ring having composition $Ti_2Si_2O_4$ (**1.XXVIII**). Both silicon and titanium atoms in the molecule exhibit regular tetrahedral geometry. Analogously the corresponding Zr compound [*t*-Bu$_2$Si(O)OZrCl$_2$]$_2$ was also prepared from the reaction between dilithium salt of *t*-Bu$_2$Si(OH)$_2$ and $ZrCl_4$.[41]

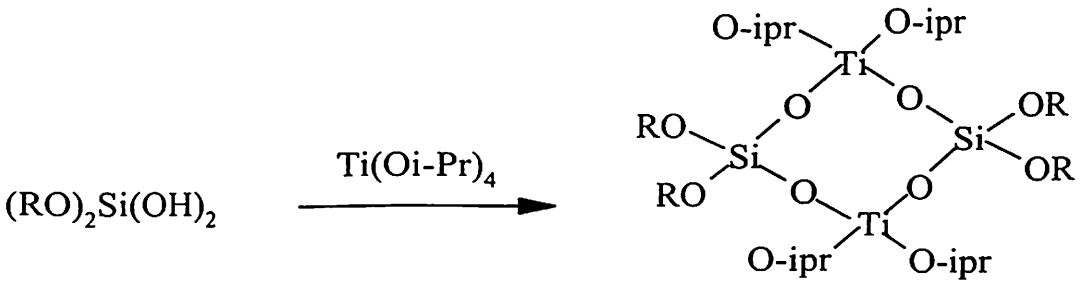

1.XXVII

Equation 1.19

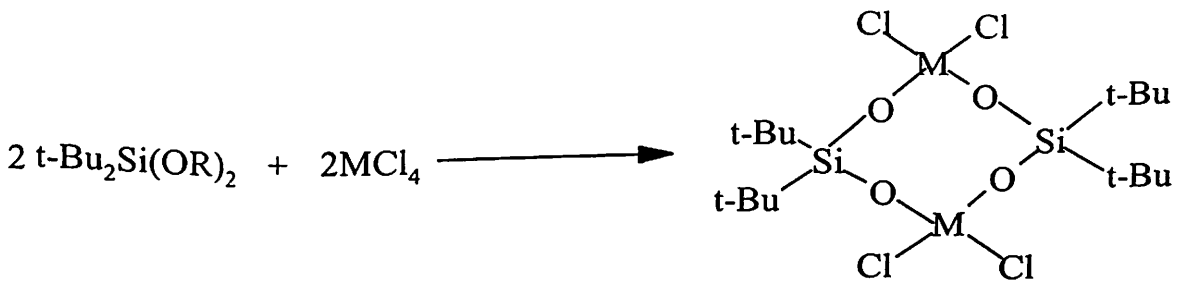

1.XXVIII

M = Ti, R = H
M = Zr, R = Li

Equation 1.20

Cyclopentadienyl substituted titanasiloxane $[t\text{-}Bu_2Si(O)OTiCpCl]_2$ ( ) can be prepared directly by the reaction of $CpTiCl_3$ with $t\text{-}Bu_2Si(OLi)_2$. The reaction of the silanediol $Ph_2Si(OH)_2$ with zirconium amido derivative, $Zr(NEt_2)_4$ leads to the formation of the dianonic *tris*-chelate metallasiloxane $[NEt_2H_2]_2[(Ph_4Si_2O_3)_3Zr]$ (**1.XXX**). In this reaction the silanediol prior to co-ordination to zirconium, gets converted into disilanol by condensation of two molecules through elimination of water. In the case of zirconocene central zirconium atom is co-ordinated by six oxygen atoms in a distorted octahedral geometry.[42]

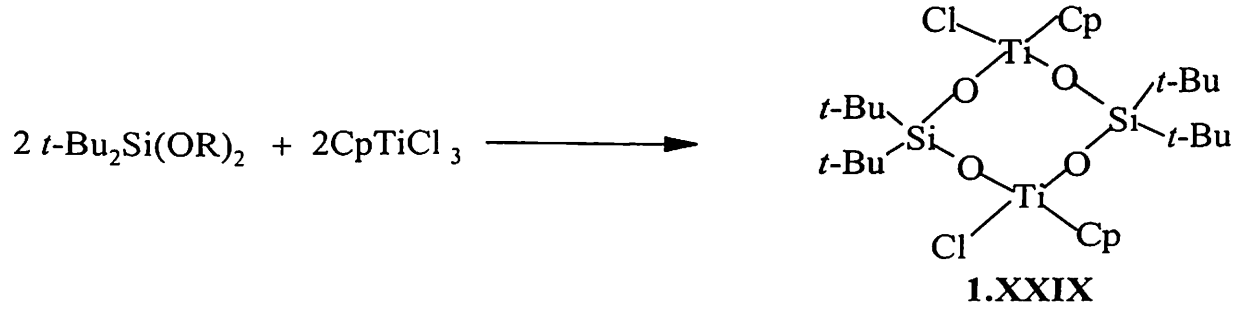

1.XXIX

Equation 1.21

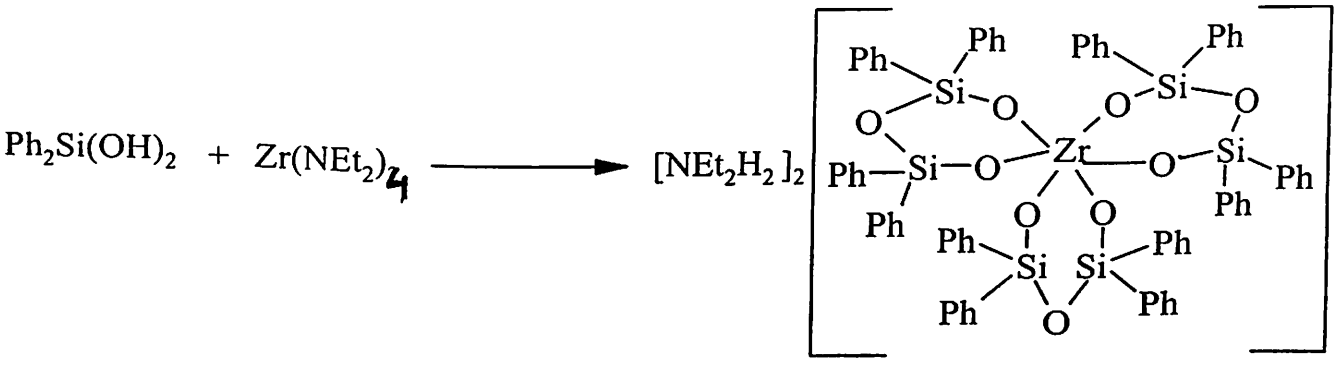

1.XXX

Equation 1.22

Disilanols are also used as building blocks for a variety of metallasiloxanes.[43] The disilanols are capable of chelating to form six member rings containing the central metal. The reactions leading to group 4 metallasiloxanes from disilanols are described in equation 1.25 and 1.24

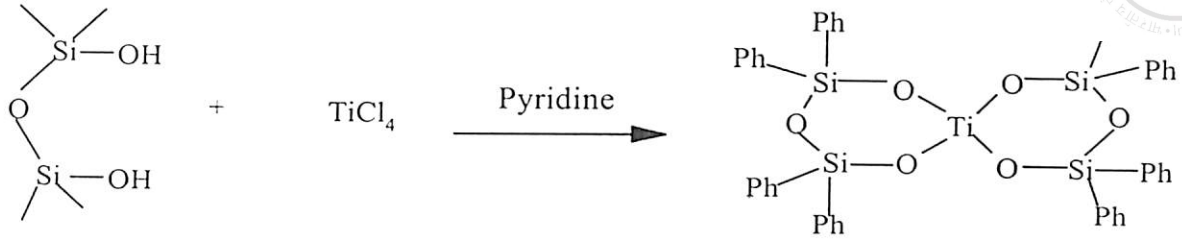

Equation 1.23

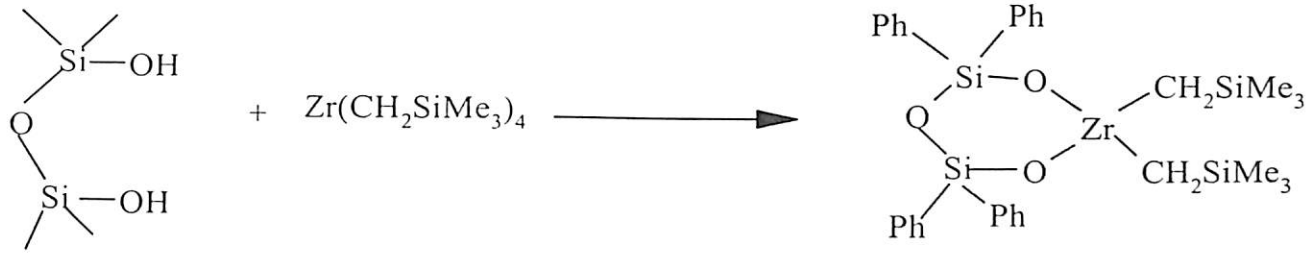

Equation 1.24

In a similar manner metallasiloxane derivative of Group 5, Group 7, Group 9 and main group metals can be prepared from disilanols. Few interesting structures of such compounds are shown in **1.XXXI, 1.XXXII, 1.XXXIII**.

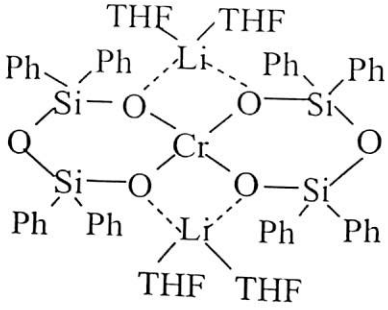

THF= Tetrahydrofuran

1. XXXI

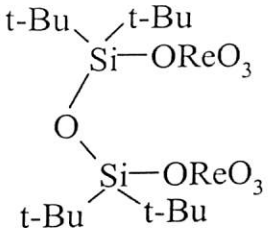

1. XXXII

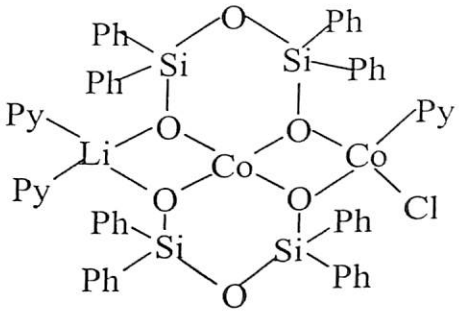

Py= pyridine

1. XXXIII

Reactions of simple silanediol and disilanols with titanium halides or titanium amides give cyclic titanasiloxanes. Three-dimensional titanasiloxanes can be prepared by reaction of titanium amide with silanol or silanediol. Such reactions serve as a synthetic path for preparation of model compounds for Ti doped Zeolites.[44, 45] The cubic titanasiloxanes can be prepared by a single step synthesis from the reaction of titanium orthoesters and

silanetriols.[46] The driving force for formation of zeolite like structure is the elin ıe corresponding alcohol, which results in the subsequent assembly of the three-dimensional SiOTi frameworks.

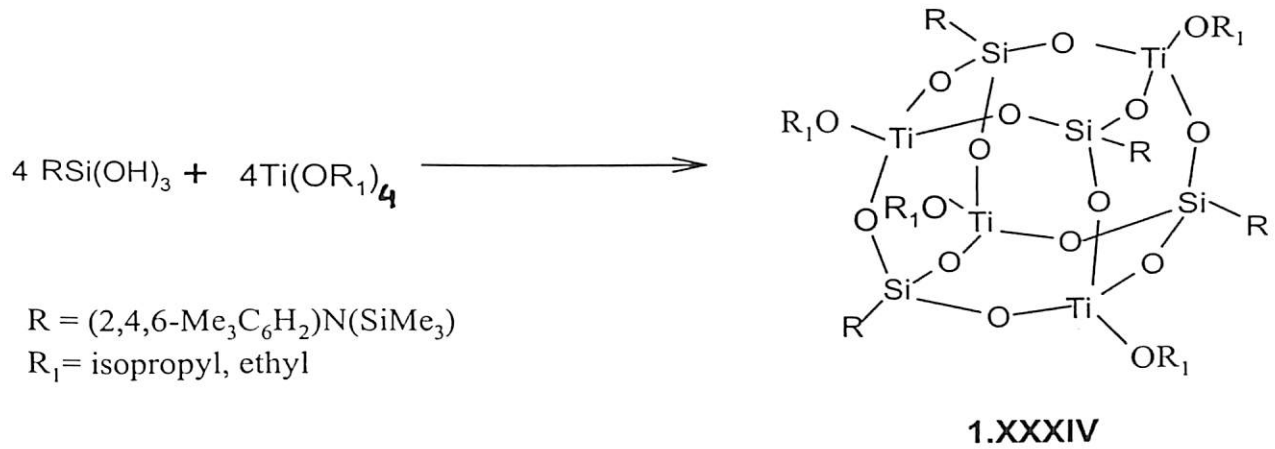

1.XXXIV

Equation 1.25

In analogous manners three-dimensional network of aluminiumosiloxane, indiumsiloxane, galliumsiloxane etc. can be prepared from the reaction of trisilanols and MMe_3 where M = Al, In, Ga etc. In all these networks cubic metallasiloxanes, $M_4Si_4O_{12}$ polyhedrons are present.[47] The sides of the cubic framework comprise six $M_2Si_2O_4$ eight-member rings, which adopt an approximate C_4 crown conformation. The OSiO angles in all compounds remain close to a tetrahedral geometry.

I. 5 (iv) Silsesquioxane

The hydrolysis of silicon trichlorides is a complicated process and usually does not lead to the expected trihydroxy compounds, but undergoes polycondensation in solution resulting in the formation of three-dimensional silsesquioxanes having network of *closo* cubic geometry. Such compounds have empirical formula $RSiO_{3/2}$. Incompletely condensed polyhedral silsesquioxanes is possible to isolate by carefully controlling the steric parameters for the R group and the reaction condition.[48]

The cross-linked silicon oxygen networks, containing simple or functi residues on every silicon to give silsesquioxanes are common[49,50] Silsesquioxane can have different structures such as random structure, ladder structure, cage structure and partial cage structure. They are also sometimes called by the name *ormosils* (organically modified siloxane). A representative silsequioxane is shown in the fig **1.XXXV** .

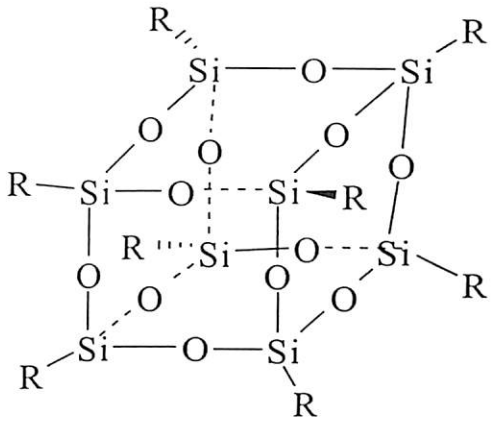

1.XXXV

To prepare mono-substituted silsesquioxane, there are three conventional synthetic routes[50]

i) Co-hydrolysis of trifunctional organo or hydrosilanes. For example co-hydrolysis of $HSiCl_3$ and $PhSiCl_3$ result in the formation of $PhH_7Si_8O_{12}$ (equation 1.26)

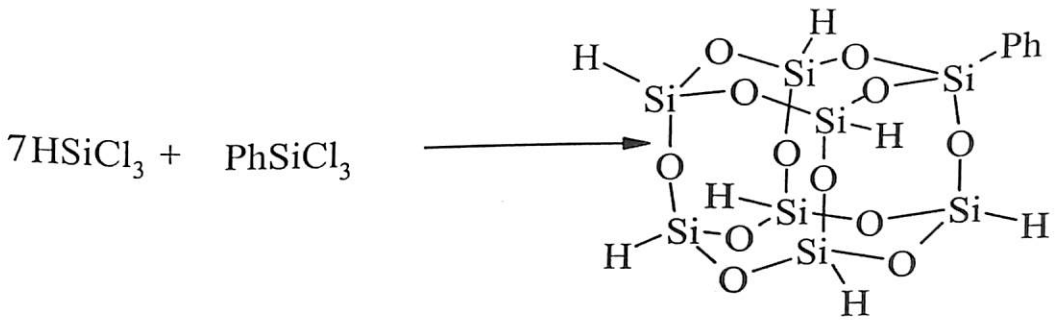

Equation 1.26

ii) Substitution reactions at silicon center with the retention of siloxane cage leads to structural modification of silsesquioxane. For this reaction hydrosilylation is a commonly used reaction (equation 1.27)

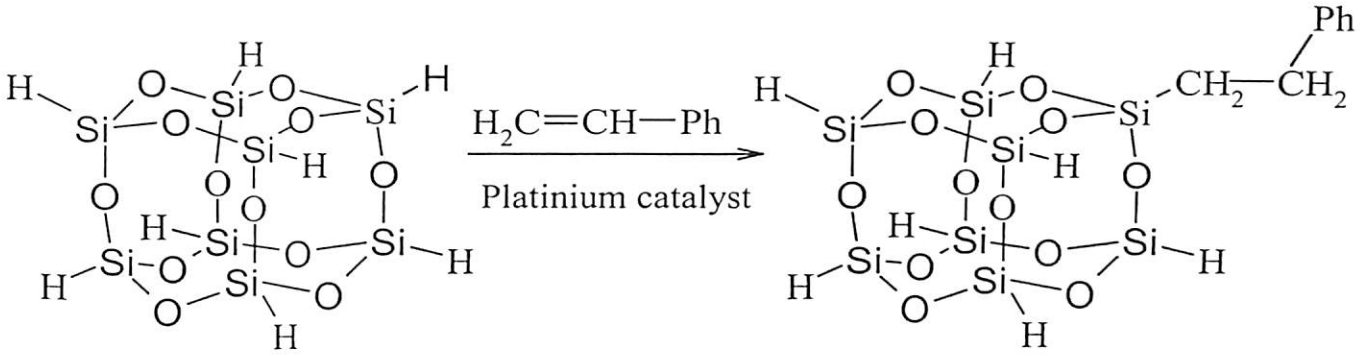

Equation 1.27

ii) By the corner capping reactions of functional group present in the incomplete cage, silsesquioxanes can be prepared.

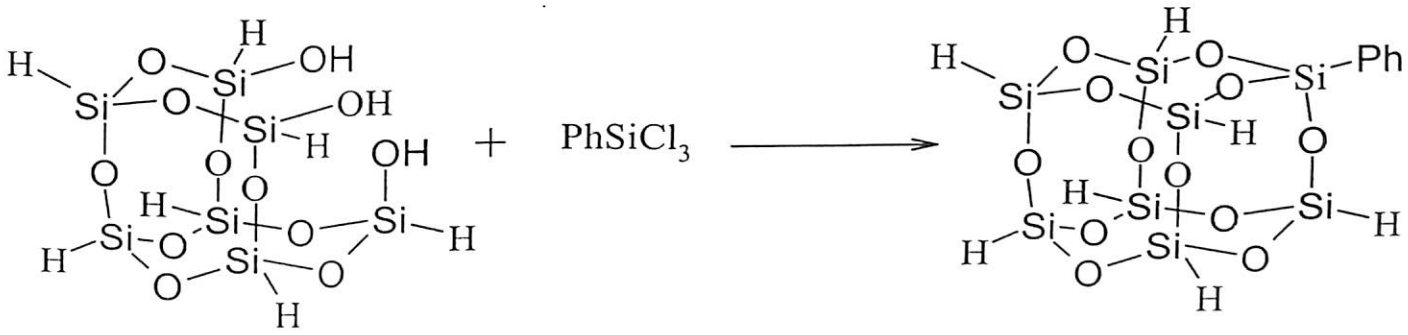

Equation 1.28

Silsesquioxane have also three subclasses; they are

a) Functional silsesquioxane. b) Nonfunctional silsesquioxane c) Bridged poly silsesquioxane

a) Functional silsesquioxane

The silsesquioxane, having one or more functional group/s like SiOH, SiH are called functional silsesquioxane(**1.XXXVI**).[50] Functional silsesquioxane are prepared from silanes having formula $RSiX_3$, where R is an organofunctional group and X is a alkoxy or halide etc. Vinyl, allyl functional, methacryl-functional, amino-functional and epoxy functional sillsesquioxane are most important structural motif from application point of view.[48]

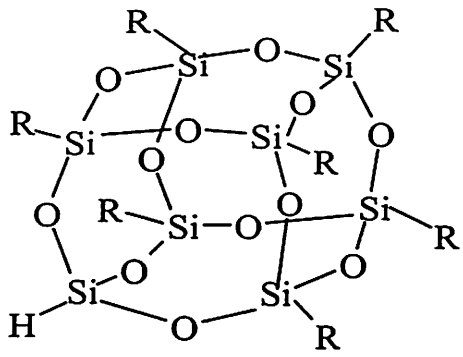

1.XXXVI

b) Nonfunctional silsesquioxane

As the name implies the silsesquioxane without any functional group are called nonfunctional silsesquioxane (**1.XXXVI**). Generally in this type of silsesquioxane all silicon atoms are bonded with an alkyl or aryl group.[49, 50] Example of nonfunctional silsesquioxanes are phenyl silsesquioxane, methylsilsesquioxane, substituted phenyl and benzyl silsesquioxanes. There are different possibilities on the structural features of a non-functional silsesquioxane. Base on the cage structure they can be prismatic cage having eight, ten or twelve silicon-oxygen bonds and categorized as T_8^R, T_{10}^R and T_{12}^R respectively.

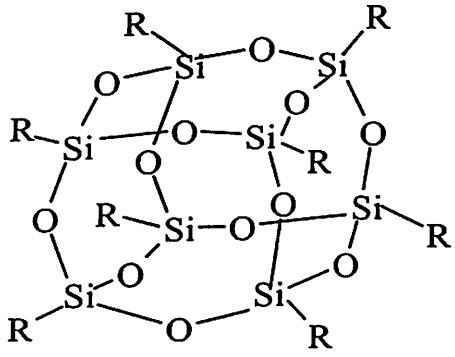

1.XXXVII

c) Bridge polysilsesquioxane:

Bridge polysilsequioxanes have three-dimensional network. They can be distinguished from other silsesquioxane as they contain organic fragment as an integral component of the network. This family of hybrid organic-inorganic materials are prepared in sol-gel processing of monomers having variable organic bridging groups and two or more trifunctional silyl groups.[51-52] Some important monomers that have been known from long time for the preparation of bridge polysilsesquioxane are shown below (**1.XXXVIII, 1.XXXIX, 1.XXXL, 1.XLI**)

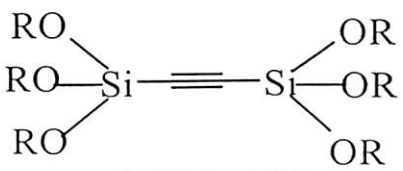

1.XXXVIII

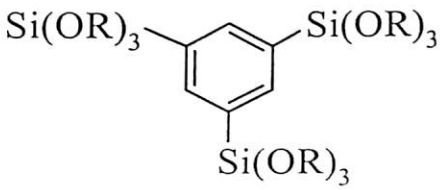

1.XXXIX

1.XXXL

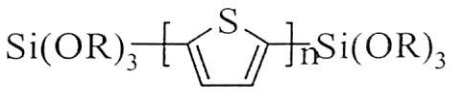

1.XLI

Figure 1.4

A representative structure of bridge poly silsesquioxane is shown **1.XLII**

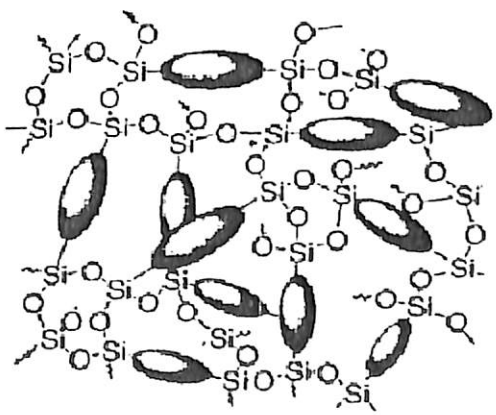

aromatic, alkene, alkyne, alkane

1.XLII

The hybrid organic-inorganic materials can be synthesized through familiar routes; hydrolytic sol-gel route [51,52] and non-hydrolytic sol-gel routes[53,54] each route has its advantages and disadvantages.

Understanding of bridge polysilsesquioxane requires discussion on hybrid organic-inorganic materials. Hybrid organic-inorganic materials are of two categories, nanocomposites and nanostructured hybrid materials. Nano-structured materials are generally prepared by hydrolysis and polycondensation of mono component hybrid organic-inorganic precursor i.e. organic unit is an integral part of the component, which is generally called building block unit.[51] On the other hand, nanocomposites are the polycondensed product of an inorganic matrix in the presence of an organic molecule acting as a host.[55] Two routes leading to the formation of nanocomposite and nanostructured hybrid materials is shown in the scheme-1.4. The bridge polysilsesquioxane falls in the category of nanostructured hybrid organic-inorganic materials.

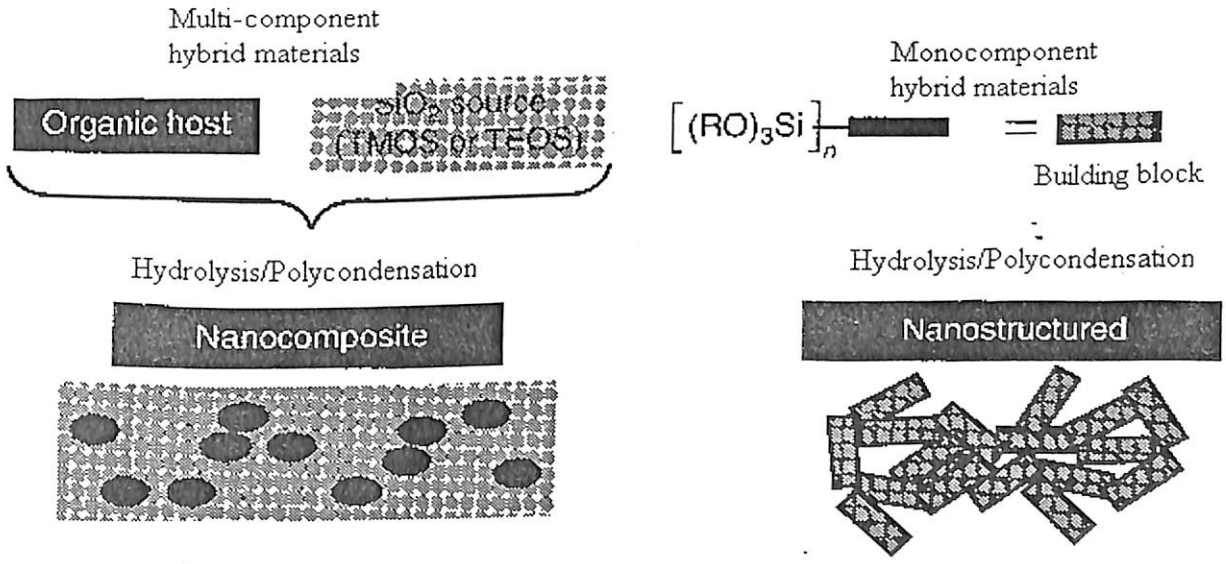

Scheme 1.4

Silsesquioxanes can be prepared by hydrolytic sol-gel route, in which hydrolysis and polymerization leads to the desired product. Polymerization process involved in this kind of

reaction is generally catalyzed by acid, base or fluoride ion. The main steps in sol gel process are shown in (scheme 1.5).[52a] The sol-gel process starts from an homogenous solution of precursor in a solvent which leads to the formation of oligomers, polymers, colloid and from colloid gel is formed. Finally the xerogel is obtained by the elimination of solvent by a drying step. The sol-gel process for silica precursor is tetraethoxysilane. Most of the hybrid organic–inorganic materials are prepared through this route. Changing any one of these steps during its formation can change the morphology of these materials. In the case of silica the size of the container can have influence on the final properties of the materials. In material science these types of gels are described as unstable solids. On the other hand, because of the high sensitivity towards the experimental conditions, it is possible to achieve very different texture by simple modifications of the kinetic parameters like temperature, pressure, concentration, solvent, catalyst, nature of leaving group etc.

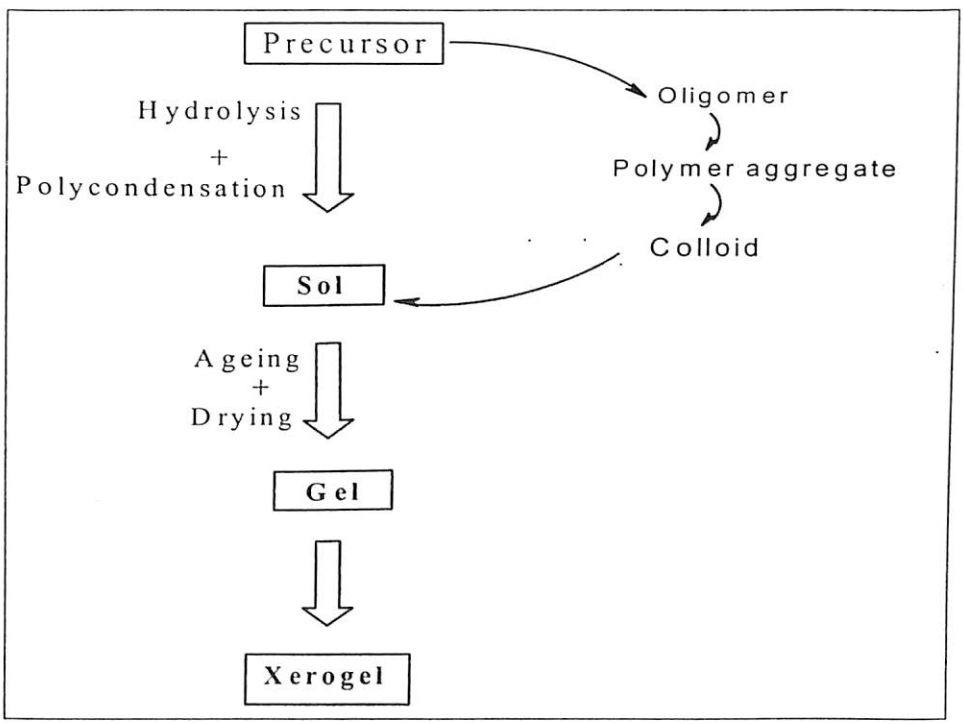

Scheme 1.5

In contrast to the hydrolytic route, there are very few reports to date on non hydrolytic route to prepare organic inorganic hybrids.[53a] Non hydrolytic sol-gel method has been developed in recent years as an alternative to the hydrolytic route.[53, 54] Very recently the synthesis of inorganic oxides *via* non-hydrolytic sol-gel routes is reported.[54] This involves the reaction of a metal halide with an oxygen donor such as an alkoxide, ether, alcohol etc. under non-aqueous conditions as shown in scheme 1.6.

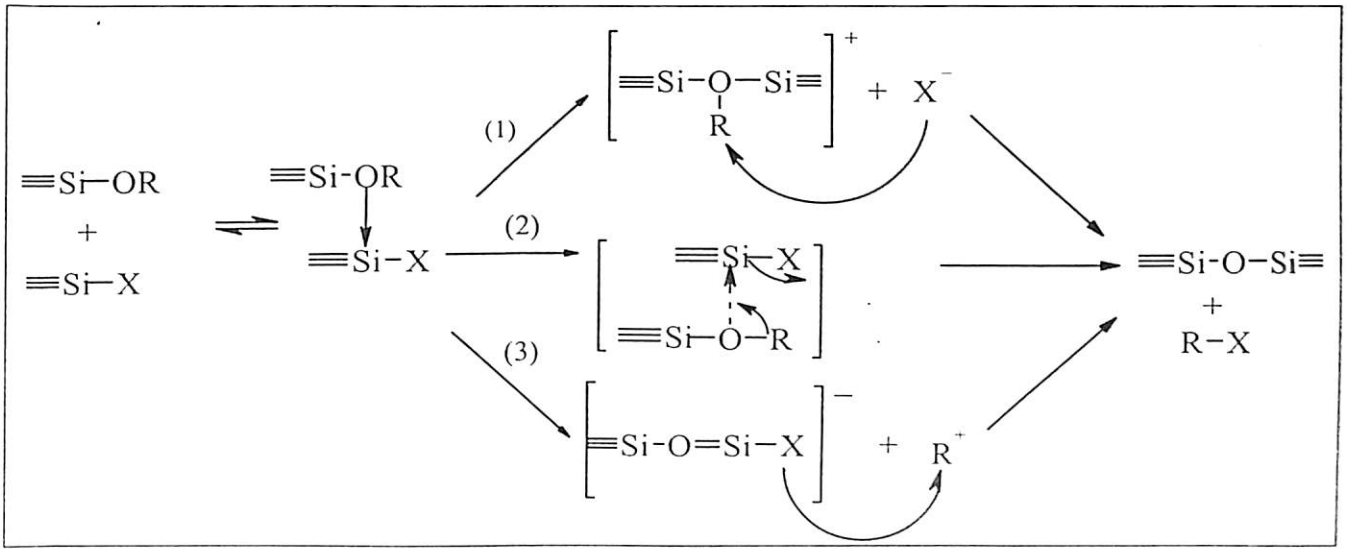

Scheme 1.6

Both the methods have their own merits some of the comparisons of the hydrolytic and non-hydrolytic sol-gel routes are given in table 1.2

Table 1.2

Hydrolytic	Non-hydrolytic
Facile, low-temperature process	Facile, low-temperature process
Homogenizing solvent used	Potentially solvent free.
Good for ionic and O-containing species	Potential problem of O-containing species
Limited compatibility of hydrophobic species	No problem with hydrophobic species
Well established	New technology, good for water sensitive species

1.5 (v) Ladder siloxane

The ladder-type polysilsesquioxane[55-57] has the general formula $(RSiO_{1.5})_n$. The *cis*-1,3,5,7-cyclotetrasiloxanetetraol is used as a versatile precursor for the synthesis of pentacyclic ladder siloxane.[58] Such synthesis of pentacyclic ladder siloxane (**1.XLVIII**) proceeds through three key steps, silylation of silanol followed by chlorodephenylation, hydrolysis and silylation again scheme 1.7

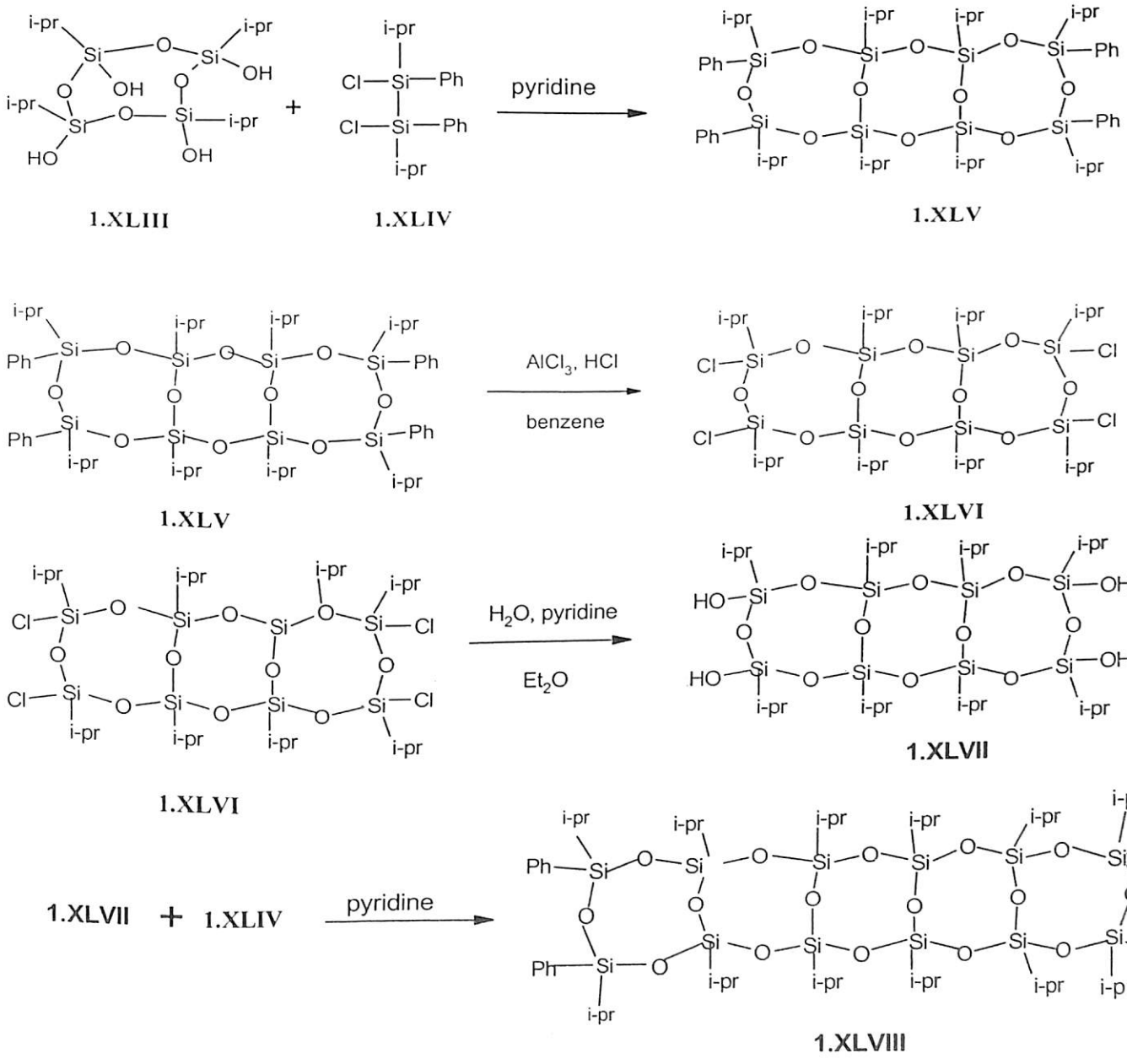

Scheme 1.7

1.5 (vi) Cyclic siloxane

Cyclic siloxanes constitute an important class of silicone precursor. The most practical method for the preparing high molecular weight polysiloxane is the ring opening polymerization of cyclic monomers.[59] The polymerization of hexamethyl cyclotrisiloxane leads to higher molecular weight polymers with low polydispersity. The cyclic dimethylsiloxanes are usually made by the hydrolysis of dichlorodimethylsilane (scheme 1.8). [60] The formation of cyclic siloxane is generally accompanied by substantial amounts of linear siloxane. The formation of linear siloxanes can be suppressed by the use of organic co-solvent for hydrolysis.[59] The reaction between dimethylsulfoxide and dimethyldichlorosilane leads to the formation of cyclic siloxane as the major product and linear siloxane are not formed[60]

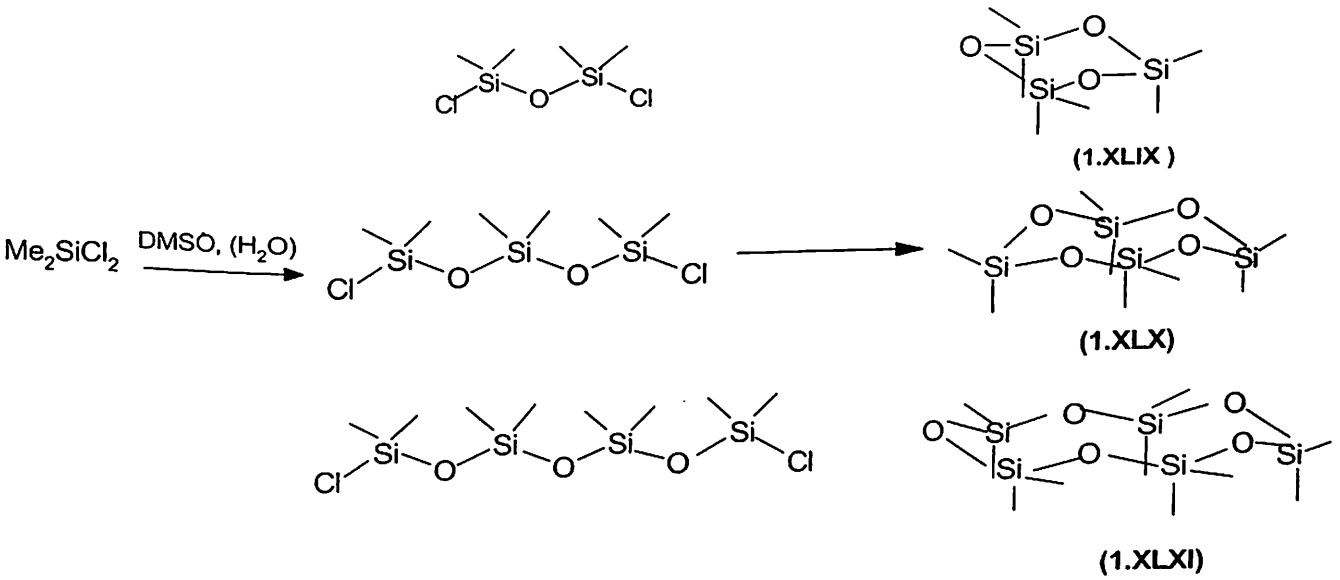

Scheme 1.8

1.6 Common reactions of hydrosilane

Hydrosilanes are important starting material for the preparation of many oragano silicon compounds.[61,62] Synthesis of silicon-silicon and silicon-heteroatom from SiH

functional compounds has lot of advantages over the synthesis of similar type [illegible]ds from the other Si-functional compound.

The pursuit of clean, straightforward alternatives to wurtz coupling reactions for the synthesis of polysilanes has focused attention on dehydrocoupling reactions of silane catalysed by transition metals.[63, 64] Dehydrogenative coupling of hydrosilanes result in the formation of silicon-silicon[65] and SiX[66] bond (X O, N, S, C etc.) scheme 1.9. The transition metal catalyzed addition of hydrosilanes to multiple bonds is generally referred to as hydrosilylation, is a well known process in organo silicon chemistry.[62] A major issue in using hydrosilanes as starting reagent to produce Si-hetero atom bonds is to find out the right catalyst for a desired transformation.

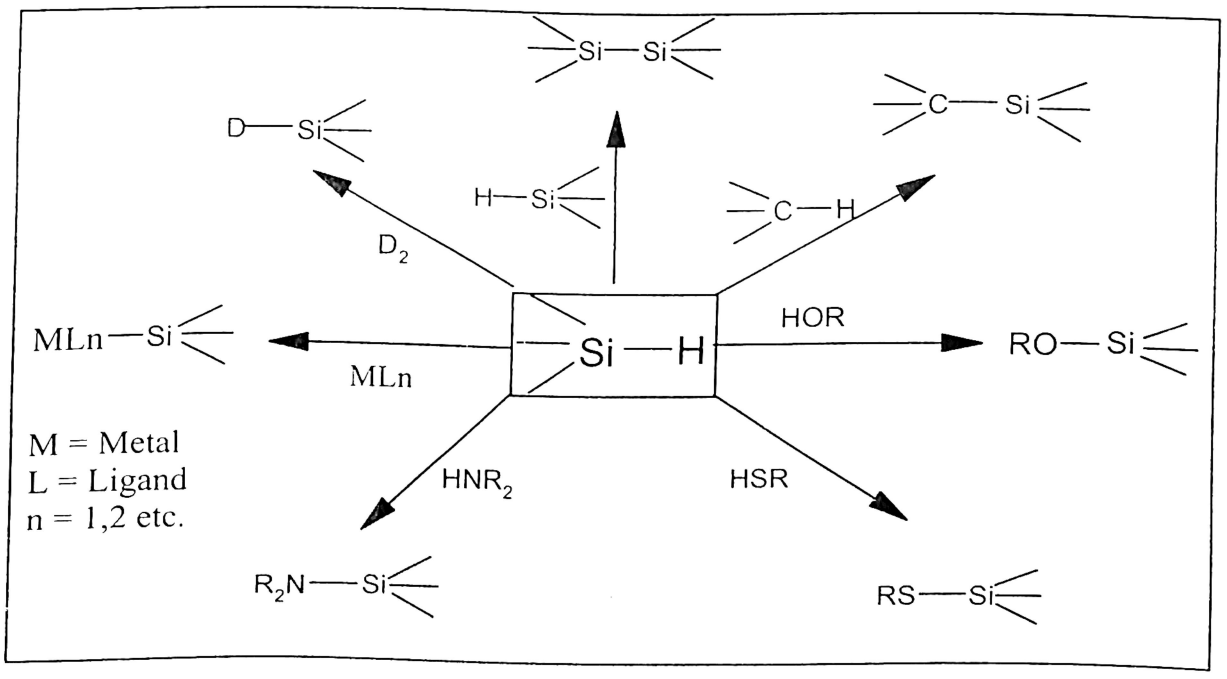

Scheme 1.9

The group-4 metallocene derivatives are considered the most active catalysts for dehydrocoupling; they are capable of producing oligomers and sometimes polymers from primary silanes. Catalyst derived from late transition metal complexes of Pt, Rh, Pd, Cu etc[66-68]produces silicon-silicon and Si-heteroatom bonds.[65, 69] Rearrangement reactions are commonly observed during these reactions.[70] Semi-labile groups such as SiH, $SiSiR_3$ and

SiPh are more reactive for redistribution than alkyl groups, but less reactive [illegible]s, alkoxide etc. One of the substrate that undergoes facile rearrangement is phenylsilane and it gives diphenysilane, triphenylsilane etc as shown in equation 1.29. Transition metal catalyzed redistribution or rearrangement between silicon atoms generally proceeds by silylene transfer mechanism[71] scheme 1.10

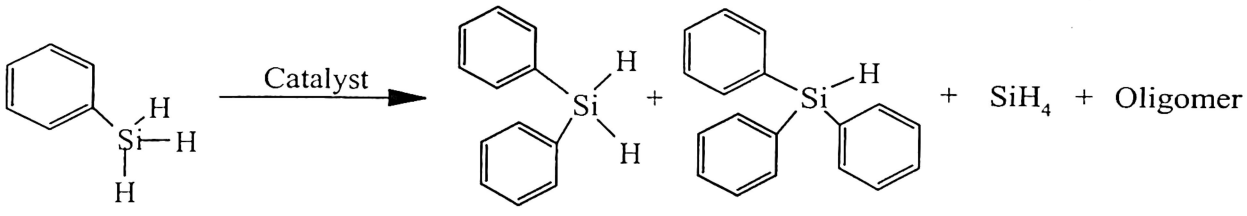

Equation 1.29

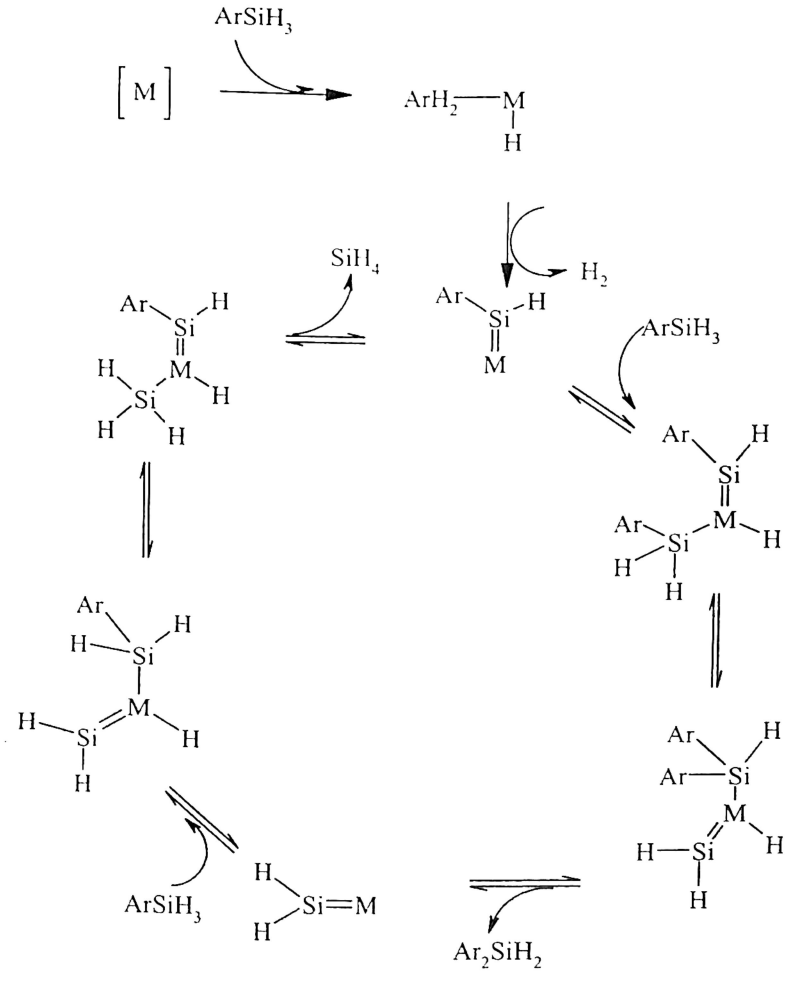

Where M = Ruthenium

Scheme 1.10

The making and breaking of SiX bonds in the co-ordination sphere n metals is a valuable preparative tool for the transformations of the organosilicon compounds. Such processes generally occur due to oxidative addition followed by reductive elimination. Oxidative addition is more likely for metal in low oxidation states like Pd(0), Rh(I), Ni(0) etc.[72-75] The oxidative addition of alkylsilanes to transition metal complexes has been studied throughly.[76] These reactions also play important role in hydrosilylation of olefins and serve as important model for analogous CH activation. The common feature of these reactions is that at some point during the catalytic cycle the silicon compounds interacts with the metal and MSi bond is formed.[72-77] The reverse reaction, often leads the formation of new SiX [1] bond by the cleavage of SiM bond.[72-77] The hydrosilylation generally follows oxidative addition and reductive elimination and the different intermediates involved are shown in scheme 1.11

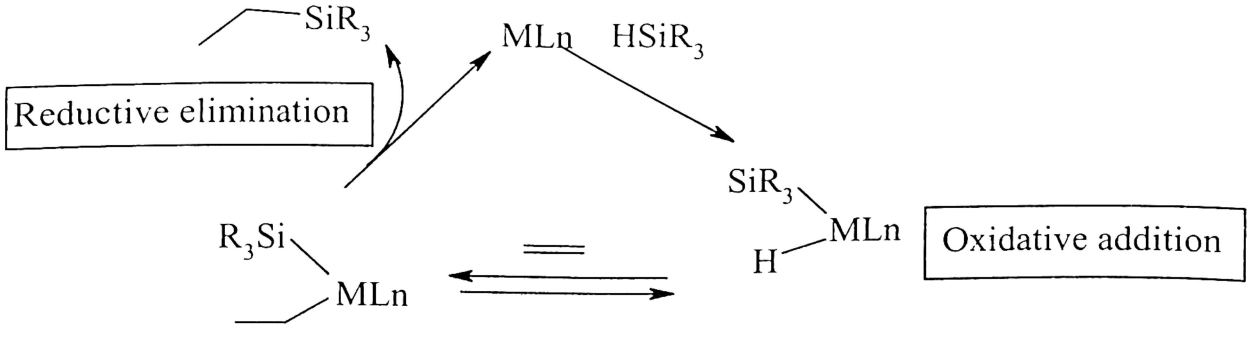

Where, M = Transition metal like Rh, Pd, Ni etc

L = Ligand

n = 0,1, 2 etc.

Scheme 1.11

However, the dehydrocoupling reaction of hydrosilanes by early transition metal catalyst involves σ-bond metathesis reaction.[78] The σ-bond metathesis is a concerted process in which σ –bonds are broken and formed in a four-center transition state[79] the mechanism

(scheme 1.12) suggests a coordinatively unsaturated hydride complex as the active species and the reaction scheme is based simply on the two steps. The first step involves the dehydrometalation of silanes with a metal hydride and second step involves coupling of metal silyl complex with a hydrosilanes to produce Si-Si bond. This step regenerates of active hydride species for further reaction. The most active catalyst precursors are therefore hydride complexes or complexes that can be rapidly converted to hydrides under the polymerization condition (scheme 1.12). The zirconocene complexes having a composition $(CpC^{*}pZrH_2)_2$ are very active catalyst for such reactions. Scandium, lanthanide, and actinide complexes are also active catalyst for σ bond metathesis.[79]

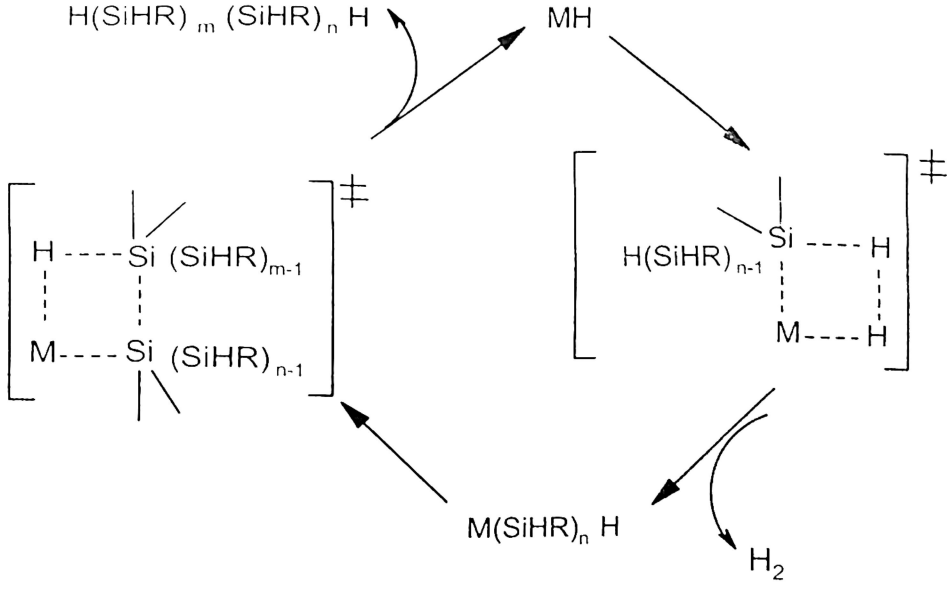

Scheme 1.12

1.7 Siloxane as a ligand and their role in supported catalyst

Recent interest in the development of environmentally benign synthesis has evoked interest in developing polymer bound metal catalyst and reagents for organic synthesis that maintain high activity and selectivity. Due to the superior mechanical and thermal properties compared to organic polymer support, inorganic supports, such as clay, zeolite or silicagel

are ideal candidates for several-supported catalysts.[80] Supported reagents are generally obtained by the introduction of a reagent into an inert, porous inorganic support.[81]

The main advantage of using silica as supported catalysts over organic polymer supported analogue are due to better availability of the active sites. The binding of chiral ligand on the silica occurs on the surface and therefore makes it easier for the reactants to interact with the chiral ligands, while the chiral ligand may be encapsulated in the polymer matrix in the case of an organic polymer supported catalyst. There are numerous potential advantages of supported reagent over conventional reagent; some of the important advantages are as follows

(i) Good dispersion of the active sites can lead to the significant improvement in reactivity.

(ii) Solids are generally easier and safer to handle than liquid or gaseous reagent.

(iii) The supported reagent is easy to remove from the final reaction mixture (filtration) hence minimizing cross contamination between inorganic and organic compounds.

The major disadvantages of the supported reagents are

(iv) The trapping of the undelivered organic molecules in the pores of supported reagent.

(v) The difficulty in ensuring good mixing of a solid-liquid or solid-liquid-gas mixture.

(vi) Leaching of active components from the support into solution.

For supported reagent, are used as model compound of silica. The silsesquioxane containing SiOH groups, having partially condensed structures can be complexed with catalytically active metal center. Metal containing silsesquioxane are extremely used for alkene polymerization,[83] alkene metathesis as well as active catalyst for alkene epoxidation.[84] The incompletely condensed silsesquioxane trisilanol has recently been reported as precursor for the soluble, titanium model compound, which is an active catalyst for the epoxidation of

alkenes.[90] The first titanium silsesquioxane known for its catalytic activity in epoxidation reactions is $(C_6H_{11})_7Si_7O_{12}Ti(\eta^5\text{-}C_5H_5)$.[85] This stable titinium complex was found to effectively and selectively catalyze alkene epoxidations when reacted with olefin in the presence tertiarybutylhydroperoxide. Similar tridentate ligated silsesquioxane titanium complexes with general formula $[TiR\{(R')_7Si_7O_{12}\}]$ (R = alkyl, cycloalkyl, alkoxy, aryloxy, siloxy; R′ = cyclopentyl, cyclohexyl, cycloheptyl) are also synthesized and are found to be active epoxidation catalyst.

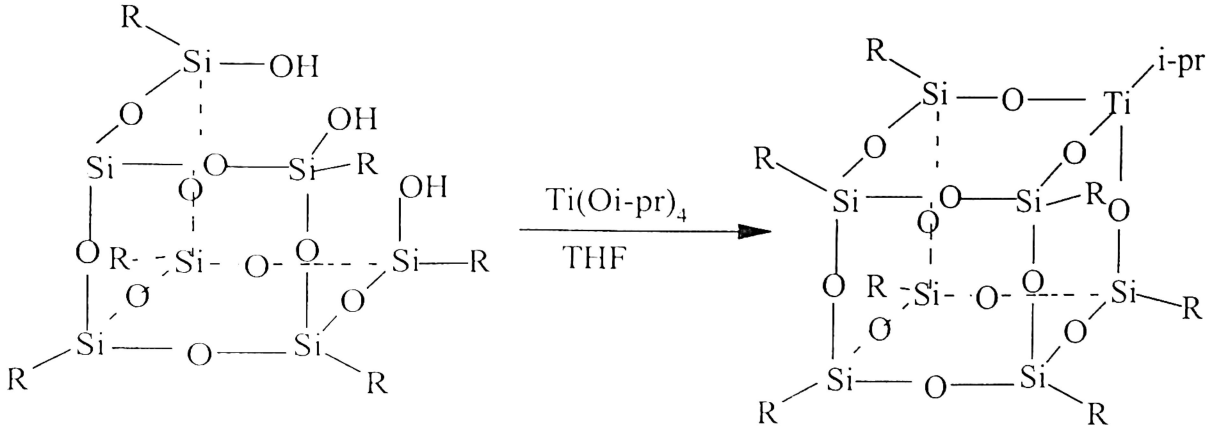

Equation 1.30

I. 8 Silicon in biological environment

Higher animals require silicon for their overall growth and bone mineralisation process.[86-87] Chicken deprived of silicon in their diet exhibits significantly poorer growth performance than those with normal quantities of silicon. Silicon compounds in some form also has adverse effect on living beings, for example inhalation of small silica particles lead to the diseases like silicosis, tuberculosis and lung cancer.

Bioactive organic compounds having OH, NH group can be readily protected by silyl groups. This has effect of hydrophilic to hydrophobic molecules. For certain drugs, one of the limiting parameters for efficacy is the degree to which they can cross liphophilic

membranes. Silylated derivatives have preferential absorption in liphophilic membranes over the corresponding OH, NH precursors. Sometimes the drug arrives at the active site after deprotection; in this case effect of silylation is simply to facilitate the delivery of the native drug is called pro-drug,[88] example of such prodrug is **1.XLXII**

Some simple C-silylated derivatives of drugs are also known. They rarely hydrolyzed at an appreciable rate under physiological conditions. Thus, they don't behave as pro-drug; they are bioactive compounds in their own way. Many potential sila-drugs have been investigated. Bioactivities of some of the sila–drugs are exemplified by the compounds **1.XLIXII – 1.XLXVII**. Compounds with structure shown as **1.XLXIII** find application as pain control (better than aspirin) and compounds **1.XLXIV** and **1.XLXV** as antitumor drugs.

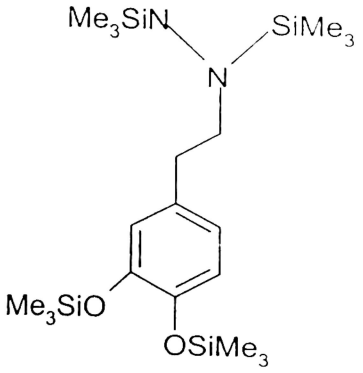

1. XLXII

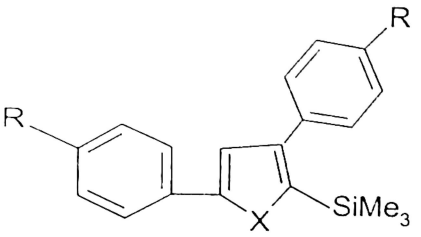

Where, X = O, R = F
X = S, R = OMe

1. XLXIII

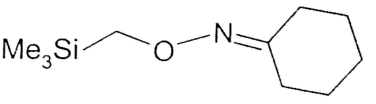

1. XLXIV

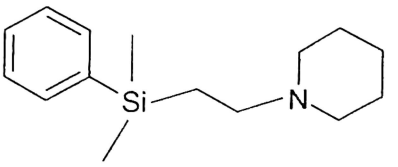

1. XLXV

I.9 Scope of the work

Siloxane additives are highly effective internal and external lubricants and have a number of significant processing advantages for surface improvements. Polydimethylsiloxane finds applications in silicon industry[89, 90] as elastomer, lubricating oil, heat resistant tiles etc. Polysiloxanes offer a wide spectrum of interesting opto-electronic properties due to polar silicon-oxygen backbone that are not generally shown by common

organic polymers.[91] Some of the outstanding properties of siloxanes are high thermal stability, flexibility at low temperature and have low dielectric constant.

Low permittivity of silicones assist them to use as a wire coatings, motor insulators, transformers etc.[92]Some siloxanes possess exceptional hydrophobicity. The resistance to liquid water has made such siloxane for moisture barriers. Chemical inertness and biological safety of poly-dimethylsiloxanes along with their spreading and lubricating properties have established them to be useful components in skin care formulation. Siloxane also finds medical application, like drug delivery system, artificial skin, and contact lenses because of its high permeability to gases.[93-94] Siloxane filled breast forms are simply the best and most realistic that science and technology has yet been able to develop. In appearance, texture, and movement they are simply the last word in mimicking the natural female breasts. Siloxanes having amino-functional group finds application in hair care products. Functionalized siloxanes also find applications in textile industry.

Siloxane with porous structure find application in selective adsorption or catalysis.[95] The ease of cleavage as well as formation of a silicon-oxygen bond makes them useful for alcohol protection.[96] The inorganic hybrid materials and nano-composites having silicon-oxygen bond are projected to have great potential as advance material. [51]

Poly-phenyl silsesquioxane is used as coating materials in electronics and optical devices. Among these, the application in photo resist property of silsesquioxane is outstanding [97a,b], they are also used as a protective coating films for semiconductor devices,[97c] magnetic recording media, and optical fiber coatings.[56d] Polymethyl silsesquioxane is used as a binder for ceramics and used as additive to materials such as cosmetics.[97e] Bridge polysilsesquioxane has been widely used for surface modification and as coating materials.[98] Incorporation of dyes into the sol gel matrix is used for wave guide, lasers, sensors, light

emitting diodes and nonlinear optical materials.[2] The combination of high surface area with chemical functionality makes them potential candidates for packing materials for HPLC column[99], catalyst support, [100] and adsorbent materials.[101]

With these backgrounds the development of new synthetic reagents for selective transformation in silicon oxygen bond would provide ways for new material design. Environmentally benign catalyst system for silicon-oxygen bond forming reactions is a central point that needs further study. The utility of the hybrid material capable of providing *nano* confinement as well as the design of surface modified *nano*-structured material needs a clear attention. New catalyst from copper, palladium, gold and rhodium for SiH bond activation can serve the purpose of nano-confinement to the metallic states. For this purpose the structurally simple air stable catalysts derived from nitrogen donor ligand could be prime interest as they may provide way for selective product formation. Keeping in view of material design the identification of active catalyst for silane for silicon-silicon or silicon-hetero atom bond formation needs clear attention. With the last objective in mind, in this thesis the catalytic aspect of Pd, Au, Rh and copper complexes are investigated.

Chapter 2

Synthesis and characterisation of few tetrachlorocuprate complexes

2.1 Background

A late transition metal complex may have several properties that help it to act as a catalyst. Some of such properties are: metal should have variable oxidation states that are interconvertible by appropriate reagent; the ligand/s in the complex should be labile enough to make room for a substrate metal interaction; the metal center should have possibility to expand /change its co-ordination number as well as co-ordination geometry. The halo complexes copper(II) have plasticity of the metal coordination sphere that leads to great variety of crystalline architectures with different coordination numbers, geometries and nuclearities [102-104]. This makes copper (II) systems excellent candidates for the study of co-relation of structure and reactivity[105-107] that could be responsible for an organic transformation. The flexible co-ordination geometry of the copper (II) and the existence of both coordinated and semicordinated ligands results in number of electronic structures and allows them to exist in a wide array. The co-ordination numbers may vary from four to six (with typically distorted geometries). Semi coordinate bond formation between oligomers requires a relative displacement of neighboring oligomers, thus forming stacks. The structural properties of tetrahalocuprate complexes are of also interest because of their wide variety of stereo chemical features and unexpected oligomeric species.[108] Several quasi-planar bridged $Cu_nX_{2n}L_2$ (X= halide, L= halide or neutral ligand) complexes of copper are known. In this class of complexes the building block is the monomeric CuX_2L_2 species having square planer geometry. The higher oligomers ($n \geq 2$) are quasi-planar chains of edge

sharing having a core of halo-bridged CuX_2L_2 . These oligomers frequently aggregate into stacks in which the copper ion complete its co-ordination sphere by forming long, semi co-ordinate bonds to chlorides ions on either one or two neighboring oligomers. The monomeric $[CuCl_{n+2}]^{-n}$ complexes exist as square planar[109], distorted tetrahedral[110], square pyramidal geometry[111]. The square planar $[CuCl_4]^{2-}$ are usually have ammonium cations and are stabilized by hydrogen bonding interactions between the ammonium cation and the chloride.[112] The halogenocuprate chemistry of the type $[CuX_4]^{2-}$ (X= Br, Cl) with inorganic and organo ammonium counter ions[113-114]are common but [HL][CuX_3L] (L = monodentate nitrogen base) are less common[115]. Some planar complexes having $[CuCl_3L]^-$ ions for example (LH)[$CuCl_3(H_2O)$] (LH = 2-aminopyridinium) are reported. Variation of the reaction condition leads to the variation of composition of products in many copper-halo complexes; for example the $(LH)_2$ $[CuCl_4]$ as well as $(LH)_2$ $[Cu_2Cl_6]$ can be

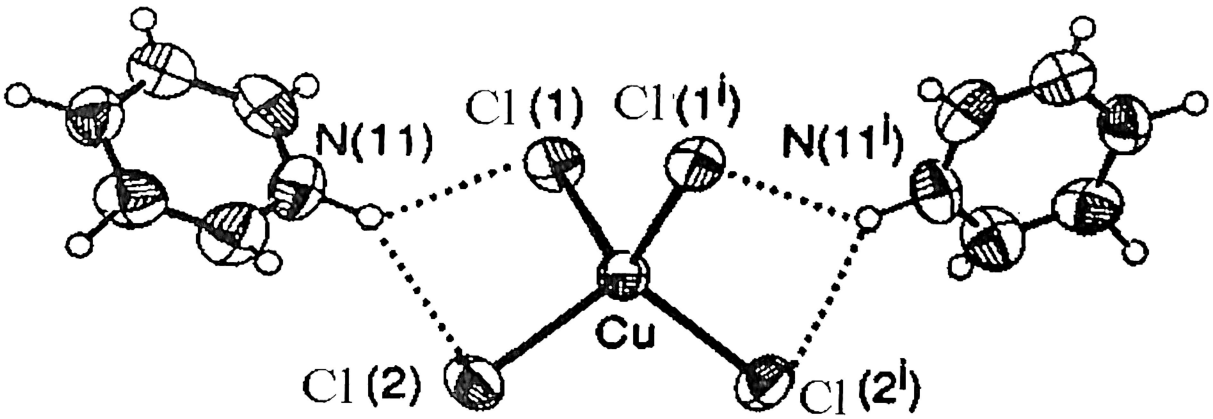

Figure 2.1 the crystal structure of *bis*-pyridinium tetrachlorocuprate complex

prepared with the same reagents but different reaction conditions.[116] While pursuing the present research on identification of tetrachlorocuprate as catalyst and characterization of them the crystal structure of *bis*-pyridinium tetrachlorocuprate is reported by some other researchers[117]. The chemistry of this complex is important due to the fact that the co-ordination ability of pyridine decreases on protonation and the H-bonding ability of the H-N^+

group enables the pyridinium cation to stabilize $[CuCl_4]^{2-}$ layer type structure.[1] The crystal structure of the *bis*-pyridinium tetrachlorocuprate complex is shown in fig1a. In *bis*-pyridinium tetrachlorocuprate (II) the Cu-Cl distances vary between 2.205 Å and 2.265 Å and the *trans*-Cl bond angles vary from 104.5 to 180^0 (i.e. limiting values of tetrahedral and square planar geometry). In *bis*-pyridinium tetrachlorocuprate (1a) there are two sets of non equivalent Cu-Cl bond of which one has 2.233(1)Å slightly shorter than the other Cu-Cl bond, which is 2.251(1) Å. Both these chloride ions take part in the network of the hydrogen bonds, and form a bifurcated bridge to the cationic proton of the pyridinium ion. The crystal structure of compound(1a) is composed of discrete $[CuCl_4^{2-}]$ polyhedra and isolated pyridinium cations (figure 2.1). The copper atom sits on a crystallographic twofold axis.

The Cl-Cu-Cl bond angles in (**1a**) vary between 97.83 and 132^0 showing geometry intermediate between square planar and tetrahedral coordination. The packing coefficient of **1a** (0.695) indicates close packing. Packing appears as separate columns of cations and anions. The cations are oriented so as to minimize electrostatic repulsion between identical charges and simultaneously maximize attraction between opposite ones. The steric demand of the pyridinium cations neighboring to each tetrachlorocuprate (II) anion, their hydrogen bonds and the shielding as a joint effect isolates the tetrachlorocuprate anions in the monomeric form. Since the nearest non covalent Cu-Cu and the shortest Cl-Cl distances are both longer than the sum of the Vander Waal radii, there is no visible interaction between tetrachlorocuprate (II) anions.

The geometry of the analogous tetrabromcuprate compounds is reported as a compressed tetrahedral geometry with two bond angles distinguished from the others (96-104^0) by their high values (123-136^0). These values again show that the geometry of the

tetrabromocuprate complexes is intermediate between the square-planar (D_{4h}) and regular tetrahedral (T_d) geometry.[118]

Different types of species can be formed from a halo-cuprate complex in solid state or solution while performing further reactions (scheme 2.1). The bromo complexes can change its co-ordination by brominating an active site of a cation. For example the complex 2-aminopyridinium(2-amino-5-bromopyridine) tribromocuprate is formed from *bis* (2-aminopyridinium)tetrabromocuprate on irradiation of the later[119]. During the synthesis of $[PyH]_2[CuCl_4]$, a polymeric $[CuCl_2(py)]_n$ is also formed.[117] By decreasing the amount of HCl in the course of the synthesis gives more amount of polymeric species. Which suggest that there is an equilibrium between these two species exists and the direction of equilibrium determined by the HCl concentration.

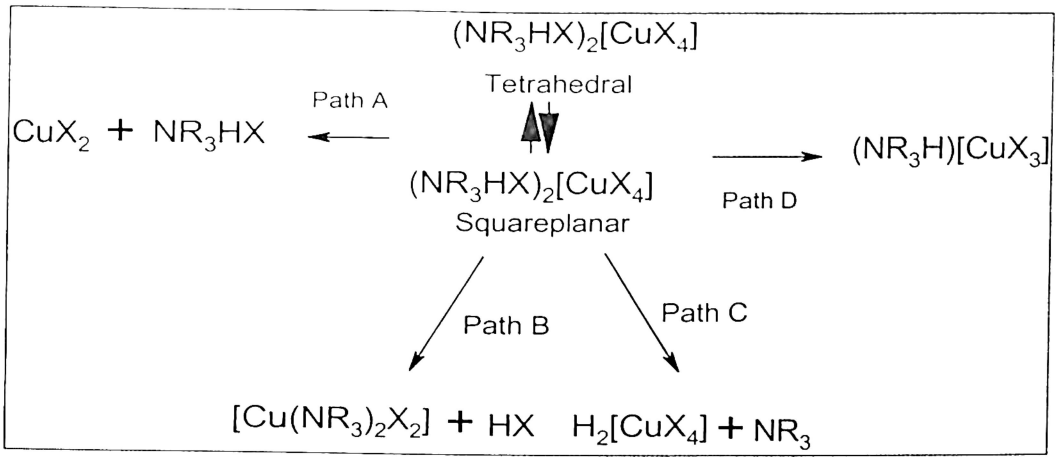

Scheme 2.1

The complex (pyrimidinium)$[CuCl_3(H_2O)]$ on heating leads to the formation of dimeric (pyrimidinium)$_2[Cu_2Cl_6]$ complex[120]. This thermal reaction shows two-endothermic transition. At the first transition temperature, the copper-water bonds break and the water molecules are free to move through the channels so formed. At the second transition temperature the water gets superheated and is eliminated from the crystal. This clears the channels, and monoprotonated cations are able to co-ordinate to the copper ion to generate a

new structure. The foregoing discussion clearly suggests that halo complexes I) may have satisfy different structures and satisfy some prerequisites to act as catalysts for organic transformations.

2.1.1 Synthesis and characterization of tetrachlorocuprate complexes

To look for the suitability of catalytic activity tetrachlorocuprate complexes five copper complexes were synthesized by a simple synthetic procedure (equation 2.2 a-c). The complexes (1a-d) were prepared by common synthetic procedure in which methanolic cupric chloride dihydrate solution was first acidified to generate the tetrachlorocuprate. Addition of the corresponding amine gave the required complex (for details refer to experimental section). Whereas, the complex (1e) was obtained from the reaction of anhydrous cupric chloride with 3,5-dimethylpyrazole.

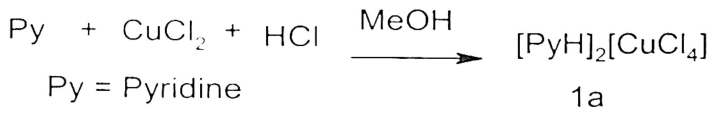

Equation 2.2a

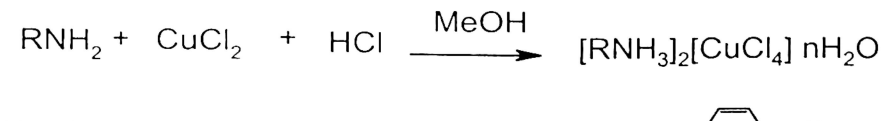

Equation 2.2b

For 1b, n = 0 ; 1c, n = 1; 1d, n= 3

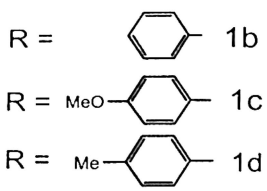

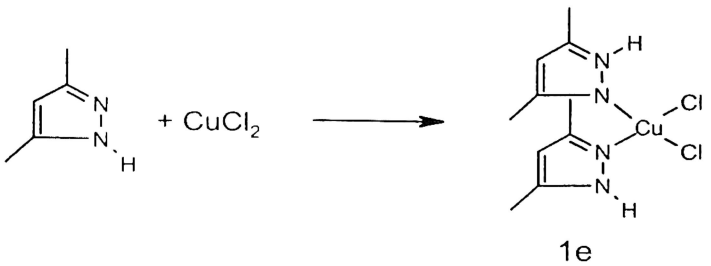

1e

Equation 2.2c

The compositions of the complexes were ascertained from the elemental analysis as well as by estimating the copper and chloride content. The *bis*-anilinium tetrachlorocuprate and *bis*-pyridinium tetrachlorocuprate complexes were found to be devoid of water of crystallization whereas the *bis*-*p*-methoxyanilinium tetrachlorocuprate and *bis*-*p*-methylanilinium tetrachlorocuprate complexes had one and three molecules of water of crystallization respectively.

The IR spectra of *bis*-pyridinium tetrachlorocuprate show the characteristics $\nu_{C=C}$ and $\nu_{C=N}$ band of the pyridinium ion appear at 1600 cm^{-1}, 1525 cm^{-1} respectively in the complex. The N-H stretching vibrations of the complex appear at 2850cm^{-1} in the complex whereas the free pyridinium shows ν_{NH} stretching at 3200cm^{-1}. The *bis*-anilinium tetrachlorocuprate has characteristic N-H stretching vibrations at 3018 cm^{-1} in contrast to aniline NH-vibration appearing at 3360cm^{-1}. The N-H bending vibrations of $-^{+}NH_3$ group of the salts (1600- 1575 cm^{-1}) are also present in the complex. Similarly the IR spectrum of *bis*-*p*-methylanilinium tetrachlorocuprate shows a very broad absorption band at 3000 cm^{-1} in which both the OH and NH stretching are merged; whereas, *bis*-*p*-methoxy anilinium tetrachlorocuprate shows very broad and strong absorption peaks at 3456cm^{-1} and 3045cm^{-1} due to O-H and NH stretching arising from the water of crystallization and anilinium cation.

The absorption maximum in the UV-visible spectra of acetonitrile solution of the complexes are listed in the table 2.1. Each of these complexes 1a-1d shows three absorbance. One of the absorption occurs in the visible region and the other two in the UV region. The absorption in the visible region in each case is assigned to the d-d transition and occurs due to the transition from ^{2}E to ^{2}T state. The absorption in the region 300 –350 nm are assigned to ligand to metal charge transfer transition. There is another absorption in the region of 240-280 nm due to the π- π^*-transition from the counterion. The extinction coefficients of the

absorptions of *bis*-*p*-methoxyanilinium tetrachlorocuprate and *bis*-*p*-methylanilinium tetrachlorocuprate complexes are higher than the values for *bis*-anilinium tetrachlorocuprate and *bis*-pyridinium tetrachlorocuprate, suggesting in the former two complexes distortion from the tetrahedral geometry is more than the later two. The UV and visible spectrum of *bis*-anilinium tetrachlorocuprate complex in acetonitrile is shown separately in figure 2.2.

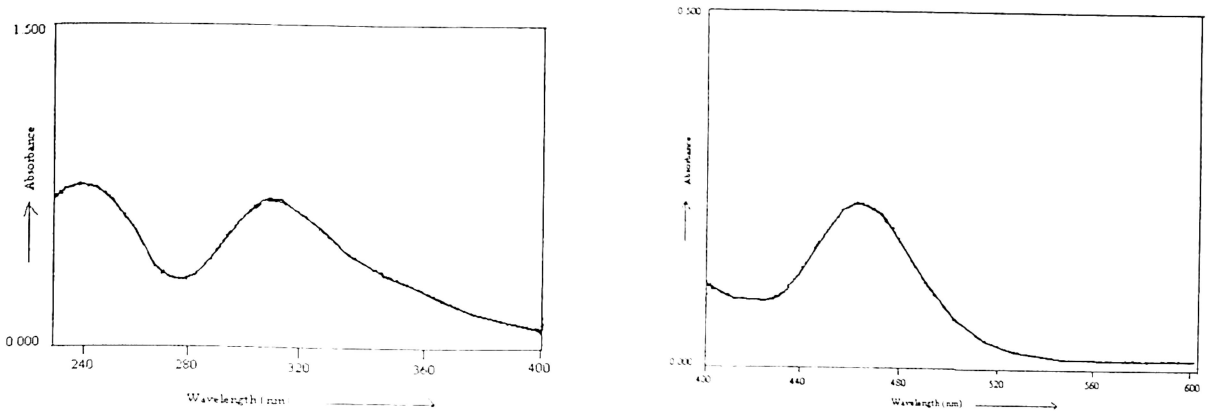

Figure 2.2 UV and Visible spectra of *bis*-anilinium tetrachlorocuprate in acetonitrile (3.3×10^{-3} mmol in 3ml acetonitrile)

Table 2.1. The UV-visible absorptions of tetrachlocuprate complexes

Complex	π- π* transition (extinction co-efficient in Litre $mol^{-1}cm^{-1}$)	LMCT (extinction co-efficient Litre $mol^{-1}cm^{-1}$)	d-d transition (extinction co-efficient Litre mol^{-1} cm^{-1})
1a	242 nm (700)	313 nm (728)	474 nm (650)
1b	246 nm (217)	309 nm (644)	461 nm (217)
1c	274 nm (1700)	311 nm (1498)	461 nm (1262)
1d	250 nm (2446)	308 nm (2282)	458 nm (803)

2.1.2 Solvatochromicity of the complexes

The UV-visible spectrum of the tetrachlorocopper(II) complexes are solvent dependant. For example $[PyH]_2[CuCl_4]$ in acetonitrile show an absorption at 474 nm which on addition of methanol shifts to 437 nm. Whereas the *bis-p*-methoxyanilinium tetrachlorocuprate monohydrate (1c), shows a large change in λ_{max} when the spectra are recorded in different sovents such as acetonitrile and methanol. This makes them suitable candidate for the study of solvatochromicity.

An acetonitrile solution of *p*-methoxyanilinium tetrachlorocuprate monohydrate has an absorption maximum at 460 nm (ε = 1262 cm^{-1}) in acetonitrile whereas the complex in methanol has absorption at 570 nm. The change that takes place on addition of each aliquot of methanol to an acetonitrile solution of *bis-p*-methoxyanilinium tetrachlorocuprate monohydrate is shown in figure 2.3.

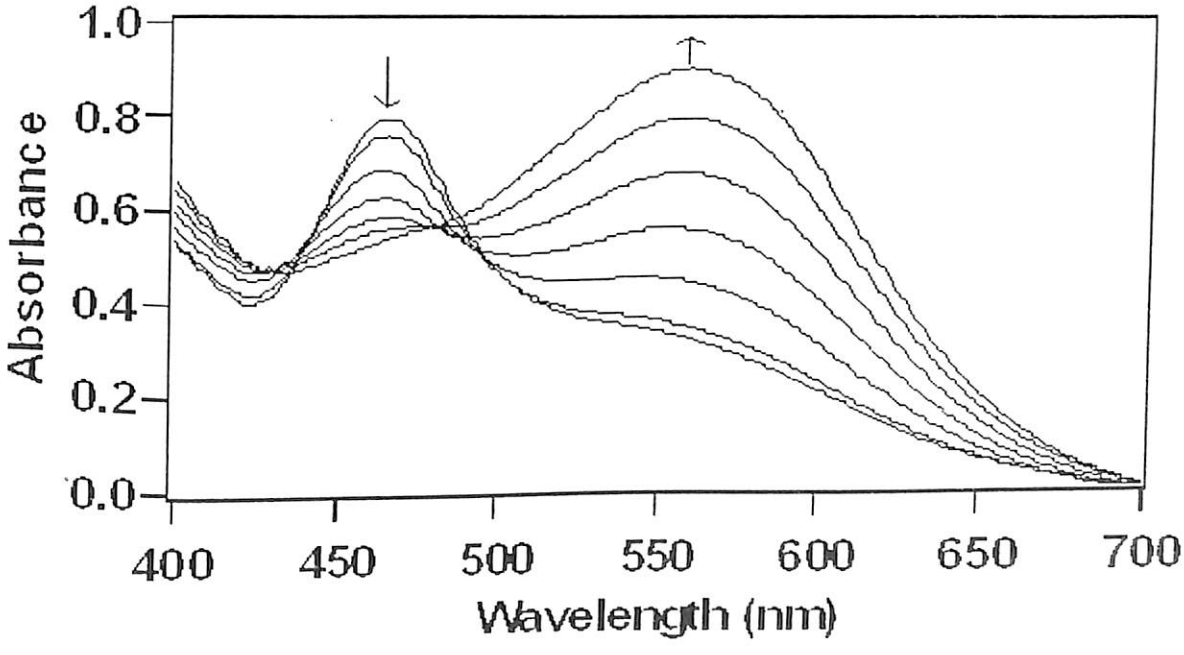

Figure 2.3 The change in the visible spectra of (1c) (0.2 mmol) in acetonitrile (2 ml) on addition of aliquots of methanol (25 µl, 0.64 mmol)

Once the optical absorption of the compound changes from 460 to addition of methanol to acetonitrile solution of *p*-methoxy anilinium tetrachlorocuprate, it can not be brought back to the original state having absorption at 460 nm by adding acetonitrile. But addition of hydrochloric acid solution leads to regeneration of the absorption at 460 nm and while doing this; the absorption at 570nm is lost. However due to effect of dilution the intensity of absorption becomes lower than the original value (fig 2.4). After restoration of the 460nm absorption, the absorption at 570nm can be regained if methanol is added. Since the methanol allows the growth of absorption at 570 nm and addition of chloride ion pushes it to the state having absorption at 460 nm a dissociative path should be responsible for such phenomenon. It is thus proposed that addition of methanol allows the halogen to dissociate from the co-ordination sphere. This process would result in a $[Cu_2Cl_6]^{2-}$ complex. However, the literature reports that the dimeric $[CuCl_3]^-$ species can be formed from the tetrahalocuprates[120]. Since a halogen exchange process takes place during the solvatochromic shift, it can be pushed back and forth by adding appropriate reagent. Thus the sovatochromicity of the *bis-p*-methoxy tetrachlorocuprate complex is due to structural interconversion between monomeric and dimeric structure, which can be represented by the equilibrium (equation 2.3)

$$[p\text{-}MeOC_6H_4NH_3]_2[CuCl_4] \underset{HCl}{\overset{MeOH}{\rightleftharpoons}} [p\text{-}MeOC_6H_4NH_3]Cl + [p\text{-}MeOC_6H_4NH_3]_2[Cu_2Cl_6]$$

Equation 2.3

The clear change in color on addition of methanol to the acetonitrile solution of *bis-p*-methoxy tetrachlorocuprate and its interconversion to another species makes it a potential candidate for recognizing alcoholic solutions. So various alcohols, such as methanol, ethanol and *iso*-propanol were used for such studies. It is found that similar effect on the change of

absorption in each case is observed. Bulky hydroxy compounds such as calixar as weakly co-ordinating hydroxy compounds such as phenols are not capable of changing the visible-spectra of the complex **1c.**

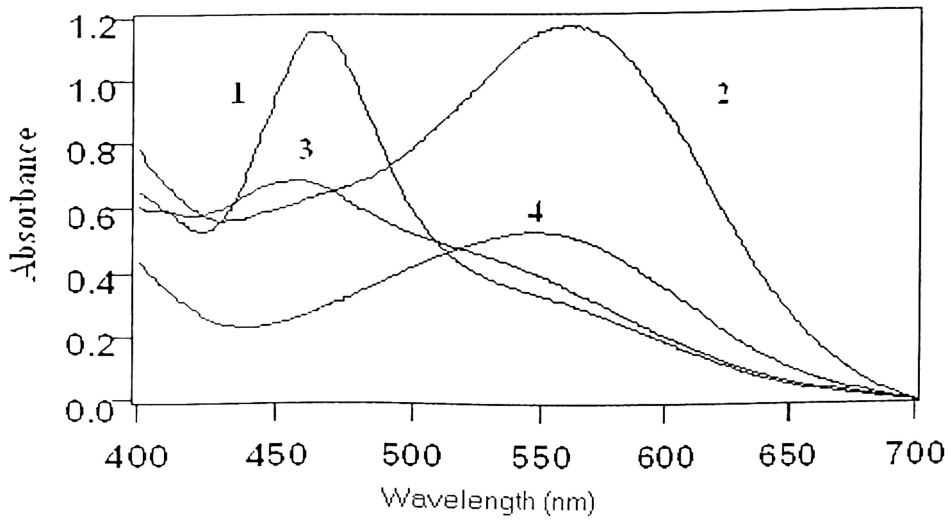

Figure 2.4 The visible spectrum of (1c) 0.25 mmol) in acetonitrile (2 ml); (2) on addition of methanol (0.2 ml, 5.3 mmol); (3) on addition of HCl (0.32 mmol); (4) on addition of methanol (0. 8ml, 21.2 mmol)

The IR spectra of the *bis-p*-methoxyanilinium tetrachlorocuprate sample before dissolving in methanol and after dissolving in methanol are different. In the case of freshly prepared sample have strong broad IR absorptions at 3045cm^{-1} and 3456cm^{-1} whereas the sample on dissolving in methanol the absorption peak of the sample appears as single absorption at 2900cm^{-1}. In addition to this there is a clear difference in the absorptions 810cm^{-1}, this absorption gives rise to two absorptions at 810 and 830cm^{-1} after recrystallisation from methanol.

2.1.3 The electrochemical study

The redox behaviors of tetrachlorocuprate complexes were studied by cyclic voltammetry using three-electrode system comprising of Ag/AgCl reference electrode, two

platinum electrodes as working and auxiliary electrode in acetonitrile. All complexes (1c and 1d) display a quasi-reversible voltammogram in the region 400- 650 mV with different ΔE_p values and i_{pc}/i_{pa} ratio from 0.92 to 1.34 at a scan rate 100 mV/s. The quasi-reversible cycle is independent of the direction of the scan. The voltammetric response is assignable to the Cu (II)/Cu (I) couple as such processes are known in the literature[121]. Selected voltammetric data for the tetra chlorocuprate complexes are given in table 2.2 and a representative voltammograms is shown in figure 2.5. The electrode potentials are calibrated to the Fe^{2+}/ Fe^{3+} couple of ferrocene.

Table 2.2#: The electrochemical data of the complex 1a- 1d

Complex	E_{pc} (mV)	ΔE_{pa}(mV)	ΔE_{pa} (mV)	i_{pc}/i_{pa}
1a	429	609	180	1.34
1b	519	636	117	1.11
1c	510	627	117	0.92
1d	481	623	142	1.09

All the cyclic voltamograms are obtained from the complexes (0.0127mmol) dissolved in acetonitrile (5ml) using tetrabutylammoniumperchlorate as supporting electrolyte with two platinum as a working and auxiliary electrode and Ag/AgCl as reference electrode. All scan are + ve with scan speed (100mV/sec)

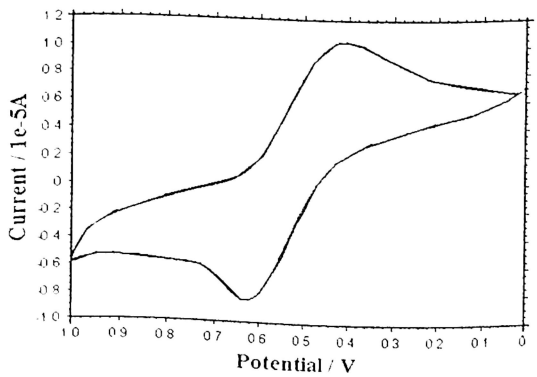

Figure 2.5 Cyclic Voltamogram of $[PyH]_2[CuCl_4]$

The complex 1a has similar redox couple in methanol solvent also but the peak p different in methanol. The methanolic solution of 1a has E_{pc} and E_{pa} at 394 mV and 527 mV. This suggests that the change of coordination is responsible for the shift in the oxidation and reduction potentials. The observation of quasireversible states are due to the fact that a polymeric structure has to be cleaved to generate a favorable tetrahedral co-ordination of copper(I) which implicates that structural change accompanies electron transfer.

This can be explained by a dissociative mechanism, which operates, on changing from one solvent to the other. Different dissociative equilibriums of the complex in solution through ligand exchange phenomenon is shown in scheme 2.2.

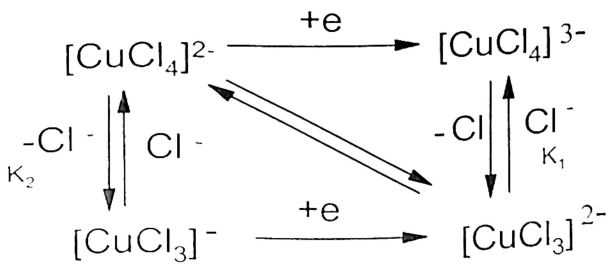

Scheme 2.2

This scheme is based on the assumption that a dissociative path may be followed prior to the reduction or a reduction of the metal center followed by a dissociative path to yield the copper(I) species. Since each of these paths involve equilibrium processes and associated with one electron transfer the equilibrium the difference in the shift in the positions of oxidation and the reduction peaks are related to the two equilibrium constants. Thus, from Nernst equation and with the formulations[122] in scheme 2.2 the relative value of K_1/K_2, $E_{red} - E_{ox} = 0.059 \log (K_1/K_2)$. The value of K_1/K_2 is calculated for the *bis*-pyridinium copper (II) complex by comparing the oxidation peak positions in two different solvents namely methanol and acetonitrile. This is done with an assumption that the copper (II) complex in methanol goes to a tri-coordinated environment, but it is in tetra co-coordinated environment

in acetonitrile. Tri-chloro copper (II) complexes are well documented in litera

K_1/K_2 is found to be 3.1 X 10^{-4} which shows that the ligand dissociation followed by reduction is the favorable process. This also makes an added advantage to the complex for co-ordination unsaturation prior to the oxidation process of a substrate to get involved in a catalytic reaction.

2.1.4 ESR spectra

Copper(II) is a d^9 system has S= ½, is ESR active. The nuclear spin quantum number of copper being I= 3/2 interaction of electron spin with nuclear spin results in hyperfine interaction. The X-band ESR spectra of the complexes were recorded at room temperature (figure 2.6). The ESR spectra for the *bis*-pyridinium tetrachlorocuprate shows a narrower isotropic signal when field set at 2500 Gauss, but it becomes more broader when field set at 3200 Gauss with g_{iso}= 2.16, which is due to characteristic flattened tetrahedral geometry of $[CuCl_4]^{2-}$. The lack of anisotropy can be explained either by dynamic Jahn-Teller effect or by strong spin exchange between centers that are randomly distorted by the static Jahn –Teller interactions. The anionic ligand to metal bond causes the ESR absorption to occur higher to DPPH standard. Tetrahedral structure for tetra-bromocuprate is already reported[119] to show isotropic ESR spectra. *Bis*-anilinium tetrachlorocuprate, also shows an isotropic signal at g_{iso}=2.0. But for *bis-p*-methylanilinium tetrachlorocuprate trihydrate and *bis-p*-methoxyanilinium tetrachlorocuprate monohydrate has distorted signal, which indicates that the geometry of the complex is distorted from tetrahedral to square planar. Thus, the counterions have a role on the structure of the complexes that are reflected in the ESR spectra. Since the spectra were recorded at room temperature the hyperfine-coupling is not seen in the spectra.

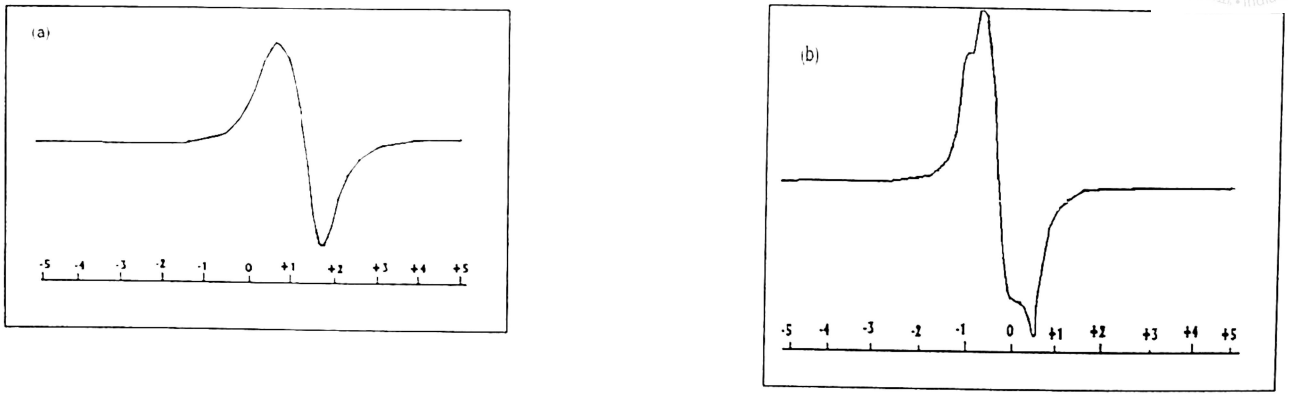

Figure 2.6 X-band powder EPR spectra of *bis*-pyridinium tetrachlorocuprate (a) and X-band EPR spectra of *bis-p*-methyl anilinium tetrachlorocuprate (b)

2.1.5 Magnetic moment

As already mentioned copper (II) is a d^9 system, thus tetrahedral complexes of copper (II) has single unpaired electron and must be paramagnetic. The spin only magnetic moment μ_s for single unpaired electron is given by the expression

$$\mu_s \text{ (in B. M.)} = g\sqrt{s(s+1)} \qquad \text{(Equation 2.4a)}$$

Where s is the absolute value of the spin quantum number and g is the gyro magnetic ratio, whose value is approximately, g = 2. Putting g = 2 and s =1/2 for single electron, spin only magnetic moment comes 1.73 B. M. (for single unpaired electron)

The magnetic moments of simple Cu(II) complexes (Those lacking Cu-Cu interactions) falls in the range 1.75 to 2.20 BM, regardless of stereochemistry of the copper(II) center.[124] The magnetic moments of the tetrachlorocuprate complexes were calculated by measuring χ (magnetic susceptibility) of the complexes and then using *Curie law*, the equation 2.4b

$$\mu = 2.84\sqrt{\chi_M T} \qquad \text{(Equation 2.4b)}$$

Where χ_M = Molar susceptibility, T = Absolute temperature.

The magnetic moments of the tetrachlorocupurate complexes after diamagnetic correction at 25 ^{0}C are listed in the table 2.3. The values show that the complexes are monomeric in nature since these values are well within the range for a single electron.

Table 2.3: Magnetic moment of tetrachlorocuprate complexes at 300K

Tetrachlorocuprate complex	Magnetic moment (BM)
$[PyH]_2[CuCl_4]$	1.78
$[C_6H_5NH_3]_2[CuCl_4]$	1.78
$[p\text{-}CH_3O\text{-}C_6H_4NH_3]_2[CuCl_4].H_2O$	1.79
$[p\text{-}CH_3\text{-}C_6H_4NH_3]_2[CuCl_4].3H_2O$	2.08

2.1.6 Crystal structure of (1e)

The 3,5-dimethylpyrazole (pz) on reaction with $CuCl_2$ in acetone gives a copper complex having composition $(pz)_2CuCl_2$. The comparison of IR absorption of the complex and the ligand suggests the complex formation (table 2.4). The NH stretching frequencies of the ligands are effected on complex formation; the absorptions at 3201cm^{-1} shifts towards higher side to 3267cm^{-1} and the absorption becomes sharp. The enhancement of intensity is attributed to the H-bonding present among the NH and anionic chloride ligand. The C=N appearing at 1598cm^{-1} of the ligand shifts to a lower side at 1567cm^{-1} suggests that the complexation of the nitrogen atom increases the delocalisation of the lone pair of electron attached to the nitrogen atom attached to a hydrogen atom.

Table 2.4.IR absorptions of 1e and 3,5-dimethylpyrazole (cm^{-1})

3,5-dimethylpyrazole	$(pz)_2CuCl_2$
3201(m), 3140(m), 3104(m), 3037(m), 2945(m), 2884(m), 2786(w), 2602(w), 1598(m), 1486(w), 1419(w), 1312(m), 1153(w), 1025(m), 851(w), 779(w), 737(w)	3267(s), 3201(s), 2924(w), 1567(s), 1470(m), 1419(s), 1275(m), 1183(m), 1050(s), 819(m), 794(s), 697(m), 615(w), 543(w), 435(w)

The dimeric nature of the copper makes the copper to have a penta co-ordinate environment with a distorted trigonal bipyramid structure. In the crystal structure Cu(1)-N(3) bond length is 1.998(3)Å which is shorter than the Cu(1)-N(2) bond length 2.015(3)Å and nonbridging Cu(1)-Cl(2) bond length is 2.2985(9) Å which is also shorter than the bridging counter part, thus the bond length of Cu(1)-Cl(1) is 2.3258(9) Å. and that of Cu(1)-Cl(1A) is 2.6703 Å (1). The bond angle of N(3)-Cu(1)-N(2) is $88.67(11)^0$, almost close to the bond angle of N(2)-Cu(1)-Cl(2) which is $88.95(8)^0$ and the bond angles of N(3)-Cu(1)-Cl(2) is $162.46(8)^0$. The bond angles of N(3)-Cu(1)-Cl(1) is $89.36(8)^0$; whereas the bond angles of N(3)-Cu(1)-Cl(1A) is $98.76(8)^0$ and Cl(2)-Cu(1)-Cl(1) is $98.76(8)^0$ shows that due to the *penta*-coordination nature of the copper center could distinguish the axial and equatorial positions of a trigonal bipyramid geometry.

The un-coordinated nitrogen of the pyrazole has an acidic proton that participates in hydrogen bonding scheme and leads to chain structure as shown in figure 2.8. The various H-bond distances and bond angles that has direct relevance to the H-bonding scheme are listed in table 2.5. In a three-dimensional network the dimeric units provides close packed structures as shown in figure 2.9.

Table 2.5. Hydrogen bond distance and angles in [Å and ^{0}] are

D-H---A	d(D-H)	d(H---A)	d(D---A)	< (DHA)
N(1)-H(1)--Cl(2)	0.86(4)	2.72(4)	3.121(3)	110(3)

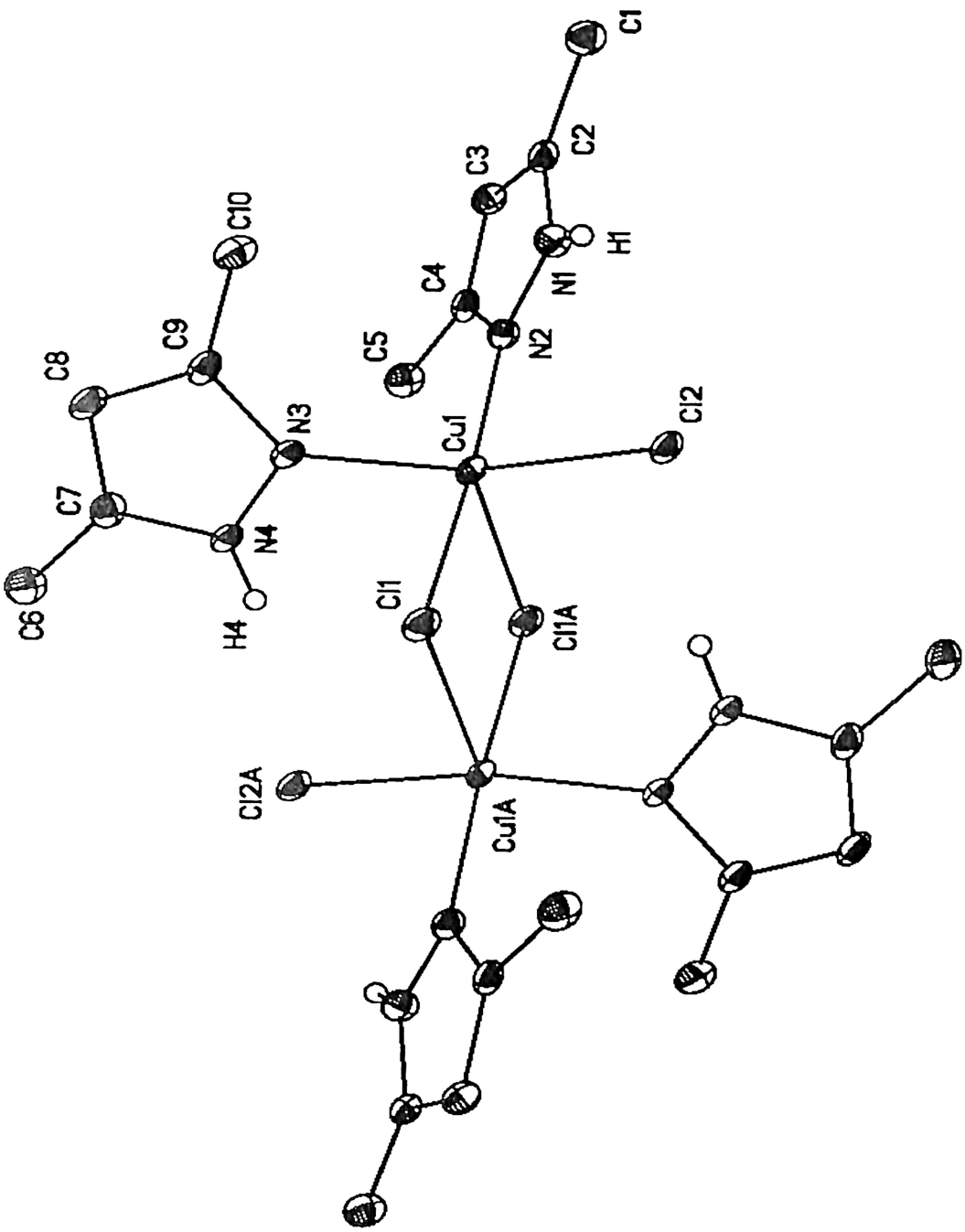

Figure 2.8: The dimeric structure of *bis*-2,4-dimethylpyrazoblecopper(II)chloride

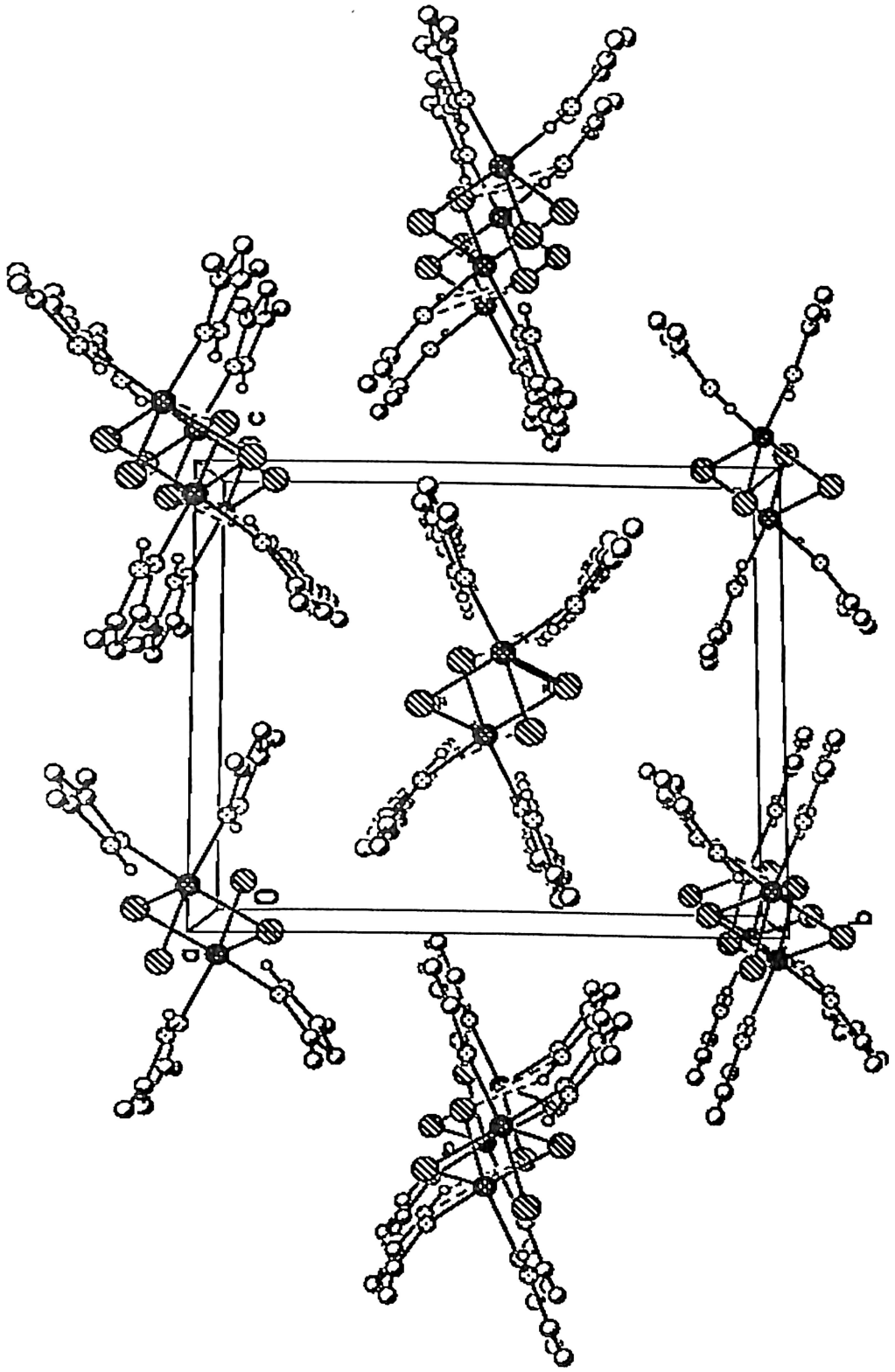

Figure 2.9 Closed pack structure of *bis*-2,4-dimethylpyrazoblecopper(II)chloride

2.1.7 Thermochemical properties

Thermochromism is a well-known phenomenon in co-ordination chemistry and is usually ascribed to temperature dependent changes in the co-ordination geometry of the chromophore[125-126]. However, the change in electronic structure via the thermal procedure is quite slow, limiting the utility of those systems. For example copper (II) complex $[Cu(DED)_2](BF_4)$, where DED = *N,N*-diethylethylenediamine[127-128], shows three absorption peaks at 515, 305 and 255 nm at room temperature. On cooling, the absorption peaks in the 515nm gets shifted to shorter wavelength, resulting in the color change from purple to red. According to literature report this phenomenon is due to the square planar structure in the law temperature (red) phase is dynamically distorted towards tetrahedral configuration in the high temperature (purple) phase.[125] Structural phase transitions are quite common in copper (II) halide salts and with hydrogen bonding cations, they are usually associated with disordering of the cation and concomitant weakening of N-H—X hydrogen bonds.[126, 129] The weakening of the hydrogen bonds increases the charge density on the halide ions of the $[CuX_4]^{2-}$ anion, which relaxes its co-ordination geometry towards tetrahedral in order to minimize the electrostatic repulsion between the halide ions. For this reason tetrahalocuprate complexes are found to be theromochromic and shows different colors due to interconversion between different structures. For several tetrachlorcuprate salts discontinuous thermochrochromic phase transitions are observed with a "greenyelloworange" colour progression as the distortion of the anion with respect to ideal tetrahedral geometry decreases. The enthalpies of the phase transitions in tetrachlorocuprate are greater than those observed in the corresponding tetrabromocuprate salts owing to the decreased ionic radii of the chloride ion over that of the bromide ion, which usually permits a larger distortion of the tetrachlorocuprate anions from the T_d geometry.[129-130]Several complexes having counter ions

derived from ammonia derivatives are usually studied for this purpose. However, due to polymerizing and oxidizing properties of anilinic compounds, the use of anilinium cations for such thermal studies is limited. Another aspect of these complexes is the ability of these complexes to release acid and exchange the coordination position of the halogens.

The thermal behavior of these complexes has been deduced from their TG/DTA and DSC curves in nitrogen atmosphere and in air. The data shows that there are three processes associated; namely, dehydration when water of crystallization is present; as in case of 1c and 1d, and organic cataions pyrolysis and phase transition in DSC curve. The thermogram of *bis*-pyridinium tetra chlorocuprate (1a) and anilinium tetra chlorocuprate 1b) has distinct differences that not only occur from the molecular weight difference but from the thermal reactivity point of view. Based on the percentage of the weight loss the following equations explain the weight loss in different tetrachlorocuprate complexes.

$(PyH)_2[CuCl_4]$	$(AnH)_2[CuCl_4]$	$(p\text{-}CH_3OC_6H_4NH_3)_2[CuCl_4].H_2O$	$(p\text{-}CH_3C_6H_4NH_3)_2[CuCl_4]3H_2O$
↓	↓	↓	↓
2PyHCl	AnH + AnHCl	$H_2O + p\text{-}CH_3OC_6H_4NH_2$ $+ p\text{-}CH_3OC_6H_4NH_3Cl$	$3H_2O + p\text{-}CH_3C_6H_4NH_2$ $+ p\text{-}CH_3C_6H_4NH_3Cl$
↓ (Theory) Loss = 63.00%	↓ Loss = 56.83% (Theory)	↓ Loss = 61.30% (Theory)	↓ Loss = 64.03% (Theory)
↓ Loss = 64.65% (Found)	↓ Loss = 55.24% (Found)	↓ Loss = 62% (Found)	↓ Loss = 62.8% (Found)
$CuCl_2$	$H[CuCl_3]$	$H[CuCl_3]$	$H[CuCl_3]$
py =pyridine	or $H_2[Cu_2Cl_6]$	or $H_2[Cu_2Cl_6]$	or $H_2[Cu_2Cl_6]$
	an =aniline		

In the case of the *bis*-anilinium-tetrachlorocuprate it may thought that the aniline being a reducing agent a part of $CuCl_2$ may get converted to CuCl on heating but this indeed is not the case as the product of thermal reaction did not show dimeric or oligomeric aniline in absence of oxygen. Furthermore the $[CuCl_3]^-$ species are well known and they prefer to remain in dimeric form if the cations are small. The above results are indicative of the fact that the pyridinium system undergoes thermal decomposition in a different manner than the corresponding anilinium analogue. In the region of 150-300^{0}C the compounds 1c and 1d losses 62% (theory 61.30%) weight, 62.8% (theory 64.03%) weight respectively that corresponds to loss of one neutral molecule of the parent anilinium hydrochloride, aniline and the water molecules of crystallization. The thermal property of complex 1a described in literature[130] suggest loss of one HCl molecules at 90^{0}C but we did not observe any loss of weight in this region in thermogravimetry but we have observed an endothermic process in DSC at this temperature.

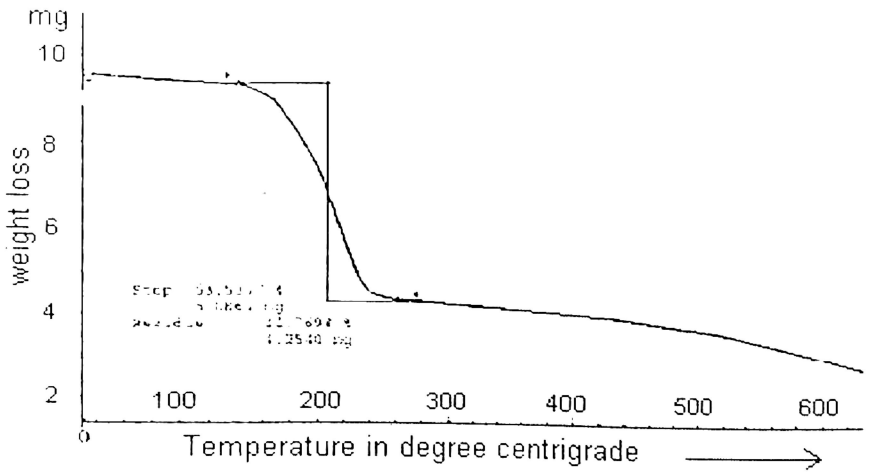

Figure 2.10 Thermogram of *bis*-anilinium tetrachlorocuprate (1b)

The compound 1a shows endothermic process at 87^{0}C and 104^{0}C in the differential scanning calorimeter. There are two endothermic processes for 1a and no weight loss in TGA was observed. These two transitions are referred to structural changes namely, at 87^{0}C, 1a

changes from tetrahedral to square planar and at 104^{0}C it exchanges halide ligands making the N, N co-ordination. The compound 1b shows an endothermic process at 102^{0}C due to change in the tetrahedral structure to square planer. Structural phase transitions are quite common in copper (II) halide salts and with hydrogen bonding cations they are usually associated with disordering of the cation and concomitant weakening of N-H...X hydrogen bonds. The weakening of the hydrogen bonds increases the charge density on the halide ions of the $[CuX_4]^{2-}$ anion, which will relax its co-ordination geometry toward tetrahedral in order to minimize the electrostatic repulsion between the halide ions.

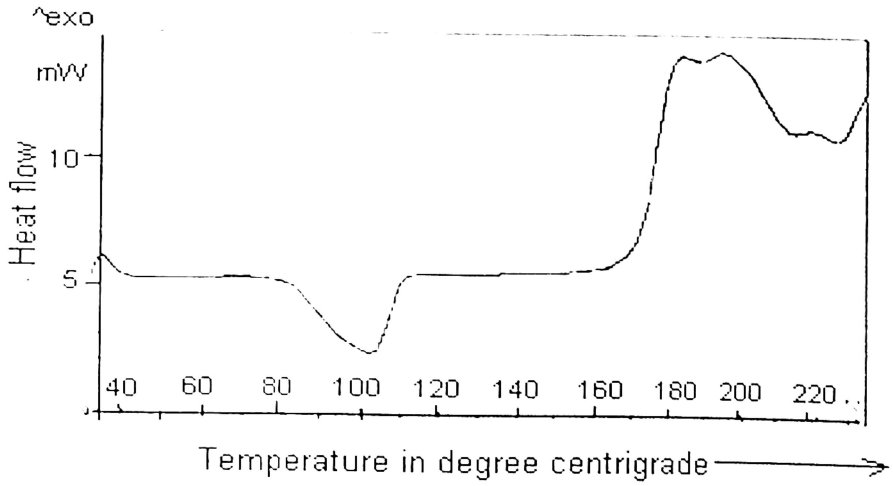

Figure 2.11 The DSC of *bis*-anilinium tetrachlorocuprate

2.1.8 Electrical property

Since the ammonium tetrachlorocuprate and many other such anionic chloro-complexes have extensive H-bonding and polymeric structures[119]. They are expected to show interesting material properties. There are many studies on magnetic properties which reveals that based on the halo-bridged core around two or multiple number copper atoms the complexes can be either ferromagentic or antiferromagnetic [118-119, 132]. There is also recent report on the interesting electrical properties arising from such systems. We have also observed that cupric chloride when trapped in a supramolecular environment created by

highly hydrogen-bonded system such as urea it shows interesting thermoelectric switching properties. In such systems the resistance vs temperature profile (figure 2.8) passes through a normal gaussian shape. Such property was explained as combination of proton conductivity with structural change[133].

The electrical properties of the tetra chlorocuprate complexes also have reflection of this endothermic process. The plot of normalized resistance versus temperature in the region of 40^0C-140^0C for complex tetra chlorocuprate 1b shows a sudden decrease in resistance in the region where the endothermic process takes place (figure 2.12). Based on the crystallographic evidences presented on the structural changes of related compounds from tetrahedral to square planar geometry, the decrease in resistance is attributed to the parallel stacking of the copper centers on transforming from tetrahedral to square planar geometry. In a square planar geometry the interaction between the d_z^2 orbital gets maximized and thereby causes enhancement of electron flow in one direction.

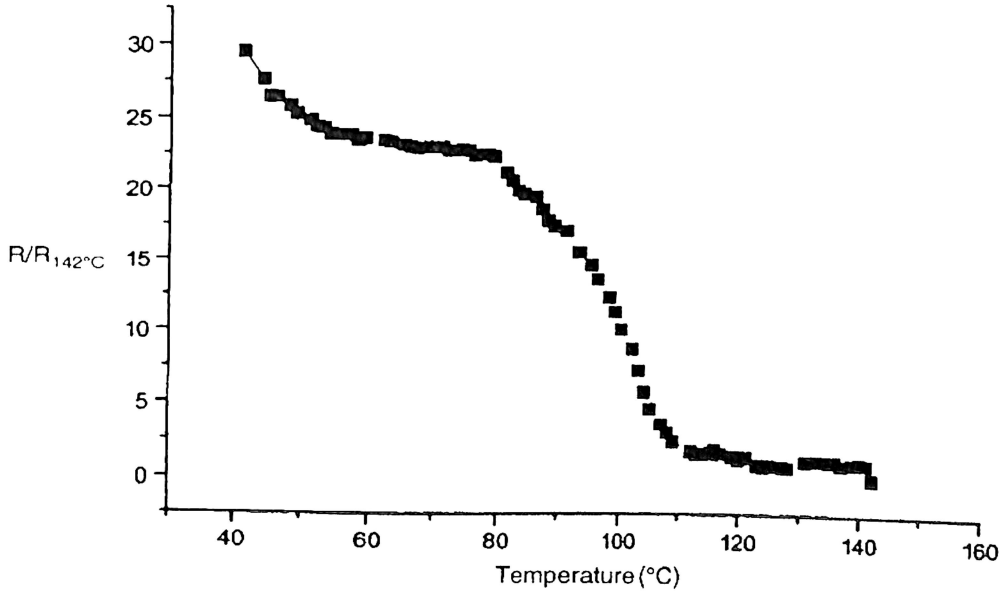

Figure 2.12: The plot of resistance normalized to resistance at 142^0C vs temperature of pallet of (1b)

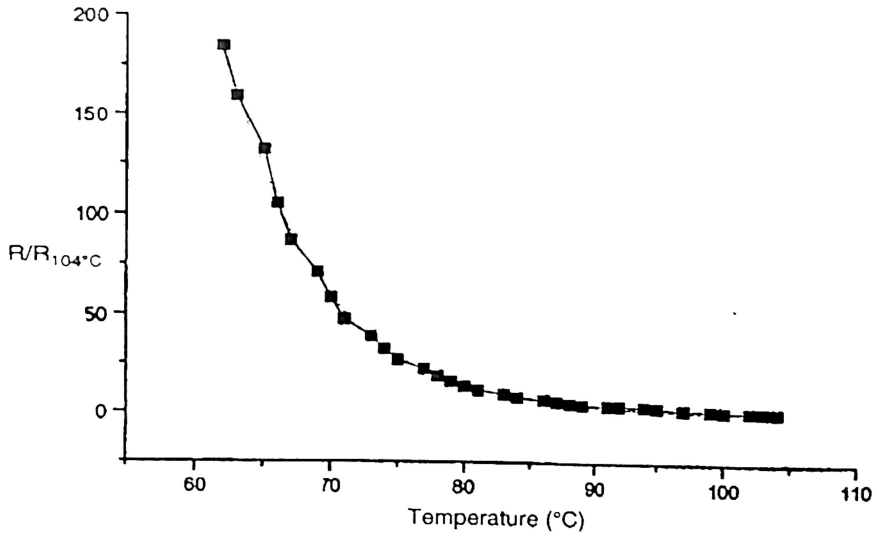

Figure 2.13: The plot of resistance normalized to resistance at 104^{0}C vs temperature of a thin film of (1c)

The tetra chlorocuprate (II) complex **1c** has a molecule of water of crystallization in the interstices of the crystals. It has a structural change at 70-108^{0}C (from DSC). The complex 1c has also a labile water molecule present in the system, which is lost at around 120-140^{0}C. The compound has a resistance vs temperature profile having an exponential shape in the region 80-140^{0}C (figure 2.13). This observation is important in biological system such as DNA nano particles it is observed that the resistances versus temperature profile are greatly influenced by the presence of water molecules. The low temperature resistance data on such system has a transition in the temperature range of 80-140^{0}C. It is already mention that the tetrahalocuprate complexes are thermochromic and their thermochromicity is generally associated with a structural change around the copper (II) centers. We had also shown that the structural changes around copper (II) can effect the resistance profile of a system and we have demonstrated the thermoelectric switching property from such possibilities.

The evidence of change in co-ordination geometry around copper (II) center is also coming from the recorded IR spectra of *bis-p*-methoxyanilinium tetrachlorocuprate

monohydrate in room temperature as well as the heated sample. The room ten spectra of this complex shows two absorptions spectra at 3456 and 3045 cm^{-1} due to O-H and N-H frequency, respectively.

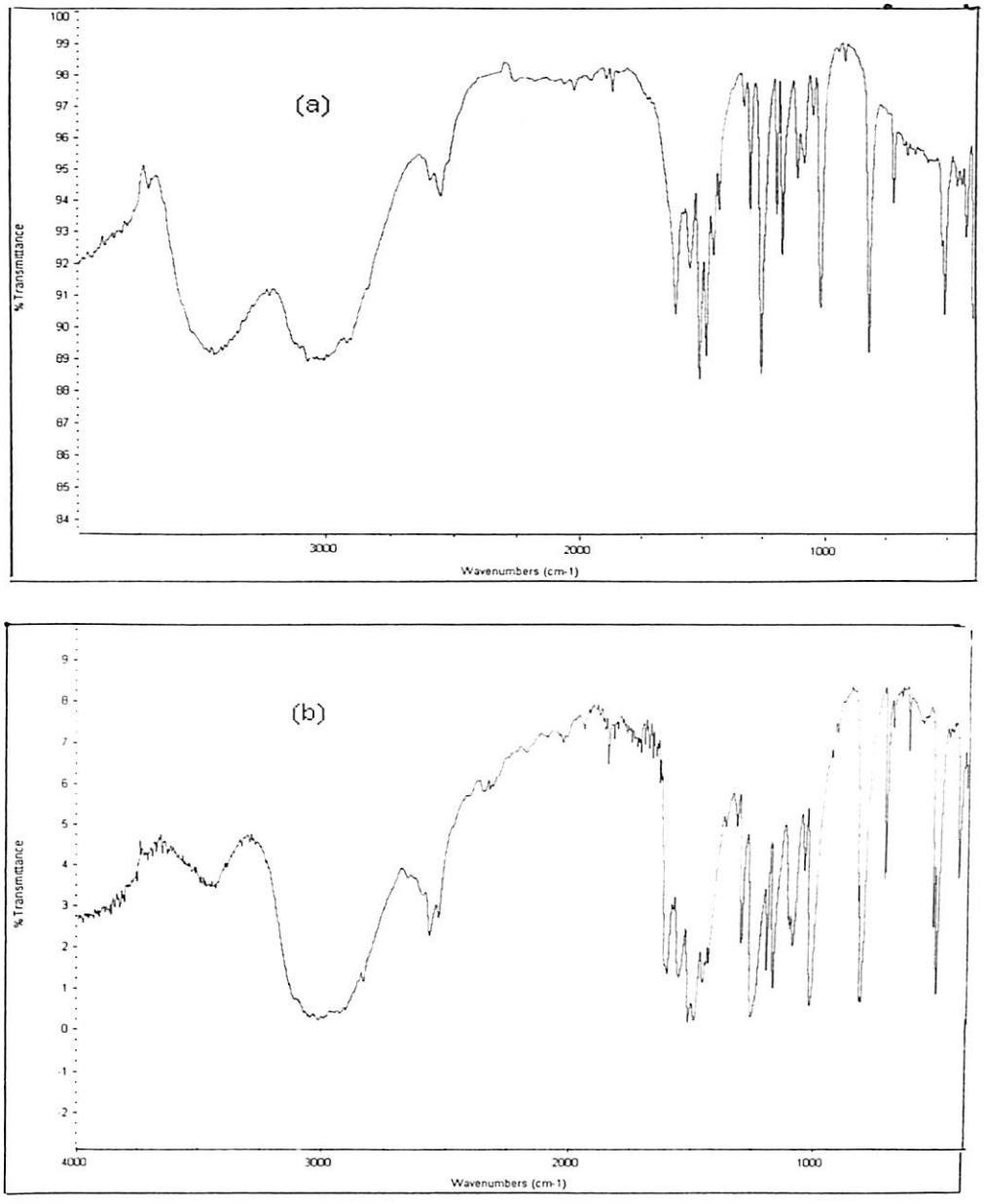

Figure 2.14 (a) IR spectra of *bis-p*-methoxyanilinium tetrachlorocuprate complex before heating (b) IR spectra of bis-*p*-methoxyanilinium tetrachlorocuprate complex after heating

The sample on heating to 100^0C result in considerable loss of absorption at 3456cm^{-1}. This shows that the loss of weakly bound water molecule as well as the change in the co-ordination geometry around the copper (II) center effects the resistance. Further proof to this

result is observed from the thermal study. The DSC of the samples has an endothe at 60-104^{0}C without loss of weight followed by another endothermic process at 115-140°C for the loss of water molecule.

Chapter 3

Copper complexes catalysed silicon-oxygen bond formation and related reactions

3.1.1 Background

Copper(I) complexes are extensively used for silicon hydrogen bond activation[134]. The copper complexes generally used for such reactions are air sensitive and their synthetic procedures are not simple. On the other hand copper (II) is a useful stable oxidation state that can be generally converted to (I) oxidation state. Silanes being reducing agents, are capable of reducing copper(II) to copper(I) prior to another organic transformation. This leaves scope for *insitu* use of copper(II) as precursor for transformation to copper (I) complexes that in turn may acts as a catalyst. In chapter 2 it is demonstrated that chlorides of tetrachlorocuprates are labile and copper(II) center can change co-ordination number causing co-ordination unsaturation. The tetrachlorocuprate complexes also possesses a quasireversible redox of Cu (II) and Cu (I) that have scope for catalytic reactions. Copper metal is also known to catalyse[135] the reaction of silicon with alkylhalide and in gas phase to give corresponding halosilanes (equation 3.1)

$$Si + RCl \xrightarrow[\text{pressure/ heat}]{Cu} R_3SiCl + R_2SiCl_2 + RSiCl_3$$

Equation 3.1

With this background and keeping in mind the emerging interest of the use of environmentally suitable catalyst, the catalytic reactivity of different tetrachlorocuprates with different silanes were investigated.

3.1.2 Tetrachlorocopper(II) catalysed silicon-oxygen bond form reaction

Silicon oxygen bonds are much stable than carbon oxygen bond but silicon-oxygen bond is much more labile than carbon-oxygen bond. In literature it has been already reported that metallic copper[136-137]and copper (I) hydride[135]complex for example $[Ph_3PCuH]_6$ is a useful catalyst for silicon-oxygen bond formation in the reactions between silanes and alcohols. Although, the metallic copper powder can be used for silicon-oxygen bond formation of silanes the reaction is limited to substrates containing phenyl groups attached to silicon and also requires drastic reaction conditions. It was found that tetrachlorocuprates having anilinium, *p*-methoxyanilinium, *p*-methylanilinium, and pyridinium cations are fairly good catalysts for silicon oxygen bond forming reactions through alcoholysis of silane. The complexes are capable of converting 10-equivalent of the substrates with respect to one mole of the catalyst. The reactions proceeds at room temperature slowly but can be completed within 3-6 hours when carried out at 40-70^{0}C. The tetrachlorocuprate catalyzed silicon-oxygen bond forming reactions can be represented by the equation 3.2 and 3.3.

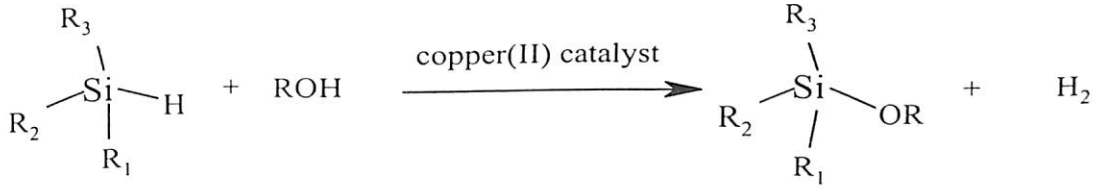

$R_1 = R_2 = R_3 = -C_6H_5-$

$R_1 = R_2 = R_3 = -CH_2CH_3$

Equation 3.2

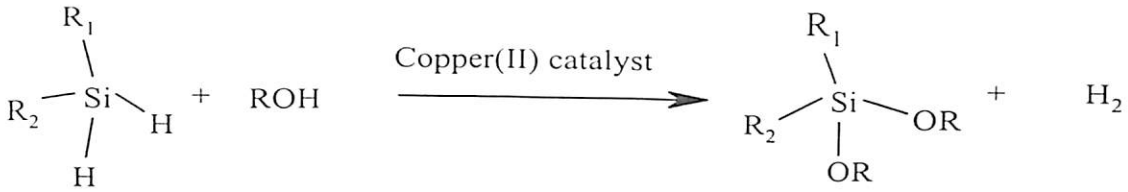

$R_1 = R_2 = -C_6H_5$; $R_1 = CH_3$, $R_2 = C_6H_5$

Equation 3.3

These reactions were performed under neutral and mild conditions. Since these reactions gave only hydrogen gas as by-product separation was not difficult. However the usual problem of purification of siloxane by column chromatography was observed; as many times the silica gel was found to be capable of degrading the silicon-oxygen bond thereby decreasing the isolated yield after column chromatography.[138-139]

The reaction was studied with both monohydrosilanes and dihydrosilanes. The reactions with various primary and secondary alcohols such as methanol, ethanol, isopropanol and allylalcohol were carried out. These reactions gave the corresponding silylethers and they are listed in table 3.1 and 3.2. The reaction was not applicable to tertiary butylalcohol (equation 3.4). For example the reaction of triphenylsilane with

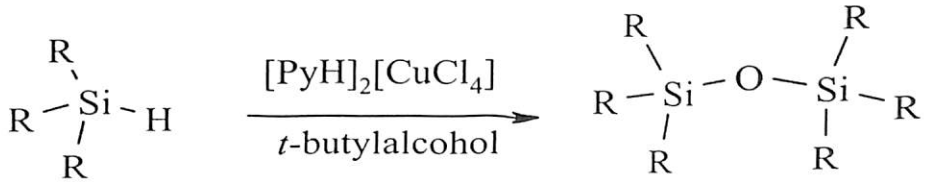

$R = -C_6H_5$, $-C_2H_5$

Equation 3.4

Table 3.1. *Bis*-pyridinium tetrachlorocuprate catalysed silylethers from mono-hydrosilanes

Silane	Alcohol	Reaction condition (Yield)	Product (yield)
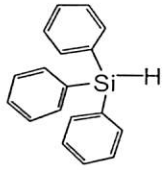	CH_3OH	40^0 C for 3hrs (60)	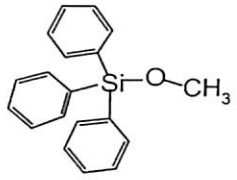 3a
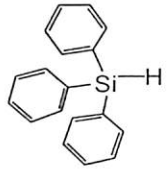	CH_3CH_2OH	40^0 C for 3hrs (57)	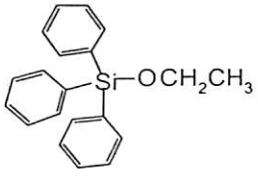 3b
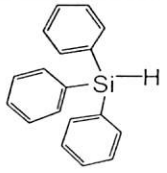	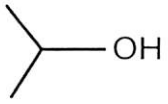	60^0 C for 6hrs (40)	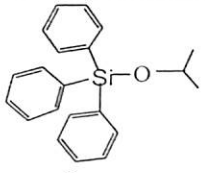 3c
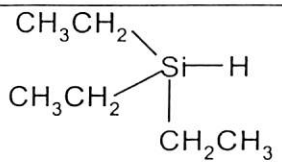	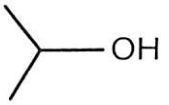	60^0 C for 6hr (50)	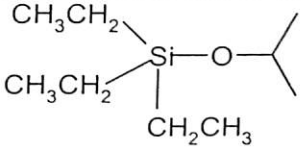 3d
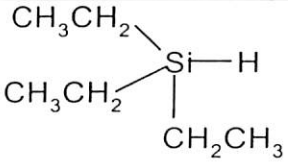	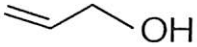	60^0 C for 7hrs (60)	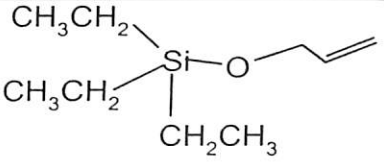 3e

Table 3.2. *Bis*-pyridinium tetrachlorocuprate catalysed silylethers from dihydro

Silane	Alcohol	Reaction condition and isolated yield	Product
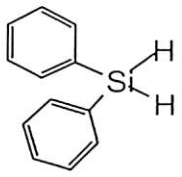	CH_3OH	60^0C for 3hrs (55)	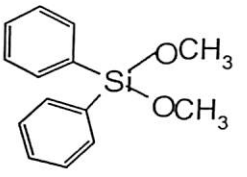 3f
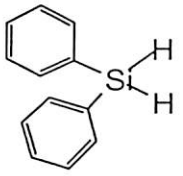	CH_3CH_2OH	60^0C for 3hrs (60)	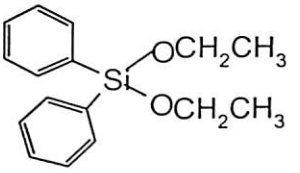 3g
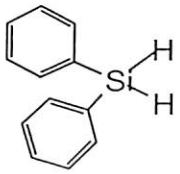	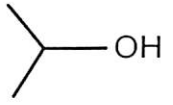	60^0C for 5hrs (40)	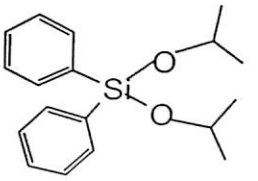 3h
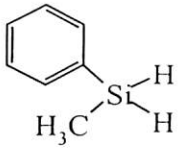	CH_3CH_2OH	50^0C for 3hrs (60)	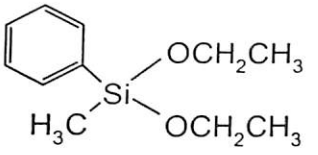 3i

tertiary butylalcohol in the presence of *bis*-pyridinium tetrachlorocuprate as catalyst led to the formation of the di-triphenylsiloxane only. In this reaction all the silane was consumed. This suggested that the water present in the reaction competes with the alcohol. The identity of the ditriphenylsilylether was established from its ^1H NMR and ^{13}C NMR and IR. It had ^1H NMR peaks at 7.3-7.7δ due to the phenyl group whereas it had the ^{13}C signals from the phenyl groups at 127.9δ, 129.4δ, 134.3δ, and 134.9δ respectively. In IR spectra it had the silicon-oxygen stretching frequency at 1068 cm^{-1} and the compound was devoid of Si-H

frequency that was originally observed in the parent silane at 2150 cm^{-1}. The al reacted with triphenylsilane and gave silylether. In this case the double bond of the allyl group was not reduced. The phenols were found to be not suitable for these catalytic reactions. The reaction was very effective to dihydrosilanes, in which exclusively disubstituted silylethers were formed. The monohydrosilylethers were not observed in the reaction mixtures. Different alcohols such as methanol, ethanol and isopropanol were reacted with diphenylsilane and methylphenylsilane in the presence of catalytic amount of *bis*-pyridinium tetrachlorocuprate. These reactions were carried out with different catalyst systems and *bis*-pyridinium tetrachlorocuprate was found to be the most suitable catalyst. This compound has the advantage that it has a ligand, which is stable, but *bis*-anilinium tetrachlorocuprate complex has a deficiency that they underwent oxidation when left under aerial condition. The relative rates of different tetrachlorocuprate catalysts were determined by monitoring the alcoholysis reaction between diphenylsilane and ethanol with help of GC. This was done by taking out solution from the concerned reaction mixtures using a micro syringe, followed by injection into a Hewllet Packard GC with a SE-30 capillary column, with flame ionization detector. The products were compared with authentic samples. The plot of change of concentration of diphenylsilane vs time obtained from different catalysts are shown in the figure 3.1. it was observed that about 80% of the silane reacted with alcohols and forms the corresponding silane within half an hour. The reactions than slows down and some amount of diphenylsilane remain unreacted even after two and half hour. The comparison plot of change of concentration of diphenylsilane on reaction with ethanol where catalyst a = *bis*-anilinium tetrachlorocuprate, b=*bis*-*p*-methylanilinium tetrachlorocuprate, c=*bis*- *p*-methoxyanilinium tetrachlorocuprate, d = *bis*-pyridinium tetrachlorocuprate showed that they follow similar trend in the product formation. It suggests that the counter ion does

not have a role in the reaction. It is also indicative of the fact that there could be a and copper(I) couple that would be responsible for these reactions or the metallic copper that may be formed could participate in the catalytic reactions.

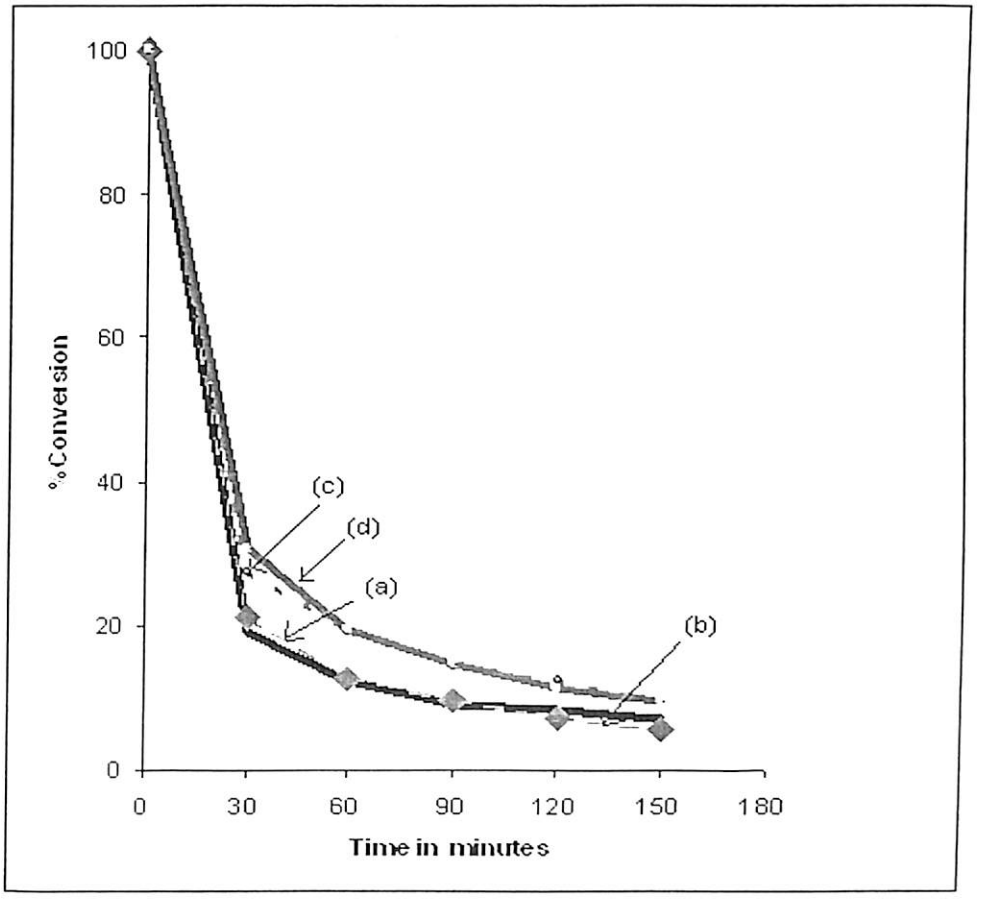

Figure 3.1 Conversion of diphenylsilane (0.01mmol) to diethoxy diphenylsilane by different tetrachlorocuprate complexes (0.008mmol) Where a = *bis*-anilinium tetrachlorocuprate, b = *bis-p*-methylanilinium tetrachlorocuprate, c = *bis-p*-methoxyanilinium tetrachlorocuprate, d = *bis*-pyridinium tetrachlorocuprate

To understand possible involvement of a copper(I) species in the reaction of the copper catalysed silicon-oxygen bond forming reactions, such reactions were also monitored by UV-Visible spectroscopy. It was found that all these reactions initially passes through decolourisation of copper(II) solution suggesting a reduction of copper(II) to copper(I) complex. The regeneration of the catalyst in the course of these reactions was very clear from visible spectroscopy. For example, the pyridinium tetrachlorocuprate had a well-defined

absorption peak at 467nm. The absorption maximum decreased on reacti diphenylsilane in the presence of ethanol (figure 3.2 the graph marked as **a**). The reaction led to decolorisation of the solution, suggesting the conversion of copper (II) to copper (I). However, after the consumption of the diphenylsilane the absorption peak at 467 nm reappeared, suggesting that the Cu (II) was regenerated (figure 3.2 marked as **b**).

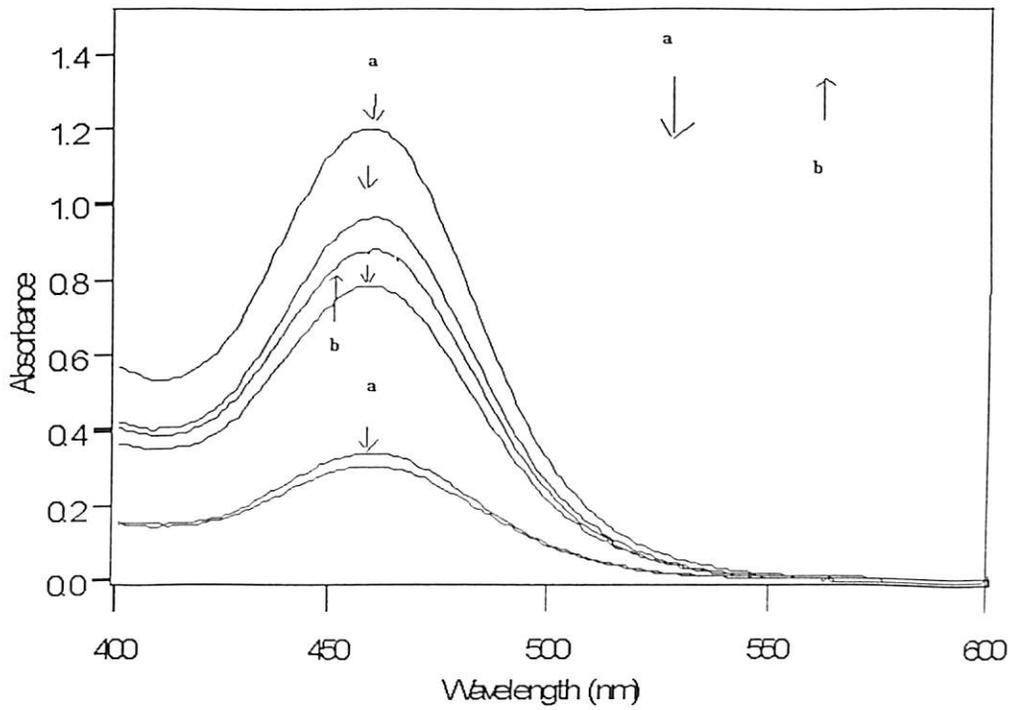

Figure 3.2 The change in absorption at 467 nm with time(every three minute interval) of a solution of *bis*- pyridinium tetrachlorocuprate in ethanol on addition of diphenylsilane

Performing the reaction at different concentrations of the *bis*-pyridinium tetrachlorocuprate complex, the relative rate of the decrease in the absorption at 467 nm was studied during its reaction with diphenylsilane and ethanol. It was observed that the time taken to reach the minimum absorption was dependent on the catalyst concentration. Visible spectra showed that as the concentration of the copper (II) catalyst was increased, the time required for a decrease in the absorption at 467 nm was increased. For example, the reaction of diphenylsilane (0.1 mmol), *bis*-pyridinium tetrachlorocuprate (0.011 mmol) with ethanol (3.4 mmol) in acetonitrile (4 ml) has a minimum absorption at 467 nm after 15 min figure 3.3

(a) but the reaction of diphenylsilane (0.1 mmol) *bis*-pyridinium tetrachlorocup mmol) with ethanol (3.4 mmol) in acetonitrile (4 ml) had minimum absorption after 20 min figure 3.3(b). In the later case, the regeneration of the catalyst was slower, because higher amount of the catalyst was used than in the former case.

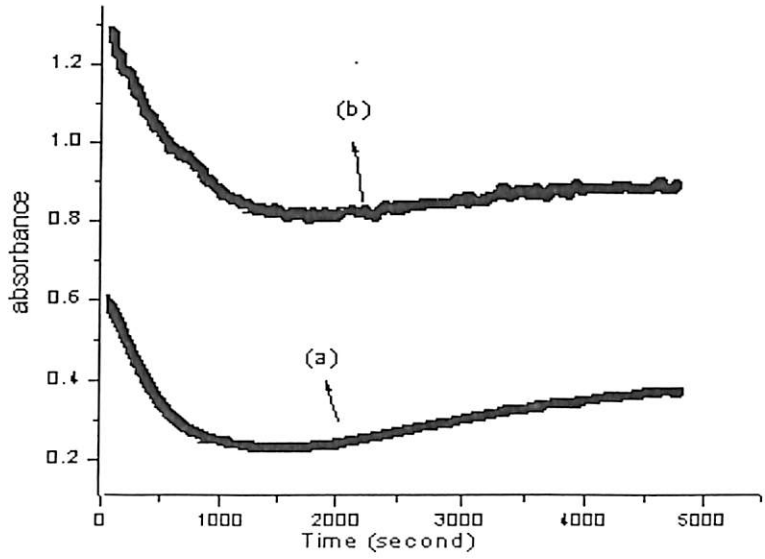

Figure 3.3 The reaction of diphenylsilane (0.1 mmol), *bis*-pyridinium tetrachlorocuprate (0.011 mmol) with ethanol (3.4 mmol) in acetonitrile (4 ml) has a minimum absorption at 467 nm after 15 min figure 3.3 (a) but the reaction of diphenylsilane (0.1 mmol) pyridinium tetrachlorocuprate (0.02 mmol) with ethanol (3.4 mmol) in acetonitrile (4 ml) has minimum absorption after 20 min figure 3.3(b).

These observations suggested that once silane was added to the solution of *bis*-pyridinium tetrachlorocuprates it reduced the copper(II) to copper(I); thereby decolorizing the solution. As the reaction proceeded the silanes got consumed and the copper(II) state was regenerated, such observation implied that interchange of copper(II) and copper(I) during the reaction. We had tested the reactivity of the anhydrous cupric chloride for silicon-oxygen bond forming reactions. It was found to be not suitable for such catalytic reactions. For example the reaction of triphenylsilane in methanol in the presence of cupric chloride gave di-triphenyl silylether. The result is attributed to the fact that the silicon-oxygen bonds are acid sensitive and if at all a methylsilylether was formed in this reaction it would have got

hydrolysed to corresponding silanol. Which on further reaction gave triphenylsilylether.

As discussed earlier the dihydrosilanes are good substrates that get difunctionalisation on reaction with alcohol, quantitative products were formed through catalytic reaction. Thus, the tetrachlorocuprate complexes should be good catalyst for the synthesis of silicon-oxygen bonded oligomers from polyhydric alcohol. It was found that the silicon-oxygen bond formation could be extended to synthesize oligomers from the reaction of dihydrosilanes(equation 3.5) and trihydrosilane with polyhydroxyalcohols (equation 3.6).

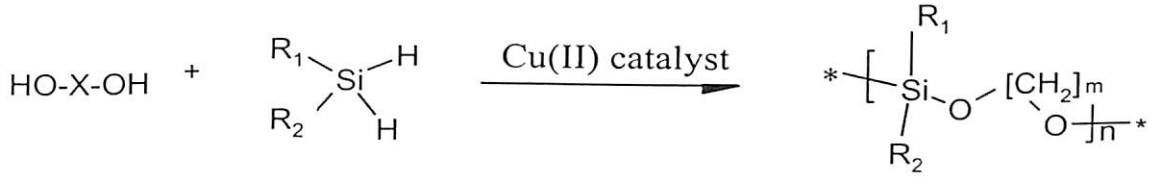

$R_1 = R_2 = Ph$, $X = CH_2CH_2$	3k
$R_1 = R_2 = Ph$, $X = CH_2CH_2CH_2$	3l
$R_1 = R_2 = Ph$, $X = CH_2CH{=}CHCH_2$	3m
$R1 = Ph$, $R_2 = Me$, $X = CH_2CH{=}CHCH_2$	3n
$R_1 = Ph$, $R_2 = Me$, $X = CH_2CH_2$	3o
$R_1 = Ph$, $R_2 = Me$, $X = CH_2CH_2CH_2$	3p

Equation 3.5

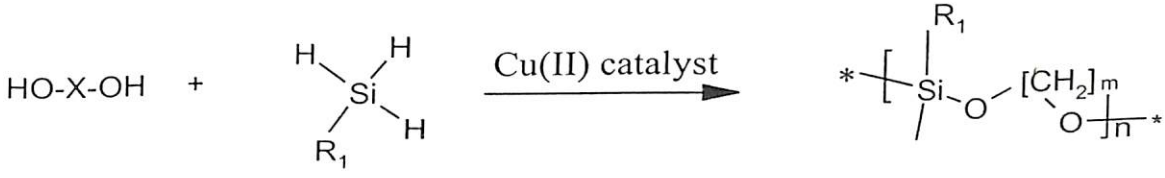

$R_1 = Ph$, $X = CH_2CH_2$ 3q

Equation 3.6

Several diols such as 1,2-ethylenediol, 1,3-propanediol, *cis*-l, 4-dihydroxy-2-butene were reacted (equation 3.5 and 3.6) with diphenylsilane and methylphenylsilane in the

presence off tetrachlorocuprate complexes as catalyst. These reactions led to silicon bonded low molecular weight oligomers. The ^{1}H NMR and ^{13}C NMR of the products were indicative of the fact that they comprised of uniform structure. The spectra of two illustrative examples of the oligomers sythesised by tetrachlorocuprate are shown in figure 3.4 and 3.5. The ^{1}H NMR of the oligomer (3o) (figure 3.4.) showed its phenyl group signals at 7.3-7.8δ and the ethylene groups appeared at 3.7δ; the methyl groups attached to the silicon center appeared as a multiplet at 0.57-0.14δ. The peaks are labeled in the NMR spectra figure 3.4.

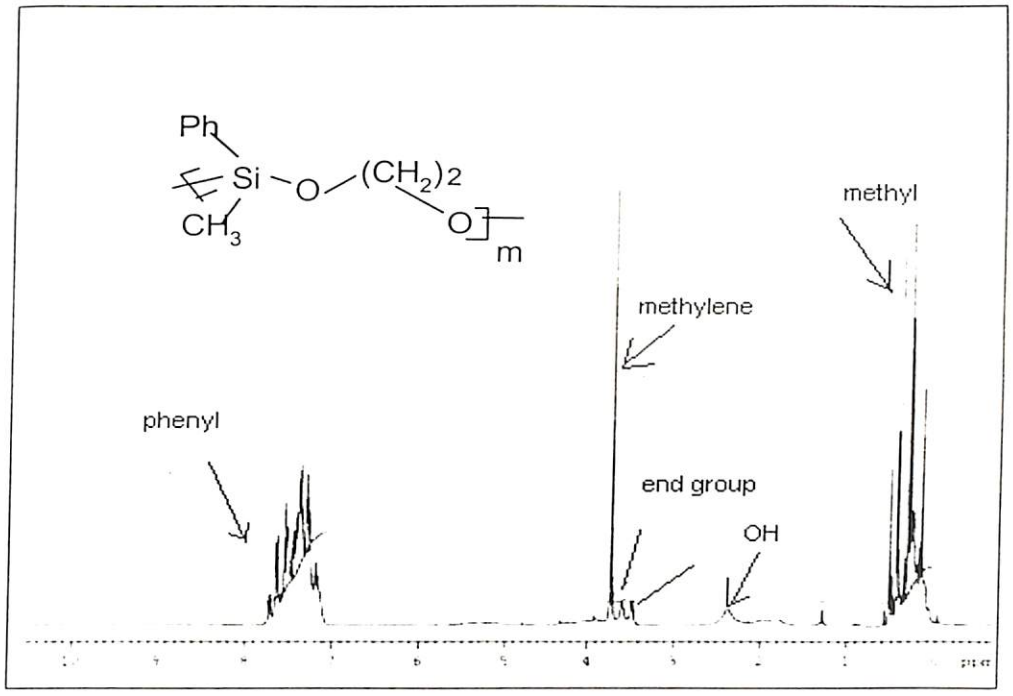

Figure 3.4 ^{1}H NMR spectra (400 MHz) of oligomer of phenylsilane and ethylene glycol

There were also small peaks in the region of methylene group (marked as end group) that arise from the -CH_2CH_2OH end group in the oligomer. The two set of –CH_2 groups Si-O-CH_2- and Si-O-CH_2-CH_2 were observed separately because of their magnetic nonequivalence. In addition to these there is a small OH signal at 2.3δ that may arises from the –OH end group that form through the hydrolytic cleavage of Si-H bond. The ^{13}C NMR

spectra of the oligomer have signals at 136.8, 133.3, 129.8, 127.4δ due to aromat and signal at 63.4δ is due to ethylene carbon. The methyl carbon attached to the silicon center (figure 3.5) appear at -0.1δ. The end group signals can be seen in the IR spectra of the oligomer also. The IR spectra had OH stretching frequency at 3367cm^{-1}, however it was devoid of any Si-H frequency. The oligomer also had the Si-O stretching at 1076 cm^{-1}.

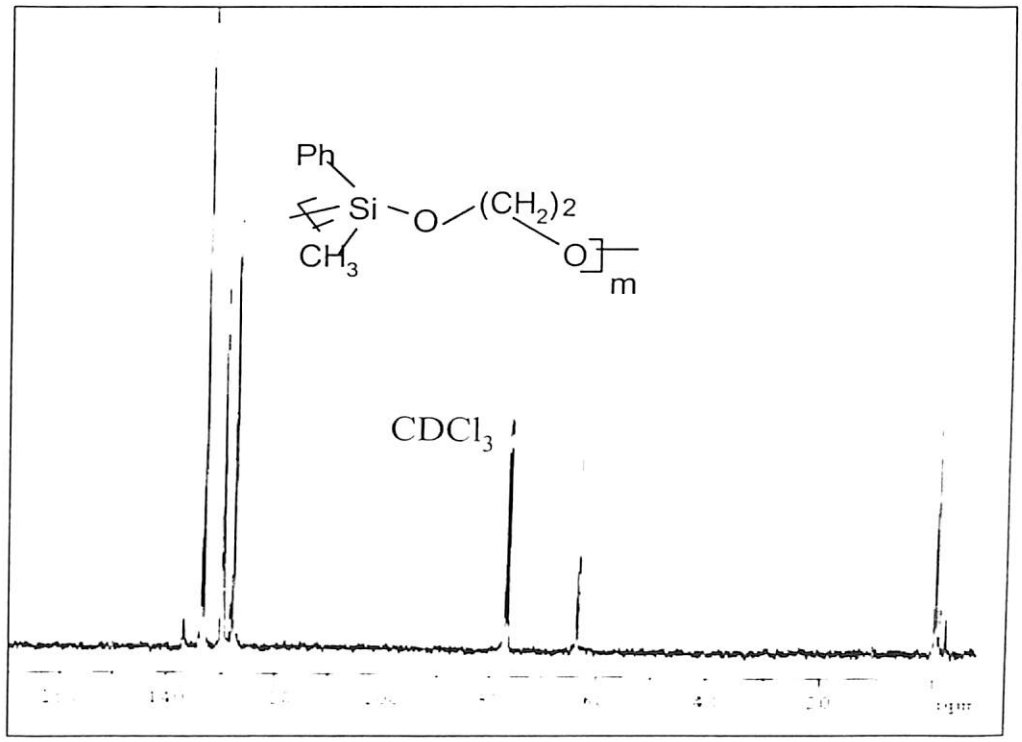

Figure 3.5 ^{13}C NMR spectra (400MHz) of oligomer of phenylsilane and ethylene glycol

Similarly the siloxane oligomer of *cis*-butenediol with diphenylsilane was also prepared. This oligomer is of interest because an oligomer having silicon-oxygen bond and the double bond are potential candidate for further functional modifications. The transition metal catalysts derived from late transition metal are generally capable of hydrosilyaltion.[69] But in the case of tetrachlorocuprate catalysis, it was observed that neither hydrogenation nor hydrosilylation of the siloxane oligomer derived from *cis*-butendiol and diphenylsilane took place. The proton NMR of this product is shown in the figure (3.6). The signals from the

$-CH_2OSi$ appears at 4.1δ and the proton of $-CH=CH-$ appear at 5.7δ in addit signals, the multiplet at 7.2-7.8δ due to phenyl groups that are attached to the silicon center. In this oligomer also there are minor signals that arises from the end groups, which are presumably from $-CH_2CH=CHCH_2OH$ and OH are also appeared. The IR spectrum also shows the presence of OH group with strong absorptions at 3437 cm^{-1}. The IR spectra showed the presence of double bond as it had the medium intensity absorption for C=C at 1646 cm^{-1}.

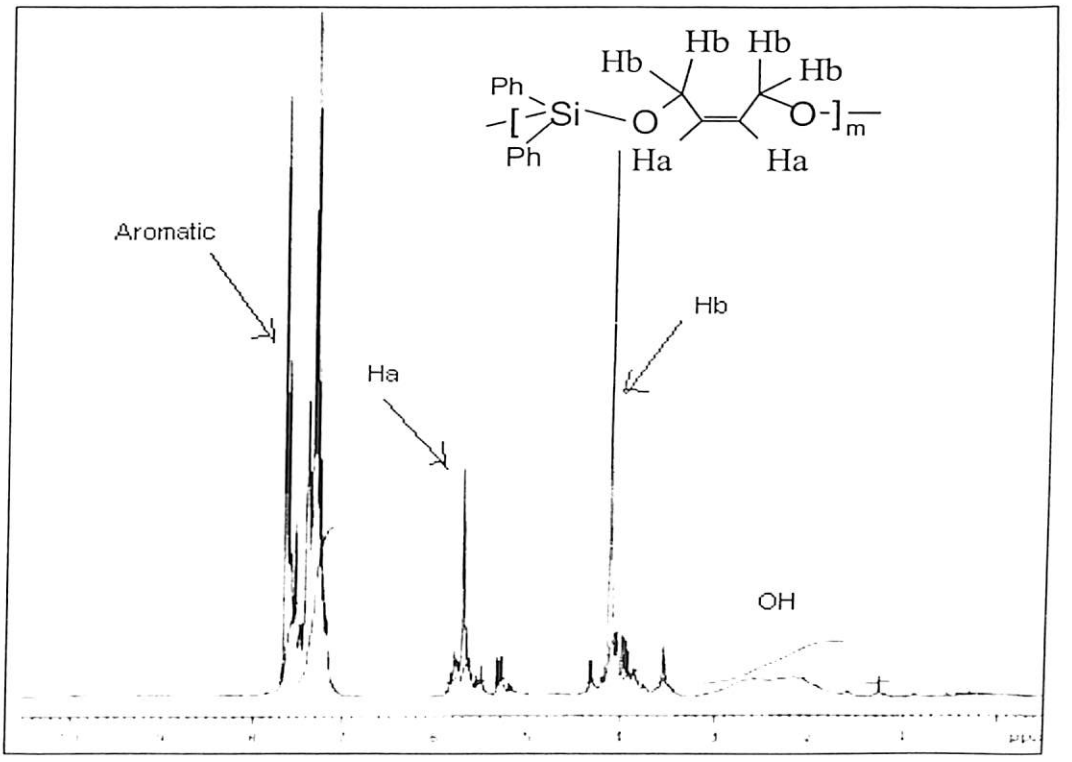

Figure 3.6 ^1H NMR spectra (400 MHz) of siloxane oligomer of diphenylsilane and *cis*-butenediol

3.1.3 Gel-permeation chromatogram of siloxane oligomer

In a polymerization reaction a number of polymer chain starts growing simultaneously, but all of them do not get terminated after growing to the same size.[140-141] The chain termination is a random process, hence, each polymer molecule formed can have different number of monomer units and thus different molecular weights. Thus, unlike a simple chemical compound, each of which has the same molecular weights, whereas a

polymer or oligmer contains molecules, each of which can have different molecu

The molecular weights of polymer or oligomer samples viewed statistically and expressed as weighted average molecular weight (M_w) and number average molecular weight (M_n). Thus to know a polymer properly, one must have a knowledge of both the average molecular weight as well as its dispersion pattern. This dispersity with respect to the lowest to the highest molecular weight homologues is expressed by a simple molecular weight distribution curve.

Gel Permeation Chromatography has been proved to be an effective technique to ascertain the distribution of molecular weight of polymeric/oligomeric compounds. The molecular weight distributions and dispersity of the oligomers were determined (Table 3.3) and it was found that the polydispersity of each of the oligomers were close to unity. This implies that the molecular weight distributions of the oligomers are very narrow. The M_w values were found to lie in the range 900- 3000 with respect to polystyrene as standard. This shows that the oligomers comprise minimum of 8 to 10 monomeric blocks. The molecular weight and the yield of different oligomers synthesized by tetrachlorocuprates are shown in table 3.3.

The molecular weights of these oligomers were determined by GPC and are listed in the table 3.3. The chromatograms of the oligomers were simple and unimodal suggesting that majority of the oligomeric species were having similar chain length. The chromatogram of siloxane oligomer (table 3.3 entry 3k) prepared from the dehydrogenative condensation reaction between diphenylsilane and ethyleneglycol and its molecular weight distribution are shown in figure 3.7. The oligomer has M_w and M_n values with respect to polystyrene as standard are 1667 and 1659 respectively. This indicates that it is a very low molecular weight oligomer comprising of 8-10 repeated monomeric units. The polydispersity of this oligomer

is again very close to unity showed it to have narrow distribution of molecular v uniform chain length.

In order to increase the molecular weight of the oligomer the reactions were carried out for prolonged time as well as increasing the catalyst concentration. Both the attempts were not successful and it was observed that prolonged heating and more catalysts lead to less yield. This suggested that silicon-oxygen bond formed initially might be degraded by the same catalyst system.

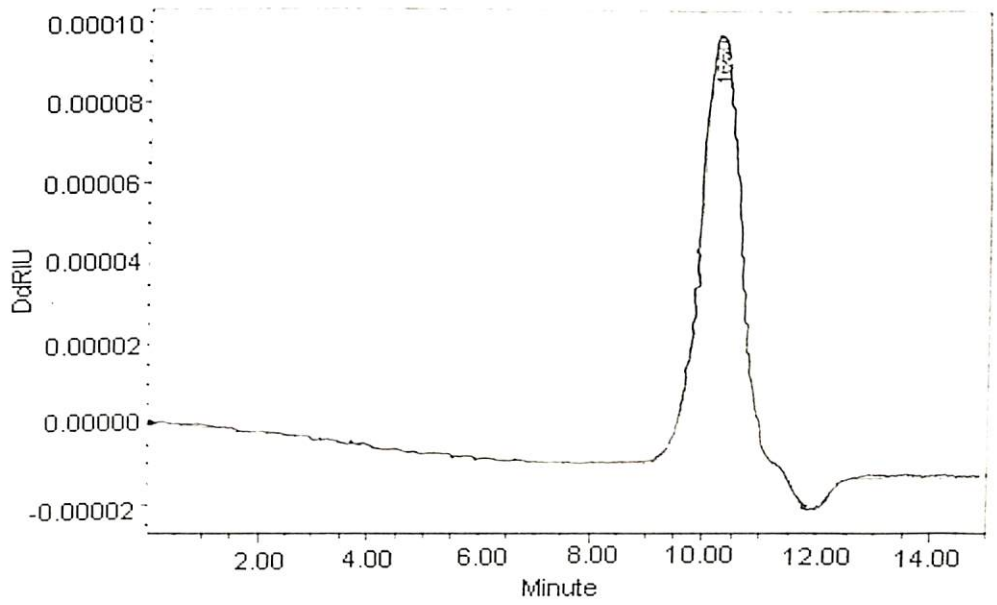

Chromatogram of the siloxane oligomer 3k

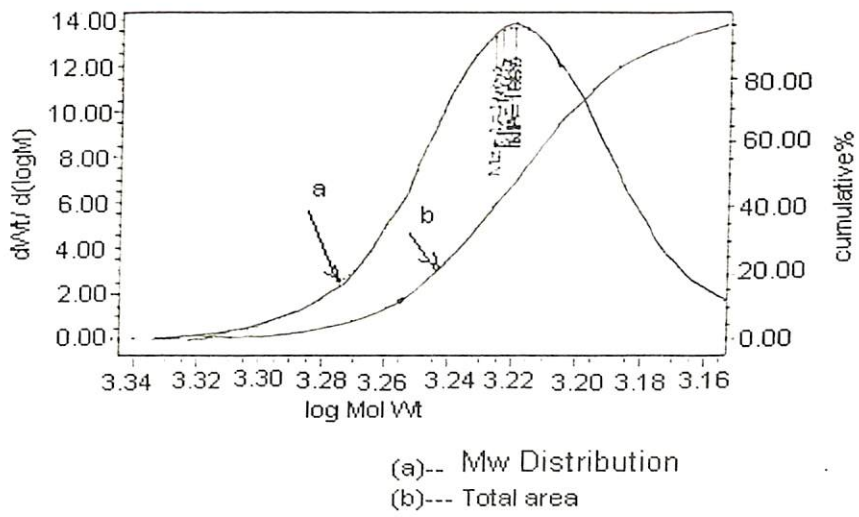

Figure 3.7 Molecular weight distribution graph of the oligomer 3k

Similarly the chromatogram along with distribution graph of siloxane oligomer condensation product of methylphenylsilane with *cis*-butenediol (table 3.3 entry 3n) is shown in the figure 3.8. This oligomer has M_w and M_n values are 1088 and 1077 respectively indicating that it is a very low molecular weight oligomer. The polydispersity of this oligomer is again very close to unity.

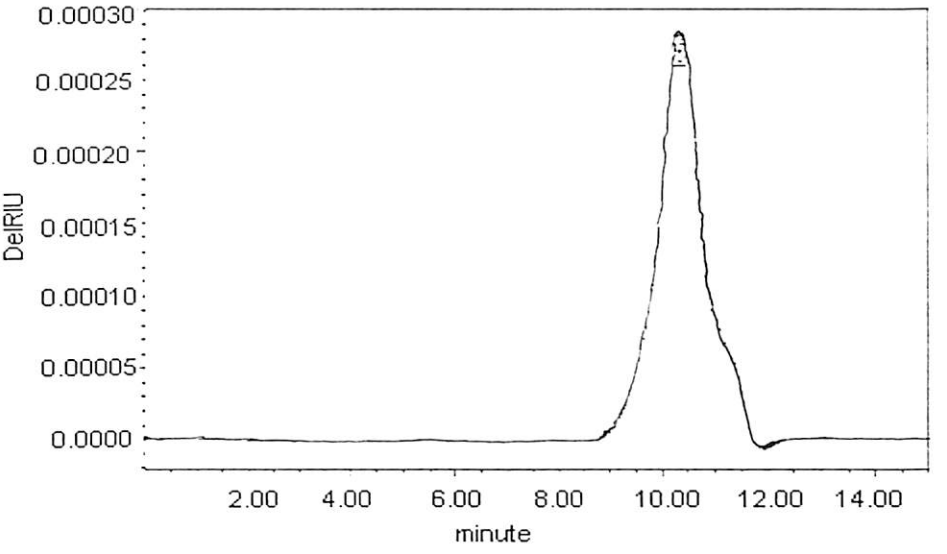

Chromatogram of the oligomer 3n (table 3.3)

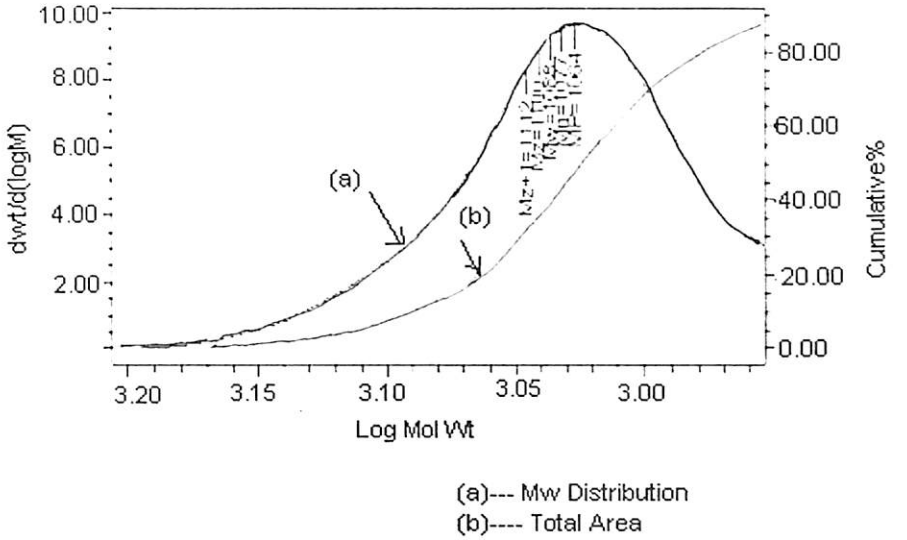

Figure 3.8 Molecular weight distribution graph of the oligomer 3n (table 3.3)

Table 3.3. Oligomerisation reactions by copper complexes

Silane	Alcohol	Oligomer	M_w values (% yield)
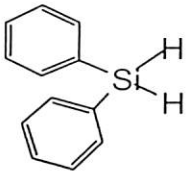	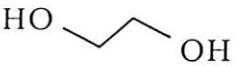	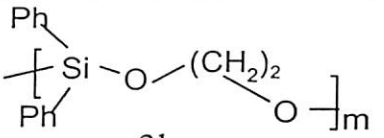 3k	M_w = 1667 (60) M_n = 1659
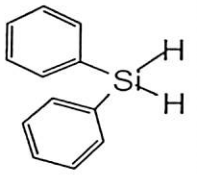		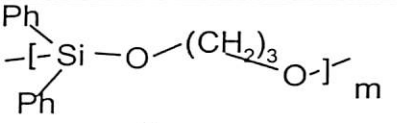 3l	M_w = 1663 (70) M_n = 1656
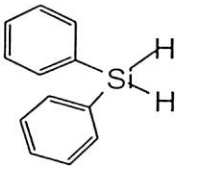		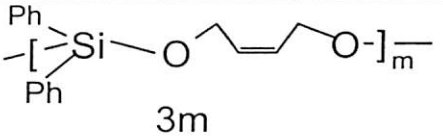 3m	M_w = 2754 (68) M_n = 2738
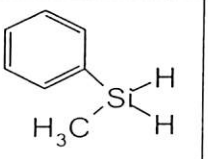	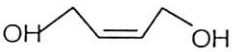	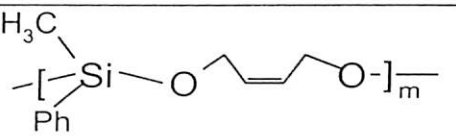 3n	M_w = 1088 (70) M_n = 1077
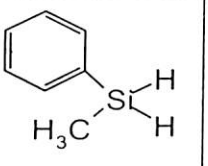	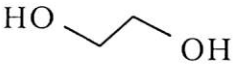	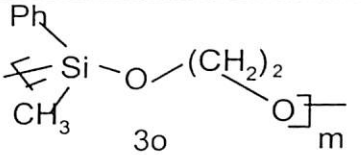 3o	M_w = 1698 (78) M_n = 1683
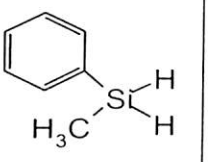		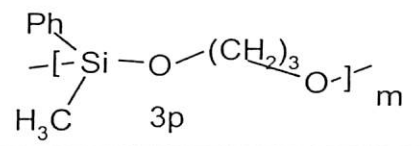 3p	M_w = 1623 (80) M_n = 1616
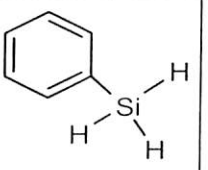	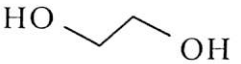	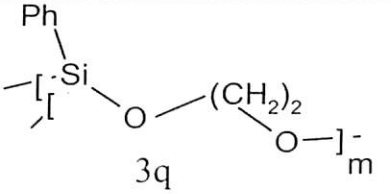 3q	M_w = 3788 (90) M_n = 3788

As the oligomerisation reaction was found to be very effective for dihydro had extended the reaction to the trihydrosilane. For this purpose the reaction between the phenylsilane with ethyleneglycol in the presence of *bis*-pyridinium tetrachlorocuprate was carried out. The reaction was found to be very rapid and completed within 30 minutes. The product formed was characterized by NMR spectroscopy and other analytical techniques. It has shown a relatively simple NMR showing the presence of bridging methyl and the phenyl groups (figure 3.9a). In proton NMR there were minor signal around 2-3 ppm arising due to the end group. These were assigned to OH either from–CH_2OH or to Si-OH. ^{13}C NMR showed the characteristic pattern of the C_6H_5Si group having three signals 128.2, 130.93, 134.5δ and ethylene carbon appear at 64.05 δ. Since there was no Si-H frequency observed in the region of 2100- 2200 cm^{-1} of IR; the oligomer should have a three dimensional network.

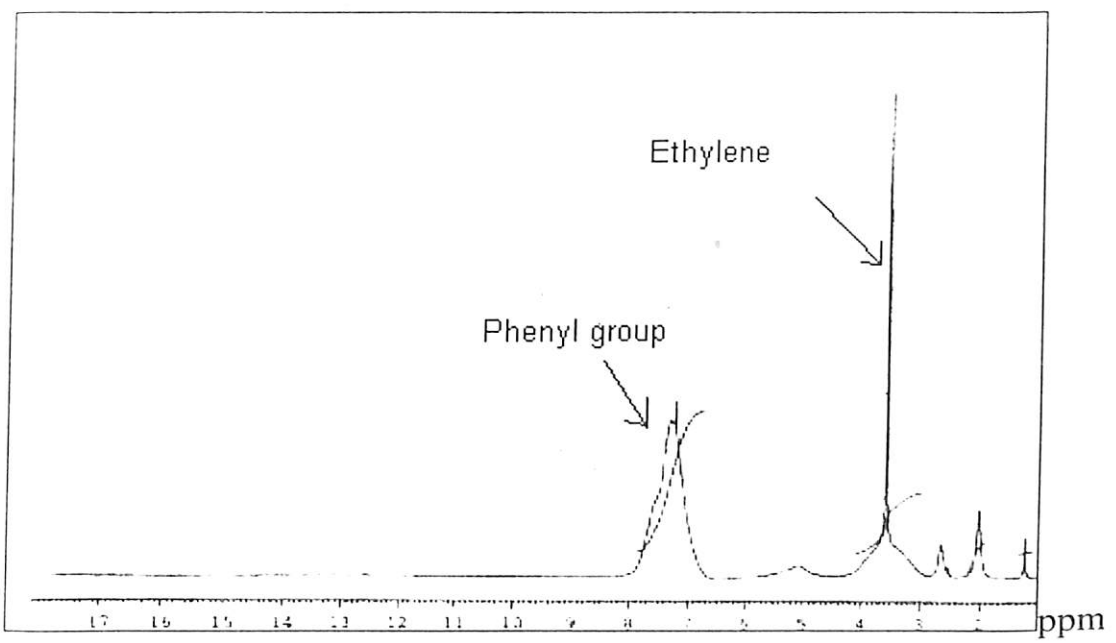

Figure 3.9a ^1H NMR spectra (400MHz) of the oligomer of phenylsilane and ethyleneglycol

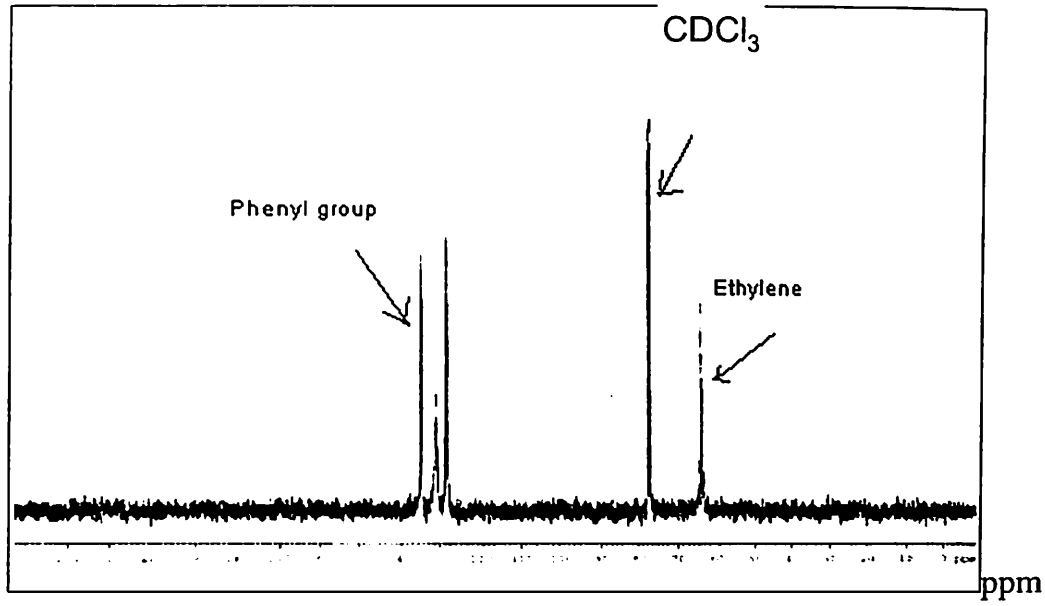

Figure 3.9b ^{13}C NMR spectra (400 MHz) of the oligomer of phenylsilane and ethyleneglycol

During this reaction deposition of metallic copper was observed. In order to ascertain this the XRD pattern of the oligomer was recorded and it showed the presence of metallic copper particle attached to the oligomer.[142-144] The powder XRD on comparison with standard sample revealed it to have peak for Cu (111) and Cu (200) diffraction at the identical place of standard metallic copper figure 3.10. Apart from these two signal a small peak shown by # arising from the siloxane was observed. The broadening of the signals was attributed to the presence of amorphous siloxane embedding the copper particles.

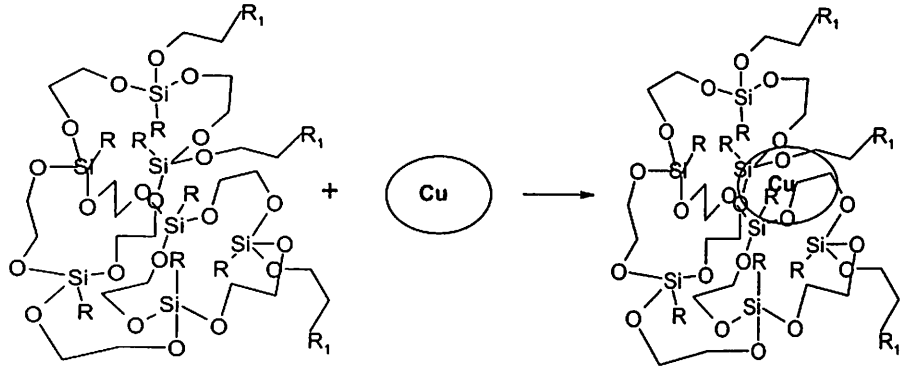

Where R_1 = extension of the siloxane framework , R = phenyl

A cross-linked structure to trap copper colloids

Scheme 3.2

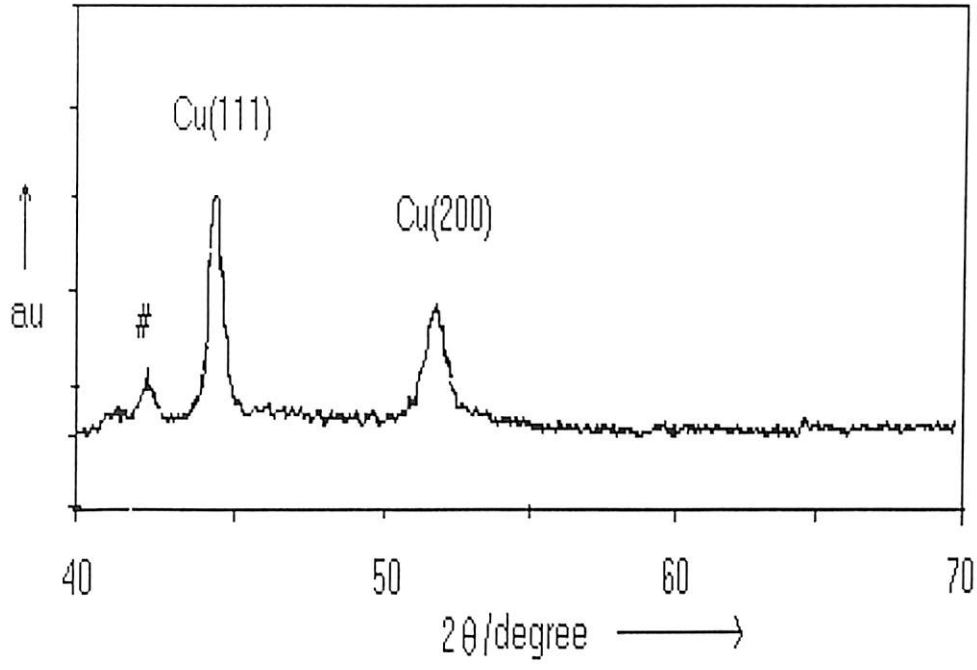

Figure 3.10 XRD of the copper colloid deposited over the glass plate from the reaction of phenylsilane with ethyleneglycol.

The SEM photograph also confirmed the presence of copper particles. The figure 3.11 shows the SEM photograph of oligomer of phenylsilane and ethyleneglycol (table 3.3 entry 3q)

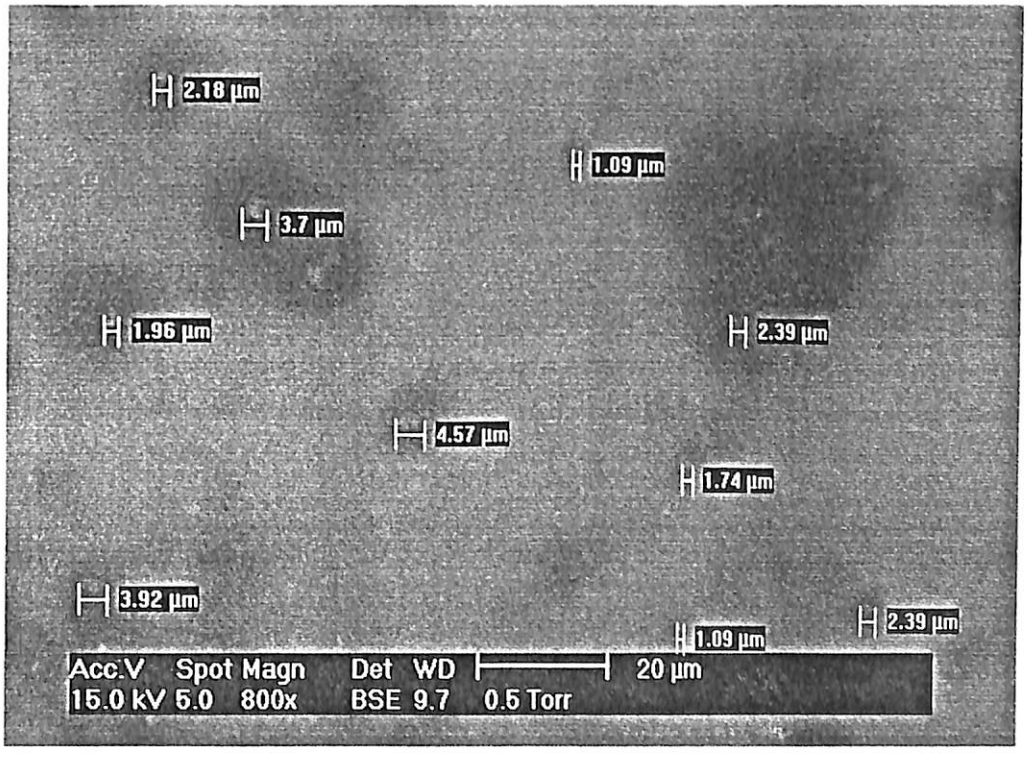

Figure3.11 SEM photograph of the metallic copper particle deposited by the reaction of phenylsilane and ethyleneglycol.

These copper particles were found to be embedded in oily mass in the SEM phot is supported by the data obtained from the surface analysis, which suggests that copper particles are above a layer of silicon. This is attributed to the siloxane matrix that is stabilizing the copper particles. The sizes of the particles were found to be in the order of 2.5 μm. The copper metallic particles are not stable and slowly undergo oxidation when exposed to air. However, they are stable under inert atmosphere. In the literature it is reported that the metallic particle of nano-dimensional size are not stable in aerial condition.[145] These results showed that the copper metal could be deposited in an electroless path by choosing suitable substrates under a mild condition thereby provides a relatively simple method for copper metal powder deposition over electro deposition[146-148]and spin coating[146] procedure. The study also complements the electroless chemical deposition of metal particles of control dimension [146,149] The possibility of substrate design for particle size control could be an added advantage of the method. The roles of metallic copper particles in organic synthesis as a catalyst are well known[150]. The copper metallic particle deposited by our method has been tested for further catalytic reactions with silanes. The copper particles are first deposited by the reaction of phenylsilane with ethyleneglycol from *bis*-pyridinium tetrachlorocuprate. For understanding of reactivity of the copper metallic particles; the reaction of triphenylsilane with ethanol in the presence of the metallic particles (10mol%) were carried out. It was observed that this reaction was assisted by the copper metallic particles and this suggested the possible participation of copper particles in zero oxidation state in the copper catalysed dehydrogenative coupling reactions. For example the reaction of triphenylsilane with ethanol gave the corresponding silylether at 60^0C with the copper particles (with approximately 10mole % conversion in 4hrs) prepared by an independent reaction of *bis*-pyridinium tetrachlorocuprate with phenylsilane and glycerol.

Based on all these observations and results from the silicon oxygen bc reaction the following reaction mechanism may be proposed for tetrachlorocuprate catalysed silicon-oxygen bond forming reactions scheme 3.3.

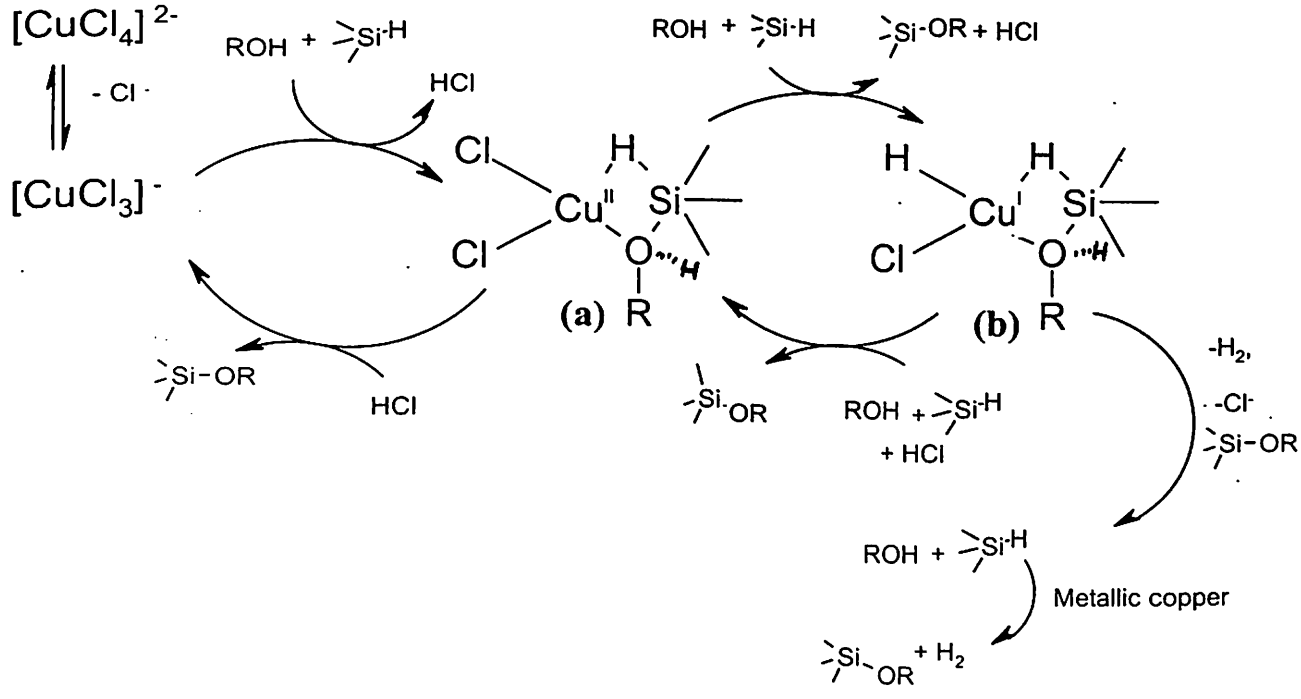

Scheme 3.3

In this mechanism both Cu(II), Cu(I) as well as metallic copper particles takes part in the reaction between alcohol and silane to give silylether. From entire study on dissociation of $[CuCl_4]^{2-}$ to $[CuCl_3]^-$ species it is presumed that in protic solvent $[CuCl_3]^-$ ions formed which underwent further reaction. Tetrachlorocuprate can directly react with alcohol and silane to generate HCl and copper silane intermediate (**a**) in which the oxidation states of copper is Cu(II). This copper silane intermediate can also formed from $[CuCl_3]^-$ complex. This intermediate (**a**) reacts further with alcohols and silane to give silylether and generates HCl, in this process intermediate (**a**) is transformed to another intermediate (**b**) where the oxidation states of copper is Cu(I). The intermediate (**b**) liberates H_2 (g), HCl and generates

silylether, in this process Cu(I) is transformed to metallic state which reacts alcohol and silane to give silylether. On the other hand the intermediate (**b**) again may react with alcohols and silane to give silylether in this process (**b**) is transformed to (**a**), similarly intermediate (**a**) in presence of HCl can give silylether and produce back the catalyst.

3.1.4 Deposition of metallic gold particle by the reaction of silanes and dihydric alcohols

In the literature it is reported that gold metallic particle can be deposited by reductive method.[151-152] Since gold belongs to the same group of copper, we carried out similar reductive reactions with gold also. It was found that the reaction of phenylsilane and ethyleneglycol in the presence of $H_2[AuCl_4]$ gives metallic gold particle. The SEM photograph of gold deposited by the reaction of phenylsilane and ethyleneglycol as well as reaction of methyl phenylsilane and ethyleneglycol is shown in figure 3.12. The SEM photograph shows that in this case gold is not supported over siloxane. This result is also confirmed from the XRD of the deposited gold particle (figure 3.13). Sharpness of the XRD peaks clearly indicates the free nature of the gold particle i.e. they are unsupported by siloxane. It is also interesting to note that the gold deposition is much faster than the copper and is instantaneous. Thus it is believed that the copper particle deposition follows secondary process of siloxane formation while the reduction of gold is a primary process having very less probability of being attached to the oligomer formed. The identity of gold particles were ascertained by SEM as well as XRD. The XRD has clear peaks at (100), (200) and (220) plane respectively.

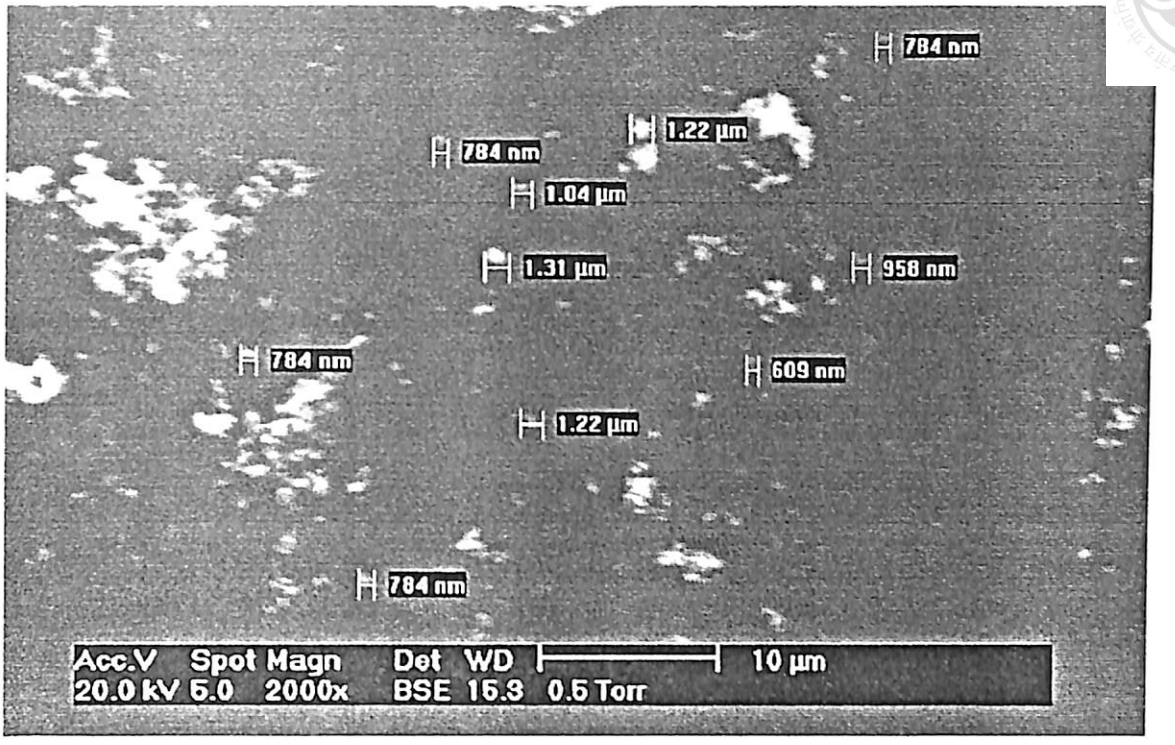

Figure 3.12 SEM photograph of the gold particle deposited by phenylsilane and ethyleneglycol on reaction with $H_2[AuCl_4]$

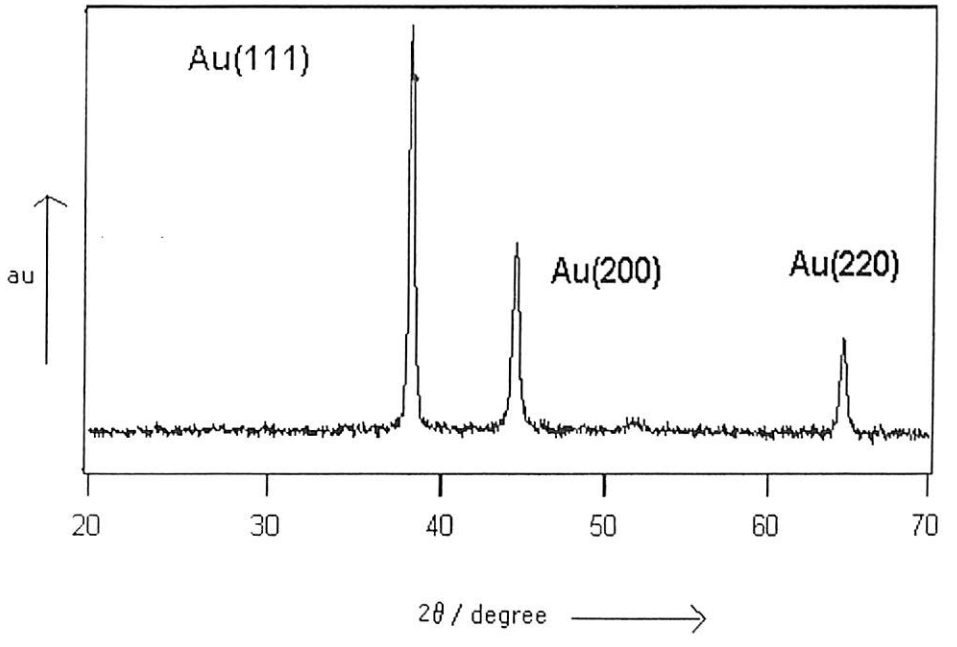

Figure 3.13 XRD of gold particle deposited by the reaction of phenylsilane and ethyleneglycol with $H_2[AuCl_4]$

Variation of substrate changes the particle sizes. The deposited gold particle copper has different average particle size and the details of the result from SEM are given in the table 3.4.

Table 3. 4

Sample	Details	Average particle size
$MePhSiH_2$ + $H_2[AuCl_4]$ + Ethyleneglycol	Sample contains a single type of structure with relatively similar mesh size	Single mesh size= 412.4 µm
$PhSiH_3$ + $H_2[AuCl_4]$ + Ethyleneglycol	Sample contains a single type of structure with relatively similar mesh size	Single mesh size= 948nm
$MePhSiH_2$ + *bis*-pyridinium tetrachlouprate + Ethyleneglycol	Sample contains a structure of two different mesh-sizes	Large mesh size= 535.3µm Small mesh size=1.64 µm
$PhSiH_3$ + *bis*-pyridinium tetrachlouprate + Ethyleneglycol	Sample contains large structures, as well as smaller fragments, which were measured. These fragments appear to be surrounded by "dark pools", possibly water or oil.	Single mesh size= 2.5 µm

The 1,3,5 trihydroxybenzene has tetrameric structure and exists in an ordered form in solid state. Thus expecting the effect of such orderly structure on the deposition of gold particles the patterning were attempted. But the attempt was not successful. In all cases the metallic gold particles were obtained having uniform particles size ranging from 0.9-5.37µm (see SEM photo expt. Section). The patterning of the gold were attempted with the 1,3,5 trihydroxybenzene and phenylsilane but the attempt was not successful.

3.1.5 Some related oxidative reactions catalysed by tetrachloro complexes

It is already mentioned that the phenols are not good substrate for tetrachlorocuprate catalysed silicon-oxygen bond forming reaction. When phenol and silane are heated together with tetrachlorocuprate a black solution was obtained which contains a mixture of compounds that could not be characterized. So we looked for the reactivity of different aromatic compounds with tetrachlorocuprates. Several reactions with *bis*-pyridinium trachlorocuprate in presence of co-oxidants were carried out are shown in the scheme 3.4

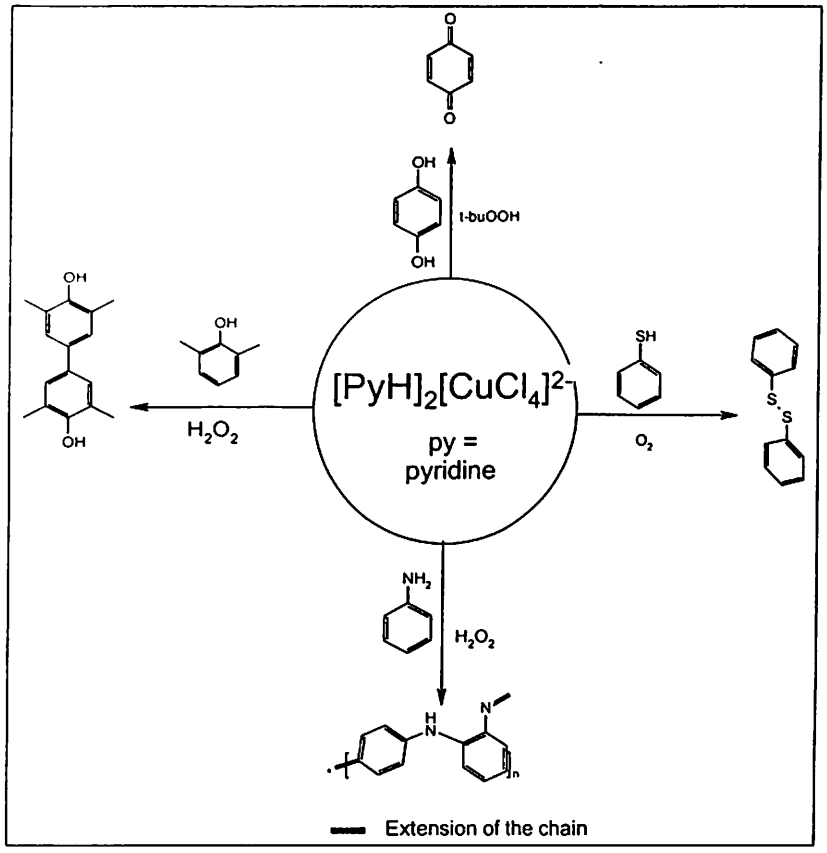

Scheme 3.4

The oxidation of 2,6-dimethylphenol by *bis*-pyridinium tetrachlorocuprate with H_2O_2 as co-oxidant gives the 4,4-dihydroxy-3,5,3,5-tetramethylbiphenyl(I) major and 4-(3,6-dimethylcyclohexa-2,5-dienone)-methylidene-2,6-dimethyl-cyclohexadienone(II) minor.

The major product was purified and characterized. The mass spectrum of the c shown in the figure 3.14.

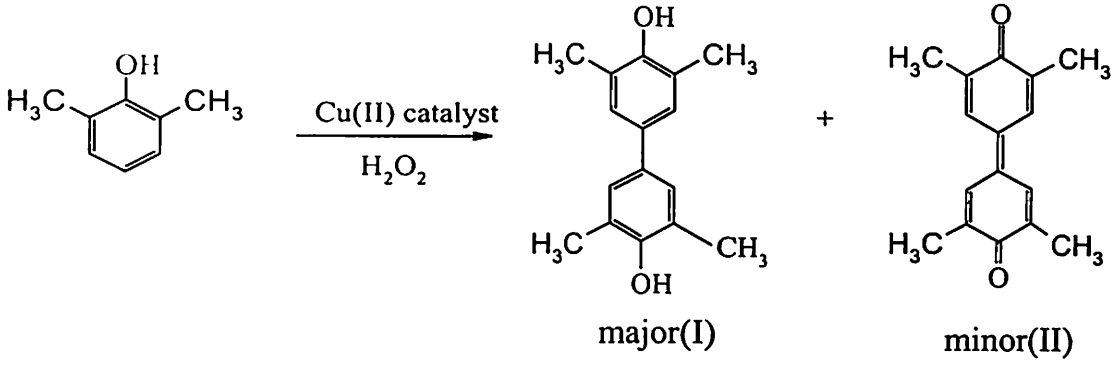

Equation 3.7

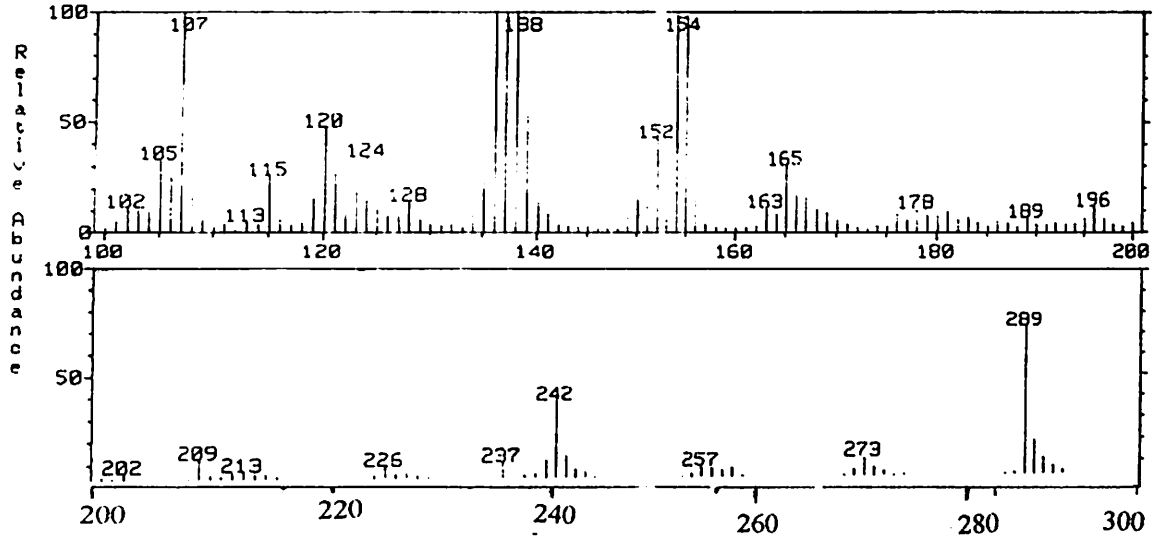

Figure 3.14 The FAB mass spectra of 4,4-dihydroxy-3,5,3,5-tetramethylbiphenyl (I) in m-Nitrobenzyl alcohol matrix

The FAB mass spectrum of the above compound was recorded at room temperature and m-nitrobenzylalcohol was used as the matrix. Thus peaks appear at m/z 136, 137, 154, 289 are due matrix. The molecular ion peak is at m/z 242 and other fragmentized peaks at 226, 213, 209, 202, 196, 189 etc. are present.

The oxidative polymerization of 2,6-dimethylphenol is an important reaction and it leads to novel phenylene oxide polymers[153] However in such reaction formation of 4-(3,6-

dimethylcyclohexa-2,5-dienone)-methylidene-2,6-dimethyl-cyclohexadienone(II) the polymerization process[154]. In the *bis*-pyridinium tetrachlorocuprate catalysed reaction this product 4,4-dihydroxy-3,5,3,5-tetramethylbiphenyl (I). The product (II) may be formed from the oxidation of (I) by copper catalyst. The dimeric compound (II) has absorption at 414 nm with a very high extinction coefficient 9.05×10^{4} Litre mol^{-1} cm^{-1} . The methanolic solution of the *bis*-pyridinium tetrachlorocopper complex does not have absorption in this region. So advantage of this point was taken and the reaction was monitored with different catalyst concentrations. The growth of absorption maximum at 414nm is shown in figure 3.15.

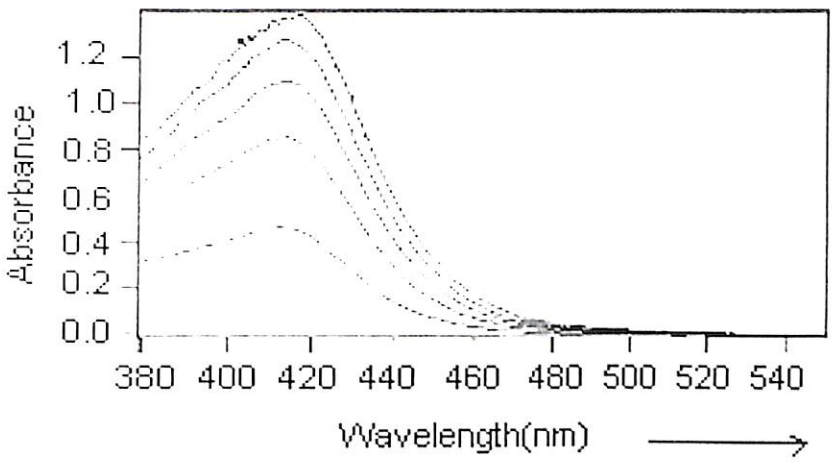

Figure 3:15 Visible spectroscopic study of reaction of 2,6-dimethylphenol (12.8mg, 0.105mmol) by *bis*-pyridinium tetrachlorocuprate (3mg, 0.01mmol) in the presence of hydrogen peroxide (30µl , 30%)in methanol ($3cm^3$)

The effect of concentration of copper(II) complex for three different ratios of copper and the substrate is illustrated in figure 3.16. From the figure it is apparent that the reaction can operate with catalyst concentration of one tenth of the ratio of substrate to catalyst but increase of catalyst concentration does not significantly effect the formation of 4-(3,6-dimethylcyclohexa-2,5-dienone)-methylidene-2,6-dimethyl-cyclohexadienone(II). Control experiments with hydrogen peroxide without the catalyst under the similar reaction condition

did not give C-C coupled product of 2,6-dimethylphenol; this was confirmed by study also. This result suggested that side product was initially formed in the reaction did not increase and formation of this product was independent of catalyst concentration.

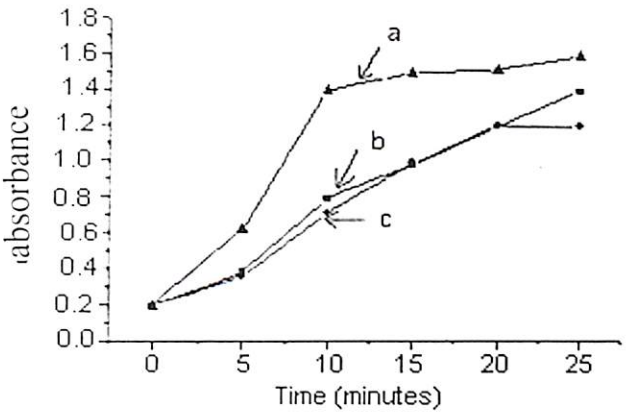

Figure 3:16 The concentration dependence of catalyst on dimerisation of 2,6-dimethyl phenol by *bis*-pyridinium tetrachlorocuprate (1a) along with H_2O_2 at 30^0C measured at 414nm (a) phenol: (1a) = 30: 1; (b) phenol: (1a) = 10:1; (c) phenol: (1a) = 6: 1

initially formed in the reaction did not increase and formation of this product was independent of catalyst concentration.

Aromatic dihydroxy compounds such as 1,4-dihydroxy benzene 1,4-dihydroxy naphthalene reacted with catalytic amount of *bis*-pyridinium tetrachlorocuprate in the presence of tertiary butyl hydroperoxide as an co-oxidant. Similarly, the reaction of aromatic thiol such as thiophenol gives corresponding disulfide when reacted with catalytic amount *bis*-pyridinium tetrachlorocuprate. These study oxidative reactions of the activated aromatic by tetrachlorocuprate suggests that the activated aromatic substrates prefers oxidative transformations rather than O-silylation reaction. .

Chapter 4

Palladium catalysed silicon-oxygen bond formation

4.1.1 Background

The copper (II) catalysed silicon-oxygen bond forming reactions described in the earlier chapter has several limitations. Some of the disadvantages of the copper (II) catalysed silicon-oxygen bond forming reactions are a) the copper (II) catalysed silicon-oxygen bond forming reactions are relatively slower than the lower transition metal complexes c) these reactions proceed at elevated temperature d) ratio of substrate to catalyst required in the reactions are relatively less d) aromatic hydroxy compounds do not react with silane in the presence of copper (II) catalyst e) oxidative reaction of phenolic compounds is possible. In order to overcome these limitations there is need for search for new catalyst for these reactions.

It is reported in the literature that the group-8 metals and metal halides catalyse the dehydrogenative condensation of silane with amines, alcohols and thiols.[156-160]Although numerous studies on the scope of these processes have been made, such a study are generally focused on monohydrosilanes. This is possibly due to the disproportionation reactions of polyhydrosilanes.[161] Among the catalysts, rhodium catalyzed silicon-oxygen bond-forming reactions have been extensively studied.[162] Palladium catalyzed silicon-oxygen bond forming reactions are known, study on the versatility of such reactions are not investigated.[163] In addition to these we have illustrated earlier that copper(I) can be an active catalyst for Si-H bond activation. copper(I) has a d^{10} electronic configuration. The literature suggests that palladium(0) can be formed *in situ* during palladium(II) catalysed reactions of silane and can

be an active catalyst. Palladium(0) has also d^{10} electronic configuration and thus in reactivity of palladium(0) and copper(I) is expected.

Palladium complexes have very wide applications in organic reactions as catalysts. Palladium complexes are among the most readily available easily prepared and easily handled transition metal catalysts. Their real synthetic utilities relies in the specificity and functional group tolerance.[164-165] It can tolerate functional groups like carbonyl and hydroxyl group, so palladium complex catalyzed reactions can be carried out without protection of this functional group. Another advantage of palladium catalysed reactions is that they are not very sensitive to oxygen and moisture (except those with phosphorous based ligand) or even to acid. They permit unconventional transformations and give the synthetic chemist a wide range of choice of starting materials.

It is generally the facile redox interchange between the Pd(0) and Pd(II) oxidation states that is responsible for the catalytic chemistry that are caused by palladium complexes. The most common starting materials for most palladium complexes is palladium (II) chloride; it is a chloro-bridged polymer, insoluble in most organic solvent (scheme 1.I). The polymeric structure can be easily broken by donor ligands (L) resulting in monomeric $PdCl_2L_2$ complexes stable to air and soluble in most common organic solvents. The nitrile complexes $[PdCl_2(RCN)_2]$ are labile to easily vacate coordination site making them excellent choice for catalysis.

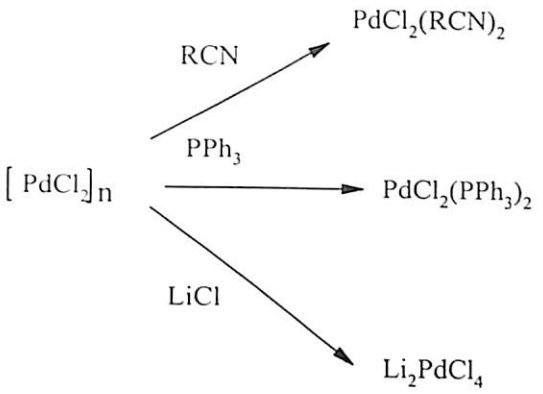

Scheme 4.I

In contrast to the nitrile ligand, the phosphine are less labile and are also infrequently used in catalysis, one frequently used catalyst precursor of choice for palladium(0) catalyzed processes is $[(PPh_3)_2PdCl_2]$. Palladium(II) salts can be used as source of palladium(0), for example, $Pd(OAc)_2$ is easily reduced to Pd(0) complexes *in situ* in the presence of phosphine ligands with several reducing agents,[166] such as $NaBH_4$, $LiAlH_4$, alcohols etc.

It has been reported in the literature that palladium(0) and palladium(II) complexes are the active catalyst for silicon-oxygen bond forming reactions[163, 167]. Palladium supported on charcoal[168] and bulk palladium metal, palladium generated in situ from $PdCl_2$ by trialkylsilane as the reducing agent are active catalyst for silicon-oxygen bond forming reaction. Most of the palladium complexes, which were used for silicon-oxygen bond forming reactions, have phosphorous-based ligand, which are air as well as moisture sensitive.[169] The search of air stable palladium complexes as catalysts is important as siloxanes are abundant in nature and their formation in aerobic condition is desirable. With this aim we prepared a series of air stable palladium (II) complexes having bidentate nitrogen donor ligand and their catalytic activity towards silicon-oxygen bond forming reactions were studied. Air stable palladium (II) complexes having nitrogen as donor ligand with composition $PdLCl_2$ [where L = N, N′-tetramethylethylenediamine (TMEDA), N, N′-tetraethylethylenediamine (TEEDA), N, N′ diethylenediamine(DED) etc] were studied as

catalyst for Si-O bond forming reactions. They have the structural features as sho 4.1.

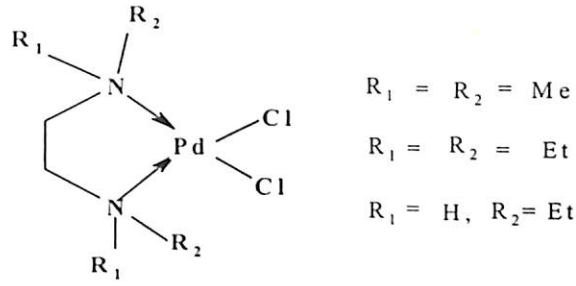

Figure 4.1

The palladium complexes were synthesized by general synthetic procedure by refluxing $PdCl_2$ in dry acetonitrile solution and then adding the desired ligand in hot solution (refer to experimental section.). The characterisations of these complexes were done by recording their elemental analysis and also by estimating chloride. Their structures were established from their spectroscopic features. As an illustrative case the IR spectra of $Pd(TMEDA)Cl_2$ is shown in figure 4.2. The tetramethylethylenediamine has stretching frequency due to methyl group in the region 2950 and 2717 cm^{-1} on complexation these appear at 3025 and 2845cm^{-1} respectively. Medium intensity C-N stretching frequency present at 1260cm^{-1} appears in the complex at 1285cm^{-1}.

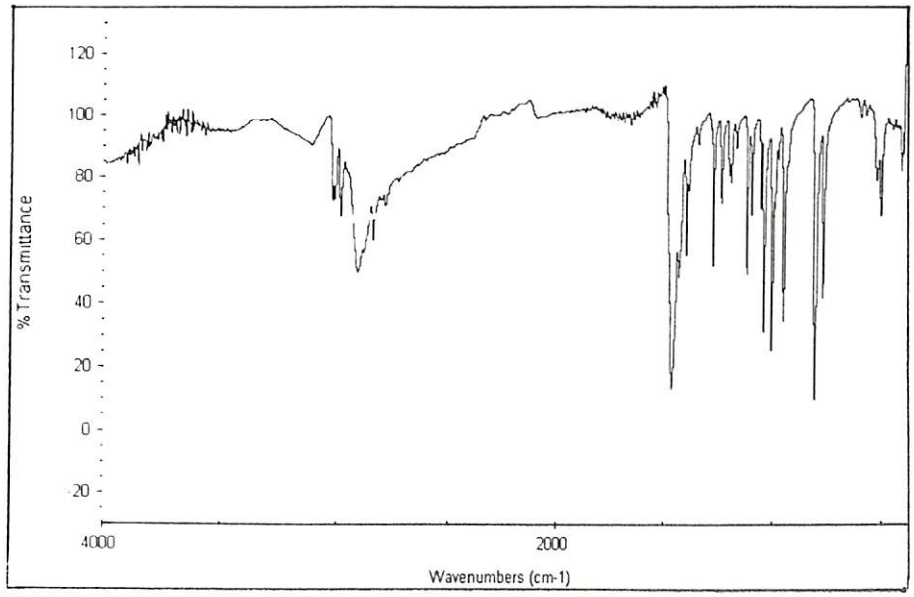

Figure 4.2 IR (KBr) spectra of $Pd(TMEDA)Cl_2$

4.1.2 Palladium catalysed silicon-oxygen bond forming reactions

We observed that these palladium complexes(figure 4.1) are capable of catalyzing silicon-oxygen bond forming reactions of different silanes with various alcohols and phenols. The silylethers could be prepared in quantitative yield by palladium complex catalyzed reactions. The dihydro- and monohydrosilanes can be converted to corresponding silylethers on reaction with alcohols and phenols, which is shown in equation 4.1and 4.2.

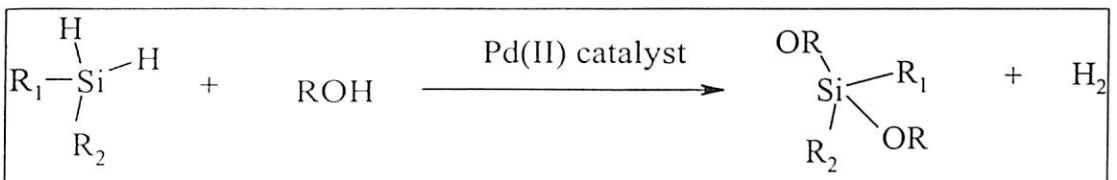

R = alkyl or aryl
$R_1 = R_2 = Ph$
$R_1 = Ph, R_2 = Me$

Equation 4.1

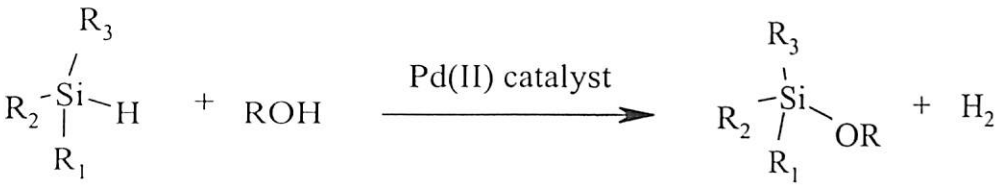

R = alkyl or aryl
$R_1 = R_2 = R_3 = Ph$
$R_1 = R_2 = R_3 = Et$

Equation 4.2

The progress of the reactions was monitored by thin layer chromatography and gas chromatography. These reactions accompanied evolution of hydrogen that could be visible from the gas bubbles during these reactions. On completion of the reaction hydrogen gas

evolution ceases. Wide ranges of alcohols were converted to corresponding sily

list of alcohols that were converted to silylethers along with the reaction conditions is given in tables 4.1 and table 4.2. A wide variety of primary, secondary and tertiary alcohols

Table 4.1. Pd(TMEDA)Cl_2 catalysed Si-O bond formation on monohydrosilanes

Substrate	Alcohol/ Phenol	Product	Reaction condition (Isolated % yield)
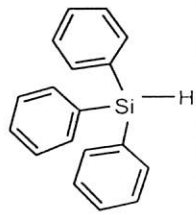	CH_3OH	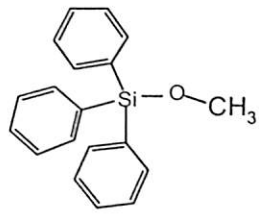	40^0C, 2 hrs (93)
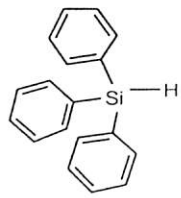	CH_3CH_2OH	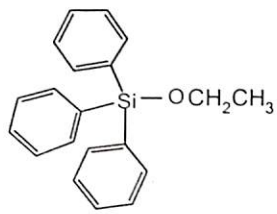	40^0C, 2 hrs (90)
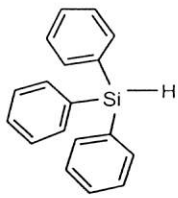	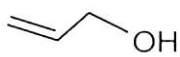	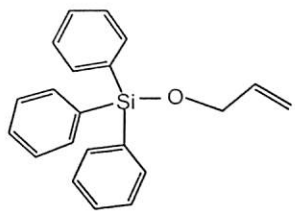	40^0C, 1.5 hrs (92)
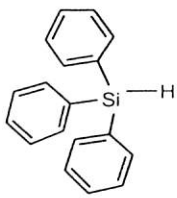	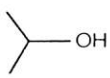	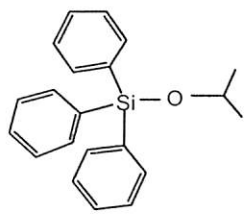	40^0C, 1.5 hrs (92)
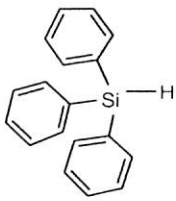	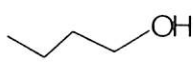	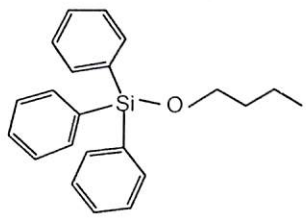	40^0C, 3 hrs (80)

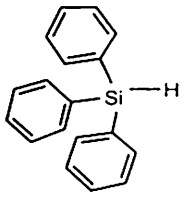	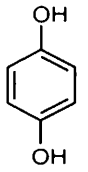	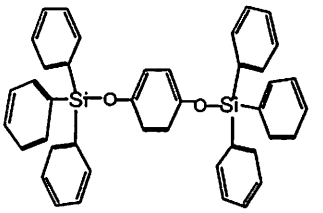	40^0C, 2 nrs (85)
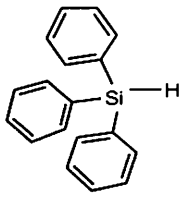	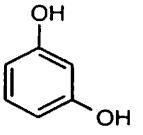	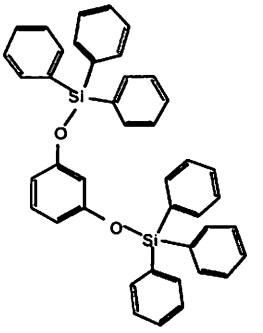	50^0C, 5 hrs (55)
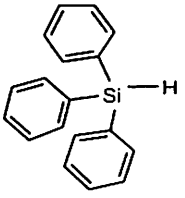	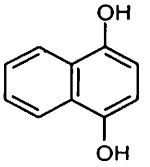	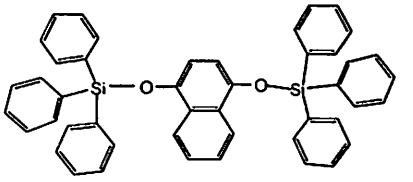	50^0C, 5 hrs (50)
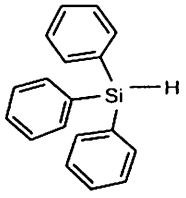	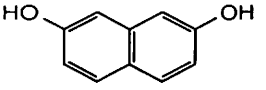	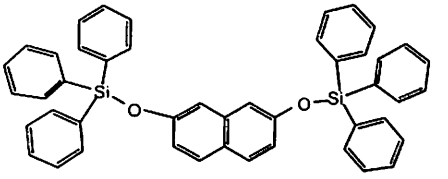	50^0C, 2 hrs (30)
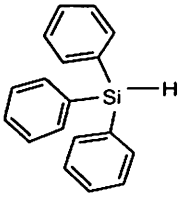	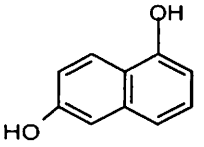	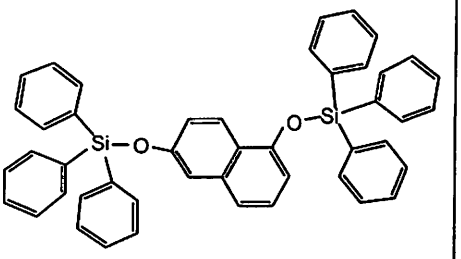	50^0C, 2 hrs (67)
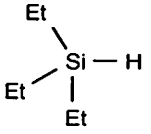	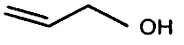	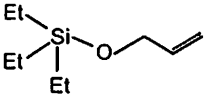	45^0C, 1.5 hrs (80)
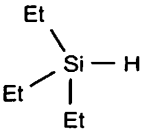	CH_3CH_2OH	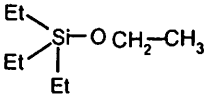	45^0C, 1.5 hrs (85)

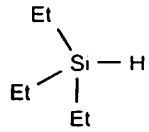	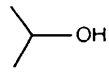	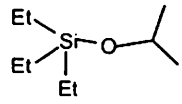	45^{0}C, 1.5 hrs (70)
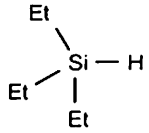	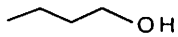	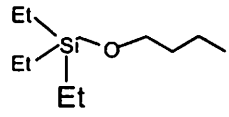	45^{0}C, 1.5 hrs (82)
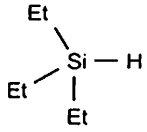	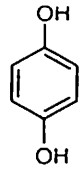	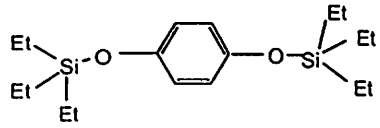	45^{0}C, 1.5 hrs (56)
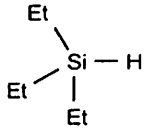	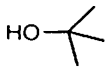	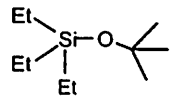	45^{0}C, 2.5 hrs (40)
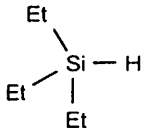	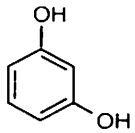	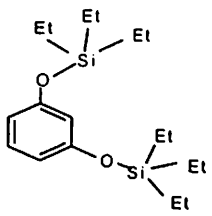	45^{0}C, 2 hrs (50)
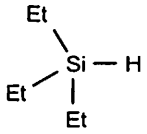	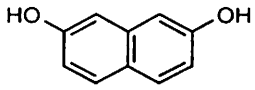	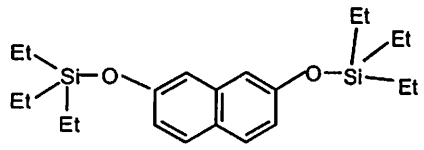	60^{0}C, 2 hrs (55)
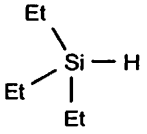	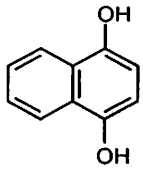	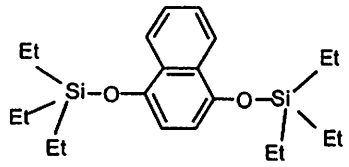	60^{0}C, 2 hrs (50)

Table 4.2. $Pd(TMEDA)Cl_2$ catalysed Si-O bond formation on dihydrosilan

Substrate	Alcohol/ Phenol	Product	Reaction condition
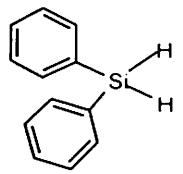	CH_3OH	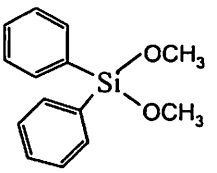	RT, 1.5 hrs. (55)
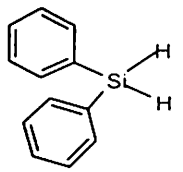	CH_3CH_2OH	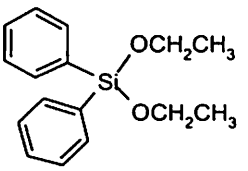	RT, 1.5 hrs. (50)
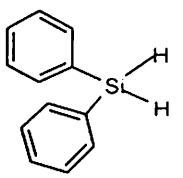	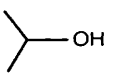	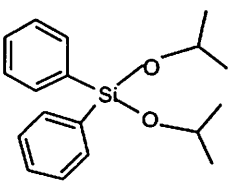	RT, 2 hrs. (45)
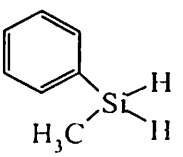	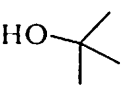	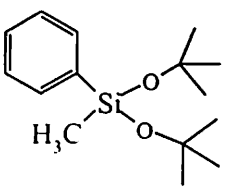	RT, 1.5 hrs. (57)
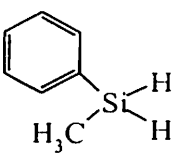	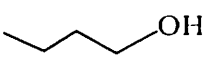	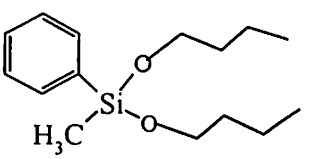	RT, 1.5 hrs. (30)
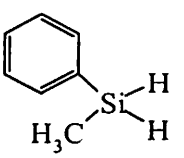	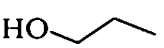	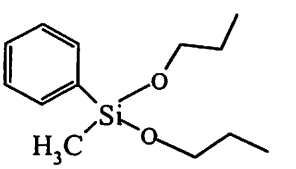	RT, 1.5 hrs. (40)
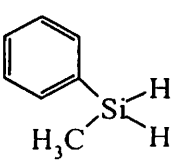	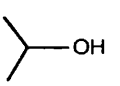	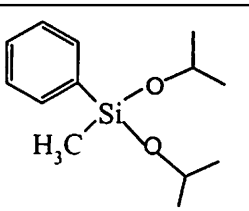	RT, 2 hrs. (80)

could be converted to the corresponding silylethers. The quantitative reaction can be seen either by the NMR spectra of the crude mixture. For example the reaction of triphenylsilane

with methanol in the presence of catalytic amount of Pd(TMEDA) triphenylsilylether as only the product. The proton NMR spectra of the crude reaction mixture after filtration show exclusive formation of the methylsilyl ether. The product has two sets of signals, the signal at 7.4-7.5δ (m, 15H) is due to aromatic proton and signal at 3.6δ (s, 3H) is

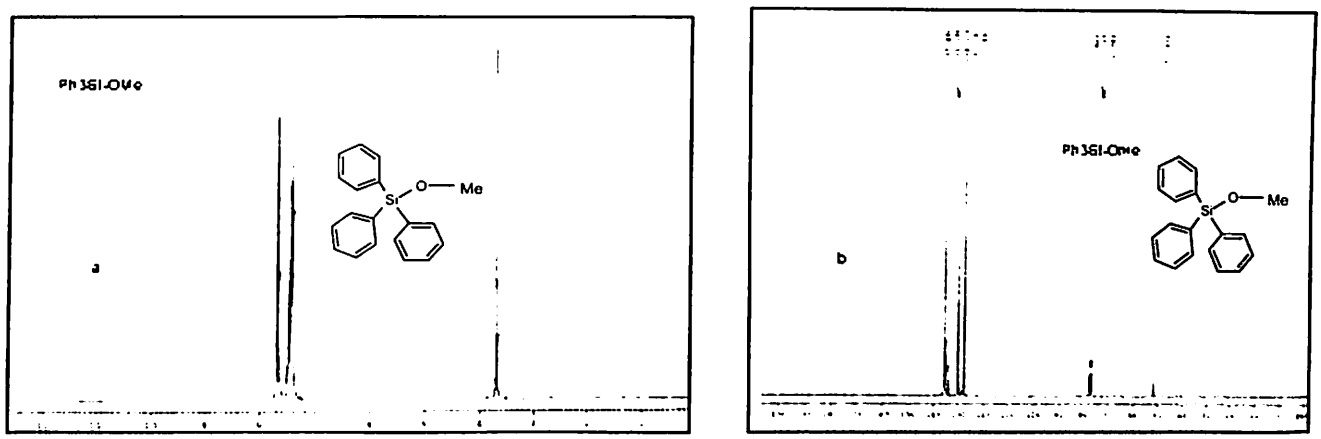

Figure 4.3 (a) ^{1}H NMR spectra (b) ^{13}C NMR spectra of the crude product from the reaction between methanol and triphenylsilane catalyzed by $Pd(TMEDA)Cl_2$

3.6δ (s, 3H) is due to methoxy proton. It is reflected in the ^{13}C NMR of the compound also; the ^{13}C NMR has two sets of signal, one set of four signals at 127.9, 130.1, 134.0, 135.4δ is due to aromatic carbon and signal at 51.9δ is due to methoxy carbon. The catalyst could be precipitated by adding hexane to the reaction solution hence, these reactions have a very simple workup procedure. In this type of palladium catalyzed silicon-oxygen bond forming reactions we observed that phenols reacts much slower (generally heating is required) than an aliphatic primary alcohols. In terms of reactivity dihydrosilanes were more reactive than monohydrosilanes. The reactions were applicable to double bond containing alcohol such as allylic alcohols. In these reactions the double bond were not affected. For example the reaction of triphenylsilane with allyl alcohol gave the corresponding allylsilylether. The ^{1}H NMR and the ^{13}C NMR clearly discerns the identity of the product. The compound Ph_3Si-

OCH_2-CH=CH_2 has signals at 7.3-7.7δ due to aromatic protons and signal at 6.0δ CH=) proton and signal at 5.2δ is due the proton β to the allylic position. The signal due to-OCH_2- protons appears at 4.4δ. In ^{13}C NMR the compound has signals at 64.7 δ due to OCH_2 carbon, signal at 136.7δ is due (CH=) carbon and signal at 114.71δ is due to (=CH_2) carbon. In addition to this the signal due to aromatic carbons appear at 135.2, 134.2, 130.1, 127.9δ. The reaction is applicable to the tertiary alcohol also, for example the reaction of triethylsilane with tertiary butyl alcohol gave the corresponding silylether of *t*-butanol in near quantitatiive yield when carried out with 10mol% of Pd(TMEDA)Cl_2 catalyst.

Since Si-H frequency appears in the region of 2100-2200cm^{-1} and in this region, the other substrates including the catalyst has no absorbance, the product transformations could be ascertained by monitoring the Si-H frequency in the product. The Si-O bond formation in the product also becomes apparent in each of the cases, as the Si-O stretching appear as strong absorptions in the region of 1100-1200cm^{-1}.

The reaction is very effective for dihydrosilanes and various alcohols were reacted with dihydrosilanes such as diphenylsilane and methylphenylsilane to give the corresponding silylethers. These reactions were very specific for di-substitutions and led only dialkoxysilylethers, while attempting to prepare the mono-alkoxysilylethers invariably the siloxanes of the parent silane were isolated.

Different dihydroxy phenols could be converted to their ethers in quantitative yield. These reactions are useful as it would give an idea on the suitability of the catalyst for oligomerisation reaction. Among the various dihydroxy aromatic the reactions of 1,4 dihydroxy, 1,3-dihydroxy phenol and 1,4-naphthalenediol, 1,6-naphthalenediol, 2,7-naphthalenediol with triethylsilane, triphenylsilane etc gave the corresponding ethers. The

mass spectra of two naphthyl ethers are shown in figure 4.4. In all cases the m/ similar but the fragmentation patterns are different.

For example the fragmentation pattern of the product of 1,4-naphthalenediol and triphenylsilanes are (in m/z) 105, 181, 199, 259, 443, 521, 676. Whereas the fragmentation pattern of the product of 2,7-naphthalenediol and triphenylsilane are (in m/z) 105, 136, 165, 181, 199, 207, 259, 379, 457, 521, 599, 676. The presence of common peak at m/z 676 is due to molecular ion peak and peak at m/z 259 is due to $(C_6H_5)_3Si^+$ (base peak). The other peaks are due to the loss of phenyl group from the molecular ion peak and base peak respectively.

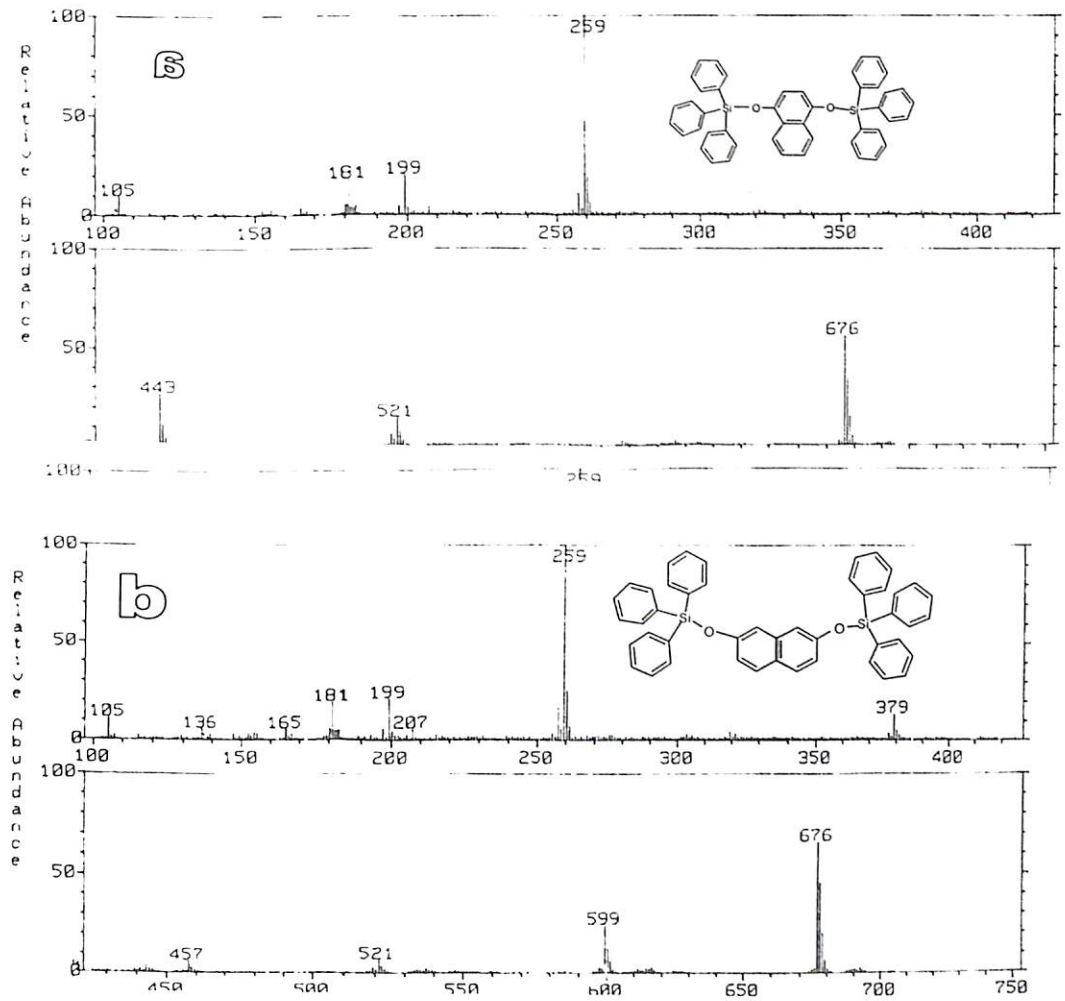

Figure 4.4 (a) Mass spectra of the condensed product of 1,4-naphthalenediol and triphenylsilane (b) Mass spectra of the condensed product of 2,7-naphthalenediol and triphenylsilane.

The relative catalytic efficiency of different palladium (II) complexes (TMEDA) Cl_2, Pd (DED)Cl_2, Pd (COD)Cl_2, Pd (TEEDA)Cl_2 were studied by the alcoholysis reactions of triphenylsilanes with ethanol and monitoring the reactions after definite interval of time in GC (figure 4.5). The kinetics of the reaction between triphenylsilane and ethanol was monitored in the presence of different catalysts. The product formation versus time is plotted for the reaction of triphenylsilane (0.065mmol) with ethanol in presence of different catalyst (0.0037 mmol) is shown in the figure 4.5. There is a definite induction time in each case and the induction time is dependent on the catalyst.

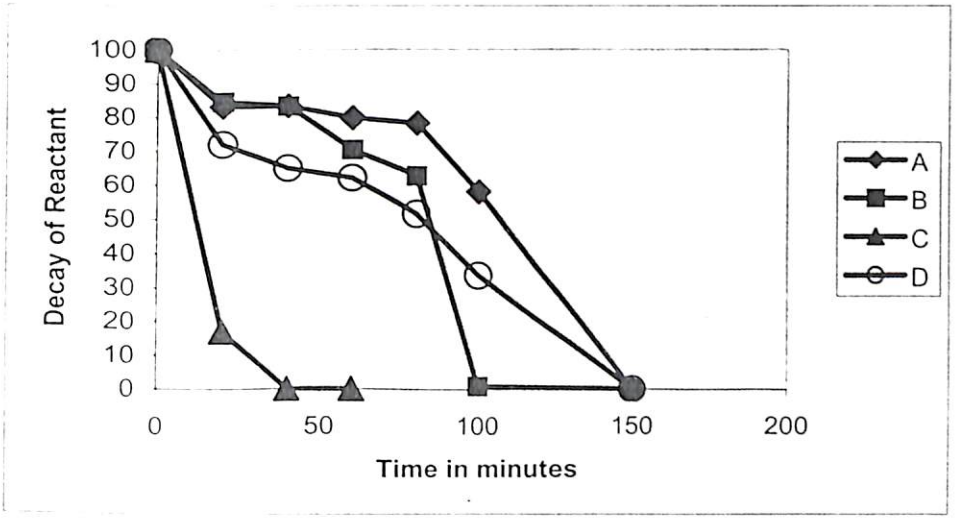

Figure 4.5 The decay of triphenylsilane during its reactions with A = Pd (TMEDA) Cl_2; B = Pd (DED) Cl_2; C = Pd (COD) Cl_2; D= Pd (TEEDA) Cl_2

The reaction gave exclusively silylether without any other side product. No degradation of the product to side product was also observed during these reactions. The decay profile as shown in figure 4.5 of the triphenylsilane showed that for each catalyst there was an induction period after which the reactions become very fast; this is possibly due to palladium colloid formation, which is more active catalyst for silicon-oxygen bond formation. Participation of colloidal palladium in silicon-oxygen bond forming reactions have been already reported by many authors.[167] The reactions of [Pd(COD)Cl_2]$_2$ was found to

(where COD is 1,4-cyclo-octadiene) be the fastest among all these reactio attributed to the dimeric nature of the compound and possible involvement of the palladium (0) species that is stabilized by the olefinic cyclo-octadienene ligand.

Based on the earlier results available in the literature about the possibility of palladium(0) being formed during reactions of palladium complexes and silanes and also observation of a induction period the palladium(II) undergoing an oxidative addition to palladium (IV) is less likely. Such process in fact should not be favorable as silanes being a source of hydride maintain a reductive environment. The oxidative addition of Si-H to palladium (II) center to form cationic palladium (IV) species is very unlikely process. The formation of palladium colloids either by the reaction of homogeneous solutions of Pd $(hfacac)_2$ (hfacac = $CF_3COCHCOCF_3$) in heptane, diethylether, methylene chloride, or acetone with Et_3SiH and other silanes or by the reaction of $Pd(OAc)_2$ in the solvent DMA was demonstrated to be an active catalyst for the hydrogenation, dehydrohalogenation and silylation of a alcohols.[170-171] In a recent study on silylation of sugars through silane alcoholysis by palladium catalyst a mechanism involving chloro ligand exchange was proposed (scheme 4.II).[167] In this reaction the halogen plays a crucial role.

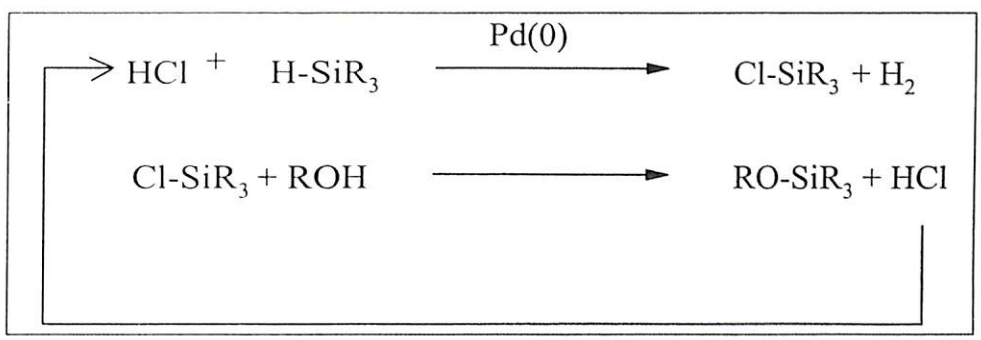

Scheme 4.II

The evidence of the involvement of above mechanism in sugar silylation came from the fact that the powdered palladium black could be activated in *situ* by small amount of silylchloride (equimolar to palladium) to give moderately active silane alcoholysis catalyst,

which did not show colloid formation. Again powdered palladium metal did catalytic activity for the silylation of sugar substrate, this suggests that, with the $PdCl_2$-generated colloid, chloride might play an active role in silane alcoholysis. This gives an idea of possible formation of Si-Cl catalytically in low steady-state concentration on the palladium surface and forms the actual reactive species as shown in the scheme 4.II. Since in this mechanism, transient presence of free hydrochloric acid is required, the reaction should be inhibited by the addition of a base and indeed this happens on addition of a base.

In an alternative mechanism silane may first reduce palladium (II) to palladium (0), which in turn may act as a true catalyst (scheme 4.III). In this mechanistic pathways palladium (0) undergo bond metathesis reactions, in which the oxidation state of the palladium (0) remains unchanged on addition of silanes and alcohols and a four-member cyclic transition state is formed during the reaction. This process is called bond metathesis and it is a concerted process in which sigma bonds are broken and formed in a four-centered transition state simultaneously. This mechanism should be independent of chloride concentration. Since we have used nitrogen donor ligand they can serve as acid scavenger and facilitate such mechanism. Based on this we proposed the following reaction scheme 4.III is more favorable process in the palladium catalysed silicon-oxygen bond forming reaction reported in this work.

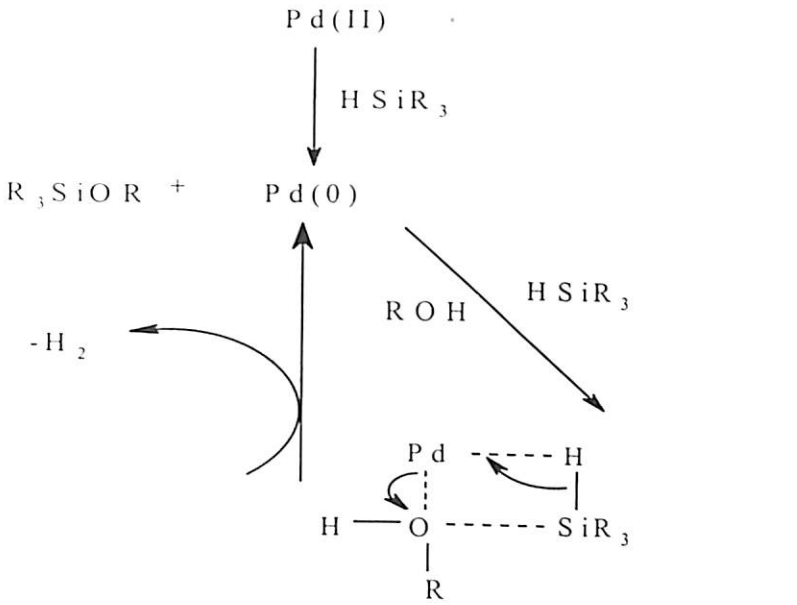

Scheme 4.III

Third mechanistic pathways, involving hydride intermediate is shown in scheme 4.IV. In this scheme silane first reduces palladium(II) to palladium(0), the true catalyst, which then undergo oxidative addition of silanes finally reductive elimination of the hydrogen and formation of the desired product give back palladium(0).

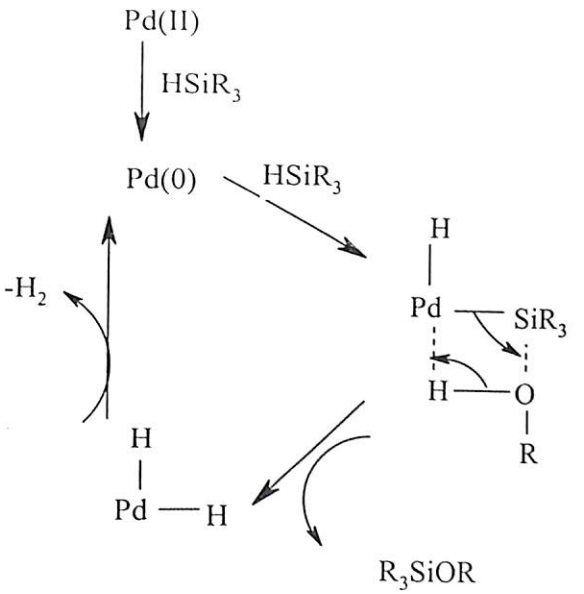

Scheme 4.IV

The formation of palladium colloid during the course of the present reactions is supported by XRD study also. The presence of induction period in this type of reactions

indicates that the preferred reaction path shown in scheme 4.III is more favoral reactions described in this chapter.

The reaction was extended to synthesis siloxane oligomers from the reaction of dihydrosilane with 1,4-dihydroxy, 1,3-dihydroxy phenols as well from different naphthalene diols. One of the reaction of 1,4-naphthalenediol with dipjenylsilane is shown in equation 4.3.

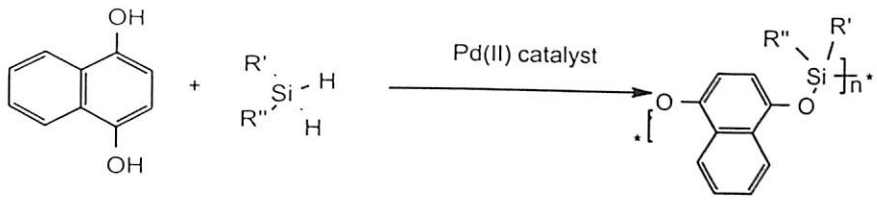

Where R' = Ph and R" = Ph or Me

Equation 4.3

The NMR spectra of the oligomers are useful in ascertaining the identity of the oligomers as well as identifying the end group present in the oligomers. For example the ^1H NMR spectra of the oligomer of the condensed product of 2,3-naphthalenediol with diphenylsilane has a signal at 7.0δ –7.9δ due to naphthyl proton as well as very weak signal at 1.8δ due to Si-OH proton.

The oligomers of various dihydroxy aromatic compounds with dihydrosilane are listed in table 4.3 along with their molecular weight data and yield. The polydispersity of the oligomers were found to be close to unity. This implies that the molecular weight distributions of the oligomers are very narrow. M_w values of the oligomers are in the range 1000-7000. An illustrative case the chromatogram along with distribution graph of siloxane oligomer prepared from diphenylsilane and 1,4-naphthalenediol is shown in the figure 4.6. This oligomer has M_w and M_n values are 4310 and 4303.

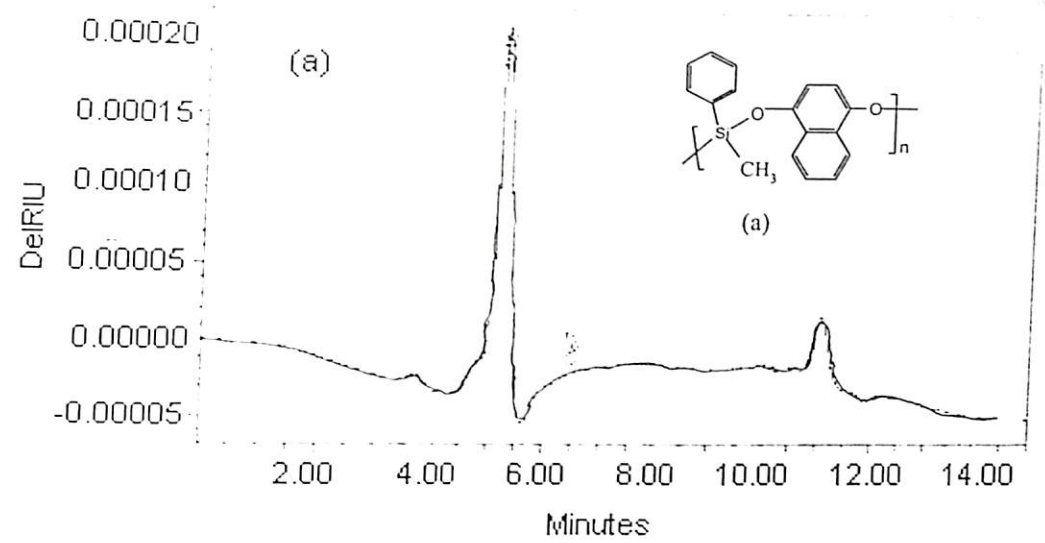

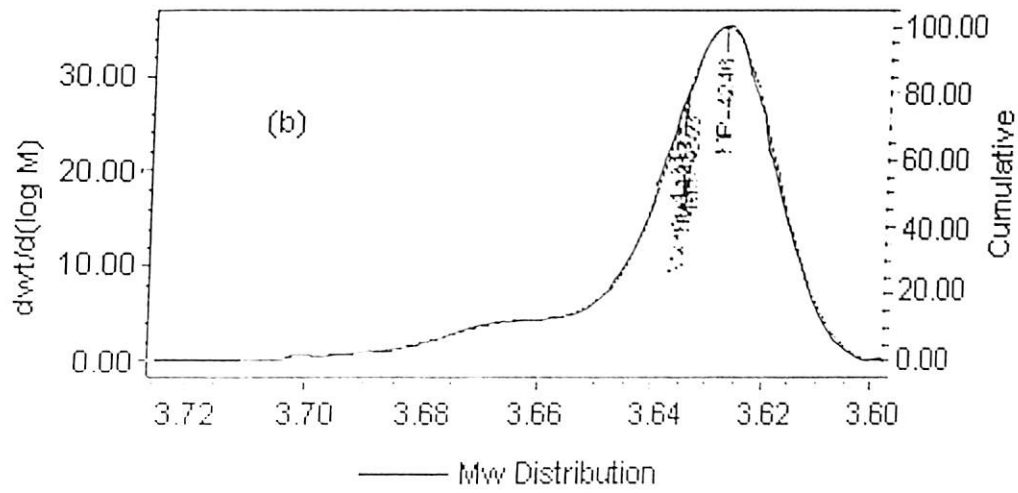

Figure 4.6 Chromatogram (a) and distribution graph (b) of siloxane oligomer

Table 4.3. Palladium catalysed formation of siloxane oligomers

Silane	Diol	Siloxane	M_w and M_n values
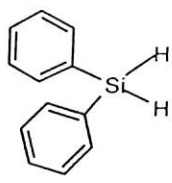	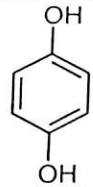	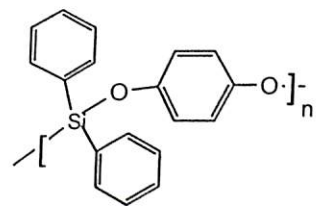	$M_w = 3401$ $M_n = 3327$
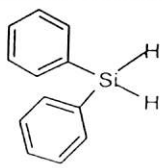	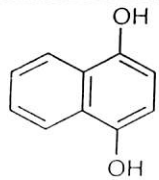	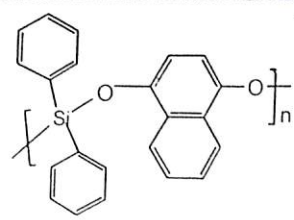	$M_w = 4310, 3100$ $M_n = 4303, 3041$

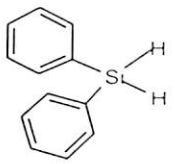	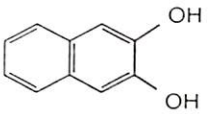	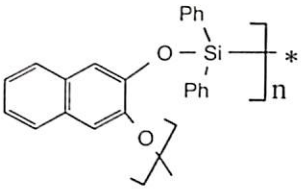	$M_w = 978$ $M_n = 949$
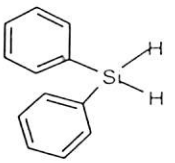	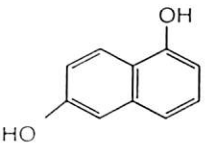	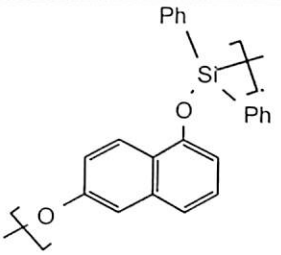	$M_w = 3306$ $M_n = 3139$
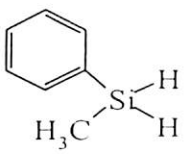	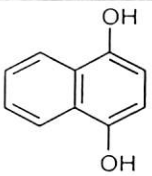	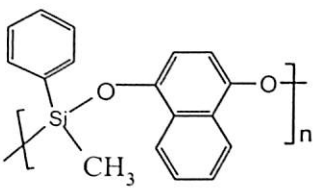	$M_w = 7004, 3291$ $M_n = 5946, 3285$
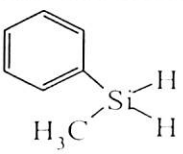	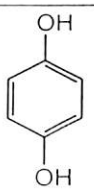	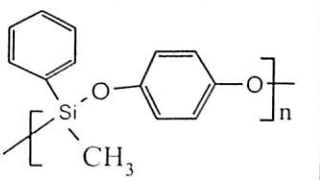	$M_w = 1391$ $M_n = 1293$
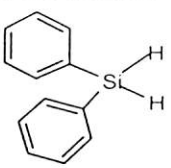		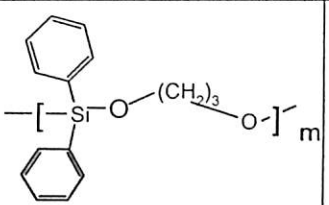	$M_w = 1763$ $M_n = 1736$
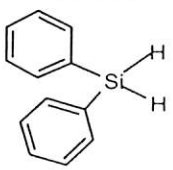	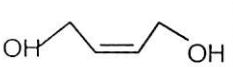	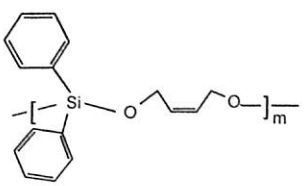	$M_w = 2854$ $M_n = 2828$

The quinone are known to react with the silane in the presence of RhCl(PI siloxane with aromatic backbone. The reaction of 1,4-benzoquinone with triethylsilane, triphenylsilane were carried out in the presence of $Pd(TMEDA)Cl_2$ and it was found that disylalated derivatives were formed (equation 4.4)

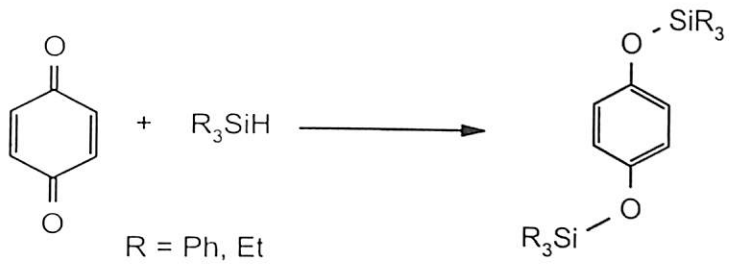

Equation 4.4

This provides another routes for the synthesis of siloxane oligomers from the reductive coupling reactions of dihydrosilane with aromatic diones (equation 4.5). Several oligomers were synthesized and their yield and the molecular weights are listed in table 4.4

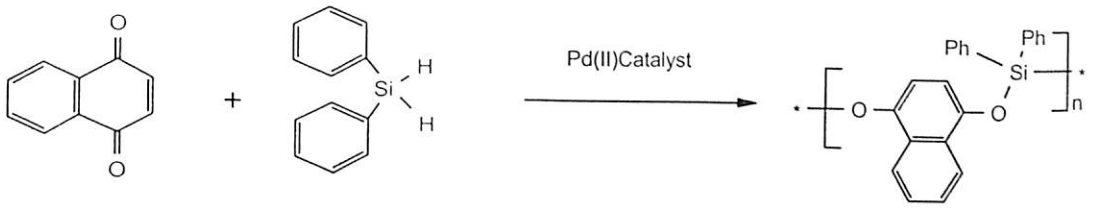

Equation 4.5

Table 4.4. Palladium catalysed Si-O bonded oligomers from quinines by Pd(TMEDA)Cl_2 as catalyst

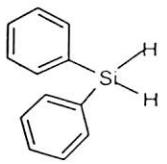	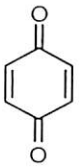	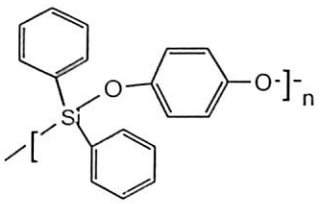 5a	$M_w = 1026$ $M_n = 971$
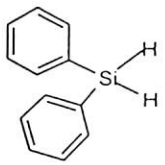	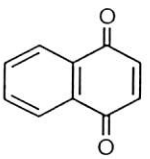	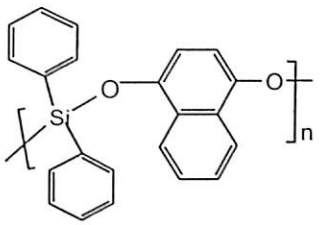 5b	$M_w = 3730, 1861$ $M_n = 3683, 1848$
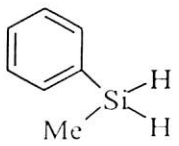	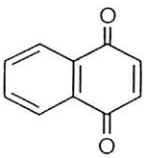	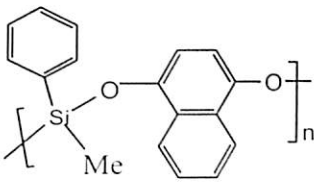 5c	$M_w = 4904$ $M_n = 4470$
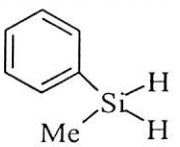	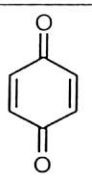	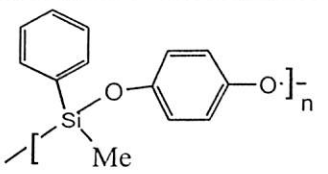 5d	$M_w = 1360$ $M_n = 1187$

The reductive coupling reactions of quinone with silanes to give siloxane oligomers are supposed to proceeds via three major steps. In the first step hydrogenation of 1,4 quinone give reduced product, in the second step 1,4-hydrosilylation of quinone to give siloxy phenols.[163] In the final step dehydrogenative silylation of OH groups of 1, 4-aromatic diols with 1,4-hydrosilylated product to give siloxane oligomers, as depicited in the scheme 4.V

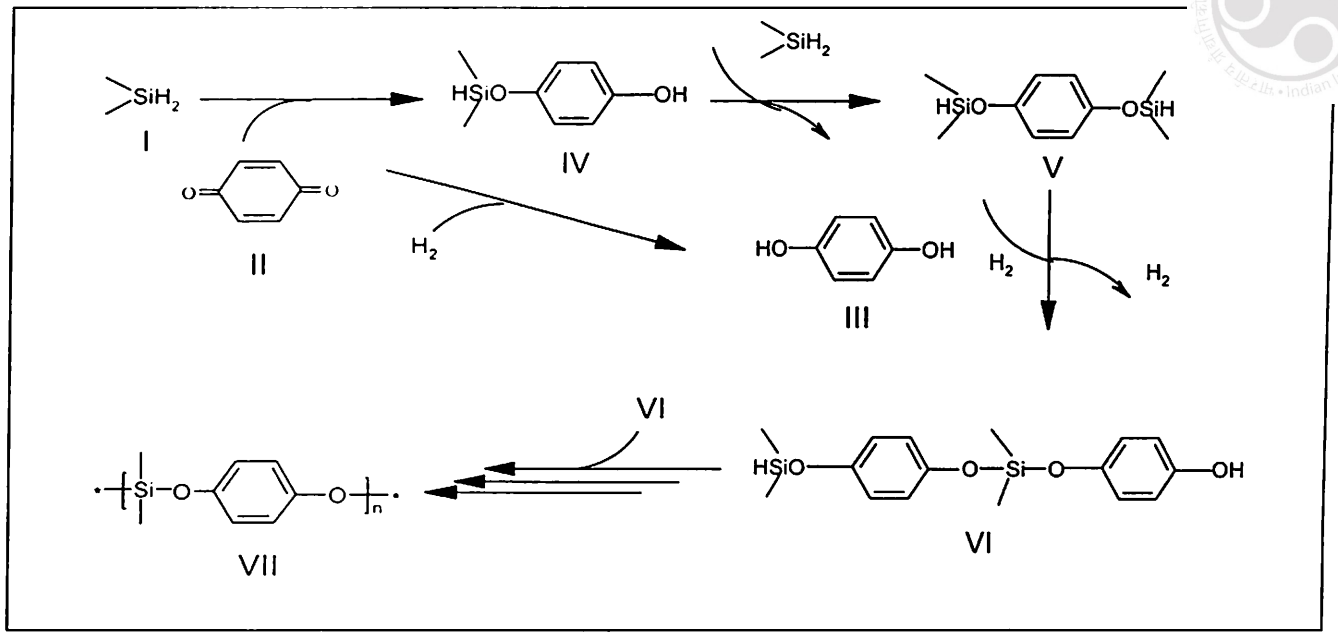

Scheme 4.V

In the case of quinone an initial reduction followed by a formation of charge transfer complex is possible. This mechanism involving a charge transfer complex of quinone and dihydroxy aromatics is proposed by monitoring the change in UV-Visible spectra of the reaction of 1,4-naphthalenediol with diphenylsilane in the presence of Pd (TMEDA) Cl_2 with time and making a differentiation of this reaction with the reaction of diphenylsilane and 1,4-naphthoquinone in the presence of same catalyst. In the former reaction one isosbestic point at 355 nm was observed, whereas in the latter reaction two-isosbestic point one at 370 nm and 355 nm was observed (for figure please refer to experimental section). The observation of a common isosbestic point in two independent reactions indicates that these reactions pass through a common intermediate. The isosbestic point at 355 nm is due to Si-O bond formation, whereas the isosbestic point at 370 nm occurs due to the reductive process of naphthoquinone. As both the reactions pass through a common intermediate, the favored reaction mechanism in these reactions is the one involving oxidative addition and reductive elimination (scheme 4.VI).

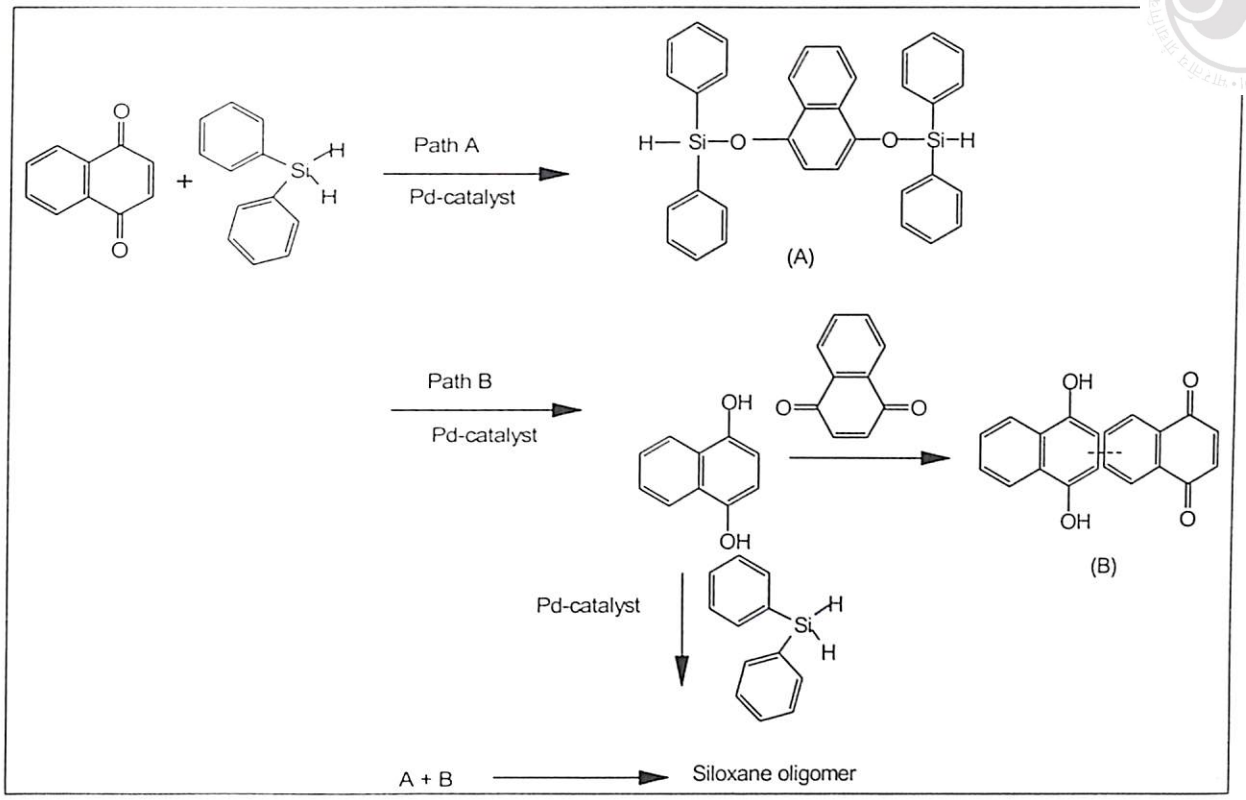

Scheme 4.VI

In the naphthoquinone reduction reaction the absorption maximum at 355 nm is assigned to a charge transfer complex (B) that can be formed by interaction of partially reduced naphthoquinone with naphthalenediol. Finally charge transfer complex **B** as well as **A** can participate in the reaction to form siloxane oligomers.

Since the oligomers show narrow molecular weight distribution, mass spectral studies can be of great help in ascertaining the exact molecular weight of the oligomers. The mass fragments of the oligomers can be of help to describe the uniformity and the fragmentation pattern. For, this purpose the FAB Mass spectra of oligomers 4b was recorded.

The highest m/z value in the FAB mass spectrum of **5b** was observed at 1439. This m/z value corresponds to four units of diphenyl silane and three naphthalenic units with palladium (II) attached to tetramethylethylenediamine (equation 4.6, structure I). The m/z signal at 1439 is a broad spread from 1436-1444 due to the isotopic abundance palladium. In structure (**I**) the palladium is anchored through Si-O-Pd and Si-Pd bonds. This m/z value may

arise from due to colloidal palladium that has oxidatively added to the oligomer mass spectra could be due to degradation of the oligomers and may occur due to colloidal palladium formation during coupling reactions, and trapped in the stacks of the siloxane Colloidal metal formation during dehydrogenative coupling is well documented. The palladium atom thus deposited may be responsible for the molecular mass and FAB mass spectrum.

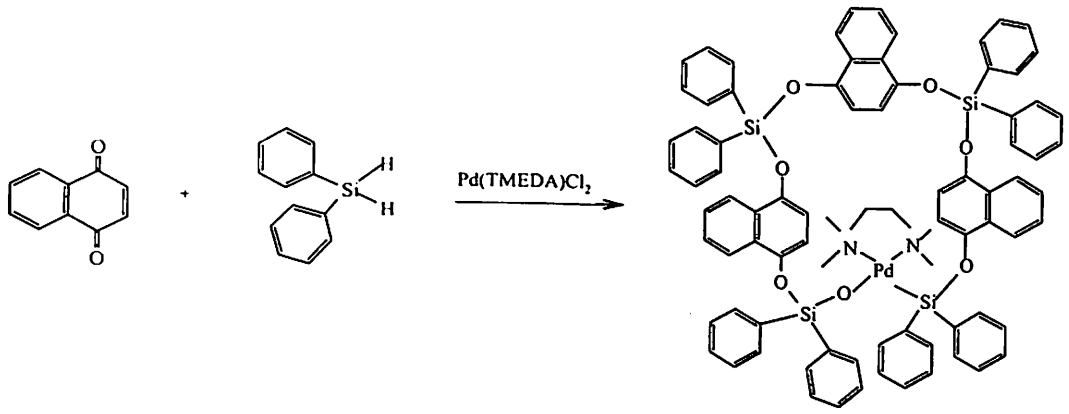

I

Equation 4.6

4.1.3 Rearrangement reaction of silanes

We had already mentioned that silane undergo a facile rearrangement reactions in the presence of transition metal catalyst [161,172-173] During the course of our study we found that palladium catalysed reactions of phenylsilane and quiononic compounds give siloxane oligomer. The mass spectra of these siloxane oligomer shows that the backbone of the oligomer contains rearranged phenylsilane units. For example, the palladium-catalysed reaction of phenylsilane with 1,4-benzoquinone results siloxane oligomer, the mass spectra of this oligomer shows it is a low molecular weight oligomer having highest m/z at 857. The mass fragments of this oligomer show the unrearranged as well as rearrange siloxane having diphenylsilylene units in the siloxane backbone. These results prompted us to study the

rearrangement reactions of silane in the presence of palladium catalyst. The rea reaction of phenylsilane and diphenylsilane can be represented by the following equation.

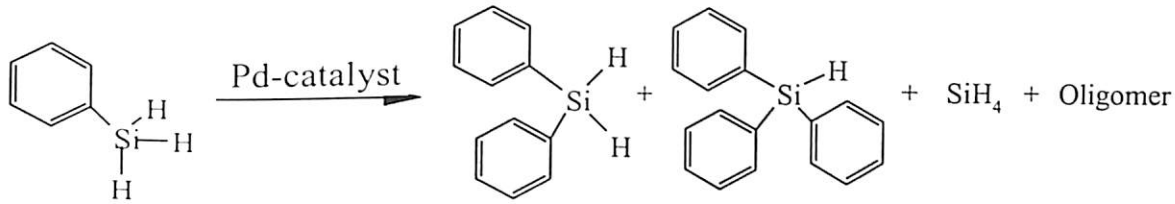

Equation 4.7

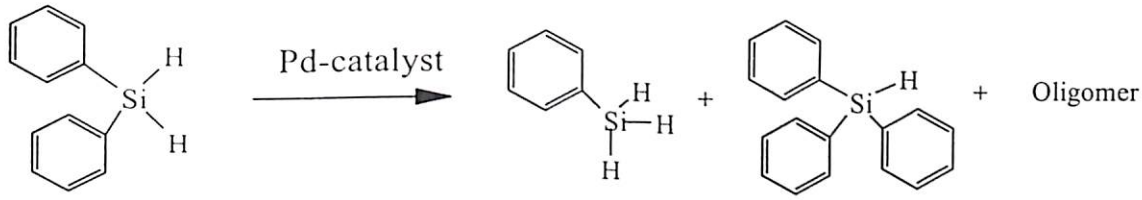

Equation 4.8

It was observed that these rearrangement reactions were catalysed by various palladium(II) complexes. The results on the rearrangement of phenylsilane and diphenylsilane after 30 minutes of reaction at 25^0C by different Pd-catalysts are shown in the table 4.5 and 4.6.

Table 4.5 [a]. Rearrangement reaction of phenylsilane by different palladium complexes

Catalyst	Phenylsilane	Diphenylsilane	Triphenylsilane
$PdCl_2$	Nil	36	63
$Pd(TMEDA)Cl_2$	Nil	66	33
$Pd(TEEDA)Cl_2$	Nil	59	41

[a] In all cases the reactions were carried out by mixing phenylsilane (0.1mmol) with palladium catalyst (0.001) in dichloromethane (2ml). The reaction mixtures were stirred at 25^0C for 30minutes. The products were analysed by GC using SE-30 column with oven temperature 180^0C and detector and injector temperature 230^0C.

Table 4.6 Rearrangement of diphenylsilane by different palladium complexes[1]

Catalyst	Phenylsilane	Diphenylsilane	Triphenylsilane
$PdCl_2$	1	82	17
$Pd(TMEDA)Cl_2$	98	Nil	Nil
$Pd(TEEDA)Cl_2$	100	Nil	Nil
$Pd(PPh_3)_2Cl_2$	5	94	Nil

[b] In all cases the reactions were carried out by mixing diphenylsilane (0.1mmol) and palladium catalyst (0.001) in dichloromethane (2ml). The reaction mixtures were stirred at 25^{0}C for 30minutes. The products were analysed by GC using SE-30 column with oven temperature 180^{0}C and detector and injector temperature 230^{0}C.

4.1.4 Comparative study of palladium catalysed and rhodium catalyzed silicon-oxygen bond forming reactions

Among the most effective catalyst for dehydrogenative coupling reactions of silanes are the $RhCl(PPh_3)_3$ and $[IrH_2S_2(PPh_3)_2]$[174-175] where S= CH_3OH. Several reports on the use of $RhCl(PPh_3)_3$ suggests that it has distinct advantages over palladium catalyzed Si-O bond forming reactions.[176-177] The reaction of phenolic compounds with dihydrosilane gives monohydrosilylethers, which can be converted to the corresponding di-aryloxy ether. In the present investigation it is already pointed out the reaction of 1,4-benzoquinones can be effected by Pd-complexes as catalyst to give the corresponding silylethers. But literature suggests that such reactions also can be carried out by $RhCl(PPh_3)_3$ catalyst. This reaction has another advantage as it can form monosilylether from reaction of dihydrosilanes with 1,4-benzoquinone or 1,4-naphthoquinone, which would serve as precursor for further functionalization on the remaining Si-H group (equation 4.9)

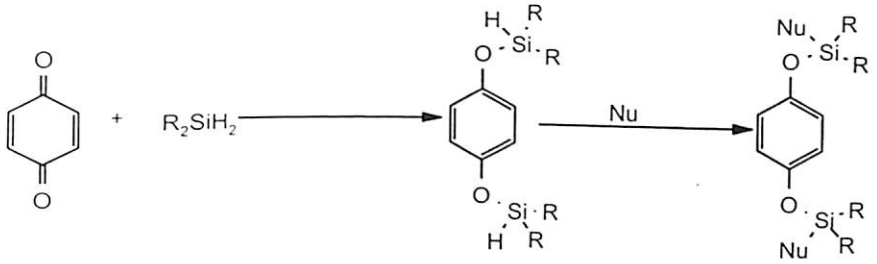

Equation 4.9

It was also demonstrated in an earlier study that diphenylsilane [159]could sequentially be substituted to give dithioether as shown in scheme 4.VII

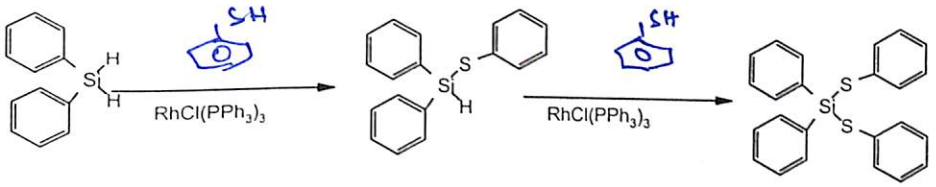

Scheme 4.VII

The reaction of 1,4-benzoquinone with diphenylsilane as well as 1,4-naphthoquinone was carried out. Between these two reactions the former reaction does not lead to the desired product but leads to a mixture of products. However the later reaction can lead specifically give the disilylated monomeric product, which is stable under inert atmosphere. In the reaction of 1,4-napthoquinone with diphenysilane gives only diaryloxyether (Equation 4.10)

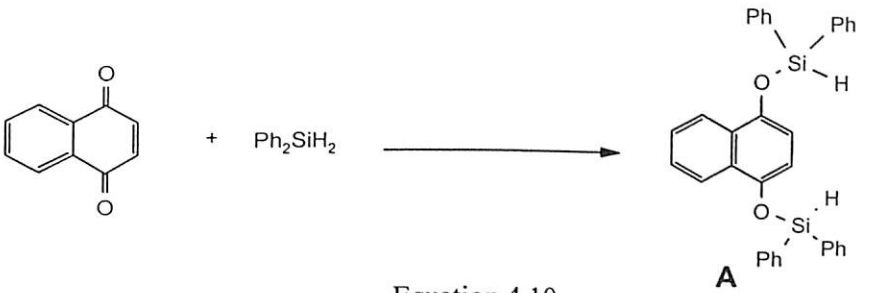

Equation 4.10

The identity of the product is ascertained from the spectroscopic data of the compound. It has the Si-H frequency appearing at 2150 cm^{-1}(s). In addition to this other ring stretching frequency at 3050cm^{-1}(w) and Si-O frequency appears at 1080 cm^{-1}(s). The compound is devoid of the carbonyl stretching that was originally present for the parent compound at 1660

cm^{-1}. The compound has the signals arising from each center. The ^{13}C NMR has th at 146.0 δ, 134.6δ, 133.0δ, 130.5δ, 128.0δ, 124.9δ, 122.4δ, 111.3δ due to aromatic carbon ^{1}H NMR spectra has signal at 8.49 δ (2H, Ha, naphthyl) 7.68 δ(8H, *ortho* C_6H_5) 7.30δ(2H, Hb, naphthyl), 7.18-7.09(12H, m, *meta* and *para* C_6H_5) 6.74δ(2H, s, Hc, naphthyl), 5.92 (2H, br, SiH). However the reaction of 1:2 ratio of naphthoquinone with diphenylsilane does not lead to a single product but a mixture of mono and disilylated derivative. The peaks in ^{1}H NMR spectra (fig 4.7) assigned as * are due to the monosilylated derivative. However, the product separation from this reaction mixture was not possible.

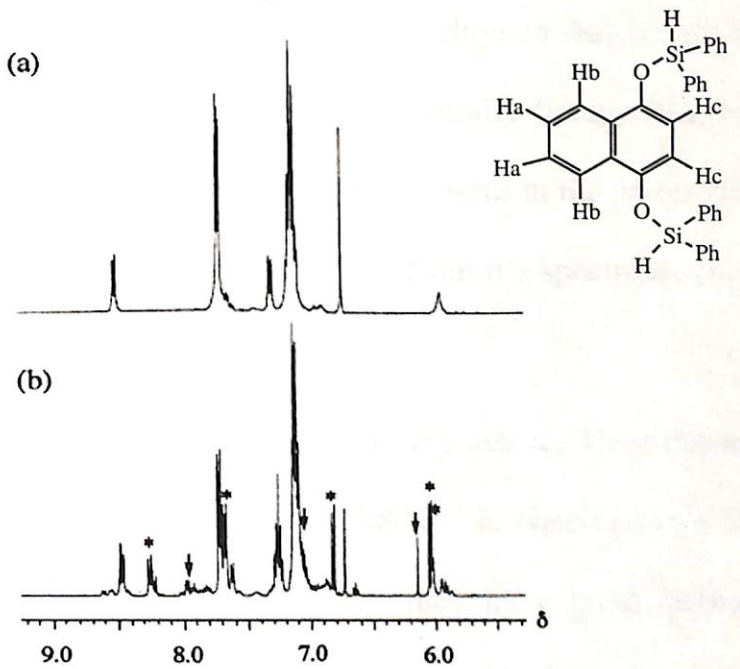

Figure 4.7 ^{1}H NMR (400 MHz) spectra of a C_6D_6 (0.53 ml) solution of (a) Ph_2SiH_2 (0.20 mmol) and 1,4-naphthoquinone (0.10 mmol) in the presence of $RhCl(PPh_3)_3$ (0.01 mmol) and (b) equimolar ratio of Ph_2SiH_2 and 1,4-naphthoquinone. The signals with asterisk and with arrows are due to monosilylated product and 1,4-naphthoquinone, respectively.

In order to probe the sequential Si-H bond activation of diphenylsilane by $RhCl(PPh_3)_3$; the diaryloxyether prepared from the reaction between diphenylsilane with 1,4-naphthoquinone (**A**) was reacted with two equivalent of thiophenol in the presence of

catalytic amount of $RhCl(PPh_3)_3$. This reaction led to the formation of dithioe

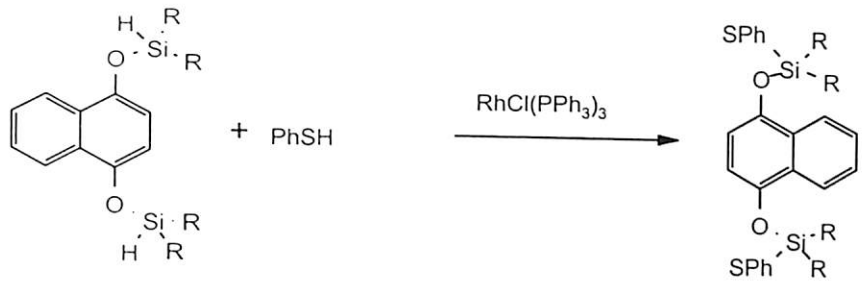

A $R = C_6H_5$- B

Equation 4.11

(equation 4.11) by formation of Si-SPh group. This showed that the reactivity of two Si-H bond of diphenylsilane is different and can be sequentially functionalised. The product (**B**) did not have the Si-H frequency that was originally present in the parent diaryloxyether (**A** in equation 4.10). The thioether (**B**) was characterised from it's spectroscopic features.

4.1.5 Thermal properties of the oligomers

The siloxane oligomers are thermally not very stable. They decompose on heating, and a continuous weight loss in the region 180^0-800^0C is observed in each case suggesting degradation of oligomer above 200^0C. However, they have good thermal stability in the range 30-180^0C. The continuous weight loss indicates hydrolytic cleavage of Si-O bonds to give smaller molecular weight products.

4.1.6 Electrical properties of siloxane oligomer

The electrical properties of siloxane composites are of interest to material chemist. Since the siloxane oligomers that are reported here has a backbone containing an aromatic group separted by an Si-O bond they are expected to show interesting electrical property. The resistance versus temperature profile of siloxane oligomer prepared from the reaction of 1,4-naphthalenediol and 1,4-naphthoquinone with diphenylsilane in the presence of

Pd(TMEDA)Cl_2 catalyst is shown in the figure 4.8. The resistance versus temper in this case shows an increase in resistance with increase in temperature and after a certain limiting temperature resistance falls with further increase in temperature i.e. thermoelectric switching behavior is obtained from the siloxane oligomer. On cooling the same path was not followed, it means that it was an irreversible effect. The irreversible effect of thermoelectric switching property is believed due to change of geometry around palladium, which is embedded in the siloxane network. On the other hand resistance versus temperature curve of siloxane oligomer prepared from 1,4-naphthoquinone with diphenylsilane in the presence of $PdCl_2$ catalyst decreases continuously with increase in temperature.

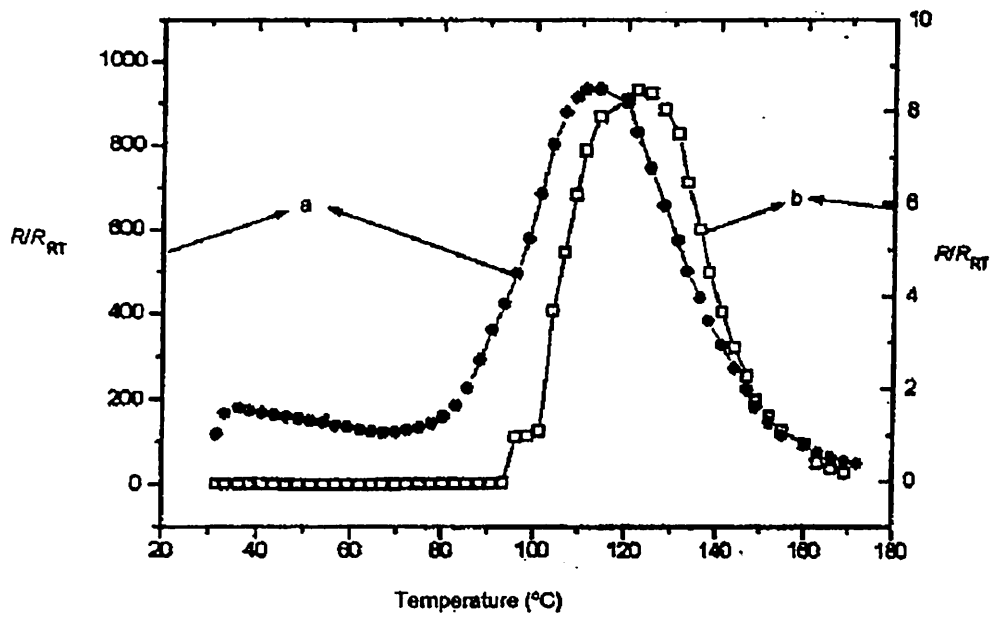

Figure 4.8 Plot of resistance R normalized to resistance at room temperature R_{RT} versus temperature of the siloxane prepared by Pd (TMEDA) Cl_2 catalyst from the reaction of (a) 1, 4-naphthalenediol and (b) 1,4-naphthoquinone with diphenylsilane.

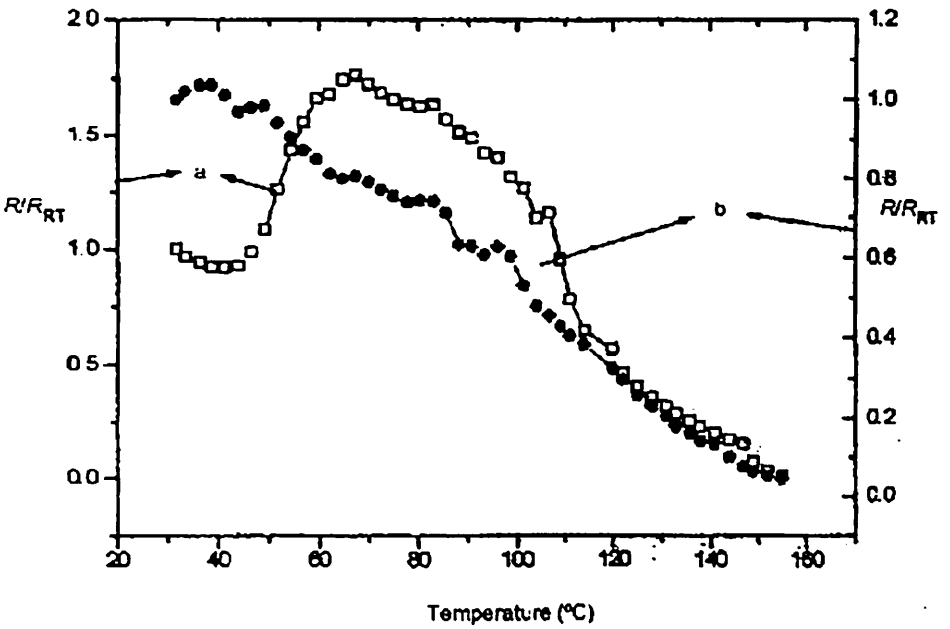

Figure 4.9 Plot of resistance R normalized to resistance at room temperature R_{RT} Vs temperature of the siloxane prepared from the reaction of 1,4-naphthoquinone with diphenylsilane by (a) $Pd(TEEDA)Cl_2$ and (b) $PdCl_2$ as catalyst

The siloxane oligomers under consideration have sp^2-hybridized C-O bonds attached to silicon. These can impart delocalization in the system through involvement of d-orbitals of silicon as well as the lone pair of electrons on oxygen. Since the siloxanes oligomers were prepared by the dehydrogenative coupling reactions of silanes and diols or by the reductive coupling reactions of silanes with dione in presence of catalyst derived from metal. Thus, the difference in the resistance versus temperature plots of the films indicates the property originates from the environment of the metal ion. In the present case we suggest that the change in co-ordination around the metal center in the siloxane oligomer is responsible for such property. This is also supported by far IR studies. We also recorded the IR spectra of the two siloxane prepared from 1, 4-naphthoquinone with diphenylsilane in the presence of $Pd(TMEDA)Cl_2$ (a) and the same reaction in presence of $PdCl_2$ (b). In the former case two absorptions at 3400cm^{-1} and 1680cm^{-1} due to O-H stretching frequency and overtone absorptions, which were absent in the latter case. A considerable decrease in the intensity of O-H stretching frequency in (b) was observed on heating the sample above 150^{0}C.

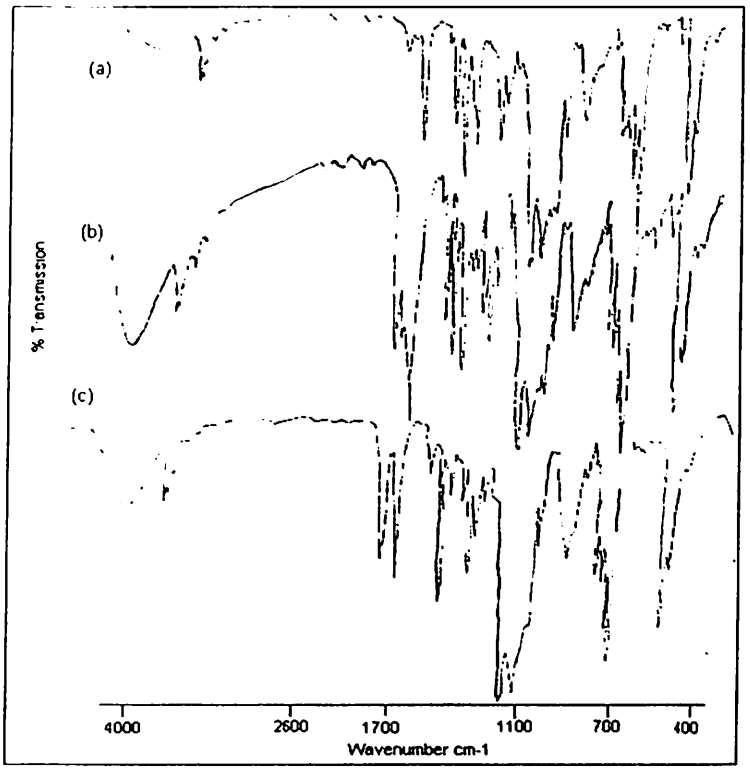

Figure 4.10 IR (KBr) spectra of siloxane prepared from the reaction of diphenylsilane and 1,4-napththoquinone by (a) $PdCl_2$ (b) Pd (TMEDA)Cl_2 (c) Pd (TMEDA)Cl_2 after heating the siloxane to 150^0C

Further proof of the loss of water molecules during heating from 30^0C to 180^0C was supported by thermogravimetriy analysis, where the siloxanes prepared from 1,4-naphthoquinone with diphenylsilane by $PdCl_2$, Pd(TMEDA)Cl_2 and Pd(TEEDA)Cl_2 have losses weight 0%, 1.5% and 3.7% respectively in this region. Differential scanning calorimetry (DSC) of the sample prepared by catalytic reactions with Pd(TMEDA)Cl_2 showed an endothermic process at the temperature where the resistance reached maximum values in the figure 4.8. Thus all evidences suggest that the thermoelectric switching property of the siloxane oligomer were due to the loss of water molecules from the siloxane interstices. The loss of water molecule changes the environment around the palladium and results in a decrease in resistance from a limiting temperature. The change in geometrical environment around the palladium centered is also confirmed from the far-IR spectra of the siloxane oligomers of 1,4-naphthalenediol and diphenylsilane. The far-IR spectra of this

siloxane oligomer at room temperature as well as after heating at 200^{0}C show strc 517 and 488 cm^{-1}, and this remain unchanged on heating. These bands are attributed to the Si-O framework on the basis of literature report on ortho-silicate. The only change observed is that a weak absorption appeared at 418cm^{-1} and this absorption splits into two absorptions at 418 and 405cm^{-1}. This again qualitatively supports a probable change of co-ordination around palladium.

Chapter 5

Experimental Section

5.1 General Instruments/Equipment used for analytical purpose

5.1.1 Infrared spectra

Infrared spectra of the compounds were recorded either on a Nicolet Impact-410 Fourier transform infrared spectrophotometer or a Perkin-Elmer infrared spectrophotometer. Spectra were recorded either as KBr pellets or as neat samples.

5.1.2 UV-visible spectra

UV-visible spectra were recorded on a Hitachi U-2001 UV-visible spectrophotometer by dissolving the stipulated amount of the substrate/s in appropriate solvent. The solutions were generally taken on a quartz cell, which was then placed into the sample chamber along with another one containing the solvent. Time scan were recorded by setting the instrument at the appropriate wavelength after determination of λ_{max} from independent experiment and then monitoring the absorbance with time.

5.1.3 Cyclic Voltammetry

The cyclic voltammograms of the compounds were recorded with an electrochemical analyser (CH instrument) with three-electrode system comprising of Ag/AgCl reference electrode, two platinium electrodes as working and auxillary electrodes. The measurements were done in dry acetronitrile (HPLC grade, distilled over CaH_2) or in methanol with tetrabutylammonium perchlorate as supporting electrolyte. The EMF values are with reference to ferrocene as standard.

The electrochemical studies were performed by dissolving 3-5mg each of the complex in acetonitrile (5 ml) with 200-250 mg of the tetrabutylammonium perchlorate as supporting electrolyte with scan speed 100 mV/s. Both positive and negative scan were recorded. Dry nitrogen gas was passed through the solution before recording of the voltamogram.

5.1.4 Elemental analysis

The elemental analyses were done on a Perkin-Elmer PE 2400 series II CHN analyser 2400. For a few samples, the elemental analyses were done at Central Drug Research Institute, Lucknow.

5.1.5 Electron Spin Resonance Spectra

The ESR measurements were done on the X-band of an EPR-E-112 ESR spectrometer at Regional Sophisticated Instrumentation Center, Indian Institute of Technology, Madras. A quartz cell was used for X-band measurements. In all these measurements diphenyl picryl hydrazyl radical (DPPH) was used as the standard.

5.1.6 Gel Permeation Chromatography

The GPC were done on a Water 600 GPC system with Refractive Index detector (Waters 2421 RI detector) with ultrastyragel ® column and THF as eluent. The flow rate was 1 ml/ min. The calibration curves for GPC analyses were obtained using polystyrene standard.

5.1.7 Nuclear Magnetic Resonance spectra

Majority of the ^{1}H NMR and ^{13}C NMR spectra were recorded either on a Bruker 400 MHz or on a JEOL EX-400 NMR spectrometer using TMS as internal standard. These were recorded at Sophisticated Instrumentation Facility, Indian Institute of Science, Bangalore or Regional Sophisticated Instrumentation Center, Central Drug Research Institute, Lucknow.

5.1.8 Conductivity Measurement

Conductivity of the material was measured over a range of temperature on a Hewlett Packard 34401 multimeter, Keithley 6512 programmable electrometer and agronics 93-C DC power supply unit. These measurements were based on the principle of measuring the resistivity changes as well as resistance with change of temperature.

Materials under investigations were taken either as thin film, made by spre solution of a concentrated sample on a small thin mica sheet. After removing the ... by slow evaporation.. The mica sheet was placed between the two probes and copper block such that the two probes just touch the film. The resistance versus resistivity was recorded. The temperature was obtained from the corresponding resistivity by using the standard conversion table. In an alternative method a thin pellet was made by using a hydrolytic press.

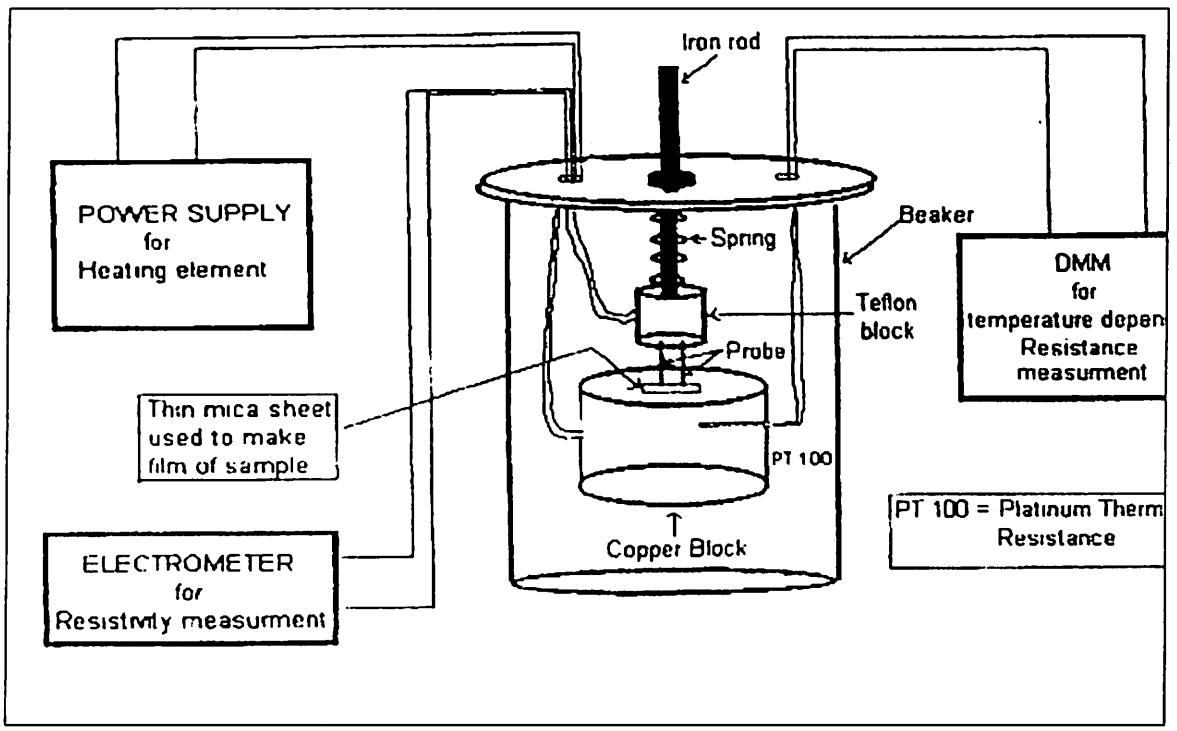

Figure 5.1 Two probe setup for conductivity measurement.

5.1.9 Gas Chromatographic Analysis

Catalytic reactions were monitored by gas chromatography on a Hewlett Packard HP 6890 GC system with the aid of FID detector by using SE-30 capillary column. In most of the cases, oven, injector and detector temperature were set at 150^0C, 220^0C and 220^0C respectively. In all cases N_2 was used as a carrier gas with 7 bar inlet pressure. The results were recorded on an HP 3395 integrator.

5.1.10 Magnetic moment measurement

The measurement of magnetic moment was carried out on a Sherwood Scientific Magnetic Susceptibility Balance. Weighed amount of the finely ground solid sample was taken in a previously weighed sample tube. Before this, the empty sample tube into the tube guide of the instrument and magnetic deflection caused by the tube was recorded as R_0. The sample tube with the sample stated above was then inserted into the tube guide and magnetic deflection caused by the tube was then recorded as R. The mass susceptibility, X_g was then calculated using the equation (A).

$$Xg = \frac{C_{Bal} l(R - R_0)}{10^9 m} \qquad \text{Equation (A)}$$

Where,

l = Sample length (cm)

m = Sample mass (gm)

R = Reading for tube plus sample

R_0 = Empty tube reading

C_{Bal} = Balance calibration constant

The molar susceptibility,

$$X_M = X_g \times M$$

Where, M = The molecular or formula weight of the substance.

For compounds containing a paramagnetic ion, X_M will be less than the susceptibility per gram atom of the paramagnetic ion, X_A, because of the diamagnetic contribution of the other groups or ligand present. Since magnetic moments are additive, X_A can be obtained from X_M by the addition of the appropriate corrections.

$$X_A = X_M - \sum_l X_l$$

Where, $\sum X_l$ = Diamagnetic correction.

The effective magnetic moments (μ_M) were calculated from the equation.

$$\mu = 2.84\chi_M T \qquad \text{(Equation 5.1.)}$$

5.1.11 FAB mass

The FAB mass spectra were recorded on a JEOL SX 102/DA-600(spectrometer/Data System using Argon/Xenon (6kV, 10mA) as the FAB gas. The accelerating voltage was 10 kV and the spectra were recorded at room temperature. M-Nitrobenzyl alcohol (NBA) was used as the matrix unless specified otherwise. The matrix peak may appear at m/z 136, 137, 154, 289, 307 in the absence of any metal ions

5.1.12 MALDI mass

The Matrix Assisted Laser Desorption Ionization (MALDI) mass spectra were recorded at Indian institute of Chemical Technology, Hyderabad and Indian Institute of Science Bangalore. The LSI mass spectra were recorded on a VG Auto Spec Mass spectrometer using either glycerol or m-nitrobenzyl alcohol as matrix.

5.1.13 Thermal analysis

The thermal analysis were carried out with a Mettler Toledo TGA/ SDTA 851^e and Mettler Toledo DSC 821^e thermal analyzer. The thermogravimetric (TG) measurements were conducted under pure nitrogen gas in an aluminium crucible. Differential Scanning Calorimetric experiments were done under air in aluminum or in a platinum crucible. In both DSC and TG, the heating rate maintained as either 5^0C or 10^0 C/min.

5.1.14 Characterisation using X-ray diffraction

A commercial X-ray diffraction system for powder samples (Seifert XRD 3003 T/T) was used for the verification of metallic particles present or not, for this purpose Cu K_α radiation (1.541 Å) with a Nickel filter was used. The instrument was calibrated with a standard Si reference. The X-ray generator was operated with an acceleration voltage of 40 kV and tube current of 30 mA. The theta-theta goniometer was used in the reflection (Bragg-Brentano) geometry (figure 5.2). The XRD data provides the variation of intensity/counts per second (cps), recorded by the detector (scintillation counter) as a

function of 2θ, where θ is the glancing angle. XRD patterns were recorded by from 10^0 to 70^0 in steps of 0.002^0.

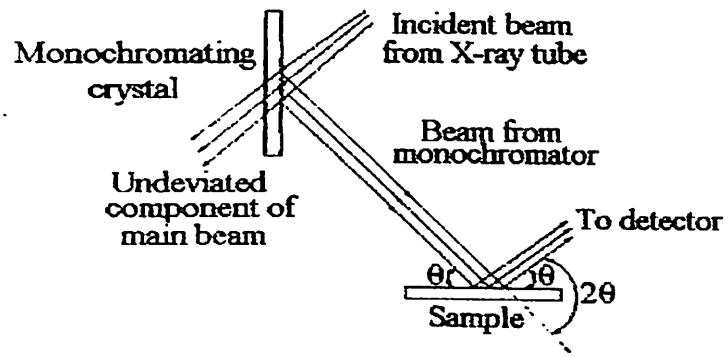

Figure 5.2: Ray diagram of an X-ray diffractometer.

For the structural analysis of a thin film deposited on a glass substrate, grazing incidence diffraction (GID) technique was used. GID technique works only with very smooth surfaces since surface variations normal to the incident beam can upset the total external reflection condition. A focused incident beam contains a range of incident directions and therefore not all the photons would land below the critical angle for total external reflection. Therefore, a compact and collimated beam of X-rays is required for a good GID. In the present studies, a söller slit assembly called the Grazing Incidence Device was used for obtaining a collimated beam of x-rays suitable for GID work.

5.1.15 General Experimental Section

All the solvents and reagents employed were of reagent grade (AR grade) and used as purchased without further purification, unless otherwise stated, and were obtained from E. Marck, Sigma-Aldrich, SRL, Qualigens. Silica gel (60-120 mesh size) was used for column chromatography. Reactions were monitored by TLC on silica gel GF_{254} (0.25 mm)

5.1.16 SEM

Scanning electron microscope photographs were obtained from University Durham UK.

Experimental section of Chapter 2

5.2.1 Typical procedure for the synthesis of tetrachlorocuprate complexes

Copper (II) chloride dihydrate (600 mg, 3.5 mmol) was dissolved in 5ml methanol and this solution was acidified with hydrochloric acid (11.6 N, 0.3 ml). A dark brown colored solution was obtained. To this solution the amine (10 mmol) or pyridine (10 mmol) was added drop wise with constant stirring. The reaction mixture was stirred at room temperature for another one hour. Addition of diethyl ether (40 ml) to the resultant reaction mixture led to the precipitation of the desired complex.

The analytical data for the complexes:

(1a) *Bis*-pyridinium tetrachlorocuprate

Isolated yield = 32%

IR (KBr): 3071 (bs), 1599 (s), 1524 (s), 1482 (s), 1444 (s), 1327 (s), 1183 (m), 1044(m), 905 (w), 745 (s), 676 (s) cm^{-1}.

(1b) *Bis*-anilinium tetrachlorocuprate:

Isolated yield = 40%

IR (KBr):3012 (bs), 1553 (s), 1493 (s), 1306 (w), 1095 (m), 744 (s), 684 (s), 472 (s)cm^{-1}

(1c) *Bis*- *p*-methoxy anilinium tetrachlorocuprate(II) monohydrate

Isolated yield = 23%;

IR (KBr): 3456 (bm), 3054 (bm), 1619 (m), 1519 (s), 1493 (s), 1307 (w), 1267 (s), 1220 (m), 1122 (w), 823 (s), 511(s) cm^{-1}.

(1d) *Bis*- *p*-methyl anilinium tetrachlorcuprater(II) trihydrate

Isolated yield = 12%

IR (KBr): 3087 (s), 2574 (s), 1599 (s), 1506 (s), 1201 (s), 1102 (s), 823 (s), 578 (w), 489 (w) cm^{-1}.

Table 2.1 Elemental analysis of the complex 1a, 1b, 1c, 1d

Composition		C%	H%	N%	Formula of the complex
$C_{10}H_{12}N_2CuCl_4$	Calculated =	32.83	3.28	7.66	$[C_5H_5NH]_2[CuCl_4]$
	Found =	32.86	3.26	7.07	(1a)
$C_{12}H_{16}N_2CuCl_4$	Calculated =	36.78	4.06	7.15	
	Found =	36.59	4.09	7.07	$[C_6H_5NH_3]_2[CuCl_4]$ (1b)
$C_{14}H_{22}N_2O_3CuCl_4$	Calculated =	35.63	4.35	5.93	
	Found =	35.81	4.66	5.96	$[p\text{-}O\text{-}CH_3C_6H_4NH_3]_2[CuCl_4].H_2O$ (1c)
$C_{14}H_{26}N_2O_3CuCl_4$	Calculated =	35.33	5.04	5.88	
	Found =	35.49	5.49	5.91	$[p\text{-}CH_3C_6H_4NH_3]_2[CuCl_4].3H_2O$ (1d)

5.2.2 Cyclic voltammogram of tetrachlorocurate complex:

The cyclic voltammograms of two tetrachlorocuprate complex were recorded by dissolving (0.0127mmol) of complex in acetonitrile (5ml) and using tertabutylammoniumperchlorate as supporting electrolyte with two platinum as a working and auxiliary electrode and Ag/AgCl as reference electrode. All scan are + ve with a scan speed 100mV/sec. The -ve scan also were recorded to check the reversibility and it was observed to give same features The cyclic voltammogram of **1d** and **1c** are shown below..

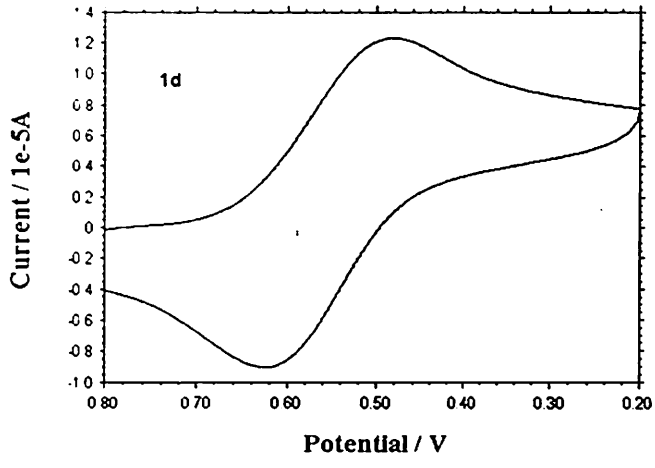

$[p\text{-}CH_3C_6H_4NH_3]_2[CuCl_4].3H_2O$ (1d)

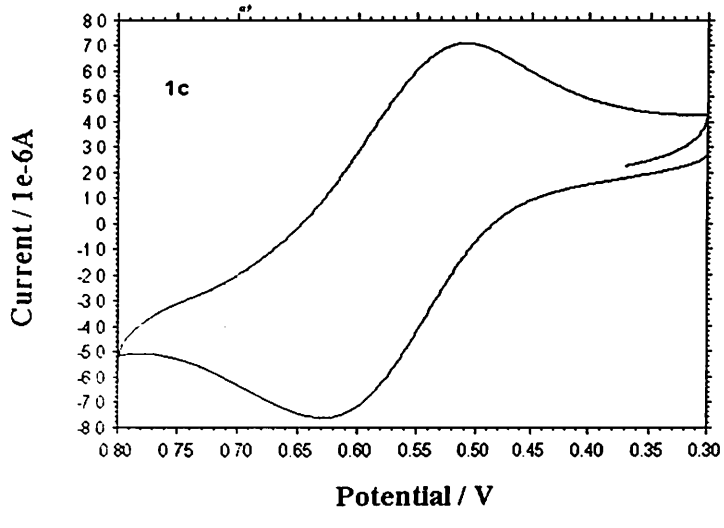

$[p\text{-}O\text{-}CH_3C_6H_4NH_3]_2[CuCl_4].H_2O$ (1c)

5.2.3 Procedure for the synthesis of $(pz)_2CuCl_2$

Copper (II) chloride dihydrate (510 mg, 3 mmol) was dissolved in acetone (10ml). To this solution the 3,5-dimethyl pyrazole (576 mg, 6 mmol) was added with constant stirring for half an hour which results formation of complex.

Yield = 600 mg (55%).

Crystal was obtained by dissolving the complex in methanol.

5.2.4 Crystal data of the complex $(pz)_2CuCl_2$

Table 5.1. Crystal data and structure refinement for $(pz)_2CuCl_2$

Identification code	03srv021	
Empirical formula	C10 H16 Cl2 Cu N4	
Formula weight	326.71	
Temperature	120(2) K	
Wavelength	0.71073 Å	
Crystal system	Monoclinic	
Space group	P 21/c	
Unit cell dimensions	a = 8.7017(17) Å	α= 90°.
	b = 13.440(3) Å	β= 106.135(8)°.
	c = 11.849(2) Å	γ = 90°.
Volume	1331.1(4) $Å^3$	
Z	4	
Density (calculated)	1.630 Mg/m^3	
Absorption coefficient	2.025 mm^{-1}	
F(000)	668	
Crystal size	0.40 x 0.22 x 0.12 mm^3	
Theta range for data collection	2.34 to 30.21°.	
Index ranges	-11<=h<=12, -18<=k<=18, -13<=l<=16	
Reflections collected	8925	
Independent reflections	3620 [R(int) = 0.0316]	
Completeness to theta = 30.21°	91.4 %	
Absorption correction	Integration	
Refinement method	Full-matrix least-squares on F^2	
Data / restraints / parameters	3620 / 0 / 218	
Goodness-of-fit on F^2	1.122	
Final R indices [I>2sigma(I)]	R1 = 0.0441, wR2 = 0.0991	
R indices (all data)	R1 = 0.0622, wR2 = 0.1051	
Largest diff. peak and hole	0.677 and -0.983 $e.Å^{-3}$	

Table 5.2. Atomic coordinates (x 10^4) and equivalent isotropic displacement parameters ($Å^2$x 1(
For $(pz)_2CuCl_2$. U(eq) is defined as one third of the trace of the orthogonalized U^{ij} tensor.

	x	y	z	U(eq)
Cu(1)	2878(1)	143(1)	9157(1)	13(1)
Cl(1)	4379(1)	-1159(1)	10206(1)	16(1)
Cl(2)	1908(1)	543(1)	10717(1)	15(1)
N(1)	-136(3)	1217(2)	8232(2)	15(1)
N(2)	1406(3)	1172(2)	8186(2)	14(1)
C(1)	-2813(4)	1888(3)	7210(3)	18(1)
C(2)	-1051(4)	1783(2)	7367(3)	14(1)
C(3)	-50(4)	2139(2)	6734(3)	15(1)
C(4)	1470(4)	1736(2)	7260(3)	14(1)
C(5)	2952(4)	1833(3)	6876(3)	18(1)
N(3)	3113(3)	-455(2)	7670(2)	14(1)
N(4)	4583(3)	-599(2)	7508(2)	15(1)
C(6)	5968(4)	-1159(3)	6047(3)	20(1)
C(7)	4500(4)	-943(2)	6428(3)	16(1)
C(8)	2893(4)	-1035(3)	5857(3)	17(1)
C(9)	2057(4)	-726(2)	6653(3)	15(1)
C(10)	286(4)	-698(3)	6485(3)	20(1)

Table 5.3. Bond lengths [Å] and angles [°] for $(pz)_2CuCl_2$.

Cu(1)-N(3)	1.998(3)	C(5)-H(51)	0.94(4)
Cu(1)-N(2)	2.015(3)	C(5)-H(52)	0.97(4)
Cu(1)-Cl(2)	2.2985(9)	C(5)-H(53)	0.94(5)
Cu(1)-Cl(1)	2.3258(9)	N(3)-C(9)	1.346(4)
Cu(1)-Cl(1)#1	2.6703(10)	N(3)-N(4)	1.359(4)
Cl(1)-Cu(1)#1	2.6703(10)	N(4)-C(7)	1.344(4)
N(1)-C(2)	1.346(4)	N(4)-H(4)	0.84(4)
N(1)-N(2)	1.359(4)	C(6)-C(7)	1.496(5)
N(1)-H(1)	0.86(4)	C(6)-H(61)	0.94(4)
N(2)-C(4)	1.347(4)	C(6)-H(62)	0.93(5)
C(1)-C(2)	1.500(5)	C(6)-H(63)	0.80(6)
C(1)-H(11)	0.94(5)	C(7)-C(8)	1.379(5)
C(1)-H(12)	0.88(5)	C(8)-C(9)	1.405(4)
C(1)-H(13)	0.92(4)	C(8)-H(8)	0.87(5)
C(2)-C(3)	1.382(4)	C(9)-C(10)	1.499(5)
C(3)-C(4)	1.405(4)	C(10)-H(101)	0.94(4)
C(3)-H(3)	0.94(4)	C(10)-H(102)	0.89(5)
C(4)-C(5)	1.488(4)	C(10)-H(103)	0.90(6)
N(3)-Cu(1)-N(2)	88.67(11)	C(2)-C(1)-H(11)	105(3)
N(3)-Cu(1)-Cl(2)	162.46(8)	C(2)-C(1)-H(12)	116(3)
N(2)-Cu(1)-Cl(2)	88.95(8)	H(11)-C(1)-H(12)	109(4)
N(3)-Cu(1)-Cl(1)	89.36(8)	C(2)-C(1)-H(13)	110(3)
N(2)-Cu(1)-Cl(1)	174.39(8)	H(11)-C(1)-H(13)	119(4)
Cl(2)-Cu(1)-Cl(1)	91.34(3)	H(12)-C(1)-H(13)	98(4)
N(3)-Cu(1)-Cl(1)#1	98.76(8)	N(1)-C(2)-C(3)	106.3(3)
N(2)-Cu(1)-Cl(1)#1	100.76(8)	N(1)-C(2)-C(1)	121.0(3)
Cl(2)-Cu(1)-Cl(1)#1	98.76(3)	C(3)-C(2)-C(1)	132.6(3)
Cl(1)-Cu(1)-Cl(1)#1	84.74(3)	C(2)-C(3)-C(4)	106.5(3)
Cu(1)-Cl(1)-Cu(1)#1	95.26(3)	C(2)-C(3)-H(3)	130(2)
C(2)-N(1)-N(2)	112.0(3)	C(4)-C(3)-H(3)	124(2)
C(2)-N(1)-H(1)	125(3)	N(2)-C(4)-C(3)	109.3(3)
N(2)-N(1)-H(1)	123(3)	N(2)-C(4)-C(5)	122.3(3)
C(4)-N(2)-N(1)	105.9(3)	C(3)-C(4)-C(5)	128.3(3)
C(4)-N(2)-Cu(1)	133.4(2)	C(4)-C(5)-H(51)	109(3)
N(1)-N(2)-Cu(1)	119.0(2)	C(4)-C(5)-H(52)	116(2)

Table 5.4. Anisotropic displacement parameters ($Å^2 x\ 10^3$) for $(pz)_2CuCl_2$. The anisotropic displacement factor exponent takes the form: $-2?\ ^2[\ h^2\ a^{*2}U^{11} + ... + 2\ h\ k\ a^*\ b^*\ U^{12}\ ]$

	U^{11}	U^{22}	U^{33}	U^{23}	U^{13}	U^{12}
Cu(1)	16(1)	17(1)	5(1)	1(1)	1(1)	2(1)
Cl(1)	19(1)	17(1)	9(1)	2(1)	1(1)	1(1)
Cl(2)	15(1)	22(1)	8(1)	0(1)	2(1)	-1(1)
N(1)	17(1)	19(1)	11(1)	4(1)	5(1)	3(1)
N(2)	14(1)	20(1)	9(1)	1(1)	4(1)	1(1)
C(1)	18(2)	21(2)	15(2)	2(1)	3(1)	1(1)
C(2)	17(2)	16(2)	9(1)	-1(1)	2(1)	2(1)
C(3)	17(2)	17(2)	11(1)	2(1)	3(1)	0(1)
C(4)	19(2)	14(2)	8(1)	-1(1)	4(1)	0(1)
C(5)	20(2)	23(2)	12(2)	4(1)	5(1)	-1(1)
N(3)	14(1)	18(1)	8(1)	-1(1)	1(1)	1(1)
N(4)	15(1)	22(1)	8(1)	-2(1)	0(1)	2(1)
C(6)	21(2)	28(2)	14(2)	1(1)	8(1)	0(1)
C(7)	21(2)	18(2)	9(1)	1(1)	5(1)	1(1)
C(8)	19(2)	24(2)	8(1)	-2(1)	1(1)	-1(1)
C(9)	19(2)	15(2)	9(1)	0(1)	1(1)	-1(1)
C(10)	18(2)	24(2)	15(2)	-1(1)	1(1)	-2(1)

Table 5.5 Hydrogen coordinates ($x\ 10^4$) and isotropic displacement parameters ($Å^2 x\ 10^3$) for $(pz)_2CuCl_2$.

	x	y	z	U(eq)
H(1)	-490(50)	880(30)	8720(40)	26(11)
H(11)	-3250(60)	1270(40)	6940(40)	37(13)
H(12)	-3090(50)	2050(30)	7840(40)	29(11)
H(13)	-3190(50)	2440(30)	6770(40)	26(11)
H(3)	-260(50)	2590(30)	6110(40)	22(10)
H(51)	2940(50)	2450(30)	6490(40)	28(11)
H(52)	3960(40)	1820(30)	7490(30)	8(8)

5.3.1 A typical Procedure for the synthesis of silylether

Bis-pyridinium tetrachlorocuprate (47 mg, 0.13 mmol) was dissolved in alcohol (5ml) and the solution was degassed by purging with dry nitrogen. To this solution triphenylsilane (260 mg, 1 mmol) was added and the reaction mixture was stirred at 60^0C for 2-5 hrs. The progress of the reaction was monitored by TLC and GC. After completion of the reaction, the reaction mixture was concentrated by removing alcohol under reduced pressure. A paste was obtained; the paste was purified by using a short silica gel column with hexane as eluent. Isolated yield after column chromatography of the silylether were 40-60%; GC yield > 98%.

The spectroscopy data of some of the silylethers are given below.

Analytical data of silylether:

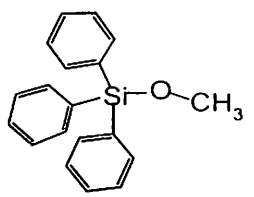

3a

IR (KBr, cm^{-1}): 3068(w), 3014(w), 2965(w), 1589(m), 1485(w), 1427(s), 1119(s), 1027(m), 998(m), 855(s), 835(s), 738(m), 712(s), 513(s)

^{1}H NMR ($CDCl_3$): (δ ppm) 7.4-7.5 (9H, m), 7.6-7.7 (6H, m), 3.6 (3H, s)

^{13}C NMR ($CDCl_3$): (δ ppm) 51.93, 127.99, 130.14, 134.03, 135.48

C, H analysis: $C_{19}H_{18}OSi$ calcd. C = 78.62, H = 6.2 found C = 78.49, H = 6.19

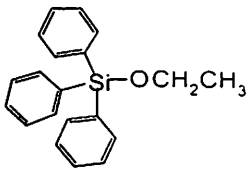

3b

IR (KBr, cm^{-1}): 3282(b), 3067(w), 3016(w), 2970(w), 1428(s), 1116(s), 1085(w), 998(w), 839(s), 737(m), 711(s), 511(s), 435(w)

^{1}H NMR ($CDCl_3$): (δ ppm) 7.3 - 7.5(9H, m), 7.5-7.8(6H, m), 3.8- 3.9(2H, q, *J*= 6.9 Hz), 1.2-1.8(3H, t, *J*= 6.9 Hz)

^{13}C NMR ($CDCl_3$): (δ ppm) 18.46, 59.85, 127.94, 130.19, 135.09, 135.49,

C, H analysis: $C_{20}H_{20}OSi$ calcd. C = 78.95, H = 6.62 found C = 78.98, H = 6.29

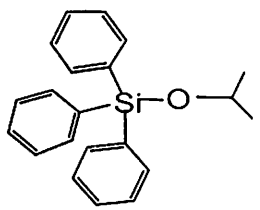

3c

IR (KBr, cm^{-1}): 3326(b), 3065(w), 3022(w), 2968(w), 2925(w), 2871(w), 1590(w), 1485(w), 1426(s), 1376(m), 1173(w), 1119(s), 1014(s), 994(m), 878(m), 835(m), 741(s), 702(s), 531(s), 508(s), 442(m)

^{1}H NMR ($CDCl_3$): (δ ppm) 7.2-7.5 (9H, m), 7.6-7.7 (6H, m), 4.2(1H, heptet, *J*= 6 Hz), 1.2(6H, d, *J*= 6 Hz)

^{13}C NMR ($CDCl_3$): (δ ppm) 25.72, 66.40, 127.81, 129.88, 135.26, 135.52

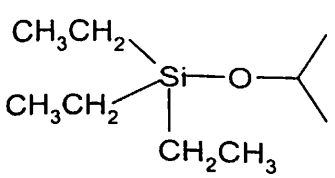

3d

IR (Thin film, cm^{-1}): 3416(bw), 2955(s), 2914(m), 2878(s), 1459(w), 1382(w), 1239(w), 1172(w), 1131(m), 1039(s), 875(w), 829(w), 742(s)

^{1}H NMR ($CDCl_3$): (δ-ppm) 3.9-4.1 (1H, m), 1.1-1.2 (6H, d, *J*= 6 Hz), 0.9-1.0 (9H,m), 0.5-0.7 (6H, m)

^{13}C NMR ($CDCl_3$): (δ-ppm) 4.92, 6.52, 25.89, 64.71

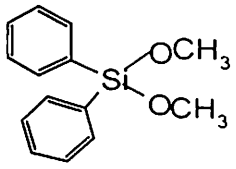

3f

IR (KBr, cm^{-1}): 3056(w), 2926(m), 2858(m), 1702(w), 1648(w), 1457(w), 1265(s), 1119(m), 740(s)

^{1}H NMR ($CDCl_3$): (δ-ppm) 7.6-7.7(4H, m), 7.3-7.4 (6H, m), 3.6(3H, s)

^{13}C NMR ($CDCl_3$): (δ-ppm) 50.96, 127.94, 130.39, 133.53, 134.38

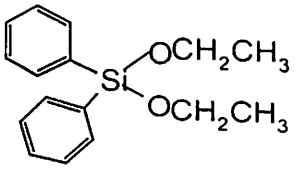

3g

IR (KBr, cm^{-1}): 3067(m), 3047(m), 3001(w), 1589(m), 1428(s), 1120(s), 822(s), 748(s), 702(s), 515(s)

^{1}H NMR ($CDCl_3$): (δ-ppm) 7.6-7.7(4H, m), 7.3-7.5(6H, m), 3.8-4.0(2H, q, *J*= 7 Hz), 1.2-1.4(3H, t, *J*= 7 Hz)

^{13}C NMR ($CDCl_3$): (δ-ppm) 18.17, 58.98, 127.82, 129.97, 133.35, 134.92

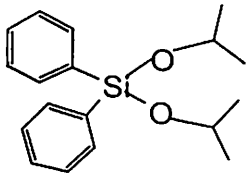

3h

IR (KBr, cm^{-1}): 3073(m), 3052(m), 3000(m), 2924(w), 1593(m), 1434(s), 1127(s), 830(s), 737(s), 707(s), 522(s)

^{1}H NMR ($CDCl_3$): (δ ppm) 7.6-7.8 (4H, m), 7.2-7.5 (6H, m), 4 (1H, m), 1.2(6H, d, *J*= 6.8 Hz)

^{13}C NMR ($CDCl_3$): (δ ppm) 135.50, 134.64, 130.52, 129.84, 66.01, 25.55

5.3.2 Visible spectroscopic study of diphenylsilane interact ethanol

The UV-Visible instrument was set at λ_{max} 467 nm and scanning for 5000 seconds, the decay of λ_{max} was monitored by adding diphenylsilane (0.1 mmol) in a mixture of *bis*-pyridinium tetrachlorocuprate (0.011 mmol), ethanol (3.4 mmol), acetonitrile (4 ml) in a quartz cuvette for one sets (a). Similarly for set (b) same λ_{max} was monitored by adding diphenylsilane (0.1 mmol) in a mixture of *bis*-pyridinium tetrachlorocuprate (0.02 mmol), ethanol (3.4 mmol), acetonitrile (4 ml) in a quartz cuvette.

5.3.3 Procedure for dehydrogenative oligomerisation of hydrosilanes with dihydroxy alcohols

Bis-pyridinium tetrachlorocuprate (40mg, 0.11mmol) was dissolved in a solution of dihydroxy alcohols (20 mmol) and acetonitrile (3ml). To this stirred solution diphenylsilane (0.2ml, 1.1mmol) was added. The reaction mixture was stirred at 60-70^{0}C for 6 hrs. The solvent and excess alcohol was removed under reduced pressure and the desired oligomer was extracted with dichloromethane (10ml). The dichloromethane was removed under reduced pressure to obtain the corresponding oligomer in 70% yield as colorless viscous liquid.

Analytical data of siloxane oligomers

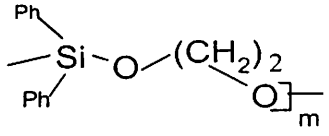

(3k)

IR (Thin film, cm^{-1}): 3436(bm), 3072(m), 3047(w), 2960(m), 2858(w), 1720(s), 1594(m), 1433(s), 1282(s), 1080(s), 873(w), 838(w), 747(s), 720(s), 701(s), 520(s)

^{1}H NMR ($CDCl_3$): (δ-ppm) 7.1-7.7(10H, m), 3.5-3.8 (4H, m)

^{13}C NMR ($CDCl_3$) (δ-ppm) 67.33, 128.29, 130.66, 134.80, 135.17

GPC (THF): M_w = 1667, M_n = 1659

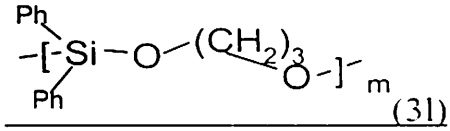

(3l)

IR (Thin film, cm^{-1}): 3440(bm), 3057(w), 2927(s), 2864(w), 2355(w), 1647(m), 1531(m), 1456(m), 1265(s), 1095(b), 741(s)

^{1}H NMR ($CDCl_3$): (δ-ppm) 7.2-7.7 (10H, m), 3.7-3.8(4H, t, *J*= 5.5 Hz), 1.7-1.8 (2H, q, J= 5.6 Hz),

^{13}C NMR ($CDCl_3$) (δ-ppm) 34.22, 61.88, 127.80, 130.15, 134.57, 134.78

GPC (THF): M_w = 1663, Mn = 1656

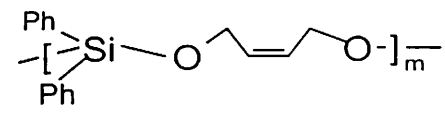

(3m)

IR (Thin film, cm^{-1}): 3437(bm), 3056(w), 2928(m), 2863(w), 1646(m), 1520(m), 1437(m), 1265(s), 1116(w), 895(w), 741(s)

^{1}H NMR ($CDCl_3$): (δ-ppm) 7.2-7.7 (10H, m), 5.6-5.7 (2H, m), 4.0-4.2 (4H, d, *J*= 4.6 Hz)

GPC (THF): M_w = 2754, Mn = 2738

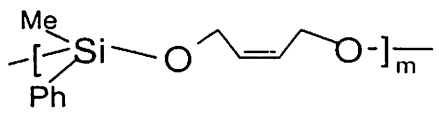

(3n)

IR (Thin film, cm^{-1}): 3442(bw), 3059(w), 2925(w), 2858(w), 1707(m), 1648(m), 1523(m), 1459(m), 1428(w), 1265(s), 1081(s), 736(s)

^{1}H NMR ($CDCl_3$): (δ-ppm) 7.2-7.7 (5H, m), 5.6-5.8(2H, m), 4.0-4.3(4H, d, *J*= 4.6), 0.2-0.5(3H, m)

GPC (THF): M_w = 1088, Mn = 1077

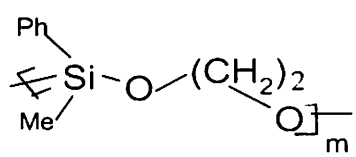

(3o)

IR (Thin film, cm^{-1}): 3436(bm), 3058(w), 2926(w), 2860(w), 1699(m), 1649(m), 1524(m), 1264(s), 1082(s), 740(s)

^{1}H NMR ($CDCl_3$): (δ-ppm) 7.1-7.8 (5H, m), 3.7 (4H, s), 0.1-0.6 (3H, m)

^{13}C NMR ($CDCl_3$) (δ-ppm) 0.22, 63.80, 127.66, 128.46, 133.33, 136.85

GPC (THF) : M_w = 1698, M_n = 1683

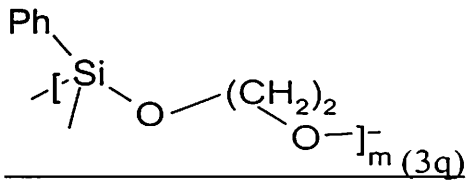

(3q)

IR (Thin film, cm^{-1}): 3393(bs), 3073(w), 2941(w), 2879(w), 1654(w), 1594(m), 1458(w), 1430(s), 1134(s), 1085(s), 1030(s), 880(w), 780(w), 739(s), 697(s), 489(s)

^{1}H NMR ($CDCl_3$): (δ-ppm) 6.7-7.8 (5H, m), 3.6(4H, s)

^{13}C NMR ($CDCl_3$) (δ-ppm) 64.61, 128.21, 130.93, 134.59,

GPC (THF) : M_w = 3788, M_n = 3788

M_w = 3236, Mn = 3232

M_w = 2470, M_n = 2449

M_w = 1786, M_n = 1768

5.3.4 Reaction of 2,6-dimethylphenol

To a solution of methanol (7ml) *bis*-pyridinium tetrachlorocuprate (35mg, 0.104mmol) was dissolved and to this solution 2,6-dimethylphenol (400mg, 3.2mmol) and hydrogen peroxide (0.5ml, 30% vol) was added. The reaction mixture on stirring at room temperature resulted in the precipitation of a red solid. The red solid was filtered, washed with hexane and dried under vacuum to give C-C bonded dimmer.

Yield =100 mg

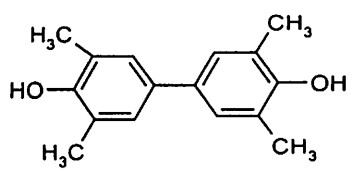

(4,4′-dihydroxy-3,5,3′,5′-tetramethylbiphenyl)

IR (KBr, cm^{-1}): 2950(w), 2924(w), 2858(w), 1654(m), 1597(s), 1377(w), 1218(m), 1039(m), 916(w), 835(w), 784(w), 481(w).

FAB mass:

242, 237, 226, 213, 209, 202,196, 189, 178, 165, 163, 154, 152, 138, 128, 124, 120, 115, 107, 105, 102.

^{1}H NMR (DMSO-d^6): δ 8.2 (2H, s, phenolic), 7.1 (4H, m,aromatic), 3.3 (s,12H)

5.3.5 Oligomerisation of aniline

Bis-pyridinium tetrachlorocuprate (30mg, 0.079mmol) was dissolved in 10ml methanol. To this solution, aniline (0.5g, 5.35mmol) and hydrogen peroxide (0.5ml, 30% vol) was added and the resulting solution was refluxed for two hours. A black solid of polyaniline was obtained. The solution was filtered and washed repeatedly with cold water (50ml). The black solid obtained was dried under reduced pressure.

Yield 150 mg

Polyaniline oligomer

IR (KBr, cm^{-1}) 3850(w), 3741(w), 3259(s), 1685.2(w), 1506(m), 1289(m), 1169(w), 747(m), 689(m).

^{1}H NMR (DMSO-d_6) (δ-ppm) 5.9-8.5(m)

^{13}C NMR (DMSO-d_6) (δ-ppm) 90.2, 115.8, 120.9, 123.7, 128.7 in addition there are signals at 89.2, 117.6. 120.1, 123.1, 127.7, 128.2, 129.3, 130.1, 138.8, 146.6, 149.9, 155.2, 180.3 9 (from the branch chain with carbonyl end group).

GPC (THF): Mn, Mw : 3479, 3546

5.3.6 Oxidation of 1,4-naphthalenediol

To a well stirred solution containing *bis*-pyridinium tetrachlorocuprate (35mg, 0.104 mmol), 1,4-naphtahlenediol (85mg, 0.53mmol) in 5ml methanol followed by tertiary butyl hydroperoxide (0.5ml, 80%) was added. The reaction mixture was stirred at room temperature for 3hrs. During this period the colour of the solution turned intense brown. The acetonitrile solvent was removed under reduced pressure; the paste obtained was extracted with dichloromethane (2 X 25ml) and was washed with water (30ml) to remove the catalyst. On removal of dichloromethane and subsequent purification by column chromatography gave 1,4-naphthoquinone. The compound was characterized by recording its NMR, IR, and comparing with authentic sample.

Yield = 50 mg

Melting point of the compound = 125^{0}C

IR (KBr, cm^{-1}): 3062(w), 3037(w), 1662(s), 1608(m), 1587(m), 1329(m), 1302(s), 1145(w), 1127(w), 1056(w), 1024(w), 864(m), 778(s), 697(w), 671(w), 445(m).

5.3.7 Oxidation of benzenethiol

Bis-pyridinium tetrachlorocuprate (35mg, 0.104mmol) was dissolved in 7ml methanol. To this solution benzenethiol (0.3 ml, 2.27mmol) was added and the reaction mixture was stirred under aerial condition at room temperature for two hrs. The solvent was removed under reduced pressure, the residue obtained was extracted with dichloromethane (2 X 25ml) and dichloromethane layer was washed with water (30ml) to remove the catalyst. On removal of dichloromethane and subsequent purification by column chromatography gave diphenyldisulphide. The compound was characterized by recording its NMR, IR, and comparing with authentic sample.

IR (KBr, cm^{-1}): 3073(w), 2924(w), 2852(w), 1577(m), 1480(m), 1438(m), 1075(m), 1024(m), 737(s), 686(s), 466(s)

^{1}H NMR ($CDCl_3$) (δ-ppm) 7.1-7.3(4H, m), 7.4-7.5(6H, m)

Melting point = 57^{0}C (reported 57^{0}C)

5.3.8 Procedure of deposition of copper

A clean glass sheet (15mm X 15mm X 1mm) was placed inside a dry Schlenk tube. To this *bis*-pyridinium tetrachlorocuprate (40mg, 0.11mmol), acetonitrile (4ml), phenylsilane (0.203 mmol) and ethyleneglycol (37.88 mmol) were added under inert atmosphere. The reaction mixture was left at room temperature for 4 hrs. Metallic copper deposited on the glass plate was taken out under inert atmosphere and characterized by recording its X-ray powder diffraction pattern.

5.3.9 General procedure for the deposition of gold

A clean glass sheet (15mm X 15mm X 1mm) was placed inside a dry beaker. To this) $H_2[AuCl_4]$ (0.088- 0.11mmol), acetonitrile (4ml), ethyleneglycol (37.88 mmol) were added. To this solution silanes (0.103 mmol) were added. Immediately metallic gold was deposited on the glass plate and the reaction mixture was kept for another four hours. The plate was then taken out and characterised by recording its X-ray powder diffraction pattern and particle size were determined by SEM.

^{1}H and ^{13}C NMR Spectral data

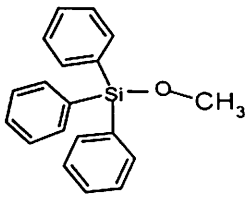

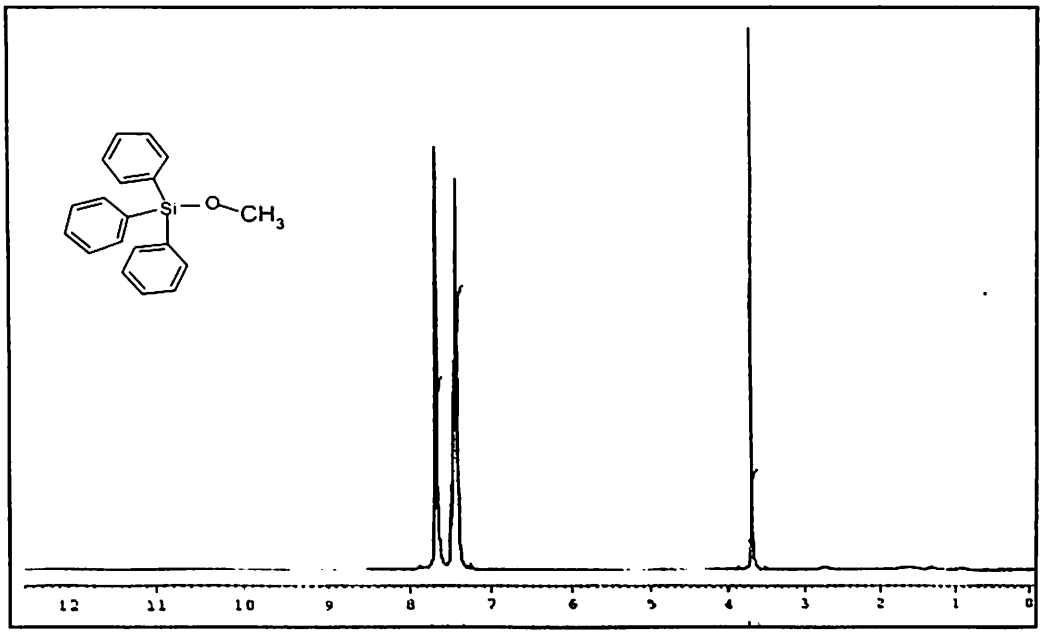

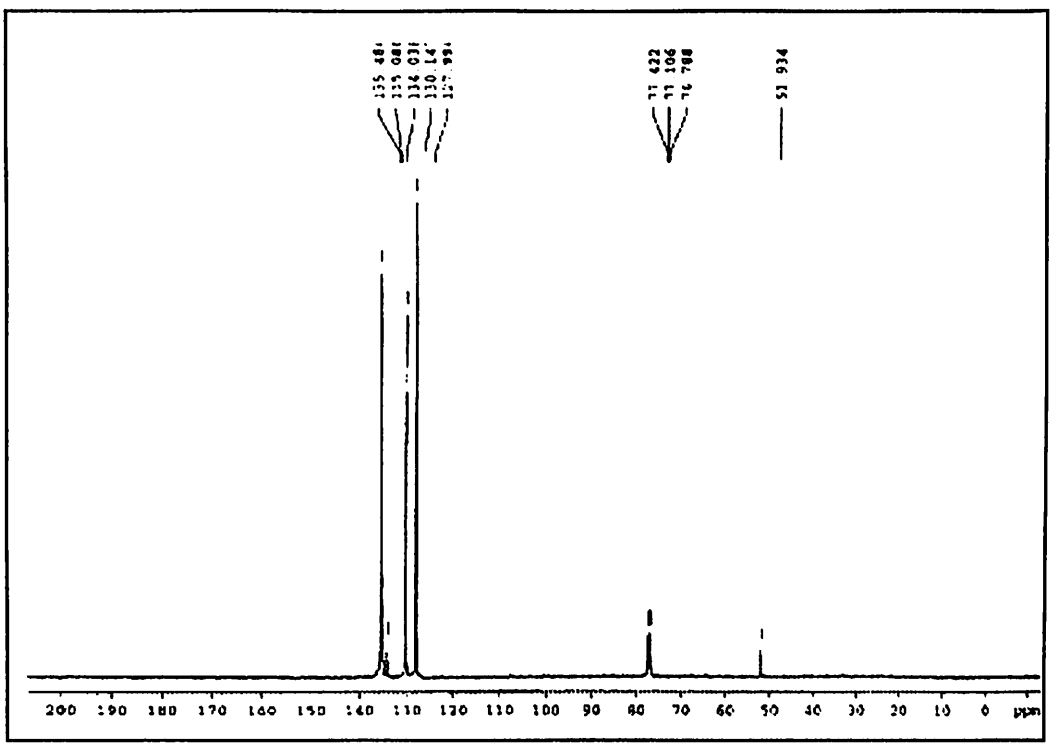

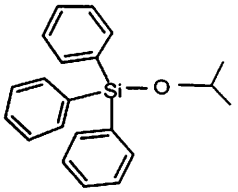

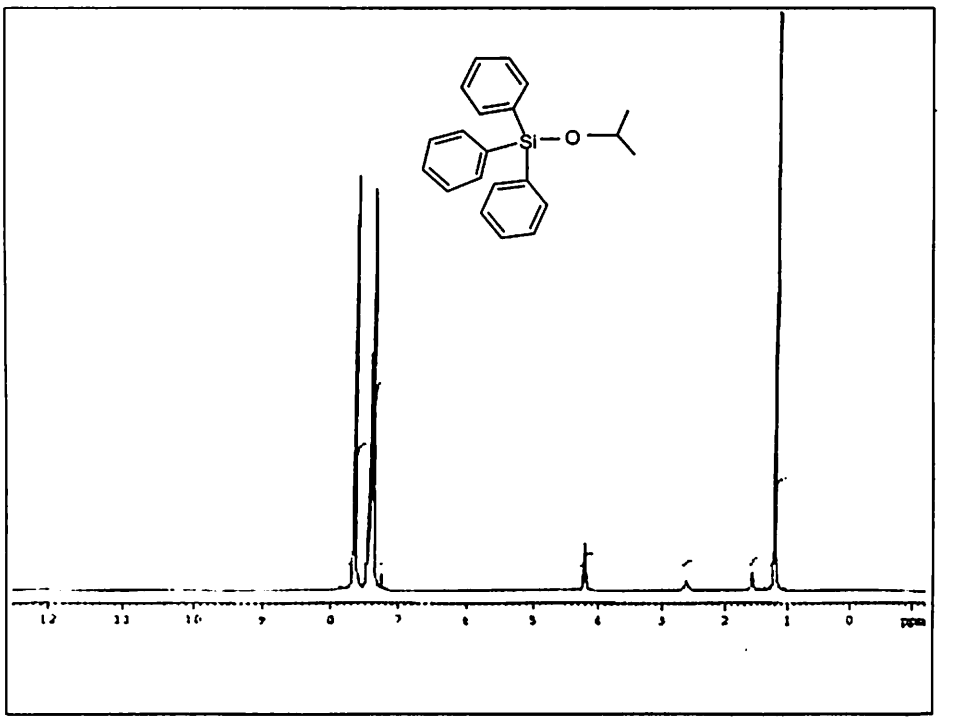

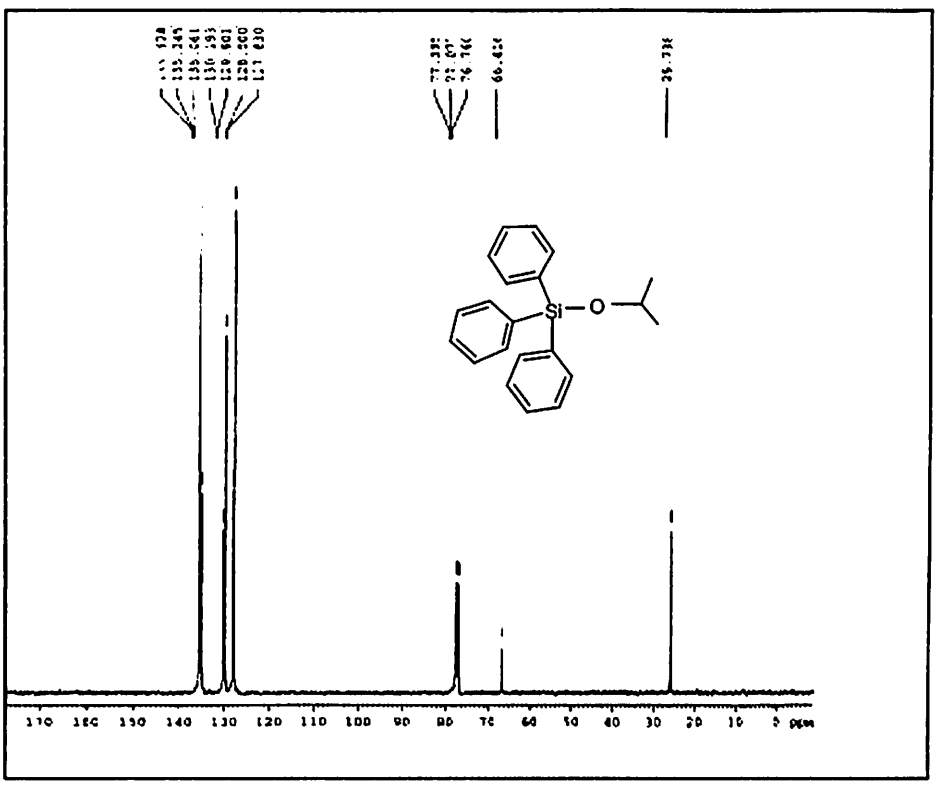

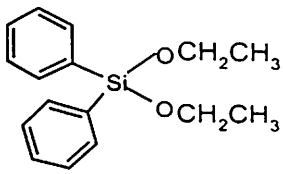
OCH2CH3
Si
OCH2CH3

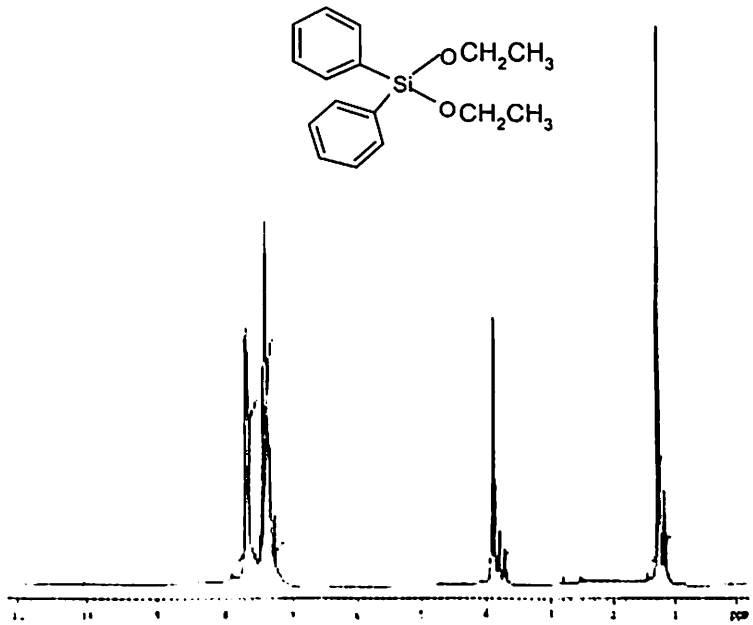
OCH2CH3
Si
OCH2CH3

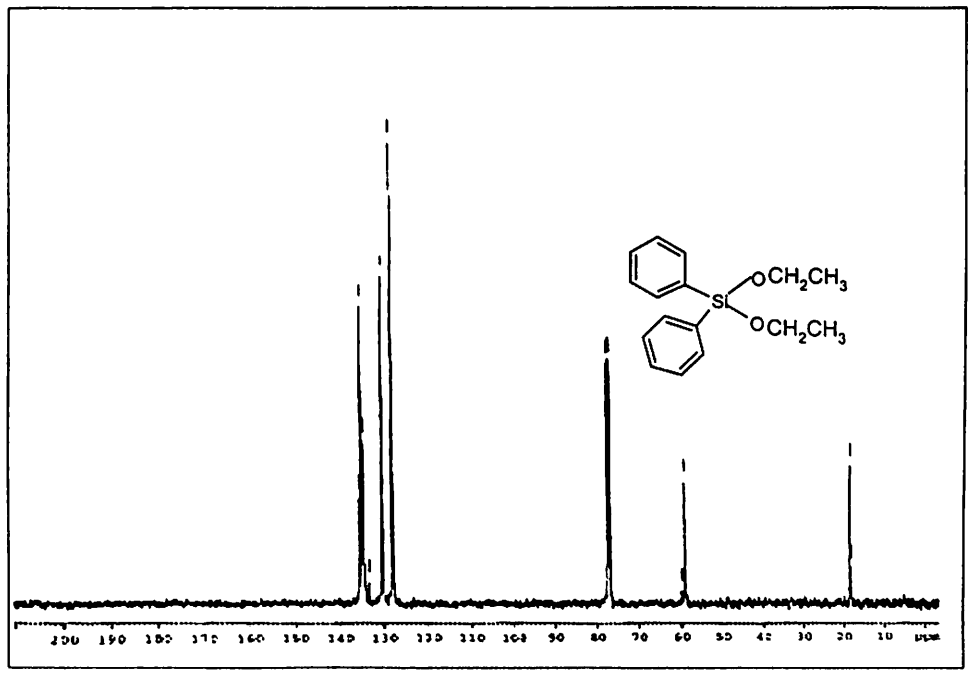
OCH2CH3
Si
OCH2CH3

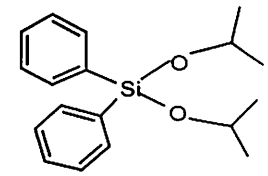

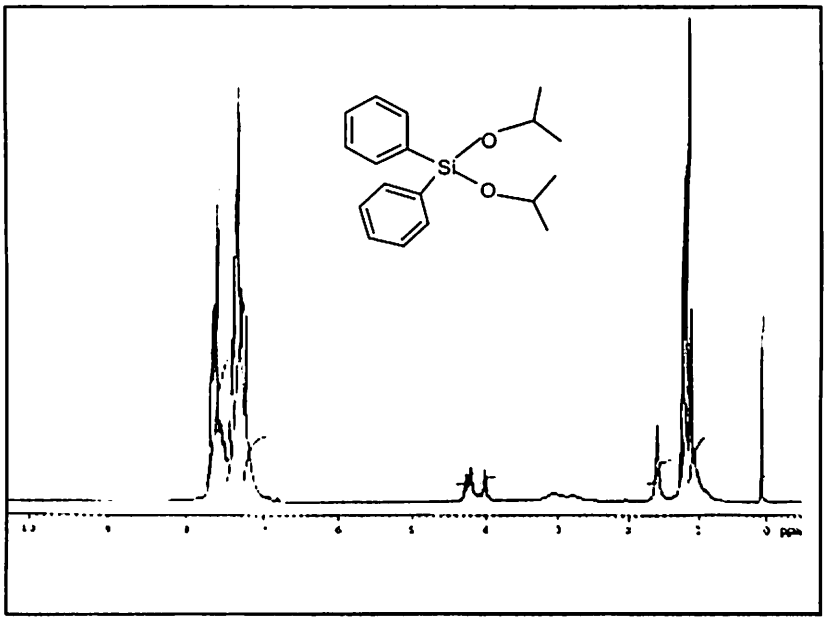

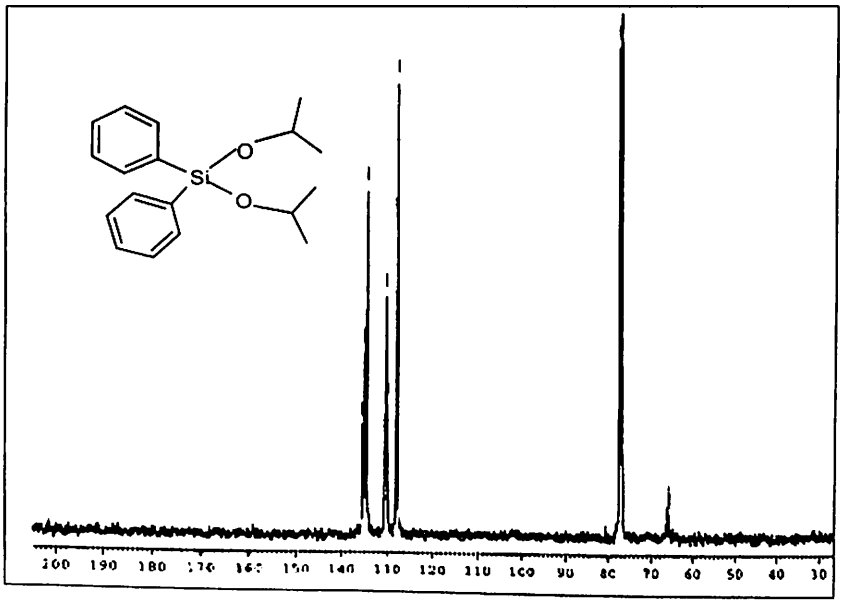

Few representative IR spectra of silylether

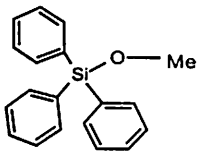

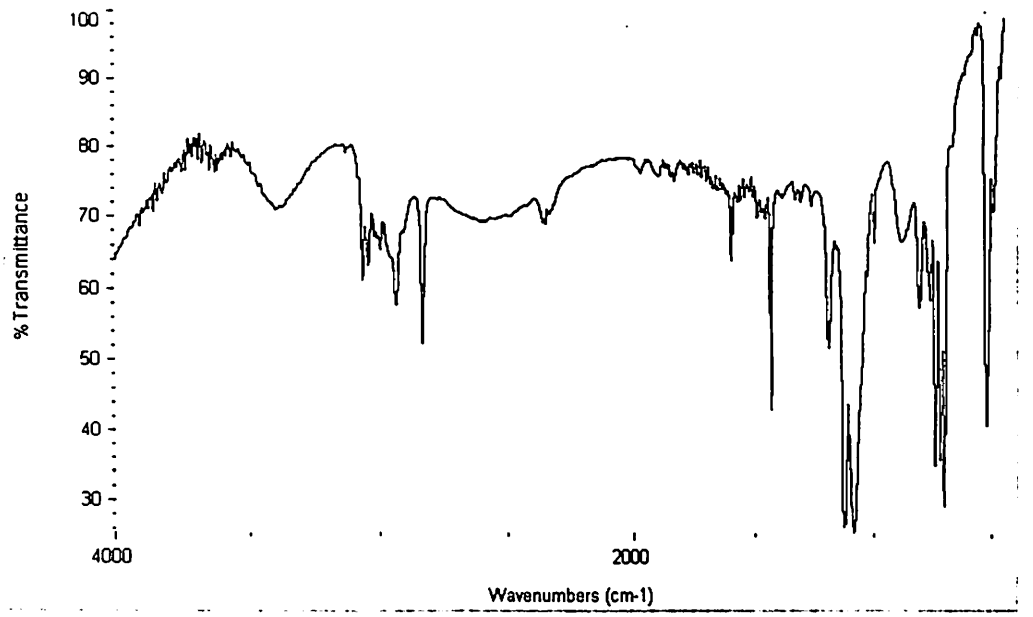

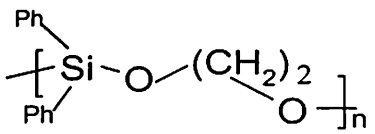

3k

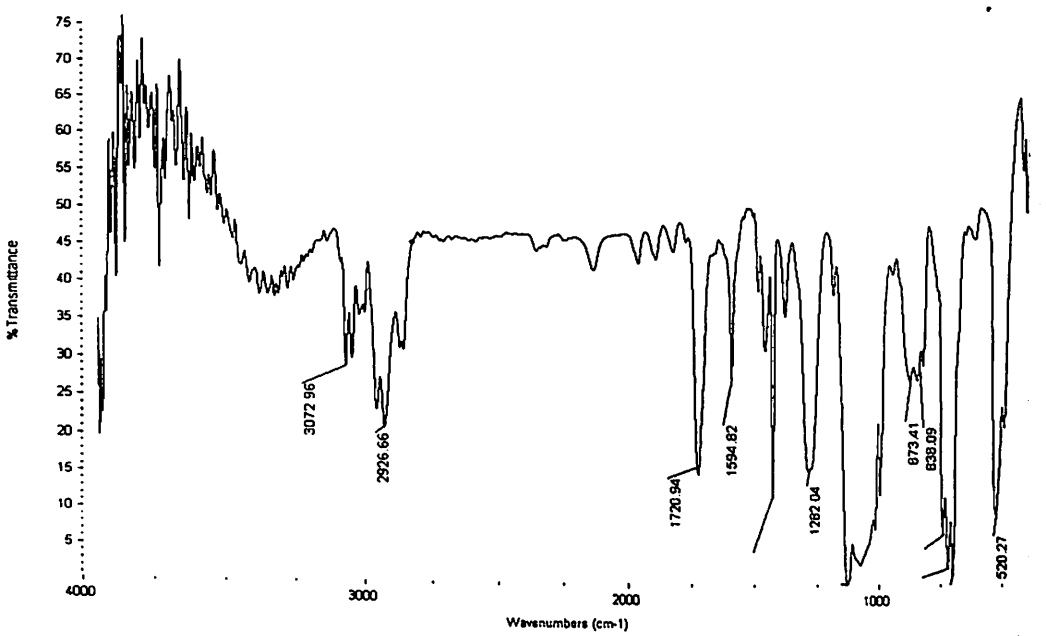

Gel permeation chromatogram

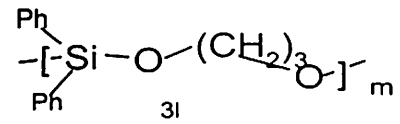

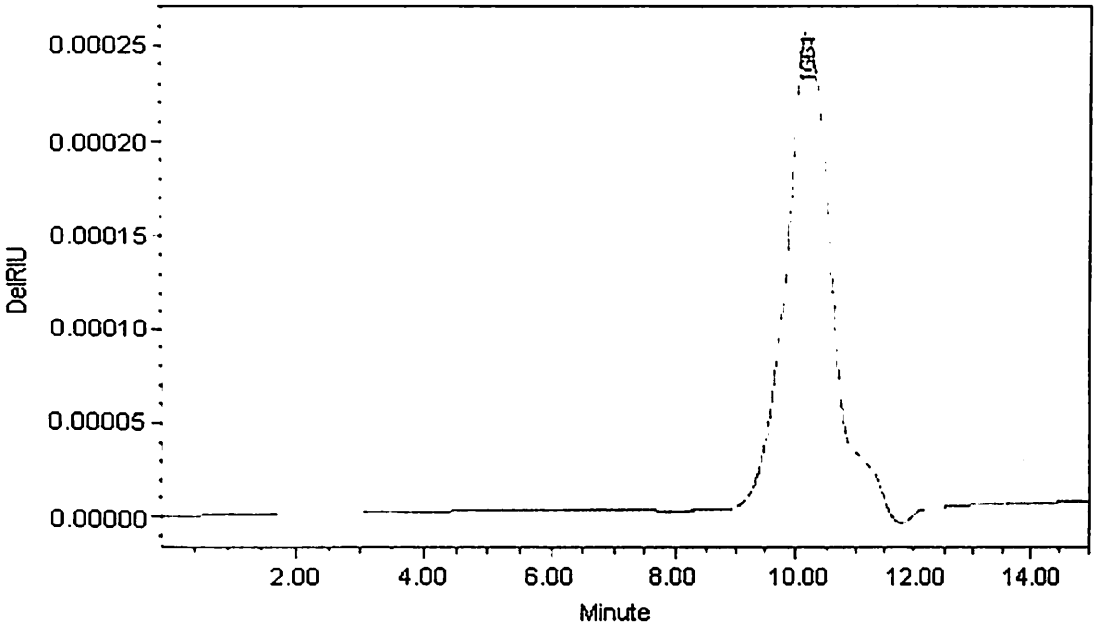

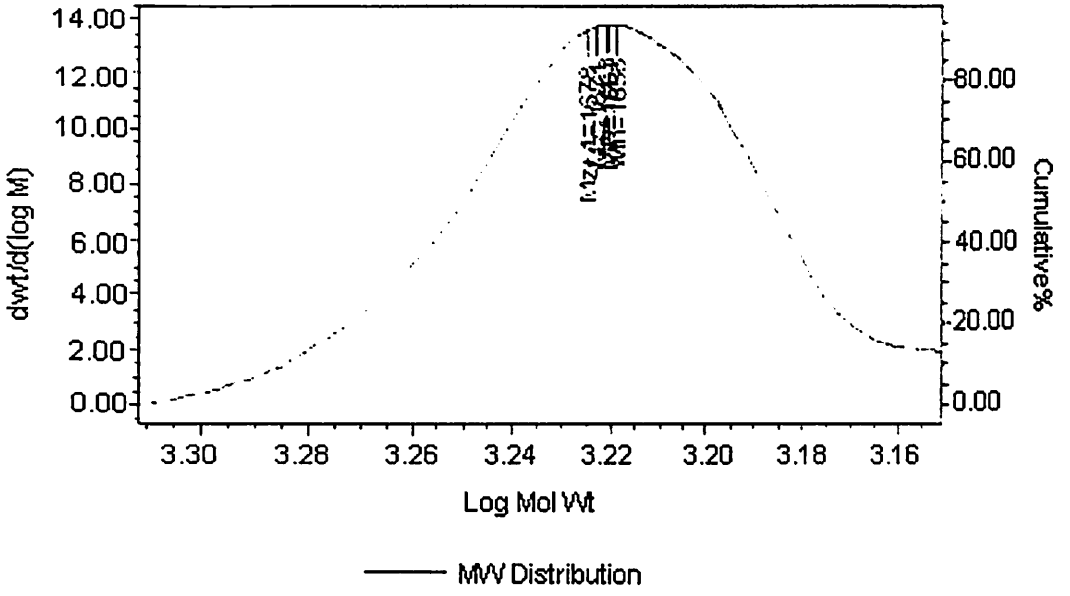

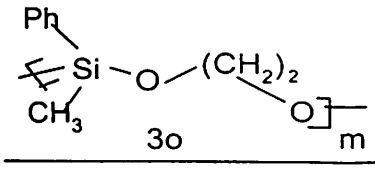

3o

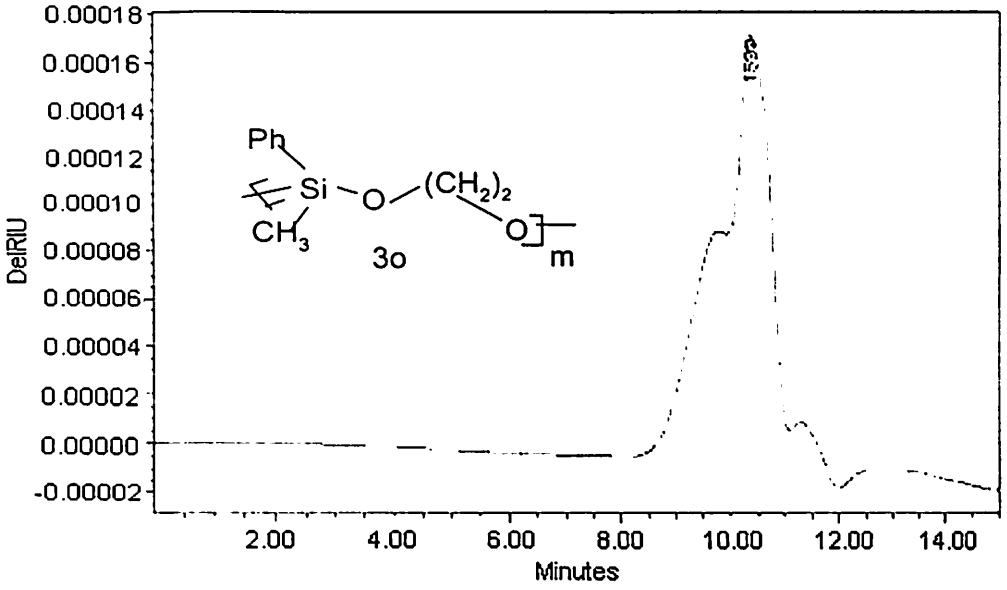

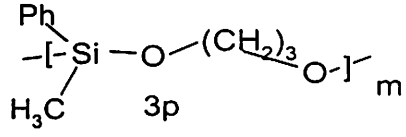

3p

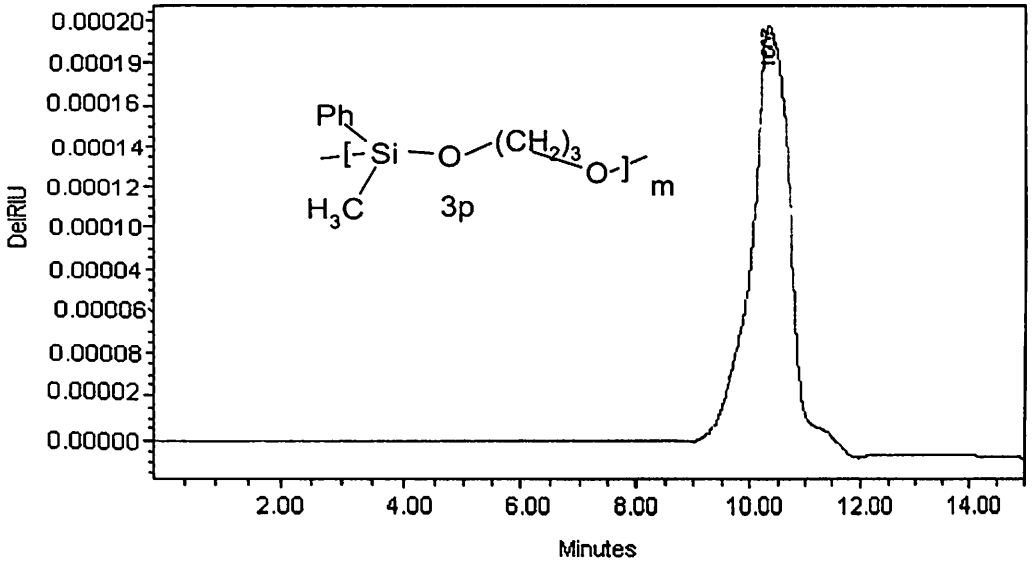

Experimental section of Chapter IV

5.4.1 General experimental procedure for the synthesis of palladium complexes

Palladium dichloride (0.4g, 2.275 mmol) was taken in 100 ml acetonitrile and refluxed for 90 minutes until a colour change from brown to red is achieved. This colour change suggests it to form $PdCl_2(CH_3CN)_2$ complex. To this hot solution of substituted ethylenediamine (2.3 mmol) was added and stirred for half-hours. The stirring resulted in the precipitation of the desired complex. The mixture was allowed to cool at room temperature and the complex was collected by filtration and washed with acetonitrile, acetone and diethyl ether and dried under vacuum.

5.a Pd(TMEDA)Cl_2

Yield = 500mg (75%)

Color of the complex = Yellow

5.b Pd(TEEDA)Cl_2

Yield = 520mg (65%)

Color of the complex = Orange

5.c Pd(DED)Cl_2

Yield = 480mg (72%)

Color of the complex = light yellow

Analytical data of the complex:

(5.a) **IR (KBr, cm^{-1})**: 3030(w), 2992(w), 2914(m), 2844(w), 1466(s), 1408(m), 1274(m), 1252(w), 1127(m), 1108(w), 1069(w), 1049(s), 1014(s), 960(s), 812(s), 777(m), 516(w)

Percentage of chloride = 23.86%, (calculated = 23.04%)

(5.b) **IR (KBr, cm^{-1}):** 2980(s), 2929(s), 2883(m), 1460(s), 1388(s), 1321(m), 1260(w), 1193(w), 1152(w), 1091(s), 1050(s), 1018(s), 799(m), 589(m)

Percentage of chloride = 20.09%, (calculated = 19.98)

(5.c) **IR (KBr, cm^{-1}):** 3477(m), 3431(m), 3119(s), 3073(s), 2975(m), 2878(m), 1454(m), 1386(w), 1137(w), 1086(m), 1034(m), 866(w), 794(w), 528(w).

Percentage of chloride = 23.94% (calculated = 24%)

5.4.2 General experimental procedure for the preparation of silylether by palladium (II) catalyst:

To a well stirred solution of alcohol (5 mmol) and silane (1mmol) in toluene (4 cm^3), the palladium catalysts (0.01 mmol) was suspended. The reaction mixture was allowed to stir for specific time at the temperature given in table 4.1 and 4.2. The black precipitate obtained was discarded after extracting the reaction mixture with hexane (20 cm^3). In most of the cases the reactions were quantitative in product formation; thus the products were obtained by removing the solvent under reduced pressure. Wherever required the products were purified by column chromatography. The products were characterized by recording their elemental analysis, IR, ^1H and ^{13}C NMR and also mass spectra in specific cases.

Since several of the compounds analytical data are reported in the copper(II) catalysed Si-O bond forming reaction only the one which were exclusively prepared by palladium catalyst are given below.

Analytical data of silylethers:

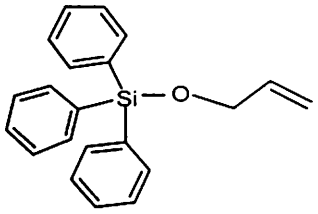

IR (Neat, cm^{-1}): 3290(b), 3073(m), 3017(m), 1597(w), 1490(w), 1428(s), 1121(s), 1031(m), 1003(m) 921(m), 843(m), 747(m), 706(s), 514(s)

^{1}H NMR ($CDCl_3$): (δ-ppm) 7.3-7.5(9H, m), 7.6-7.7(6H, m), 6.0(1H, m), 5.3(2H, d, *J*= 10.2 Hz), 4.4(2H,d, *J*= 4.3 Hz)

^{13}C NMR ($CDCl_3$): (δ-ppm) 64.71, 127.97, 130.16, 134.25, 135.27, 136.27,

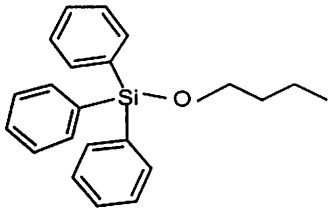

^{1}H NMR ($CDCl_3$): (δ-ppm) 7.2-7.5 (9H, m), 7.6- 7.7 (6H, m), 3.8 (2H, t, *J*= 6.04 Hz), 1.5-1.7(2H, quintet *J*= 7.2 Hz), 1.3-1.5 (2H, sextet, *J*= 7.3 Hz), 0.8Γ-1.0Γ(3H, t, J= 7.3 Hz)

^{13}C NMR ($CDCl_3$): (δ-ppm) 13.89, 19.03, 34.74, 63.77, 127.88, 129.98, 130.18, 134.59, 135.47.

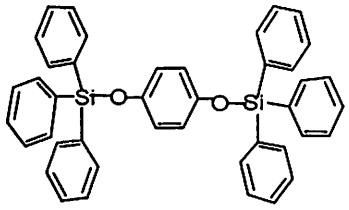

^{1}H NMR ($CDCl_3$): (δ-ppm) 7.6-7.7 (12H, m), 7.3-7.5 (18H, m), 6.7-6.8 (2H, m), 6.6.(2H, m)

^{13}C NMR ($CDCl_3$: (δ-ppm) 115.92, 120.80, 127.98, 130.30, 135.05, 135.59

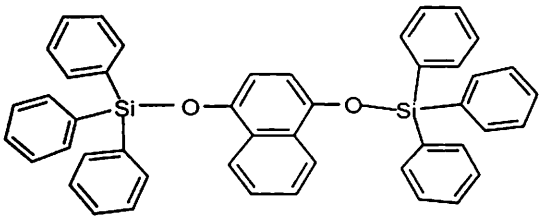

IR (KBr, cm^{-1}): 3067(w), 3057(w), 3026(w), 1674(s), 1587(s), 1495(m), 1464(m), 1438(s), 1387(m), 1341(m), 1305(s), 1269(m), 1234(m), 1126(s), 1085(m), 1008(w), 1003(w), 906(s), 860(m), 844(m), 773(m), 747(m), 716(s), 583(w), 517(s)

^{1}H NMR ($CDCl_3$): (δ-ppm) 7.3-8.3 (m)

^{13}C NMR ($CDCl_3$ (δ-ppm) 112.48, 122.62, 125.66, 128.44, 130.26, 133.79, 133.93, 138.70, 145.54

FAB mass (m/z): 105, 181, 199, 259, 443, 521, 676

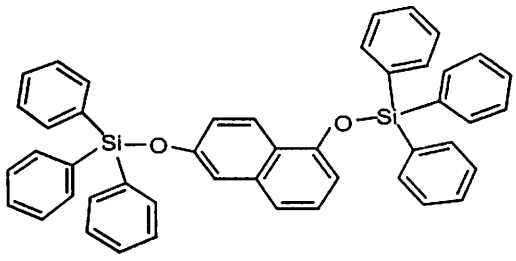

IR (KBr, cm^{-1}): 3067(m), 3047 (m), 3021(w), 1628(w), 1592(w), 1587(w), 1428 (s), 1362(m), 1264(m), 1228(m), 1116(s), 972(w), 911(m), 839(m), 747(m), 701(s), 511(s)

^{1}H NMR ($CDCl_3$): (δ-ppm) 6.6-8.3 (m)

^{13}C NMR ($CDCl_3$) (δ-ppm) 111.39, 115.08, 120.32, 121.02, 124.40, 126.28, 128.08, 129.65, 135.08

FAB mass (m/z): 105, 165, 181, 199, 259, 443, 521, 599, 676

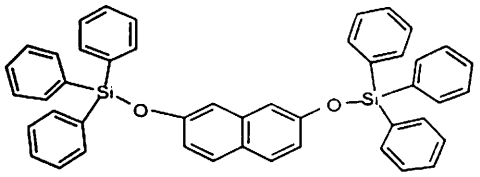

IR (KBr, cm^{-1}): 3067(w), 3042(w), 1505(m), 1433(s), 1259(w), 1213(w), 1121(s), 967(w), 921(w), 839(w), 701(s), 506(s)

^{1}H NMR ($CDCl_3$): (δ-ppm) 6.8-7.7 (m)

^{13}C NMR ($CDCl_3$ (δ-ppm) 127.97, 128.89, 129.15, 129.51, 130.14, 130.34, 135.04, 135.28, 135.58

FAB mass (m/z): 105, 136, 165, 181, 199, 207, 259, 379, 457, 521, 599, 676

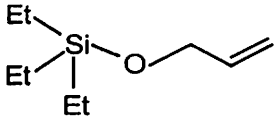

IR (Thin film, cm^{-1}): 2949(s), 2919(m), 2878(s), 1459(w), 1418(w), 1239(w), 1018(m), 834(s), 737(s)

^{1}H NMR ($CDCl_3$): (δ-ppm) 5.9-6.1 (1H, m), 5.2 (2H, d, *J*= 1.3 Hz and *J*= 17.2 Hz), 4.1 (2H, d, *J*= 3.8 Hz), 0.9-0.1 (9H, t, *J*=7.9 Hz), 0.5-0.6 (6H, q, *J*= 8 Hz).

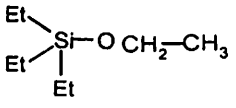

^{1}H NMR ($CDCl_3$): (δ-ppm) 3.6-3.7 (2H, q *J*= 6.9 Hz), 1.2 (3H, t *J*= 6.9), 0.9- 1.0 (9H, t, *J*= 7.9 Hz), 0.5-0.65 (6H, q, *J*= 8 Hz)

^{13}C NMR ($CDCl_3$) (δ-ppm) 5.85, 6.14, 18.66, 58.42

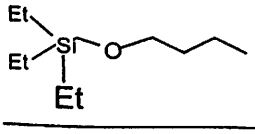

^{1}H NMR ($CDCl_3$): (δ-ppm) 3.6 (2H, t, *J*= 6.6 Hz), 2.6 (2H, m), 1.5-1.6 (2H, m), 1.3-1.4 (3H, t, *J*= 7.6 Hz), 0.9-0.1(9H, t, *J*= 5.5 Hz), 0.5-0.6 (6H, q, *J*= 7.9 Hz)

^{13}C NMR ($CDCl_3$) : (δ-ppm) 62.70, 32.89, 19.03, 13.90, 6.55, 5.86

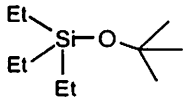

IR (KBr, cm^{-1}): 2960(s), 2919(s), 2883(s), 1470(m), 1419(m), 1239(m), 1019(s), 840(s), 748(s)

^{1}H NMR ($CDCl_3$): (δ-ppm) 1.2 (9H, s), 0.9-0.1 (9H, t, *J*= 8 Hz), 0.5-0.6 (6H, q, *J*= 7.9 Hz)

^{13}C NMR ($CDCl_3$):(δ-ppm) 32.08, 31.21, 6.51, 5.89

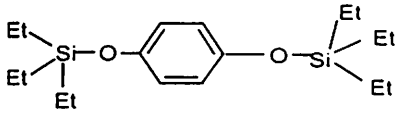

IR (Thin film, cm^{-1}): 2960(m), 2914(m), 2883(w), 1516(s), 1465(w), 1219(s), 1019(w), 912(m), 840(m), 825(m), 753(m)

^{1}H NMR ($CDCl_3$): (δ-ppm) 6.6-6.8 (4H, m), 0.9-1(18H, q, *J* = 7.8 Hz), 0.8 0.7 (8H, q, *J*= 7.9 Hz), 0.5-0.6 (4H, q, *J*= 7.9 Hz)

^{13}C NMR ($CDCl_3$) (δ-ppm) 4.98, 6.55, 14.13, 116.04, 120.63

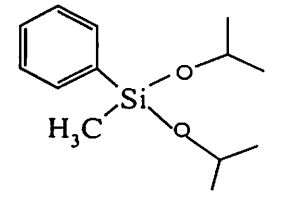

^{1}H NMR ($CDCl_3$): (δ-ppm) 7.5-7.7 (2H, m), 7.2-7.4(3H, m), 3.9-4.0 (1H, m), 1.2 (6H, d, *J*= 6.1 Hz)

^{13}C NMR ($CDCl_3$): (δ-ppm) 134.38, 133.75, 133.46, 129.89, 127.78, 64.04, 25.24, -1.49

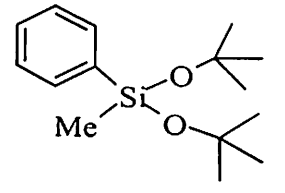

IR (Thin film, cm^{-1}): 2975(w), 3067(w), 3047(w), 1592(w), 1426(s), 1362(m), 1265(s), 1203(m), 1116(b), 865(b), 706(s), 481(s)

^{1}H NMR ($CDCl_3$): (δ-ppm) 7.5-7.7 (2H, m), 7.2-7.4 (3H, m), 1.2 (18H, s), 0.3 (3H, m)

^{13}C NMR ($CDCl_3$ (δ-ppm) -0.27, 32.05, 31.13, 127.85, 129.54, 129.98, 133.46, 134.01

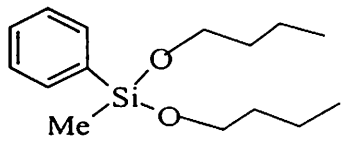

IR (Thin film, cm^{-1}): 3067(w), 2960(m), 2868(m), 1428(m), 1254(m), 1126(b), 890 (m), 788(w), 747(m), 706(m), 481(s)

^1H NMR ($CDCl_3$): (δ-ppm) 7.5-7.7 (2H, m), 7.2-7.4 (3H, m), 3.5-3.6 (2H, t, *J*= 6.6 Hz), 1.4-1.6 (2H, q, *J*= 7.8 Hz), 1.2-1.4 (2H,m), 0.7-0.9 (3H, t, *J*= 7.3 Hz), 0.1-0.3 (3H, m)

^{13}C NMR ($CDCl_3$) (δ-ppm) -1.04, 13.75, 34.71, 62.69, 127.73, 129.77, 133.45, 134.01, 137.26

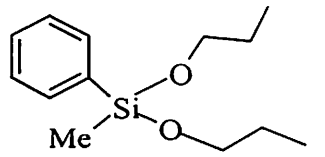

IR (Thin film, cm^{-1}): 3072(w), 2965(m), 2873(w), 1433(s), 1259(s), 1131(b), 875(b), 783(m), 747(m), 701(m), 481(s)

^1H NMR ($CDCl_3$): (δ-ppm) 7.5-7.7 (2H, m), 7.3-7.4 (3H, m), 3.5-3.6(2H, t, *J*= 6.6 Hz), 1.5-1.6(2H, m), 0.9-0.95 (3H, t, *J*= 3 Hz), 0.3-0.4 (3H, m)

^{13}C NMR ($CDCl_3$ (δ-ppm) –1.06, 10.21, 25.85, 64.69, 127.88, 130.05, 133.41, 133.74, 136.75

5.4.3 $Pd(TMEDA)Cl_2$ catalyzed reductive coupling reaction of 1,4-naphthoquinone and diphenylsilane

In a dry Schlenck tube a paste of 1,4-naphthaquinone (79 mg, 0.5 mmol) and diphenylsilane (81 mg, 0.5 mmol) was made. To this $Pd(TMEDA)Cl_2$ (9 mg, 0.037 mmol) was added and the Schlenck tube was placed in an oil bath at 90^0C for 2 hrs. The black mass obtained was washed with hexane (30 ml) and the residue thus obtained was dried under vacuum. Yield = 46 mg (65%)

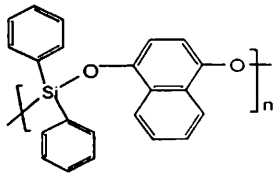

5b

IR (KBr cm^{-1}): 3360 (bm), 1618(s), 1590(s), 1550(s), 1420(s), 1390(s), 1350(s), 1230(s), 1200(s), 1090(s), 1040(s), 870(bs), 720(s), 700(s), 680(s), 660(s), 480(s)

^{1}H NMR ($CDCl_3$): (δ-ppm) 6.2-8.4 (m), 1.8 (m, from end group)

Mass (m/z): 1445-1437, 1352, 1237, 1154, 1098, 1075, 1016, 956, 937, 896, 878, 840, 814, 787, 758, 697, 676, 637, 619, 577, 559, 521

GPC (THF): M_w = 3730, M_n =3683 and M_w=1861 M_n =1848

5.4.4 Pd(TMEDA)Cl_2 catalyzed reaction of 1,4-naphthalenediol and diphenylsilane

In a dry Schlenck tube a paste of 1,4-naphthalenediol (79 mg, 0.5 mmol) and diphenylsilane (81 mg, 0.5 mmol) was made to this Pd (TMEDA) Cl_2 (9 mg, 0.037 mmol) was added and the Schlenck tube was placed in an oil bath at 90^{0}C for 2 hrs. The black mass obtained was washed with hexane (30 ml) and the residue thus obtained was dried under vacuum. Yield = 50 mg (68 %)

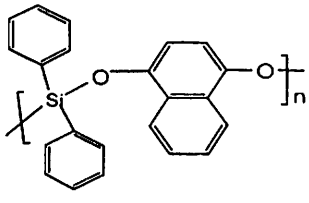

IR (KBr, cm^{-1}) 3360 (bm), 1618(s), 1590(s), 1550(s), 1420(s), 1390(s), 1350(s), 1230(s), 1200(s), 1090(s), 1040(s), 870(bs), 720(s), 700(s), 680(s), 660(s), 480(s)

^{1}H NMR ($CDCl_3$): (δ-ppm) 6.9-8.1 (naphthyl and aromatic proton), 2.7 (-OH proton, end group)

GPC (THF): M_w = 4310, M_n = 4303 and M_w =3100, M_n =3041

5.4.5 UV-visible study on the reaction of $Pd(TMEDA)Cl_2$ catalyzed reaction of 1,4-naphthalenediol and 1,4-naphthoquinone with diphenylsilane

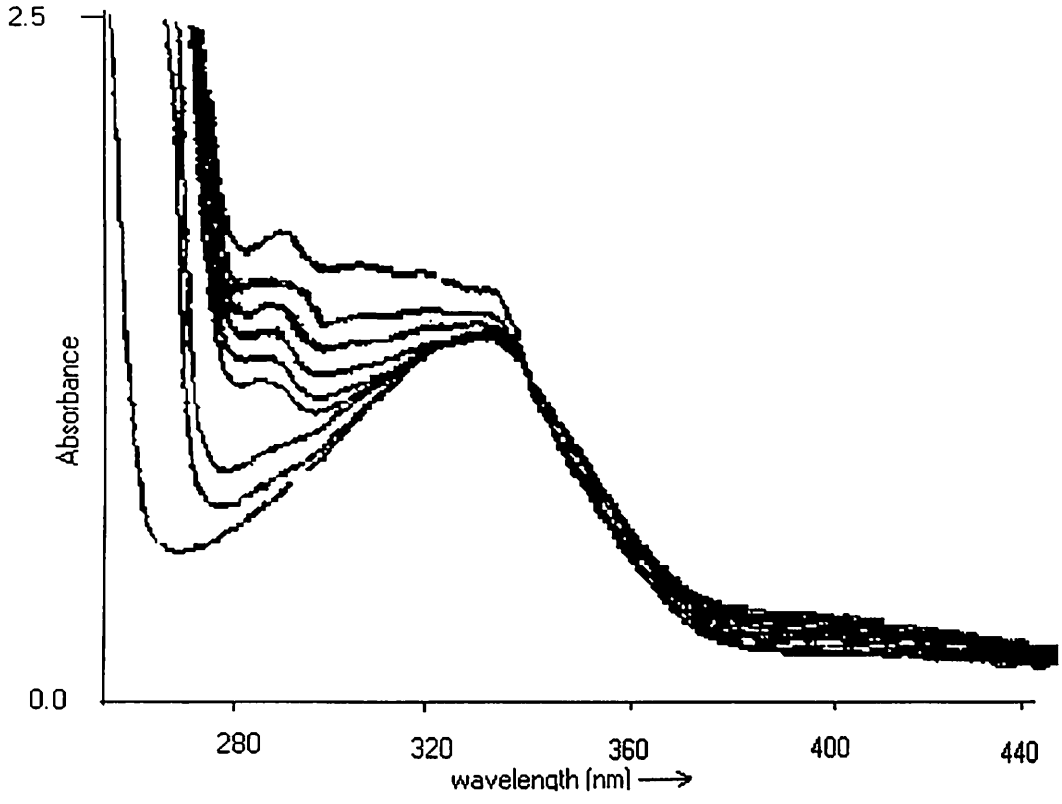

Figure 5.3 Change in absorbance during the reaction of 1,4 naphthalenediol (0.1mmol) with diphenylsilane(0.1mmol) in the presence of $Pd(TMEDA)Cl_2$(0.01mmol)in dichloromethane ($3.5cm^3$) recorded at 4 minutes time interval at 30^0C

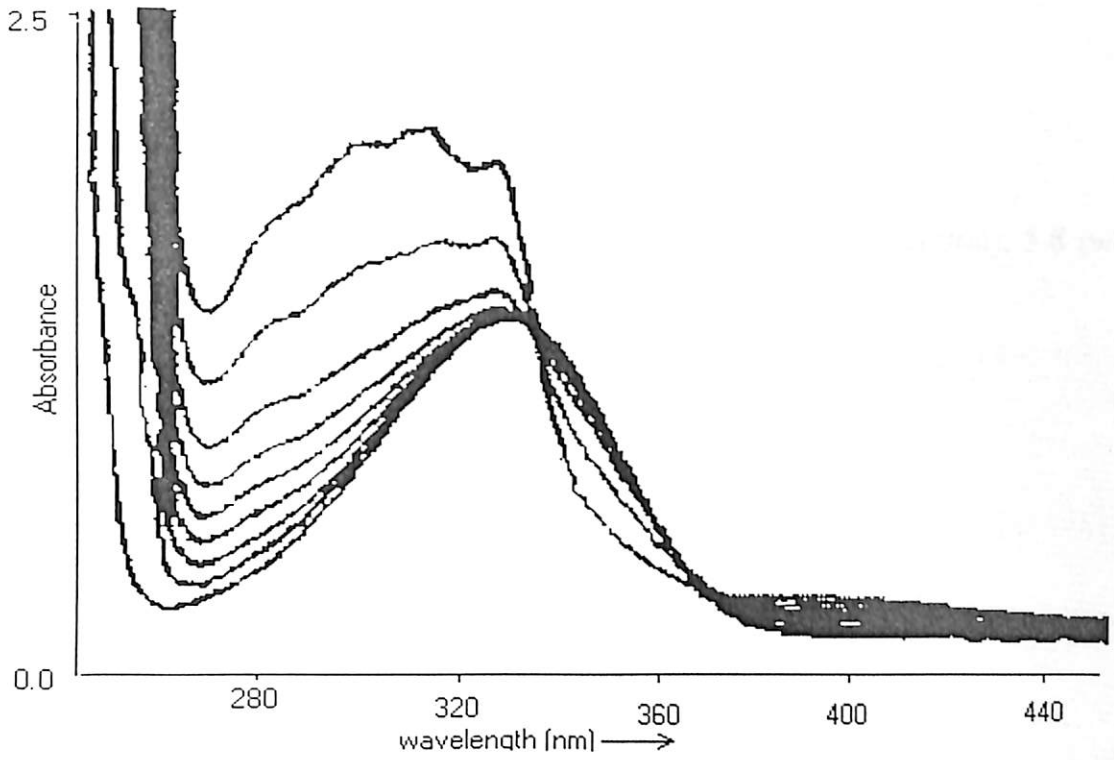

Figure 5.4 Change in absorbance during the reaction of 1,4 naphthoquinone (0.1mmol) with diphenylsilane (0.1mmol) in the presence of $Pd(TMEDA)Cl_2$ (0.01mmol)in dichloromethane ($3.5cm^3$) recorded at 4minutes time interval at 30^0C.

Analytical data of oligomer of different naphthalenediol and diphenylsilane

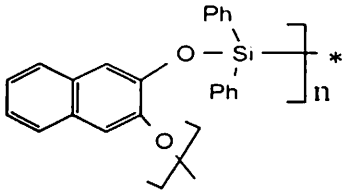

^{1}H NMR ($CDCl_3$): (δ-ppm) 6.8-7.9 (m, naphthyl and aromatic proton), 5.8 (weak signal, Si-H end group), 2.8 (-OH)

GPC (THF): M_w = 978, M_n = 949 polydispersity = 1.03

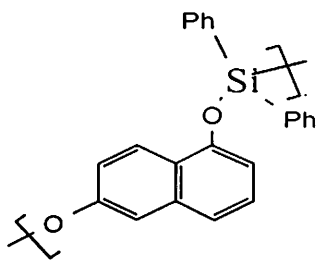

^{1}H NMR ($CDCl_3$): (δ-ppm) 7.0-8.0 (naphthyl and aromatic proton), 5.4 (weak signal, Si-H end group), 2.8 (weak signal, -OH end group)

GPC (THF): M_w = 3306, M_n = 3139, polydispersity =1.05

5.4.6 Pd(TMEDA)Cl_2 catalyzed reaction of hydroquinone with diphenylsilane

A mixture of diphenylsilane (182 mg, 1mmol) hydroquinone (101 mg, 1mmol) and Pd(TMEDA)Cl_2 (5 mg, 0.017 mmol) were heated in a dry Schlenck tube at 70^{0}C for 6hrs. The resulting black mass was washed with petroleum ether (30 ml) and the residue thus obtained was dried under vacuum. Yield = 180 mg (64%)

Analytical data

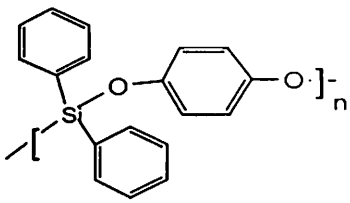

Elemental analysis: Calculated for $[C_{18}H_{14}O_2Si.0.5\ H_2O]_n$ C = 72.24, H = 5.01

Found: C = 72.45, H = 5.48%

IR (KBr cm^{-1}): 3206(bm), 1516(s), 1475(s), 1347(s), 1200(bs), 1100(s), 824(s), 752(s)

^{1}H NMR ($CDCl_3$): (δ-ppm) 6.5-8.3 (m)

GPC (THF): M_w = 3401, M_n = 3327 polydispersity = 1.02

5.4.7 Pd(TMEDA)Cl_2 catalyzed reaction of *p*-benzoquinone with diphenylsilane

In a dry Schlenck tube a paste of *p*-benzoquinone (99 mg, 1 mmol) and diphenylsilane (182 mg, 1mmol) was made to this Pd (TMEDA) Cl_2 (5 mg, 0.017 mmol) was added and the Schlenck tube was placed in a oil bath at 90^0C for 2 hrs. The resulting black mass was washed with petroleum ether (30 Cm^3) and dried under vacuum

Yield = 200 mg (71%)

Elemental analysis: Calculated for $[C_{18}H_{14}O_2Si.0.5\ H_2O]_n$ C = 72.24, H = 5.01

Found: C = 71.90, H = 5.65%

IR (KBr cm^{-1}): 3387(bm), 1591(s), 1506(s), 1123 (s), 1100(bs), 697(m)

^{1}H NMR ($CDCl_3$): (δ-ppm) 6.5-8.3 (m)

GPC (THF): M_w = 1026, M_n = 971

5.4.8 $RhCl(PPh_3)_3$ catalyzed reaction of diphenylsilane with 1,4-naphthoquinone

To a stirred solution of $RhCl(PPh_3)_3$ (10 mg, 0.01 mmol) in toluene (2 ml) 1,4-naphthoquinone was added. After dissolution of the 1,4-naphthoquinone, diphenylsilane (372 mg. 2.0 mmol) was added at one portion and the reaction mixture was allowed to stir at room temperature for 4 hrs. A colloidal solution was observed, which turns into a homogenous solution, this process was accompanied by evolution of hydrogen. After the reaction is complete, to the reaction mixture hexane (30 cm^3) was added and the catalyst was thus precipitated. The filtrate on evaporation under reduced pressure gave the desired product (**A**).

Yield = 590 mg (99%)

Elemental analysis : Calculated for $C_{34}H_{28}O_2Si_2$: C, 77.86; H, 5.34 ; found C, 77.33, H, 5.45.

IR(neat, cm^{-1}): 3050(w), 2150(s), 1610(w), 1590(m), 1510(s), 1460(w), 1430(w), 1390(w), 1240(s), 1090(s), 1030(s), 1015(s), 940(s), 820(s)

^1H NMR (benzene-d^6): (δ-ppm) 8.56(2H, dd, J=18, 10 Hz), 7.75-7.69(8H, m), 7.25(2H, dd, J=18, 10 Hz), 7.18-7.0(12H, m), 5.9(2H, s).

^{13}C NMR ($CDCl_3$): (δ-ppm) 120.0, 127.9, 130.5, 133.0, 134.5, 150.2

5.4.9 $RhCl(PPh_3)_3$ catalyzed reaction of above product (A) with thiophenol

To a solution of (**A**) (330mg, 1.0 mmol) and thiophenol in tolune (2 ml) $RhCl(PPh_3)_3$ (10 mg, 0.1 mmol) was added. The reaction mixture was allowed to stir at room temperature under inert atmosphere for 16 hrs. To the reaction mixture hexane (30 ml) was added and the catalyst was removed by filtration. On removal of solvent under reduced pressure gave the corresponding silylthioether (**B**) as light yellow oil (98%)

Elemental analysis: Calculated for $C_{46}H_{36}O_2Si_2S_2$: C= 74.59, H= 4.86, found C= H= 4.98

IR(neat, cm^{-1}): 3050(m), 1620(w), 1590(s), 1480(m), 1460(s), 1430(s), 1390(s), 1260(s), 1230(s), 1110(s), 1090(s), 1020(m), 900(s), 820(s), 740(s)

^{1}H NMR ($CDCl_3$): (δ-ppm) 8.05(2H, m) 7.9(4H, m), 7.7-7.2(20H,m), 7.1-6.9(4H, m), 6.9-6.8(6H, m),

^{13}C NMR ($CDCl_3$): (δ-ppm) 112.8, 120.4, 122.2, 126.8, 127.0, 127.9, 128.1, 128.3, 130.7, 132.6, 134.8, 135.2, 145.0

Some representative ^{1}H and ^{13}C spectra of silylether

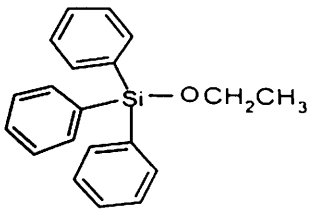

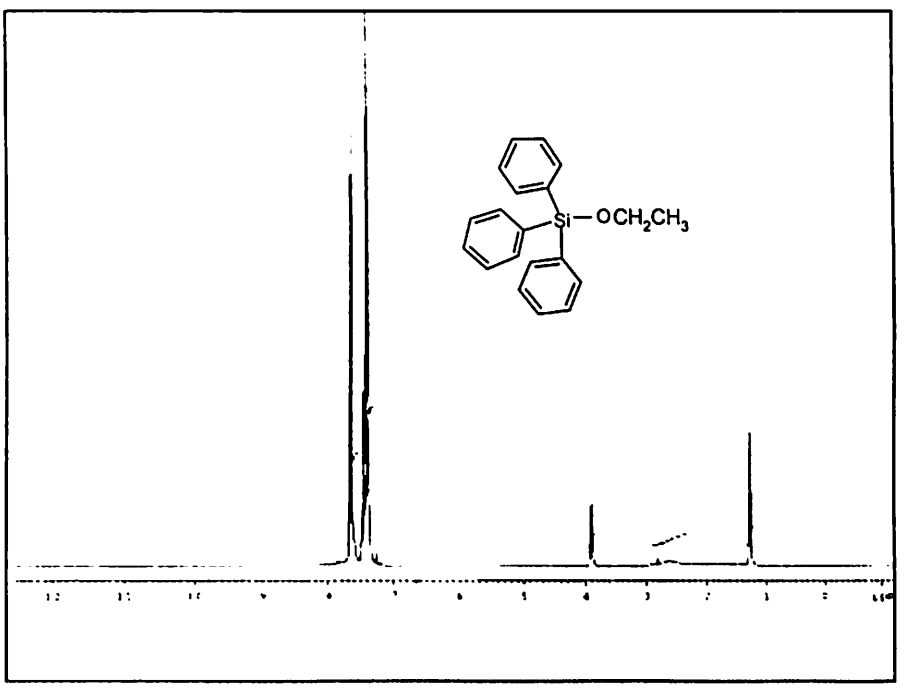

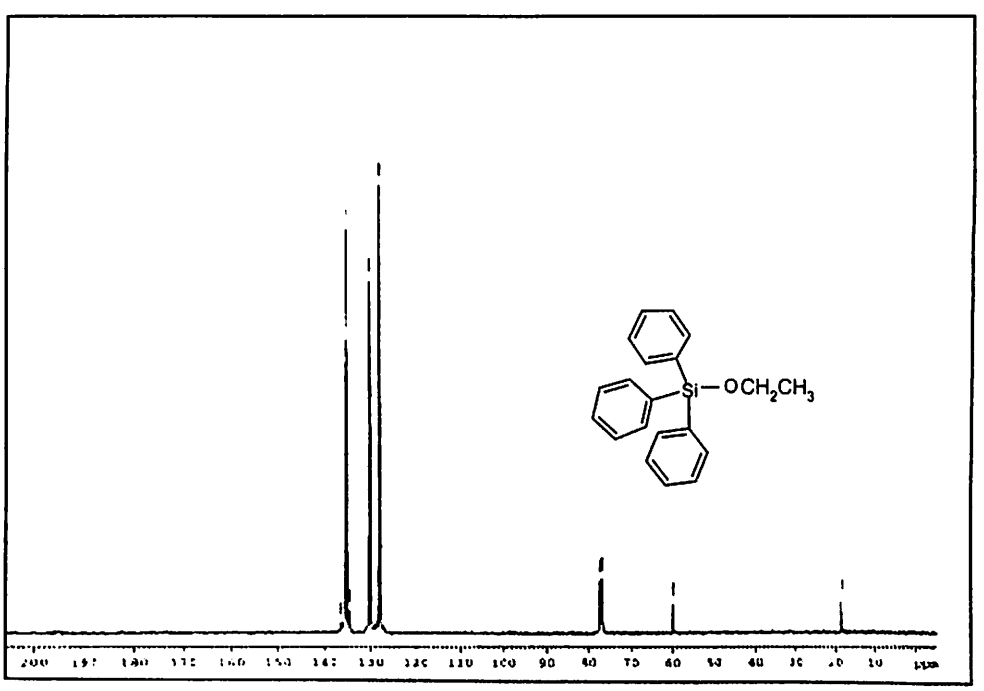

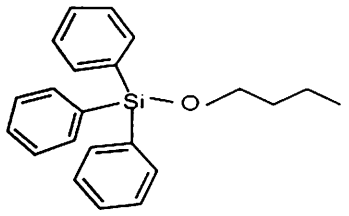

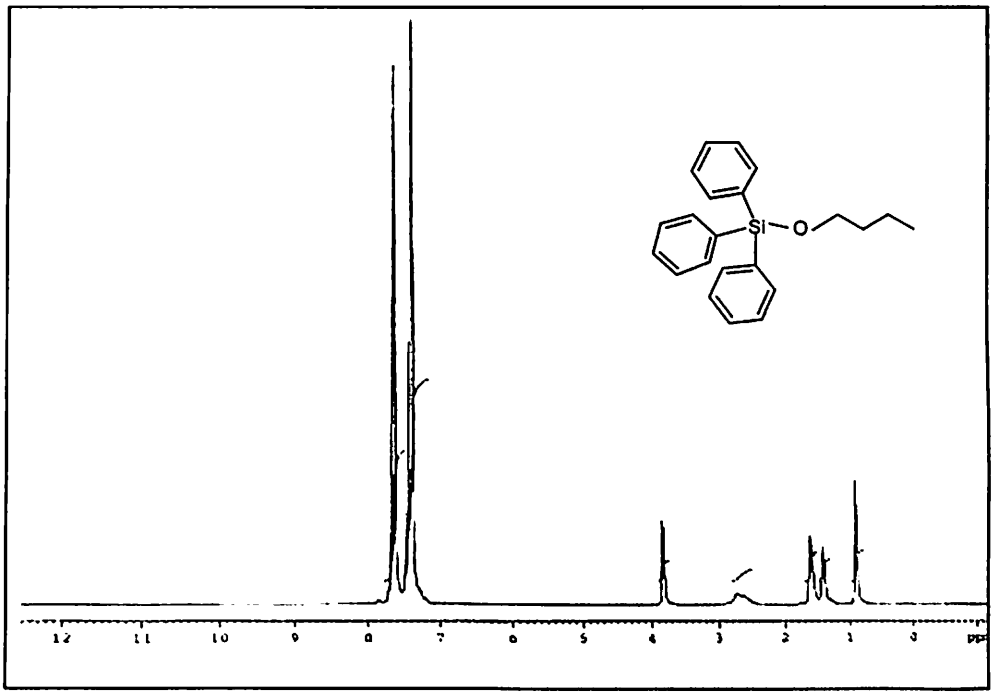

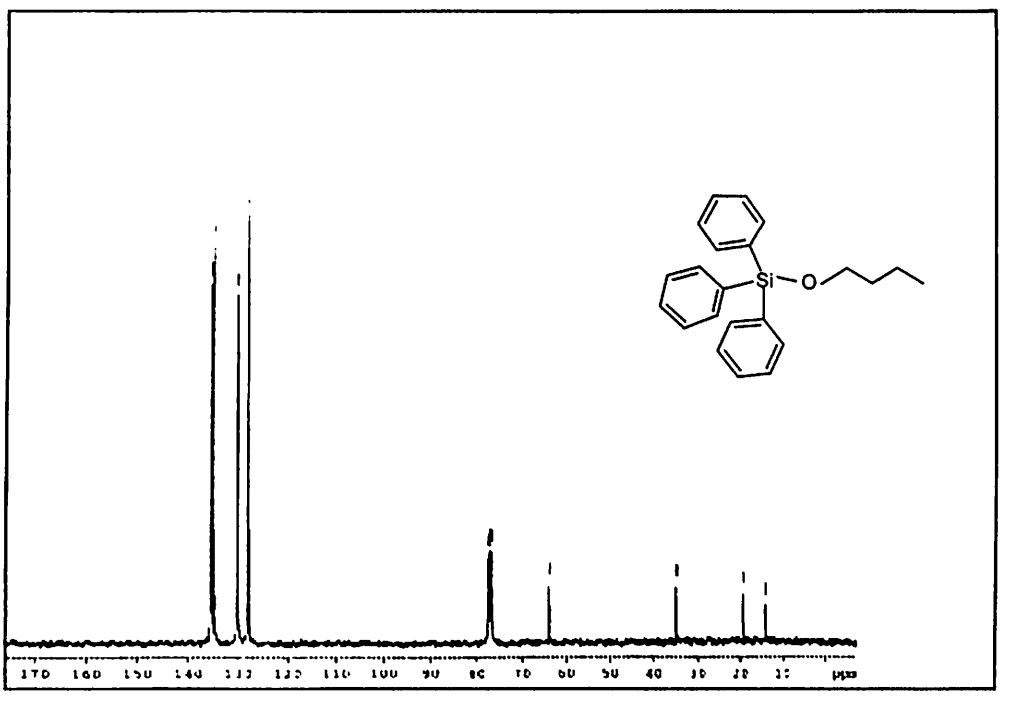

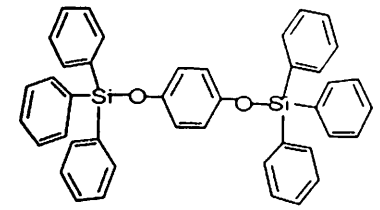

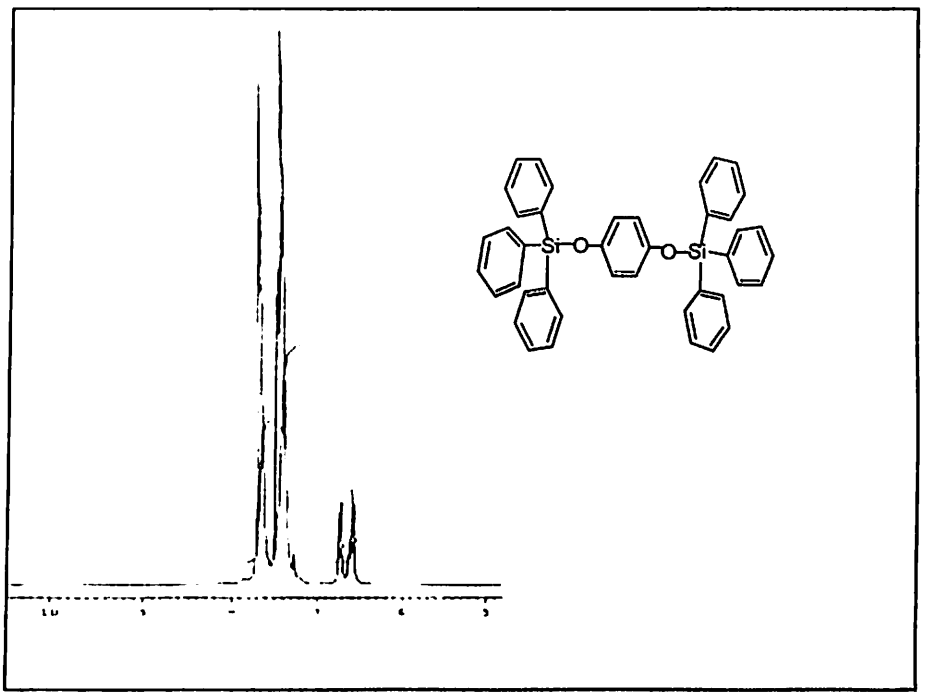

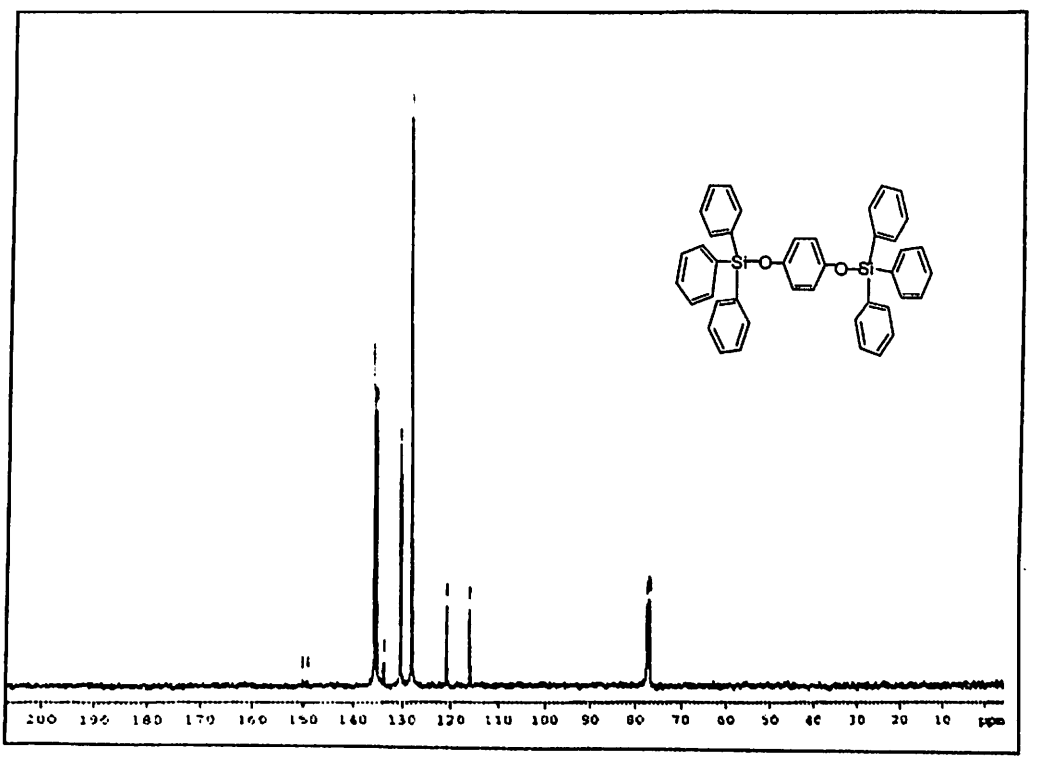

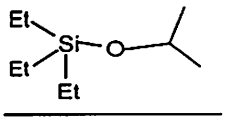
Et
Si
O
Et
Et

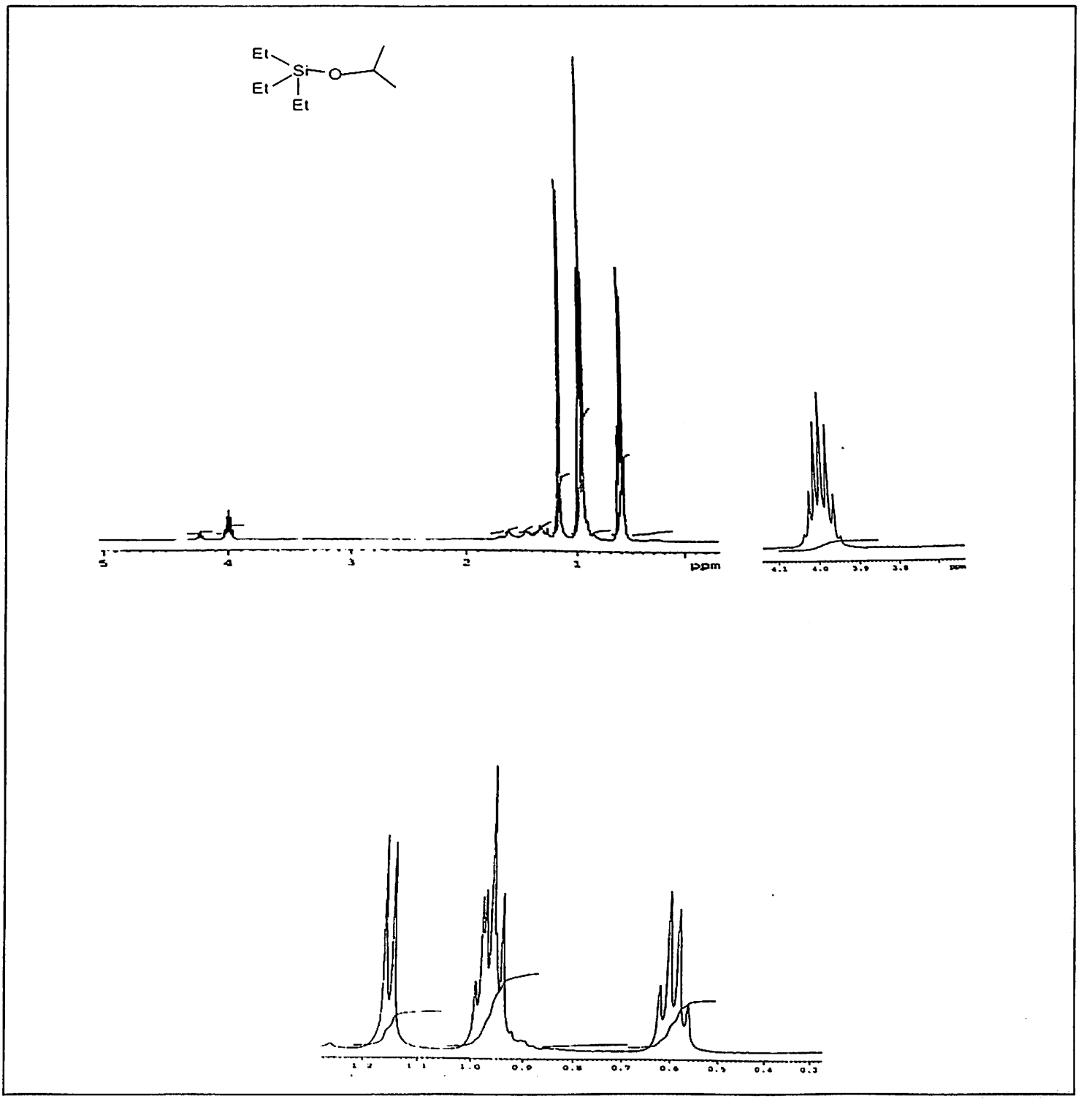
Et
Si
O
Et
Et
5
4
3
2
1
ppm
4.1
4.0
3.9
3.8
ppm
1.2
1.1
1.0
0.9
0.8
0.7
0.6
0.5
0.4
0.3

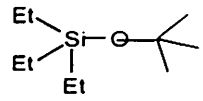

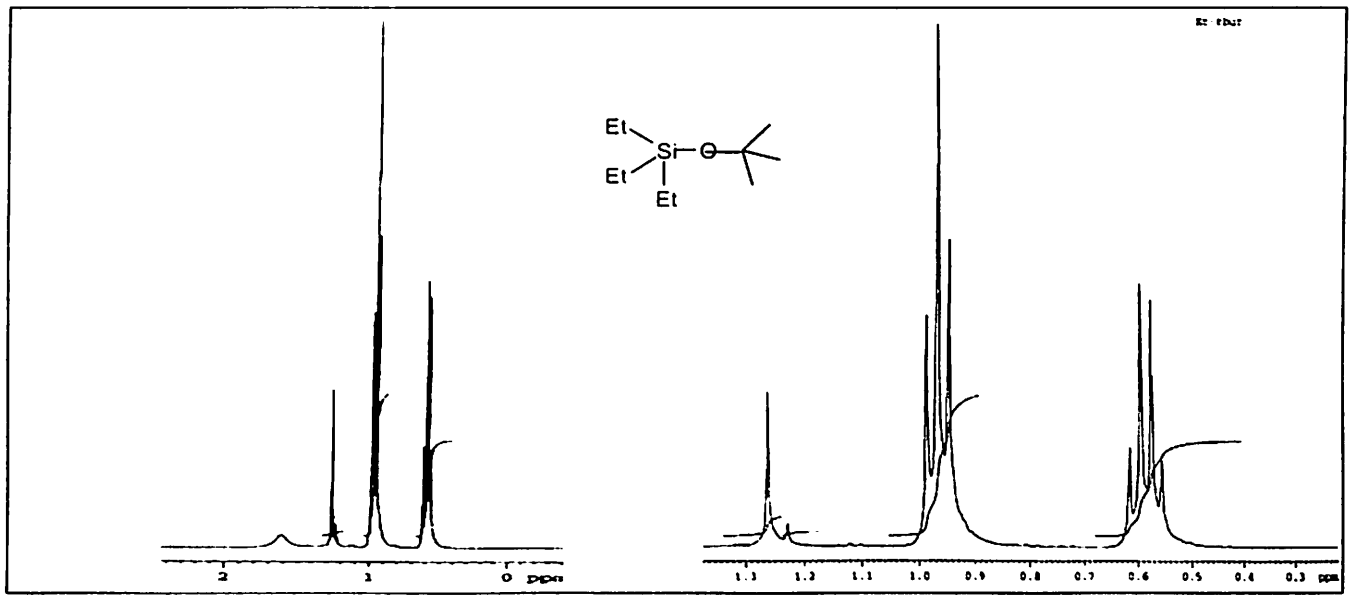

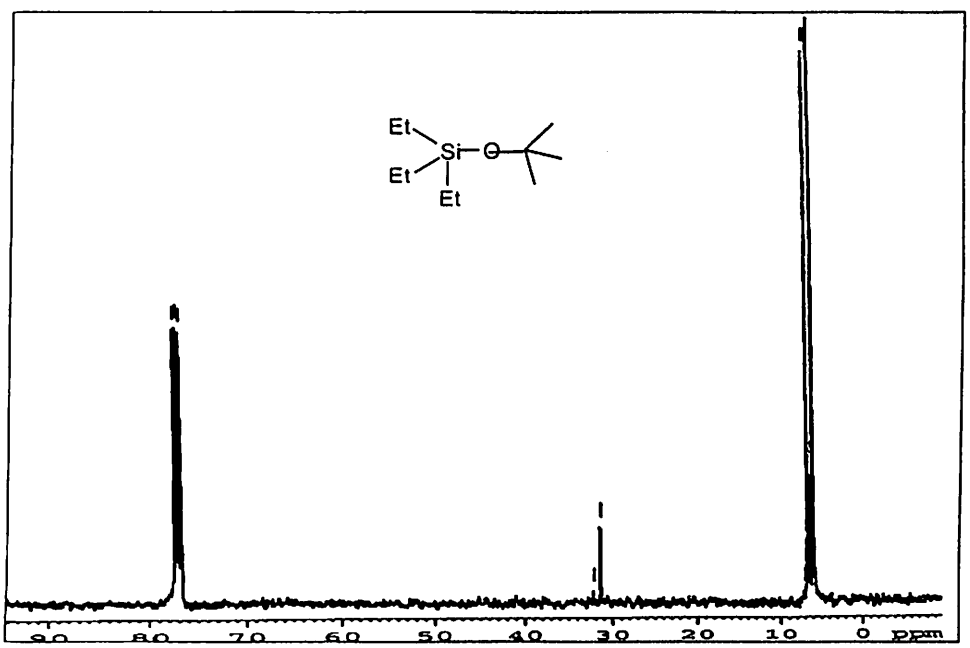

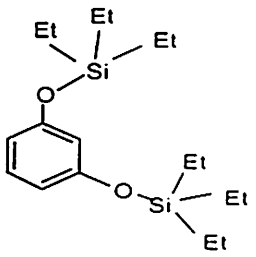
Et
Et
Et
Si
O
Et
O
Si
Et
Et

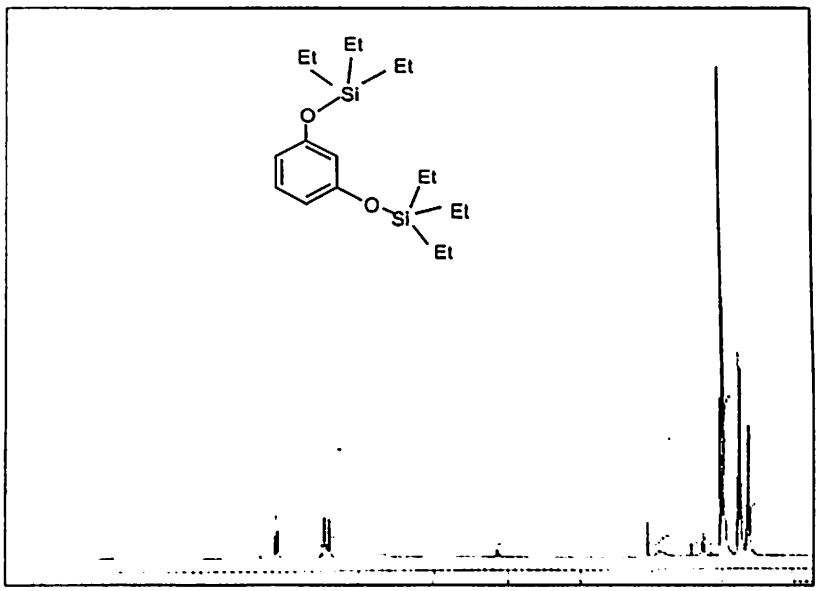
Et
Et
Et
Si
O
Et
O
Si
Et
Et

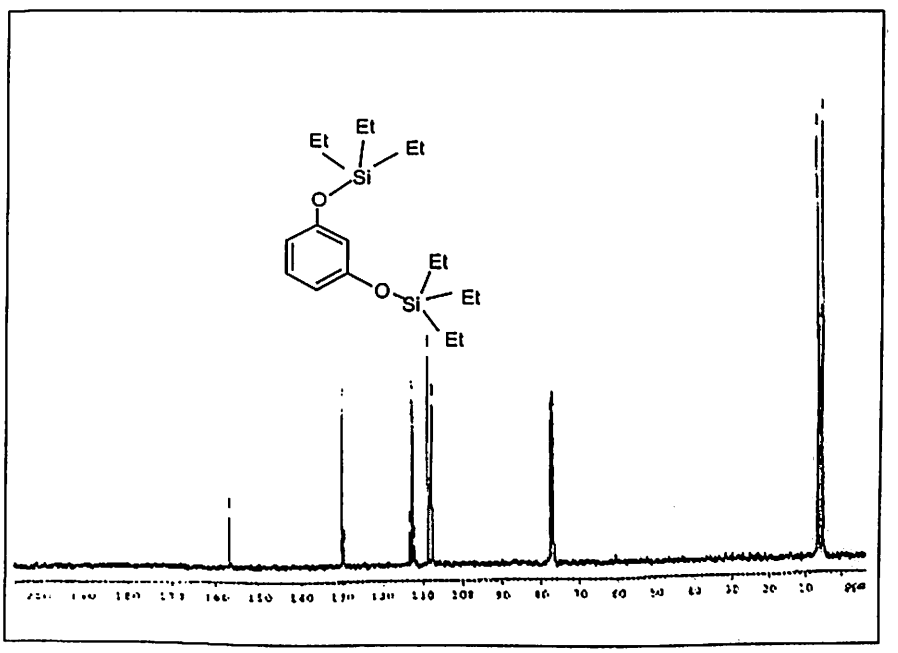
Et
Et
Et
Si
O
Et
O
Si
Et
Et

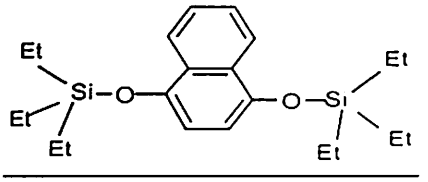
Et
Si
O
Et
Et
Et
O
Si
Et
Et
Et

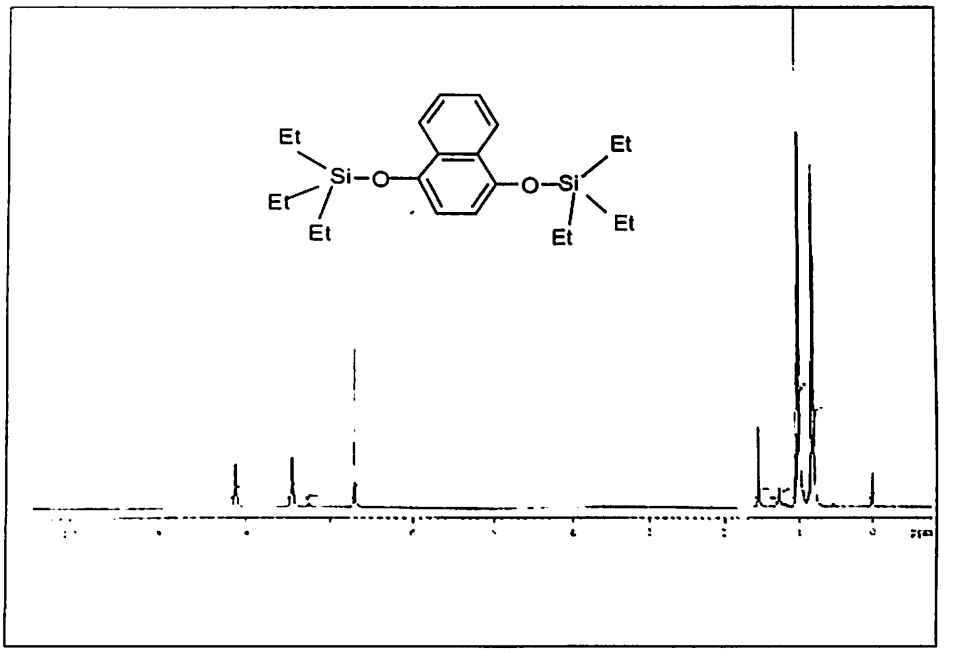
Et
Si
O
Et
Et
O
Si
Et
Et
Et

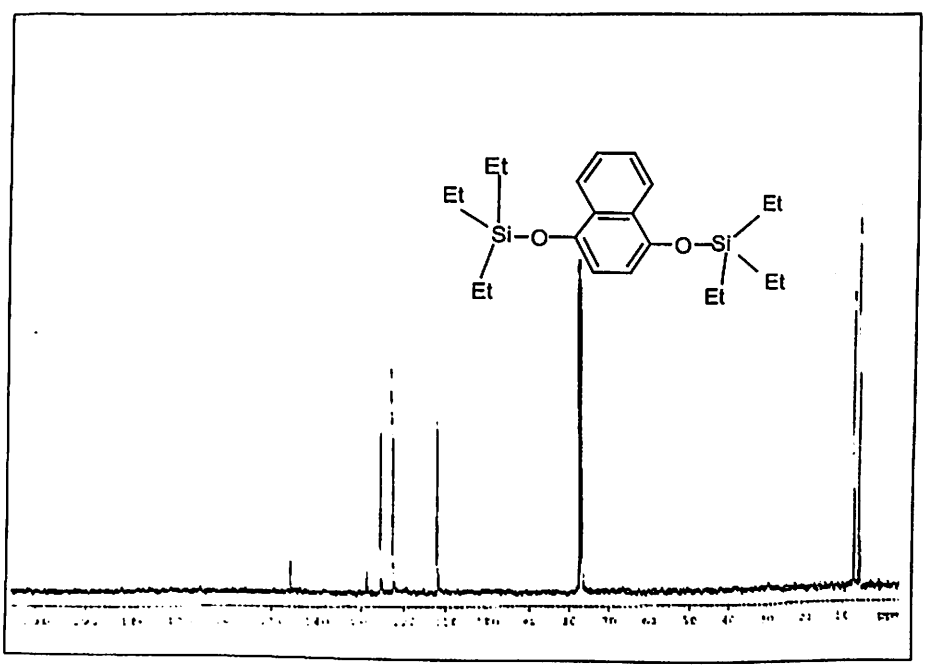
Et
Et
Si
O
Et
O
Si
Et
Et
Et

IR spectra of few silylether

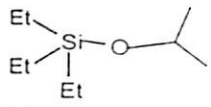

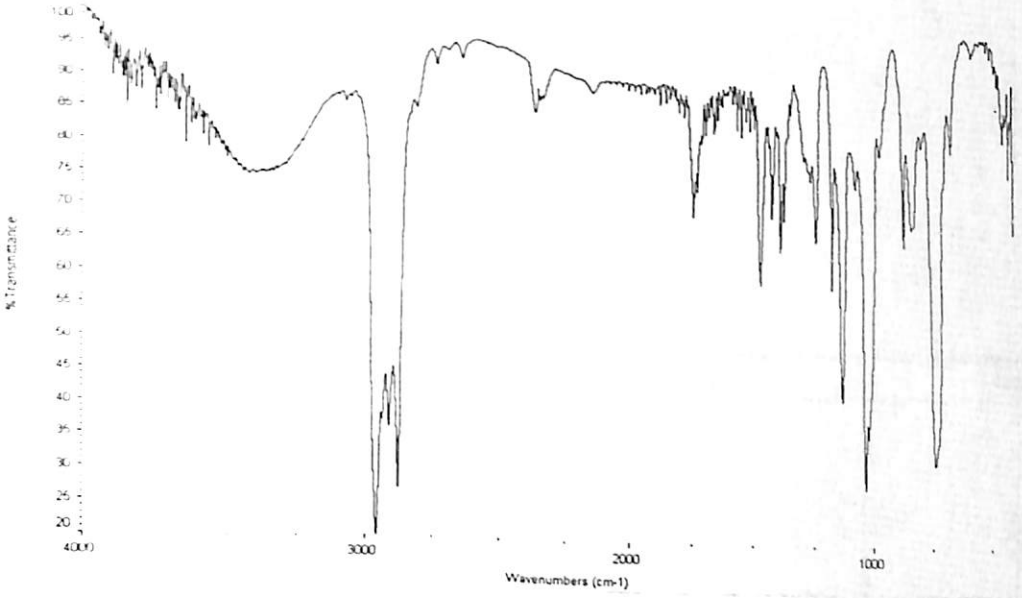

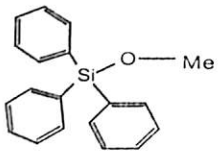

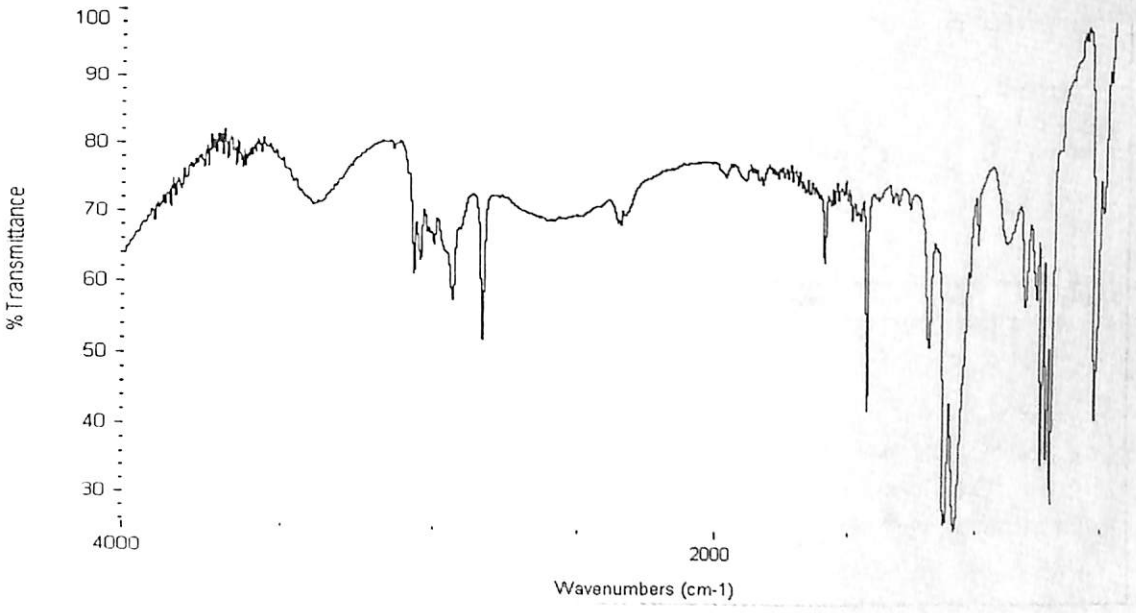

Mass spectra of few silylether:

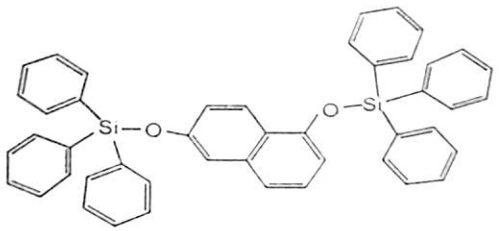

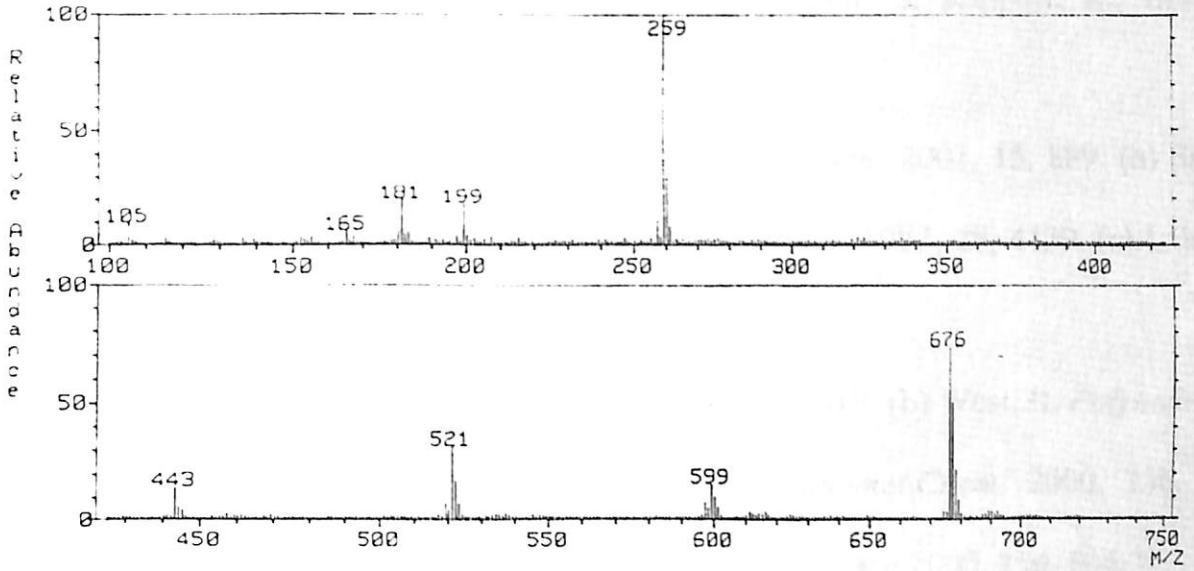

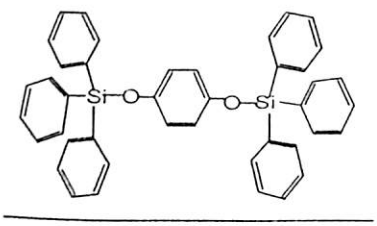

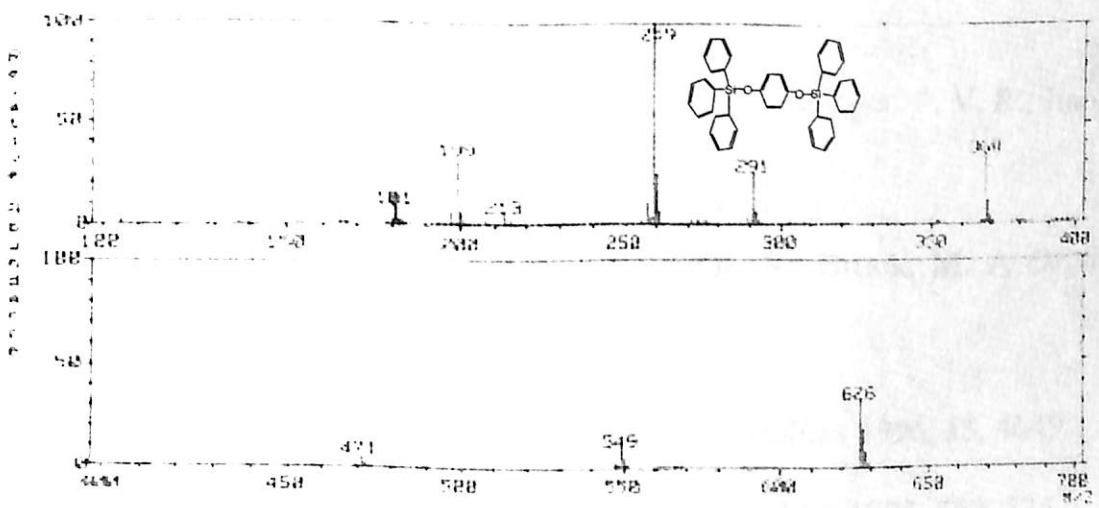

References

1. Corriu, R. J. P.; Cerveau, G.; Framery. E. *Chem.Mater.* 2000, **13**, 3373.
2. Biteau, J.; Chaput, F.; Lahlil, K.; Boilot, J. P. *Chem. Mater.* 1998, **10**, 1945.
3. Corey, J. Y. *Historical Overview and comparision of Silicon with Carbon,* In The Chemistry of Organic Silicon Compounds, Patai, S; Rapport, Z.; Eds.; Wiley: Chichester, UK, 1989, vol 1, chap1, p. 1.
4. (a) Christianopoulou, M. *Appl. Organometal. Chem.* 2001, **15**, 889. (b) Sinhababu, A.; Kawase, M.; Borchardt, R. *Tetrahedron letters.* 1987, **28**, 4139. (c) Lalonde, M.; Chan, T. H. *Synthesis* 1985, 817.
5. (a) Raabe, G and Michl, J. *Chem. Rev.* 1985, **85**, 419. (b) West, R. *Polyhedron.* 2002, **21**, 467. (c) Kira, M.; Iwamoto, T. *J. Organomet.Chem.* 2000, **236,** 611. (d) Iwamoto, T.; Tamura, M.; Kabuto, C.; Kira, M. *Science* 2000, **290**, 504.
6. Wakita, K.; Tokitoh, N.; Okazaki, R.; Nagase, S, S. *Angew. Chem. Int. Ed. Engl.* 2000, **39**, 634.
7. Tokitoh, N.; Wakita, K.; Okazaki, R.; Nagase, S.; Schleyer, P. V. R.; Jiao, H. *J. Am. Chem. Soc.* 1997, **119**, 6951.
8. Wakita, K.; Tokitoh, N.; Okazaki, R.; Nagase, S.; Schleyer, P. V. R.; Jiao, H. *J. Am. Chem. Soc.* 1999, **121**, 11336.
9. Roux, C. Le; Yang, H.; Wenzel, S.; Grigoras, S.; Brook, M. A *Organometallics.* 1998, **15**, 556.
10. Lu, P.; Paulasarri, J. K.; Weber, W. P. *Organometallics* 1996, **15**, 4649.
11. Voronkov, M. G.; Basenko, S. V. *J. Organomet. Chem* 1995, **500**, 325.
12. Corey, E. J.; Venketeswarlu, A. *J. Am. Chem. Soc.* 1972, **94**, 6190.

13. Hwu, J. R.; Wang, N. *Chem. Rev.* 1989, **89**, 1599.

14. Hart, T. W.; Metcalfe, D. A.; Scheinmann, F. *Chem. Commun.* 1979, 156.

15. Rucker, C. *Chem. Rev.* 1995, **95**, 1009.

16. Askin, D.; Angst, D.and . Danishefsky, S. *J. Org. Chem.* 1987, **52**, 622.

17. Mathias, J. *J. Orgnomet Chem.* 1986, **282**, 175.

18. Bideau, F. Le; Coradin, T.; Henique, J. and Samuel, E. *Chem. Commun.* 2001, 1408.

19. Yamashita, H.; Reddy, N. P.; Tanaka, M. *Organometallics* 1997, **16**, 5223.

20. Reddy, P. N.; Chauhan, B. P. S.; Hayashi, T.; Tanaka, M. *Chemistry Lett.* 2000, 250.

21. Lickiss, P. D. *Adv. Inorg. Chem.* 1995, **42**, 147.

22. (a) Brinker, C. J.; Scherer, G. W. *Sol-Gel Science; Academic press: San Diago*, 1989.
(b) Cypryk, M. and Apleloig, Y. *Organometallics* 2002, **21**, 2165.

23. Matsumoto, H.; Arai, T.; Watanabe, H.; Nagai, Y. *Chem. Commun.*1984, 724.

24. Boudjouk, P.; Han, B. H.; Anderson, K. R. *J. Am. Chem. Soc.* 1982, **104**, 4992.

25. Davidson, I. M. T.; Wood, I. T. *Chem. Commun.* 1982,550.

26. Kreil, C. L.; Chapman, O. L.; Burns, G. T.; Barton, T. J. *J. Am. Chem. Soc.* 1980, **102**, 841.

27. Pirrung, M. C. and. Lee, Y. R. *J. Org.Chem.* 1993, **58**, 6961.

28. Mukaiyama, T.; Banno, K.; Narasake, V. *J. Am. Chem. Soc.* 1974, **96**, 7503.

29. Mukaiyama, T. *Angew.Chem. Int. Ed. Engl.* 1977, **16**, 817.

30. Miura, K.; Nakagawa. T.; Hosomi. A. *J. Am. Chem.Soc.* 2001, **124**, 536.

31. Mortimore, M.; Cockerill, G. S.; Kocienski, P.; Treadgold, R. *Tetrahedron Lett.* 1987, **28**, 3747.

32. Rajan Babu, T. V. *J. Org. Chem.* 1984, **49**, 2083.

33. Pandey, G.; Krishna, A. *J. Org. Chem.* 1988, **53**, 2364.

34. Pandey, G. *Top. Curr.Chem.* 1993, **168**,175.

35. Doutheau, A.; Diab, Y.; Dayoub, W. *Tetrahedron Lett.* 2001, **42**, 8455.

36. Osakada, K.; Mori, A.; Koike, T.; Fujii, T. *Synlett.* 2002, **2**, 295.

37. Osakada, K.; Mori, A.; Koike, T.; Fujii, T. *Synlett.* . 2002, **2**, 298.

38. Brook, M. A.: Silicon in Organic, Organometallic, and Polymer Chemistry, John Wiley & Sons, Inc. 2000.

39. Boudjouk, P.; Chauhan, B. P. S.; *Tetrahedron Letters* 1999, **40**, 4123.

40. Haudi-Mazzah, A.; Mazzah, A.; Schmidt, H.-G.; Noltmeyer, M.; Roesky, H.W. Z *Naturforsch.* 1992, **47b**, 1085.

41. Liu, F-Q.; Uson, I.; Roesky, H.W. *J. Chem. Soc., Dalton Trans.* 1995, 2453.

42. Hossain, M. A.; Hursthouse, M. B. *Inorg. Chemic. Acta.* 1980, **44**, 259.

43. Graalmann, O.; Klingebiel, U.; Clegg, W.; Haase, M.; Sheldrick, G. M. *Chem.Ber.* 1984, **117**, 2988.

44. Bhaumik, A.; Kumar, R. *Chem. Commun.* 1995, 869.

45. Huybrechts, D. R. C.; Bruycker, D. L.; Jacobs, P. A. *Nature* 1990, **345**, 240.

46. Voigt, A.; Murgavel, R.; Chandrasekhar, V.; Winkhofer, N.; Roesky, H. W.; Schmidt, H.-G.; Uson, I. *Organometallics* 1996, **15**, 1610.

47. Brown, J. F.; Vogt, L. H. *J. Am. Chem. Soc.* 1965, **87**, 4313.

48. Baney, R. H.; Itoh, M.; Sakakibara, A.; Suzuki, T. *Chem. Rev.* 1995, **95**, 1409.

49. Marcolli, C.; Calzaferri, G. *Appl. Organometal. Chem.* 1999, **13**, 213.

50. Murugavel, R.; Bhattacharjee, M.; Roesky, H. W. *Appl.Organometal.* Chem 1999, **13**, 227.

51. Loy, D.A.; Shea, K. J. *Chem. Mater.* 2001, **13**, 3306.

52. (a) Corriu, R. J. P. and Boury, B. *Chem. Comm.* 2002, 795. (b) Schott *Mater.* 2001, **13**, 342.

53. (a) Hay, J. N; Porter, D. and Raval, H. *Chem. Commun.* 1999, 81. (b) Corriu, R. J. P and Leclercq, D. *Angew.Chem., Int. Ed.. Engl.,* 1996, **35**, 1420.

54. Hay, J. N.; Raval, H. M. *Chem. Mater.* 2001, **13**, 3396.

55. Lee, E. C.; Kimura, Y. *Polym. J.* 1998, **30**, 234.

56. Feher, F. J.; Raquel, T.; Ren-Zhi,J. *Chem. Comm.* 1999, 2513.

57. Feher, F. J.; Raquel, T.; Zhiller, J. W. *Chem. Comm.* 1999, 2309.

58. Matsumoto, H .; Suto, A.; Unno, M. *J. Am. Chem. Soc.* 2002, **124**, 1574.

59. *Siloxane Polymers*; Clarson S. J.; Semlyen, J. A.; Eds. Printice Hall: Englewood Cliffs, NJ, 1993.

60. Brook, M. A.; Grgoras, S.; Wenzel, S.; Yang, H.; Le Roux, C. *Organometallics*, 1998, **17**, 556

61. Marciniec, B.; Gulinski, J.; Urbaniak, W.; Kornetka, Z. W. *Comprehensive Handbook on hydrosilylation Chemistry*, Pergamon: Oxford, 1992.

62. Ojima, I. " *The hydrosilylation Reaction" in the Chemistry of organic silicon compounds*, Patai, S. and Rappoport (J. Wiley & Sons, New York, 1989), Chap. 25, pp. 1479-1526.

63. Imori, T.; Tilley, T. D. *Polyhedron* 1994, **13**, 2231.

64. Dioumaev, V. K.; Harrod, J. F. *J. Organomet. Chem.* 1996, **521**, 133.

65. Rosenberg, L.; Davis, C. W.; Yao *J. Am. Chem. Soc.* 2001, **123**, 5120.

66. Lewis, L. N. *J. Am. Chem. Soc.* 1990, **112**, 5998.

67. Ito, Y.; Suginome, M.; Murakami, M. *J. Org. Chem.* 1991, **56**, 1948.

68. Boudjouk, P.; Chauhan, B. P. S. *Tetrahedron lett.* 2000, **41**, 1127.

69. Yamamoto, T.; Osakada, K.; Baruah, J. B. *J. Mol. Cat. A: Chemical.* 19

70. Curtis, M. D.; Epstein, P. S. *Adv. Organomet. Chem.* 1983, **19**, 213.

71. Sakakura, T.; Kumberger, O.; Tan, R. P.; Arthur, M-P; Tanaka, M. *Chem. Comm.* 1995, 193.

72. Marciniec, B.; Krzyzanowski, P. *J. Organomet. Chem.* 1995, **261**, 493.

73. Marciniec, B.; Krzyzanowski, P.; Walczuk-Gusciora, E.; Duchmal, W. *J. Mol. Cat.* 1999, **144**, 263.

74. Marciniec, B.; Krzyzanowski, P.; and Pietraszuk, C. *Organometallics* 2001, **20,** 3423.

75. Hester, D. M.; Sun, J.; Harper, A. W. and Yang, G. K. *J. Am. Chem. Soc.* 1992, **114**, 5234.

76. Schubert, U. *Adv. Organomet. Chem.* 1990, **30**, 151.

77. Chatani, N.; Kodama, T.; Kajikawa, Y.; Murakami, H.; Kakiuchi, F.; Ikeda and Murai, S. S. *Chemistry Letters*. 2000, 14.

78. Woo, H.-G.; Walzer, J. F.; Tilley, T. D. *J. Am. Chem. Soc.* 1992, **114**, 7047.

79. Tilly, T. D. *Acc. Chem. Res.* 1993, **26**, 22.

80. Duchateau, R. *Chem. Rev.* 2002, **102**, 3525, and references therein.

81. Clark, J. H. *Catalysis of Organic Reactions by Supported Inorganic Reagents*. VCH; 1994.

82. Feher, F. J.; Blanski, R. I. *Chem. Comm.* 1990, 1614.

83. Crocker, M.; Herold, R. H. M.; Orpen, A. G. *Chem. Commun.* 1997, 2411.

84. Crocker, M.; Herold, R. H. M., *Pat.Appl*; PCT/EP96/05873.

85. Buys, I. E.; Hambley, T. W.; Houlton, D. J.; Maschmeyer, T.; Masters, A. F.; Smith, A. K.; *J. Mol. Catal*, 1994, **86**, 309.

86. Birchall, J. D. *Chem. Soc. Rev.* 1995, **24**, 351.

87. Carlisle, E. M. *Science* 1972, **178**, 619.

88. Akashi, M.; Takemoto, K. *Adv. Polym. Sci.* 1990, **97**, 107.

89. Barton, T. J.; Boudjouk, P. *Silicon-Based polymer Science. A comprehensive resource*; Zeigler, J. M.; Fearon, F. W. G., Eds.; Advances in Chemistry series; American Chemical Society: Washington, DC, 1990; vol. 224.

90. *Siloxane Polymers*; Clarson, S. J; Semlyen, J. A., Eds.; Prentice Hall : Englewood Cliffs, NJ, 1991.

91. Choi, K.M.; Shea, K. J. In *Photonic Polymer Synthesis*; Wise, G.; Trantolo, M.; Graham, B.; Eds; Marcel Dekker: New York, 1998; p-437.

92. Tomanek, A. *Silicon and Industry*, Hasner (Wacker Chemie): Munich, 1991. p146.

93. Arkles, B. *CHEMTECH*. 1983, **13**, 542.

94. Rochow, E. G. *Silicon and Silicones*; Springer-Verlag: Berlin, 1987.

95. Schubert, U. *New J. Chem.* 1994, **18**, 1049.

96. T.W. Greene and P. G. M Wutz, Protective Groups in organic synthesis, Wiley, 2nd edn., New York, 1991.

97. (a) Gozdz, A. S. *Polym. Adv. Technol.* 1994, **5**, 70. (b) McKean, D. R.; Clecak, N. J.; Pederson, L. A., *Proc. SPIE-Int.Soc. Opt. Eng.* 1990, **110**, 1262. (c) Adachi, E.; Aiba, Y.; Adachi, H. Japanese patent Kokai-H-2-277255, 1990, *Chem. Abstr.* 1991, **114**, 124250. (d) Mishima, T.; Nishimoto, H., Japanese patent Kokai- H4-271306, 1992; *Chem. Abstr.* 1993, **118**, 256251. (e) Hase, N.; Tokunaga, T.; Japanese patent Kokai- H-5-43420, 1993, *Chem. Abstr.* 1993, **119**, 34107.

98. (a) Loy, D. A.; Carpenter, J. P.; Myers, S. A.; Assink, R. A.; Small, J. H.; Shea, K. J. *J. Am. Chem. Soc.* 1996, **118**, 8501. (b) Biteau, J.; Chaput, F.; Lahlil, K.; Boilot, J. P. *Chem. Mater.* 1998, **10**, 1945.

99. Loy, D. A. Ph. D. Thesis, University of California, Irvine, CA, 1991.

100. Lindner, E.; Schneller, T.; Auer, F.; Mayer, H. A. *Angew. Chem. Int. Ed.* 1999, **38**, 2155.

101. Pohidaev, Yu. N.; Raspopina, O. Yu.; Vlasova, N. N.; Voronkov, M. G. Zh. Prikl. Khim. 1999, **72**, 586.

102. Hathaway, B. J, *Structure and Bonding* (Berlin) 1984, **57**, 55.

103. Place, H.; Willett, R.D.; Middleton, M., *J. Am. Chem. Soc.* 1988, **11**, 8639.

104. M. A., Salas; J. M., Quiros, M.; Sanchez, M. P., Romero, J., Marti, D. *Inorg. Chem.* 1994, **33**, 5477.

105. Willett, R.D *Coord. Chem. Rev.* 1991, **109**, 181.

106. Matsumoto, T.; Miyazaki, Y.; Albrecht, S. A.; Landee, C. P.; Turnbull, M. M. and Sorai, M., *J. Phys. Chem. B.* 2000, **104**, 9993.

107. Blanchette, J and Willett, R. D *Inorg. Chem.* 1988, **27**, 843.

108. (a) Coffey, T. J.; Landee, C. P.; Robinson, W. T; Turnbull, M. Winn.; Woodard, F. M. *Inorg. Chim. Acta.* 2000, **303**, 54. (b) Halverson, K., Patterson, C., Willet, R. D., *Acta Crystallogr.* 1990, **B46**, 508. (c) Bond, M. R.; Place, H.; Wang, Z.; Willett, R.D.; Liu, Y. L.; Grigereit, T. E.; Drumheller, J. E.; Tuthhill, G. F. *Inorg. Chem.* 1995, **34**, 3134. (d) Bond, M. R.; Willett, R. D. *Inorg.Chem* 1989, **28**, 3267. (e) Bond, M. R.; Willett, R. D.; Rubencaker, G. V. *Inorg. Chem.* 1990, **29**, 2713.

109. Udupa, M. R.; Kerbs, B.; *Inorg. Chim. Acta.* 1979, **33**, 241.

110. Dyrek, K.; Gosler, J.; Hodorovicz, S. A.; Hoffmann, S. K.; Oleskyn, B. J Weselucha-Brcynska, A. *Inorg. Chem.* 1987, **26**, 1481.

111. Antoline, L.; Marcotrigiano, G.; Menabue, L.; Pellacani, G. C. *J. Am. Chem. Soc.*1980, **102**, 130.

112. (a) Hunter, C. A, *Chem.Soc.Rev* 1994, 102. (b) Desiraju, G. R.; Steiner, T. The Weak Hydrogen Bond in Structural Chemistry and Biology, Oxford University Press, Oxford, 1999. (c). Frechilla, D.; Lasheras, B.; Ucelay, M.; Parrondo, E.; Craciunescu, G. and Cenarruzabeitia , E. *Arzneim. Forsch. Drug. Res.* 1991, **41**, 247. (d) Craciunescu, D. G.; Gutierrez-Rios, M. T; Parrondo-Iglesias, M, C.; Doadrio-Lopez, A.; Gaston de Iriarte and Guirvu, C., *An. Real Acad. Farm.* 1989, **55**, 329.

113. Place, H.; Willett, R.D, *Acta crystallogr. Sect. C*, 1988, **44**, 34.

114. Boeyens, J. C.; Dobson, S. M.; Ossthuizen, E. L., J. *Crystallogr. Spectrsc. Res.*, 1990, **20**, 407.

115. Thackeray, M. M.; Nassimbeni, L. R. *Acta crystallogr. Sect. B*, 1974, **30**, 2469.

116. Manfredini, T.; Pellacani, G. C; Giusti, J. G.; Pon, G.; Willett, R. D.; West, D. X. *Inorg. Chem.* 1990, **29**, 222.

117. Czugler, M.; Kotai, L.; Sreedhar, Bojja, Rockenbauer, Antal, Gacs, I. And Holly, S. *Eur. J. Inorg. Chem.* 2002, 3298.

118. Luque, A.; Sertucha, J.; Castillo, O. and Roman, P. *New. J. Chem.* 2001, **25**, 1208.

119. Luque, L.; Sertucha, J.; Lezama, L.; Rojo, T.; Roman, P. *J. Chem. Soc., Dalton Trans.*, 1997, 847.

120. Manfredini, T.; Pellacani, G. C.; Corradi, A. B.; Battaglia, L. P.; Guarini Giusti, J. G.; Pon, G.; Willet, R. D. *Inorg. Chem.* 1990, **29**, 2221.

121. Santra, B. K.; Reddy, P. A. N.; Nethaji, M.; Chakravarty, A. R. *Inorg. Chem.* 2002, **41**, 1328.

122. Balamurugan, R.; Pallaniandavar, M.; Gopalan, R. S. *Inorg. Chem.* 2001, **40**, 2246

123. Textor, M.; Dubler, E.; Oswald, H. R *Inorg. Chem.* 1974, **13**, 1361.

124. *Introduction to Magnetochemistry* by Earnshaw, A., Academic Press, New-York.

125. Kennedy, B. P.; Lever, A. B. P., *J. Am. Chem. Soc.*, 1973, **95**, 690.

126. Bloomquist, D. R.; Willet, R. D. *Coord. Chem. Rev.* 1982, **47**, 125.

127. Bray, K. L.; Drickamer, H. G.; Schmitt, E. A.; Hendrickson, D. N. *J. Am. Chem. Soc.* 1989, **111**, 2849.

128. Takahashi, K.; Nakajima, R.; Gu, Z., Yoshiki, H.; Fujishima, A.; Sato, O., *Chem. Comm.* 2002, 1578.

129. Haddad, S. and Willet, R. D, *Inorg. Chem.*, 2001, **40**, 2457.

130. Uehara, A.; Iimura, A.; Shimizu, K.; Mortia, S.; Yoshifuji, A. and Tsuchiya, R., *Thermochim. Acta*, 1984, **77**, 299.

131. Wolf, L.; Hennig, H. *Anorg. Allegm. Chem.* 1964, **329**, 301.

132. Manfredini, T.; Pellacani, G. C; Corradi, A. B.; Battaglia, L. P.; Guarini, G. G. T.; Giusti, J. G.; Pon, G.; Willett, R. D. *Inorg. Chem.* 1990, **29**, 2221.

133. Puzari, A.; Handique, J. G.; Purkayastha, A.; Baruah, J. B.; Srinivasan, A. *Indian J. Chem.* 1999, **38A**, 521.

134. Lorenz, C. and Schubert, U. *Chem. Ber.* 1995,128, 1267.

135. Clarke, M. P, *J. Organomet. Chem.*, 1989, **376**, 1.

136. Miller, W. S.; Peake, J. S.; Nebergall, W. H. *J. Am. Chem. Soc.* 1957, **79**, 5604.

137.Sternbach, B.; Mac Diarmid, A. G. *J. Am. Chem. Soc* 1959, **81**, 5109.

138. Corey, E. J.; Venkateswarlu, A. *J. Am. Chem. Soc.* 1972, **94**, 6190.

139. Brook, M. A. *Silicon in Organic and Organometallic, and Polymer Chemistry* page199.

140. Peebles, L. H.; *Molecular weight distribution in polymers*, Wiley-Interscience, New York, 1971.

141. Gowariker, V. R.; Viswanathan, N. V.; Sreedhar, J. Polymer Science, Wiley Eastern, 1986.

142. Richardson, T. J.; Slack, J. L. and Rubin M. D. *4th International Meeting on Electrochrism*, August 21-23, 2000, Uppsala, Sweden.

143. Mukhopadhya, S.; Shalini, K.; Devi, A.; Shivashankar, S. A. *Bull. Mater. Sci.* 2002, **25**, 391

144. Goswami, J.; Shivasankar, S. A.; Ananthakrishna, G. *Thin solid films*. 1997, **305**, 52.

145. Julia, H.; Becker, R.; Birkner, A.; Weiβ, J.; Fischer, R. A. *Chemm. Comm.* 2002, 68.

146. Harkness, B. R.; Rudolph, M.; Takeuchi, K. *Chem. Mater.* 2002, **14**, 1448.

147. Hof, F.; Craig, S.L.; Nuckolls, C.; Rebek, J. Jr. *Angew. Chem. Int. Ed. Engl.* 2002 **41**, 1488.

148. Sacham-Diamand, Y.; Sun, B-X; Yip, V.; Bielski, R. *Proc. Electrochem. Soc.* 1994, **94**, 136.

149. Lee, S.J.; Han, S.W.; Kim, K.; *Chem. Commun.* 2002, 442.

150. Hansen, P. L; Wagner, J. B.; Helveg, S.; Rostrup-Nielsen, J. R.; B. S. Clausen, Topsoe, H. *Science* 2002, **295**, 2053.

151. Brown, K. R.; Natan, M. J. *Langumir* 1998, **14**, 726.

152. Wear, W. W.; Reed, S. M.; Warner, M. G.; Hutchison, J. E. *J. Am. Chem. Soc.* 2000, **122**, 12890.

153. Higashimura, H.; Fugisawa, K.; Moro-oka, Y.; Kubota, M.; Shiga, A.; Terahara, A.; Uyama, H.; Kobayashi, S. *J. Am. Chem. Soc.* 1998, **120**, 8529.

155. Baesjou, P.J; Driessen, W. L.; Challa, G.; Reedijk, J. *J. Am. Chem. Soc.* 1997, **119,** 12590.

156. Gauvin, F.; Harrod, J. F.; Woo, H. G. *Adv. Organomet. Chem.* 1998, **42**, 363.

157. Laine, R. M.; Blum, Y. D.; Tse, D.; Glaser, R. Inorganic and organometallic polymers; ACS Symp. Ser. 360.

158. Chauhan, B. P. S.; Boudjouk, P. *Tetrahedron letters* 2000, 41, 1127.

159. Baruah, J. B.; Osakada, K.; Yamamoto, T. *Organometallics* 1996, **15**, 456 and references therein.

160. Lukevics, E.; Dzintara, M. *J. Organomet. Chem.* 1985, **295**, 265.

161. Sakakura, T. Kumberger, O.; Tan, R. P. Arthur, M-P; Tanaka, M. *Chem. Commun.* 1995, 193.

162. Ojima, I.; Kogure, T.; Nihonyanagi, M.; Kono, H. and Inaba, S.; *Chem. Letters* 1973, 501.

163. Reddy, P. N.; Chauhan, B. P. S.; Hyashi, T. and Tanaka, M. *Chemistry. Lett.* 2000, 250.

164. Palladium Reagents and Catalysts: innovations in Organic Synthesis. Tsuji, J, *John Wiley & Sons, 1994.*

165. Organometallics in Synthesis A Manual: Schlosser, M. *John Wiley & Sons, Second edition.*

166. Stromnova, T. A; Vargaftik, M. N. and Moiseev, I. I. J. *Organomet.* **252**, 113.

167. Chung, M.-K.; Orlova, G.; Goddard, J. D.; Harris, R.; Beveridge, T. J.; White, G. and Hallett, F. R. *J. Am .Chem. Soc.* 2002, **124,** 10508.

168. Sommer, L. H.; Lyons, J. E. *J. Am. Chem. Soc* 1969, **91**, 7061

169. (a) Sharma, H. K.; Pannell, K. H. *Chem. Rev.* 1995, **95**, 1351. (b) Yamashita, H.; Reddy, N. P.; Tanaka, M. *Organometallics* 1997, **16**, 5223.

170. Fowley, L. A.; Michos, D. Luo, X-L.; Crabtree, R. H. *Tetrahedron letts.* 1993, **34**, 3075.

171. Lissa, A.; Michos, D.; Luo, X-L.; Crabtree, R. H. *Tetrahedron letts.*1993, **34**, 3075.

172. Curtis, M. D.; Epstein, P. S. *Adv. Organomet. Chem.* 1981, **19**, 213.

173. Speier, J. L and Zimmerman, R. E. J. *Am. Chem. Soc.* 1955, **77**, 6395.

174. Baruah, J. B.; Osakada, K.; Yamamoto, T. *J. Mol. Catal* 1995, **101**, 17.

175. Luo, X-L.; Crabtree, R. H. *J. Am. Chem.Soc.*1989, **111**, 2527.

176. Corriu, R. J. P.; Moreau, J. J. E. *J. Organomet. Chem.* 1977, **127**, 7.

177. Corriu, R. J. P.; Moreau, J. J. E. *J. Organomet. Chem.*1976, **120**, 337.

LIST OF PUBLICATIONS

1. *Silicon-oxygen-bonded oligomers having thermoelectric switching properties*

   Purkayastha, A.; Baruah, J. B. *Appl. Organometal. Chem.* 2001, **15**, 693.

2. *Silicon-oxygen bonding on diphenylsilane through palladium (II)-catalysed reactions*

   Purkayastha, A.; Baruah, J. B. *Appl. Organometal. Chem.* 2000, **14**, 477.

3. *Palladium (II) catalysed Silicon-Oxygen bond formation versus rearrangement reactions*

   Purkayastha, A. ; Baruah, J. B.. *Phosphorus-sulfur-and-silicon-and the related elements.* 2001, **168**, 333.

4. *Tetra Chlorocopper(II) chemistry: delineation of optical, thermal properties.*

   Purkayastha, A. ; Baruah, J. B. *Thermochimica Acta.* 2002, **390**, 187.

5. *A new catalyst system for silylether synthesis*

   Purkayastha, A.; Baruah, J. B. *Silicon Chemistry.* 2002, **1**, 229.

6. *Some aspects of palladium and rhodium catalysis for synthesis of silylethers from Si-H bond*

   Purkayastha, A.; Baruah, J. B. *Journal of Molecular Catalysis A: Chemical.* 2003, **198**, 47.